

# Asymptotic freedom, Haldane gap and edge states of $SU(N)$ spin chains

Présentée le 14 décembre 2020

à la Faculté des sciences de base  
Chaire de théorie de la matière condensée  
Programme doctoral en physique

pour l'obtention du grade de Docteur ès Sciences

par

**Samuel GOZEL**

Acceptée sur proposition du jury

Prof. F. Carbone, président du jury  
Prof. F. Mila, Prof. I. K. Affleck, directeurs de thèse  
Prof. Ph. Lecheminant, rapporteur  
Prof. U. Schollwöck, rapporteur  
Prof. H. Rønnow, rapporteur



*À mes Parents*



“It is an odd circumstance that neither the old nor the new, by itself, is interesting;  
the absolutely old is insipid; the absolutely new makes no appeal at all.  
The old in the new is what claims the attention, – the old with a slightly new turn.”

William James



# Remerciements

J'aimerais remercier chaleureusement Frédéric Mila et Ian Affleck, mes directeurs de thèse, pour m'avoir suivi et supervisé durant ces quatre années. Je leur suis tout particulièrement reconnaissant d'avoir permis un parcours de thèse autant inhabituel qu'enrichissant. Un grand merci à Ian pour m'avoir accepté dans son groupe à Vancouver durant la première année de ma thèse, pour sa patience, sa disponibilité et son suivi méticuleux de mes travaux, qui n'auraient jamais été ce qu'ils sont sans lui. Un grand merci à Frédéric pour sa supervision constante et bienveillante, pour ses conseils avisés, pour m'avoir proposé des projets variés, m'avoir mis à disposition toutes les ressources nécessaires et pour avoir permis et initié plusieurs voyages académiques, notamment à Vancouver.

J'aimerais également remercier deux autres physiciens avec qui j'ai eu la chance de pouvoir travailler : premièrement, Didier Poilblanc, pour son enthousiasme débordant à chaque étape du projet, une réelle source de motivation. Deuxièmement, Pierre Nataf, pour son aide précieuse, pour ses encouragements et pour son humour, et ce depuis la première année de mon master déjà. Je tiens aussi à remercier Fabrizio Carbone, Henrik Rønnow, Philippe Lecheminant et Ulrich Schollwöck, les membres du jury, pour leur intérêt dans ma thèse et pour toutes leurs questions durant la défense privée. Merci également à Anna Maria pour le travail administratif, en particulier lié à mes nombreux voyages, et Aubry pour le support informatique.

Durant mon séjour à Vancouver, j'ai eu la chance de rencontrer de nombreuses personnes qui ont toutes contribué à leur façon à transformer une visite académique en une année riche en découvertes. J'aimerais premièrement remercier les membres du groupe de Ian, pour toutes les discussions scientifiques, et en particulier Kyle pour ses encouragements, pour avoir constamment partagé mes opinions sur le monde académique, mais aussi et surtout pour les week-ends prolongés sur l'Île. Je remercie également Étienne, pour avoir partagé ses vastes connaissances en physique et pour m'avoir permis de ne pas complètement oublier la langue de Molière, ainsi que les nombreux amis de SJC qui sauront se reconnaître. Du côté suisse, j'aimerais remercier les membres passés et présents du groupe CTMC, pour les nombreuses discussions scientifiques utiles et inspirantes en toute circonstance. Je tiens tout particulièrement

## Remerciements

---

à remercier Francisco, pour sa sagesse et pour avoir été celui qui me permettait de m'échapper du bureau tout en restant au bureau. Je remercie également Justin, Luc, Virgile et Samy, pour les dîners interminables à la Banane qui m'ont raccourci de nombreux après-midi de travail, ainsi que Jean et Aurélien, pour les sorties en montagne.

Finalement j'aimerais remercier mes parents ainsi que ma sœur pour leur soutien tout au long de ma thèse et de mes études, pour leur écoute et leurs conseils face à mes nombreuses incertitudes, pour m'avoir toujours encouragé à suivre la voie qui m'intéressait, et pour avoir toujours été présents dans les moments difficiles. Cette thèse n'aurait jamais vu le jour sans eux, et je ne leur en serai jamais assez reconnaissant.

*Lausanne, Novembre 2020*

Samuel Gozel



# Abstract

In this thesis we study various one-dimensional quantum spin systems with  $SU(2)$  and  $SU(N)$  symmetry. We investigate the short-distance behavior of the  $SU(2)$  Heisenberg model in the limit of large spin and show that there exists an extended regime where perturbation theory, in the form of spin-wave theory, can be successfully applied. The reason for this perturbative regime stems from the asymptotic freedom of the nonlinear sigma model onto which the Heisenberg model can be mapped. When considering observables which respect the rotational invariance of the model, we observe a cancellation of infrared divergences in the perturbative expansions, leading to a meaningful description of correlation functions. We then turn to the study of  $SU(N)$  models. Building on the representation theory of the  $SU(N)$  group and on the matrix product state (MPS) formalism, we introduce a generic method to construct Affleck-Kennedy-Lieb-Tasaki (AKLT) models having edge states described by any self-conjugate irreducible representation (irrep) of  $SU(N)$ . A simple example is given by a spin-1 AKLT model having spin-1 edge states. The phase transition between this model and the original AKLT model is shown to be continuous and to correspond to a topological phase transition described by the  $SU(2)_1$  Wess-Zumino-Witten conformal field theory universality class. In addition we study an  $SU(3)$  AKLT model for the 3-box symmetric irrep at each site. We demonstrate that the edge states are adjoint edge irreps, we extract its correlation length and provide a useful construction as an optimal MPS. Finally, we develop a density matrix renormalization group algorithm based on standard Young tableaux and subduction coefficients to make full use of the non-abelian symmetry and to investigate the  $SU(3)$  Heisenberg model with 3-box symmetric irrep at each site. We show that the model has a finite gap above the singlet ground state, in agreement with an extension of the Haldane conjecture to  $SU(3)$  chains in the fully symmetric irreps. We also argue that there are five branches of elementary excitations living in four different irreps, each of which is gapped.

**Keywords:** condensed matter physics, one-dimensional quantum magnetism, Heisenberg model, nonlinear sigma model,  $SU(N)$  symmetry, Affleck-Kennedy-Lieb-Tasaki, Young diagram, standard Young tableau, Haldane's conjecture, density matrix renormalization group, spin-wave theory, asymptotic freedom.



# Résumé

Dans cette thèse, nous étudions différents modèles quantiques de spin avec symétrie  $SU(2)$  et  $SU(N)$ . Tout au long de ce travail nous nous concentrons sur le réseau unidimensionnel. Nous étudions le comportement à courte distance du modèle de Heisenberg  $SU(2)$  dans la limite de grand spin et démontrons qu'il existe un régime étendu où la théorie des perturbations, sous la forme de théorie des ondes de spin, peut être appliquée avec succès. Ce régime perturbatif trouve son origine dans la liberté asymptotique du modèle sigma non-linéaire qui décrit le comportement à basse énergie du modèle de Heisenberg. De plus, nous démontrons que les divergences infrarouges qui apparaissent généralement dans les calculs perturbatifs à une dimension se compensent exactement lorsque les observables considérées respectent la symétrie de rotation du modèle. En conséquence, les résultats obtenus pour les fonctions de corrélations fournissent une description précise du modèle à courte distance. Nous nous penchons ensuite sur l'étude des modèles  $SU(N)$ . Après avoir décrit en détails la théorie des représentations du groupe, nous présentons une méthode générique pour construire des modèles Affleck-Kennedy-Lieb-Tasaki (AKLT) ayant des états de bord décrits par une représentation irréductible auto-conjuguée arbitraire de  $SU(N)$ . Nous illustrons cette méthode avec la construction d'un modèle AKLT de spin-1 ayant des états de bord de spin-1. Nous étudions ensuite la transition de phase entre ce modèle et le modèle AKLT original ayant des états de bord de spin-1/2. Nous démontrons en particulier que la transition est continue et décrite par la classe d'universalité de la théorie conforme des champs Wess-Zumino-Witten  $SU(2)_1$ . Cette transition est, à notre connaissance, le premier exemple concret d'une transition de phase topologique dans les chaînes de spin. Nous présentons ensuite un modèle AKLT  $SU(3)$  pour la représentation irréductible à trois boîtes symétriques sur chaque site. Nous démontrons que les états de bord sont des représentations irréductibles adjointes, nous extrayons la longueur de corrélation de l'état fondamental et introduisons une construction optimale en termes d'état de produit de matrices. Finalement, nous développons un algorithme de renormalisation du groupe de la matrice densité basé sur les tableaux de Young standards ainsi que sur les coefficients de subduction. Cela nous permet d'implémenter la symétrie  $SU(3)$  dans l'algorithme afin d'étudier le modèle de Heisenberg  $SU(3)$  avec la représentation irréductible à trois boîtes symétriques sur chaque site. Nous démontrons que le spectre du modèle a un gap fini entre l'état fondamental singulet et le premier état excité, en accord avec une extension de la conjecture de Haldane aux

## Résumé

---

chaînes  $SU(3)$  dans les représentations irréductibles totalement symétriques. En nous aidant du modèle AKLT associé, nous argumentons sur la présence dans le spectre de cinq branches d'excitations élémentaires appartenant à quatre représentations irréductibles différentes et donnant lieu à quatre gaps de Haldane distincts.

**Mots-clés :** physique de la matière condensée, magnétisme quantique unidimensionnel, modèle de Heisenberg, modèle sigma non-linéaire, symétrie  $SU(N)$ , Affleck-Kennedy-Lieb-Tasaki, diagramme de Young, tableau de Young standard, conjecture de Haldane, groupe de renormalisation de la matrice densité, théorie des ondes de spin, liberté asymptotique.

# List of acronyms

Throughout this thesis, we will make use of the few following acronyms:

AKLT	Affleck-Kennedy-Lieb-Tasaki
CFT	conformal field theory
CGC	Clebsch-Gordan coefficient
DMRG	density matrix renormalization group
ED	exact diagonalization
HP	Holstein-Primakoff
IR	infrared
IRF	interaction-round-a-face
irrep	irreducible representation
LLOS	last letter order sequence
LSMA	Lieb-Schultz-Mattis-Affleck
MPS	matrix product state
NL $\sigma$ M	nonlinear sigma model
NLSWT	nonlinear spin-wave theory
OBC	open boundary conditions
PBC	periodic boundary conditions
QMC	quantum Monte Carlo
SDC	subduction coefficient
SPT	symmetry-protected topological
SWT	spin-wave theory
SYT	standard Young tableau
UV	ultraviolet
VBS	valence-bond solid
VUMPS	variational uniform matrix product state
WZW	Wess-Zumino-Witten



# Contents

<b>Remerciements</b>	<b>i</b>
<b>Abstract (English/Français)</b>	<b>iii</b>
<b>List of acronyms</b>	<b>vii</b>
<b>1 Introduction</b>	<b>1</b>
<b>2 Asymptotic freedom in the <math>SU(2)</math> Heisenberg chain</b>	<b>5</b>
2.1 Introduction . . . . .	6
2.1.1 Failure of perturbation theory and the Mermin-Wagner-Coleman theorem . . . . .	6
2.1.2 Mapping onto the $O(3)$ nonlinear sigma model . . . . .	8
2.1.3 Renormalization group analysis of the nonlinear sigma model . . . . .	9
2.1.4 Infrared finite perturbation theory in the $NL\sigma M$ . . . . .	12
2.2 Spin-wave theory . . . . .	12
2.2.1 Equal-time correlation function . . . . .	16
2.2.2 Dynamical structure factor . . . . .	18
2.2.3 Equal-time structure factor . . . . .	23
2.3 Conclusion . . . . .	24
<b>3 Elements of group theory</b>	<b>27</b>
3.1 The permutation group . . . . .	28
3.1.1 Group definition . . . . .	28
3.1.2 Representations . . . . .	29
3.1.3 Littlewood-Richardson rules . . . . .	31
3.1.4 Standard Young tableaux . . . . .	31
3.1.5 The Yamanouchi basis and the Young rules . . . . .	34
3.1.6 The non-standard basis and the subduction coefficients . . . . .	35
3.1.7 Calculation of SDCs – the multiplicity-free case . . . . .	37
3.1.8 Calculation of SDCs – the non-multiplicity-free case . . . . .	38
3.2 The Schur-Weyl duality . . . . .	41
3.3 The $\mathfrak{su}(N)$ Lie algebra . . . . .	43
3.3.1 Preliminary definitions . . . . .	43

## Contents

---

3.3.2	The $\mathfrak{su}(N)$ Lie algebra . . . . .	44
3.3.3	Irreducible representations . . . . .	47
3.3.4	The Itzykson-Nauenberg rules . . . . .	50
3.3.5	The Clebsch-Gordan coefficients . . . . .	52
3.3.6	The relationship to the Lie group $SU(N)$ . . . . .	53
<b>4</b>	<b><math>SU(N)</math> AKLT models</b>	<b>55</b>
4.1	Generic construction of $SU(N)$ AKLT models . . . . .	56
4.1.1	AKLT states . . . . .	56
4.1.2	Parent Hamiltonians . . . . .	58
4.2	$SU(2)$ AKLT model with spin-1 edge states . . . . .	62
4.2.1	Construction of the state . . . . .	62
4.2.2	Parent Hamiltonians . . . . .	63
4.2.3	Topological phase transition . . . . .	65
4.3	$SU(3)$ AKLT model with 3-box symmetric irrep . . . . .	66
4.3.1	Original formulation with fundamental irreps . . . . .	66
4.3.2	AKLT state with adjoint edge irreps . . . . .	69
4.3.3	Parent Hamiltonian . . . . .	69
4.3.4	Perspective on the $p$ -box symmetric irrep of $SU(3)$ . . . . .	70
4.4	Conclusion . . . . .	71
<b>5</b>	<b>The 3-box symmetric <math>SU(3)</math> chain</b>	<b>73</b>
5.1	Haldane's conjecture for symmetric $SU(3)$ chains . . . . .	76
5.1.1	Statement of the conjecture . . . . .	76
5.1.2	Hints from AKLT construction and Lieb-Schultz-Mattis-Affleck theorem . . . . .	76
5.1.3	Mapping onto a nonlinear sigma model . . . . .	77
5.2	The Hamiltonian as a sum of permutations . . . . .	79
5.3	Dealing with the edge states . . . . .	81
5.4	Density matrix renormalization group with $SU(3)$ symmetry . . . . .	83
5.4.1	Non-abelian symmetries in DMRG . . . . .	83
5.4.2	Description of the algorithm . . . . .	85
5.5	The $SU(3)$ AKLT model with 3-box symmetric irrep . . . . .	99
5.6	The $SU(3)$ Heisenberg model with 3-box symmetric irrep . . . . .	101
5.6.1	Haldane gaps . . . . .	101
5.6.2	Entanglement entropy . . . . .	104
5.6.3	Analysis of the spectrum . . . . .	105
5.7	Conclusion and outlook . . . . .	106
<b>6</b>	<b>Summary and outlook</b>	<b>109</b>
<b>A</b>	<b>Crossover scale of the <math>NL\sigma M</math></b>	<b>113</b>



<b>B</b>	<b>Equal-time correlation function from the Hellmann-Feynman theorem</b>	<b>117</b>
<b>C</b>	<b>Asymptotic form of the integrals <math>J_0(n)</math> and <math>J_1(n)</math></b>	<b>131</b>
<b>D</b>	<b>Calculations at finite temperature</b>	<b>137</b>
<b>E</b>	<b>Cancellation of divergences in the equal-time structure factor</b>	<b>151</b>
<b>F</b>	<b><math>\mathfrak{su}(3)</math> generators in the symmetric irreps</b>	<b>155</b>
<b>G</b>	<b>Example of calculation of subduction coefficients</b>	<b>161</b>
<b>H</b>	<b>Example of calculation of a reduced matrix element</b>	<b>167</b>
	<b>Bibliography</b>	<b>171</b>
	<b>List of publications</b>	<b>181</b>
	<b>Curriculum Vitae</b>	<b>183</b>



# 1 Introduction

The history of quantum spin models began in the late 1920's and early 1930's with the work of Heisenberg, Bloch and Bethe who studied ferromagnetism in rigid one-dimensional arrays of atoms with spin [1–3]. After nine decades of intense investigations, the Heisenberg model is still among the most prominent models in condensed matter research. The main reason for this great success is the ability of the model to actually describe accurately the low-energy behavior of a wide range of magnetic compounds. In its simplest form, the Heisenberg model is simply given as an isotropic interaction Hamiltonian between neighboring spins lying on a lattice. This interaction stems from the overlap of the electronic wave functions which tend to align, or anti-align, the dipole moments at each site. Alternatively the antiferromagnetic Heisenberg model can be derived as the effective Hamiltonian in the Mott insulating phase of the Hubbard model. This original isotropic form has been extended to more realistic and sometimes more exotic systems making the interaction anisotropic, adding further neighbor couplings or higher-order interactions, by putting the model in external fields, by varying the spin value at each site or, more recently, by changing the symmetry group defining the transformation laws of the local “spins”. All these modifications are motivated, to some extent, by experimental realizations. In particular, the Heisenberg model and its numerous variants can describe different phases of matter, and provide tools for understanding the relevant order parameters. Tackling analytically the Heisenberg model is, however, a challenging problem, and exact solutions are only known in very specific and limited cases, even on the simplest one-dimensional lattice. In this respect, the Bethe ansatz remains one of the most famous exact solution in condensed matter physics [3]. Perturbation theory, field theory methods and bosonization have proved to be extremely useful to tackle different aspects of the model. Besides these approximation methods it appeared necessary to obtain exact, or nearly exact results, and to actually compute numerical values for some quantities. The spin models thus nurtured the development of numerical methods such as exact diagonalization (ED) [4, 5], quantum Monte Carlo (QMC) [6–8], density matrix renormalization group (DMRG) [9–11] and, more generically, the tensor network based methods [12–14].

In this thesis, we study the Heisenberg model on the one-dimensional chain lattice. Throughout the thesis we focus on isotropic models where the interaction between spins respects the symmetry group under which these spins transform. The systems under investigation can thus be called  $SU(2)$  symmetric, or  $SU(N)$  symmetric, when the spin operators belong to irreducible representations (irreps) of the  $SU(2)$  or  $SU(N)$  groups, respectively<sup>1</sup>.

The  $SU(2)$  symmetry appears as the natural symmetry for electronic spins in metallic compounds. In particular, the  $SU(2)$  symmetric one-dimensional Heisenberg model is realized to very good approximation for several values of the spin  $S$ . For instance,  $\text{CuSO}_4 \cdot 5\text{D}_2\text{O}$  is, above the Néel temperature where a transition to a three-dimensional ordered state occurs, a very good realization of the isotropic spin-1/2 Heisenberg model [15].  $\text{Ni}(\text{C}_2\text{H}_8\text{N}_2)_2\text{NO}_2(\text{ClO}_4)$ , also known as NENP, has been used to investigate the Haldane spin-1 chain, in spite of a small crystal field splitting term [16–18]. Another spin-1 chain compound is given by  $\text{CsNiCl}_3$ , but the zero-temperature one-dimensional physics is inaccessible because of a relatively high Néel temperature [19–22]. The “large spin” chains also have their experimental realizations: spin-3/2 chains are realized by compounds such as  $\text{CsVCl}_3$ ,  $\text{CsVBr}_3$  or  $\text{AgCrP}_2\text{S}_6$  [20, 23–26], the spin-2 chains by  $\text{CsCrCl}_3$  and  $\text{MnCl}_3$  [27–29] and, finally, spin-5/2 chains are obtained with  $\text{Mn}^{2+}$  ions in  $\text{SrMn}_2\text{V}_2\text{O}_8$  [30]. The experimental investigation of the spin- $S$  quasi one-dimensional Heisenberg model became of major importance after Haldane conjectured that integer spin chains have a gap while half-odd integer spin chains are gapless [31, 32].

Conversely, the  $SU(N)$  symmetry does not exist as a stable symmetry in condensed matter systems. It can appear, however, as an emergent symmetry in  $SU(2)$  spin models. For instance it is well-known that the one-dimensional bilinear-biquadratic spin-1 chain has a high-symmetry  $SU(3)$  point at equal bilinear and biquadratic couplings, the so-called Uimin-Lai-Sutherland point [33–36]. Similarly, the Kugel-Khomskii model, which describes the interaction of spin and orbital pseudo-spin operators, can be rewritten as a simple  $SU(4)$  Hamiltonian for the fundamental representation [37, 38]. The material  $\alpha\text{-ZrCl}_3$  has recently been proposed to be a candidate realization for this emergent  $SU(4)$  symmetry thanks to its strong spin-orbit coupling [39]. In fact, the realization of  $SU(N)$  spin models now relies mostly on the manipulation of ultracold atomic gases loaded in optical lattices [40–51]. Indeed when loaded in such lattices, fermionic alkaline-earth atoms such as  $^{173}\text{Yt}$  or  $^{87}\text{Sr}$  can realize Mott insulating phases of the  $SU(N)$  Hubbard model, whose low-energy physics is governed by the  $SU(N)$  Heisenberg model. The emergence of the  $SU(N)$  symmetry with  $N$  up to 10 originates from the decoupling of the nuclear spin  $I$  from the electronic angular momentum [43]. At  $1/N$  filling the atomic gas in the Mott insulating phase realizes the  $SU(N)$  Heisenberg model with  $N \leq 2I + 1$  for the fundamental irrep at each site. By using two-orbital

---

<sup>1</sup>In this thesis, by  $SU(N)$  we mean  $SU(N > 2)$ .

---

fermions, namely by exploiting the metastable  $^3P_0$  excited state of the atom it is possible to implement irreps described by a Young diagram with up to two columns. More complicated irreps, such as symmetric irreps described by a Young diagram made of a single row and more than two boxes should be under experimental reach by using the method applied for generating  $SU(2)$  spin- $S$  degrees of freedom out of spin-1/2 atoms loaded in different orbitals of the same optical well [52].

The  $SU(N)$  models offer a rich playground for exotic physics ranging from quantum spin liquids, Bose-Einstein condensation and superfluidity to symmetry-protected topological (SPT) phases. Moreover, the versatility of the optical lattices makes it possible to study the models in different geometrical configurations and, in particular, in the one-dimensional geometry. This prospect has motivated a recent quest for extending Haldane's conjecture to  $SU(N)$  chains, namely to discriminate between the models – or, more precisely, the irreps – exhibiting gapless excitations from the ones where a finite gap opens in the spectrum. The route followed to develop such conjectures is essentially an adaptation of the work of Haldane for the  $SU(2)$  Heisenberg chain. From a general perspective, the study of the one-dimensional  $SU(N)$  Heisenberg model simply consists in adapting the techniques which worked for  $SU(2)$  to the  $SU(N)$  case. This adaptation is, however, full of pitfalls. Numerically, the investigation of the  $SU(N)$  models is complicated by the large local Hilbert space dimension carried by  $SU(N)$  irreps. Moreover QMC is affected by the sign problem for  $N > 2$  as soon as the number of boxes in the Young diagram is larger than one. The DMRG, which was originally specifically designed for one-dimensional systems, is the most promising method to tackle  $SU(N)$  spin chains.

The thesis is organized in two independent parts. In the first part, Chapter 2, we revisit the  $SU(2)$  Heisenberg model in the limit of large spin. Because of the Mermin-Wagner-Coleman theorem, it is well-accepted that perturbation theory is useless in one-dimensional spin systems with a continuous symmetry [53, 54]. We demonstrate that the situation is less dramatic, and that meaningful results can actually be obtained with perturbation theory, here in the form of spin-wave theory (SWT), in spite of the absence of Goldstone bosons in one dimension. In a second part, Chapters 3-5, we turn to the study of  $SU(N)$  models. In Chapter 3 we introduce a number of notions related to the  $SU(N)$  group by building on its relationship with the permutation (or symmetric) group  $\mathcal{S}_n$ . This chapter simply aims at providing all tools required to fully grasp the developments of the next two chapters, in particular Young diagrams, standard Young tableaux (SYTs) and subduction coefficients (SDCs). In Chapter 4 we present a generic way to construct  $SU(N)$  Affleck-Kennedy-Lieb-Tasaki (AKLT) models using Young diagrams and the matrix product state (MPS) formalism. The construction being absolutely general, we illustrate it with an  $SU(2)$  example: a spin-1 AKLT state having spin-1 edge states. In view of Chapter 5 we also present in details an  $SU(3)$  AKLT model for the 3-box symmetric irrep at each site. Chapter 5 is devoted to the development of a DMRG algorithm making full use of the  $SU(3)$  symmetry

## Chapter 1. Introduction

---

to investigate the 3-box symmetric Heisenberg model, with the aim of confirming Haldane's conjecture stating that the  $p$ -box symmetric  $SU(3)$  chain is gapped when  $p$  is a multiple of three. Given the heterogeneity of the thesis, we begin and close each chapter with a specific introduction and conclusion. Finally, in Chapter 6 we summarize our results and bridge the two parts of the thesis. We also give an outlook oriented towards the rapidly evolving field of  $SU(N)$  physics.

The material presented in this thesis has been, to a large extent, published in the three following articles:

Chapter 2	Ref. [55]
Chapter 4	Ref. [56]
Chapter 5	Ref. [57]

## 2 Asymptotic freedom in the $SU(2)$ Heisenberg chain

The Haldane conjecture put forward by Haldane in 1983 was a revolution for the understanding of the one-dimensional  $SU(2)$  Heisenberg model [31, 32]. According to Haldane, the long-distance (or low-energy) behavior of the model is different for integer and half-odd integer spin: when the spin is an integer, the spectrum is gapped with exponentially decaying correlation functions, but when the spin is half-odd integer, the spectrum is gapless with power-law decay of correlations. Since Bethe's calculation on the spin-1/2 Heisenberg model and the calculation of the dispersion relation by des Cloizeaux and Pearson, it was well known that the spin-1/2 Heisenberg model is gapless [3, 58], and it was generally and erroneously thought that the gapless spectrum would occur for any value of the spin. Through the mapping of the spin chain onto a field theory, the  $O(3)$  nonlinear sigma model ( $NL\sigma M$ ) with a topological term, Haldane argued that the value of the topological angle governs the structure of the spectrum. In fact, while the gapped spectrum of the  $NL\sigma M$  with vanishing topological angle was known thanks to the work of the Zamolodchikov brothers [59], it was not known if the  $NL\sigma M$  with a topological term was gapped or gapless. The spin-1/2 chain allowed Haldane to guess the result, which was finally proven nine years later [60].

The approach followed by Haldane to understand the low-energy physics of the Heisenberg model came as a way out from the dead-end in which the community had been stuck for several decades. Indeed, perturbation theory, the most common and widely used method of quantum mechanics, is plagued with infrared (IR) divergences. This is a consequence of the Mermin-Wagner-Coleman theorem, which forbids the breaking of continuous symmetries in one-dimensional spin systems, or equivalently in  $(1+1)$ -dimensional quantum field theories [53, 54]. Any perturbative treatment of the isotropic Heisenberg model falls under the scope of the theorem: the classical ground state being the Néel state, quantum fluctuations should be introduced around this symmetry-breaking state. This is however forbidden, and the manifestation of this illegal explicit breaking of the rotation symmetry appears under the form of IR divergences in the calculation of observables of interest.

A natural question arises in this situation: in light of Haldane's conjecture and mapping onto the  $NL\sigma M$  to describe the physics of the Heisenberg chain, does the Mermin-Wagner-Coleman theorem completely rule out the possible use of perturbation theory? In fact, as we will see in this chapter, there is something more to learn from perturbation theory. We will show that perturbation theory can be reliably used in the one-dimensional Heisenberg model, provided that we use it to answer a different question than “what is the long-distance behavior of the spin chain?”, and provided we adopt a way of restoring the broken continuous symmetry. The developments rely on a major property of the  $NL\sigma M$ : it is asymptotically free [61–63]. Asymptotic freedom is a concept more widespread in high-energy physics as it describes the weak interaction of quarks at short distances. Here, we shall use the asymptotic freedom of the  $NL\sigma M$  to motivate the use of perturbation theory, and to show that the perturbative regime is actually relevant to experiments.

The chapter is organized as follows. In Section 2.1 we illustrate the consequences of the Mermin-Wagner-Coleman theorem on perturbative expansions in the spin chain through a textbook example. We then present Haldane's mapping of the Heisenberg chain onto the  $NL\sigma M$  and show that the model is asymptotically free by presenting its renormalization group analysis. We further present Elitzur's conjecture that rotationally invariant quantities are IR finite in perturbation theory. We then turn to the actual perturbative treatment of the spin chain in Section 2.2. We derive equal-time (or instantaneous) and dynamical correlation functions using SWT. Finally, Section 2.3 contains a summary and an outlook of this chapter.

At this point one should mention that the dynamical structure factor was computed to first order in perturbation theory by Takahashi using the modified SWT in Refs. [64, 65]. However neither the validity regime of the expressions was discussed, nor the equal-time correlation functions and the cancellation of infrared divergences. The content of the present chapter thus goes beyond Takahashi's derivation, in particular by understanding the consequences of asymptotic freedom on the spin chain.

## 2.1 Introduction

### 2.1.1 Failure of perturbation theory and the Mermin-Wagner-Coleman theorem

The Hamiltonian of the one-dimensional antiferromagnetic Heisenberg model with spin  $S$  is given by

$$\mathcal{H} = J \sum_i \mathbf{S}_i \cdot \mathbf{S}_{i+1} \quad (2.1)$$

where the coupling constant  $J > 0$  and where the spin operators  $\mathbf{S} = (S^x, S^y, S^z)^T$  are the generators of the  $\mathfrak{su}(2)$  Lie algebra in the spin- $S$  representation satisfying



$S^2 = S(S + 1)$ . The classical ground state of Hamiltonian (2.1) is the Néel state where nearest neighbor spins lie anti-parallel to each others. A perturbative treatment of the quantum model consists in introducing small fluctuations around the classical ground state. The Holstein-Primakoff (HP) transformation is a convenient way of introducing such fluctuations with the use of bosonic operators, which generate the so-called “spin-waves” [66]. We will go through this derivation in details in Section 2.2. Here, let us simply illustrate what happens when computing, for instance, the staggered magnetization. Choosing the  $z$ -axis as the quantization axis on which fluctuations are introduced, one has  $S_i^z = S - a_i^\dagger a_i$  for site  $i$  in the  $A$  sublattice and  $S_i^z = -S + a_i^\dagger a_i$  for site  $i$  in the  $B$  sublattice, where  $a_i^\dagger$  ( $a_i$ ) is a creation (annihilation) operator of a HP boson at site  $i$ , and where we assume the total number of bosons  $a_i^\dagger a_i \leq 2S$ . The staggered magnetization reads

$$m_{\text{stagg}} = \frac{1}{N_s} \left( \sum_{i \in A} \langle S_i^z \rangle - \sum_{i \in B} \langle S_i^z \rangle \right) \quad (2.2)$$

where  $N_s$  is the number of sites. One obtains

$$m_{\text{stagg}} = S - \frac{1}{N_s} \sum_i \langle a_i^\dagger a_i \rangle. \quad (2.3)$$

And here is the “catastrophe” [61]: the second term in Eq. (2.3) is positive and IR divergent. The staggered magnetization obtained with this calculation is thus negative infinity.

This textbook example shows the manifestation of the Mermin-Wagner-Coleman theorem. The rotation symmetry of the spin chain was explicitly broken in the perturbative approach, since we selected the Néel state as the unperturbed ground state on which quantum fluctuations are introduced. As a result of this forbidden symmetry breaking, which is artificial and does not actually happen in the spin chain, an IR divergence occurs in the first order correction to the staggered magnetization<sup>1</sup>. Going beyond the fact that the continuous symmetry of the spin chain was broken from the very beginning, one can interpret the divergence of the staggered magnetization as an indication of the absence of long-range order. Indeed, in the HP transformation, we assumed that the number of bosons is small, namely that the ground state is mainly described by the Néel state. But from the calculation,  $\langle a_i^\dagger a_i \rangle$  is actually IR divergent, contradicting the initial assumption.

---

<sup>1</sup>The zeroth order is just the classical approximation.

### 2.1.2 Mapping onto the $O(3)$ nonlinear sigma model

Haldane showed that the spin chain Hamiltonian (2.1) can be mapped, in the limit of large spin  $S$ , onto the  $O(3)$  NL $\sigma$ M with lagrangian density [31, 32]

$$\mathcal{L} = \frac{v}{2g} \left( \frac{1}{v^2} (\partial_t \phi)^2 - (\partial_x \phi)^2 \right) + \frac{\theta}{8\pi} \epsilon^{\mu\nu} \phi \cdot (\partial_\mu \phi \times \partial_\nu \phi) \quad (2.4)$$

where the different parameters take the values<sup>2</sup>

$$g = \frac{2}{S}, \quad v = 2JS, \quad \theta = 2\pi S \quad (2.5)$$

and where  $\phi$  is an  $O(3)$  vector satisfying

$$\phi^2 = 1. \quad (2.6)$$

This constraint makes the first part of the lagrangian density (2.4) interacting, although at first sight it looks like three independent scalar fields. The second term in Eq. (2.4) is topological as it can be rewritten as a total derivative. In fact, after Wick rotation to Euclidean space one has [67]

$$S_{\text{top}} = \int d^2x \mathcal{L}_{\text{top}} = i\theta \mathcal{Q} \quad (2.7)$$

where  $\mathcal{Q}$  is the Pontryagin index

$$\mathcal{Q} = \int d^2x \epsilon^{jk} \phi \cdot (\partial_j \phi \times \partial_k \phi) \in \mathbb{Z}. \quad (2.8)$$

The fact that  $\mathcal{L}_{\text{top}}$  is a total derivative can alternatively be demonstrated by showing that the variation of  $S_{\text{top}}$  vanishes under an infinitesimal transformation of the field  $\phi$ . As such, the topological term has no effect in perturbation theory. The conclusions drawn by Haldane, however, are non-perturbative by essence. When the spin  $S$  is integer, the topological angle is an integer multiple of  $2\pi$  and the topological action is thus trivial. Since the NL $\sigma$ M (2.4) has a massive one-magnon branch [59], the rotation symmetry is preserved and Haldane argued that the integer spin- $S$  Heisenberg chain is gapped<sup>3</sup>. For half-odd integer spin  $S$ , the topological angle  $\theta = \pi$  and, being aware of the gapless spectrum of the spin-1/2 Heisenberg chain, Haldane conjectured a gapless spectrum of the NL $\sigma$ M in this case. As a consequence, he assumed that the mapping of the spin chain onto the NL $\sigma$ M was not only valid for large spin, but extended up to the most quantum case of spin-1/2.

Let us now shortly discuss how the mapping can be obtained. A simple and intuitive

---

<sup>2</sup>The lattice spacing of the spin chain is set to unity throughout this thesis.

<sup>3</sup>“There are no Goldstone bosons in two dimensions” [54]. The continuous (rotation) symmetry is preserved, or restored, by quantum fluctuations.

route is to decompose the spin operators into slowly varying fields which describe the low-energy modes. These low-energy modes appear, in SWT, close to momentum 0 and  $\pi$ . We thus write [68]

$$\mathbf{S}_i \approx (-1)^i S \phi + \mathbf{l} \quad (2.9)$$

where  $\phi$  is the staggered magnetization field and  $\mathbf{l}$  is the conserved spin density and can be obtained as

$$\mathbf{l} = \frac{1}{vg} \phi \times \partial_t \phi. \quad (2.10)$$

As a consequence, the field  $\mathbf{l}$  remains always orthogonal to the order parameter  $\phi$ . Actually, a more accurate transformation is defined on two neighboring sites with [69]

$$\frac{\phi(2i + \frac{1}{2})}{\sqrt{1 + \frac{l^2(2i + \frac{1}{2})}{S(S+1)}}} = \frac{\mathbf{S}_{2i} - \mathbf{S}_{2i+1}}{2\sqrt{S(S+1)}} \quad (2.11)$$

and

$$\frac{\mathbf{l}(2i + \frac{1}{2})}{\sqrt{1 + \frac{l^2(2i + \frac{1}{2})}{S(S+1)}}} = \frac{\mathbf{S}_{2i} + \mathbf{S}_{2i+1}}{2}. \quad (2.12)$$

These transformations have the advantage to implement correctly the constraint  $\mathbf{S}_i^2 = S(S+1)$ . Inserting these expressions into the Heisenberg Hamiltonian (2.1) and performing a Legendre transform one obtains the lagrangian density of the NL $\sigma$ M in Eq. (2.4).

Alternatively one can use a spin-coherent state path integral [67, 70]. The spin coherent states  $|n\rangle$  satisfy

$$\langle n | \mathbf{S} | n \rangle = S \mathbf{n} \quad (2.13)$$

and can be explicitly expressed in terms of Schwinger bosons. The field  $\mathbf{n}$  is then decomposed as a sum of the order parameter  $\phi$  and  $\mathbf{l}$ . Integrating out the field  $\mathbf{l}$  one ends up with the action of the NL $\sigma$ M.

### 2.1.3 Renormalization group analysis of the nonlinear sigma model

The renormalization group analysis of the O(3) NL $\sigma$ M is due to Polyakov [61] who made use of Wilson's renormalization group method [71] to get the leading order term. At two-loop the  $\beta$ -function reads [61, 72]

$$\beta(g) = \frac{1}{2\pi} g^2 + \frac{1}{(2\pi)^2} g^3 + \mathcal{O}(g^4) \quad (2.14)$$

where

$$\frac{dg}{d \ln L} = \beta(g). \quad (2.15)$$

## Chapter 2. Asymptotic freedom in the $SU(2)$ Heisenberg chain

---

The positive sign in the  $\beta$ -function shows that the coupling constant  $g$  of the model flows to large values at large length scales. In other words, the model is strongly interacting at low energy and weakly interacting at short distance. This behavior, known as asymptotic freedom, is also observed in quantum chromodynamics where quarks confine at low energy but appear as nearly free particles at short distance [62, 63].

The crossover length scale  $\xi$  from the weakly interacting to the strongly interacting regime can be obtained from the  $\beta$ -function of the model [32]. Denoting by  $g_0$  the bare coupling constant,  $g_1 = \mathcal{O}(1)$  the coupling constant at scale  $\xi$  and integrating the renormalization group equation (2.15) one has

$$\ln \xi = \int_{g_0}^{g_1} \frac{dg}{\beta(g)}. \quad (2.16)$$

Using the  $\beta$ -function in Eq. (2.14) one obtains

$$\xi \propto g_0 e^{2\pi/g_0} (1 + \mathcal{O}(g_0)). \quad (2.17)$$

The proportionality factor is determined by the value of  $g_1$  and is a priori not known. An expression containing the first few higher order terms is computed in Appendix A based on the 4-loop  $\beta$ -function [73] of the  $NL\sigma M$ . Equation (2.17), however, contains the important information. Taking  $g_0 = 2/S$  as the bare coupling one gets

$$\xi \propto \frac{1}{S} e^{\pi S} (1 + \mathcal{O}(S^{-1})). \quad (2.18)$$

The crossover length scale  $\xi$  increases exponentially fast with the spin of the spin chain. The corresponding energy scale  $\Delta = v/\xi$  reads

$$\Delta \propto JS^2 e^{-\pi S} (1 + \mathcal{O}(S^{-1})). \quad (2.19)$$

In the Heisenberg spin chain, the crossover length scale  $\xi$  and energy scale  $\Delta$  correspond to the correlation length and the gap, respectively, of the model when the spin is integer. Exponential decay of correlations, namely the signature of the strong coupling regime of the spin chain, is only observed at length scales far larger than  $\xi$ , or equivalently at energy scale far below  $\Delta$ . Showing the existence of a finite gap in the integer spin chain for a large value of the spin is thus a challenging way of confirming Haldane's conjecture [8, 74, 75].

Despite the absence of a gap and correlation length when the spin is half-odd integer, the length scale  $\xi$  and energy scale  $\Delta$  are still well-defined quantities. They are the characteristic crossover length scale and energy scale which define the transition from the weak coupling regime to the strong coupling regime.

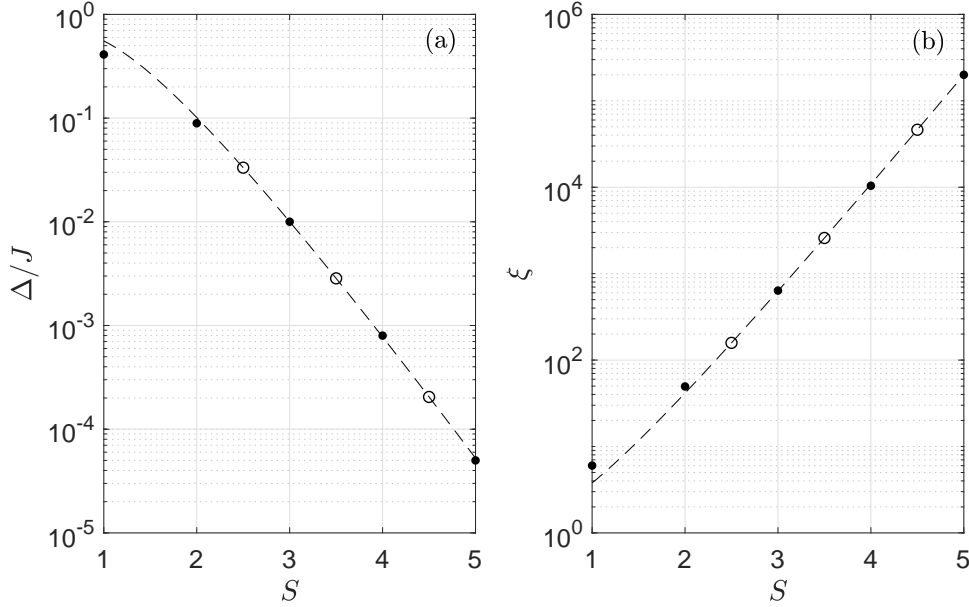


Figure 2.1: Crossover (a) energy scale  $\Delta$  and (b) length scale  $\xi$  versus spin  $S$  and fit to the scaling formulas derived in Appendix A. The fits are rather poor for small values of the spin but the exponential scaling is already observed beyond  $S = 2$ . Values for integer spin are taken from Refs. [8, 74–76] and are denoted by filled circles. The values for half-odd integer spin  $S \geq 5/2$  are extracted from the fit and are denoted by empty circles.

The large-distance, low-energy, behavior of the spin chain is thus governed by the strong coupling regime of the  $NL\sigma M$ , where the topological term plays a crucial role, and determines the exact scaling of correlation functions: exponential decay for integer spin and power-law decay for half-odd integer spin. At short distance, or high energy, however, the spin chain is in the weak coupling regime. Integer and half-odd integer spin chains are thus expected to have a universal behavior described by this weak-coupling regime. If there is a way to obtain meaningful results with perturbation theory in the weak coupling regime then these results would describe the Heisenberg chain for any value of the spin. Now recall that the crossover length scale  $\xi$  becomes very large with increasing spin. For  $S = 2$  it is  $\xi \simeq 49$  while for  $S = 3$  it is  $\xi \simeq 637$  [8]. Thus for  $S$  large enough, there is a large window of distances where the spin chain is in the weak coupling regime. By contrast, for small values of the spin the crossover length scale  $\xi$  is very short and the weak coupling regime is too narrow to have a chance to be observed. Figure 2.1 summarizes the numerical values of the crossover length scale and energy scale of the Heisenberg chain together with the scaling formulas found in Appendix A.

### 2.1.4 Infrared finite perturbation theory in the $NL\sigma M$

Although the weak coupling regime of the  $NL\sigma M$  extends to very small energies according to Eq. (2.19), it sounds a priori unfeasible to actually perform perturbative calculations in this regime because of the Mermin-Wagner-Coleman theorem. The solution, conjectured by Elitzur and rigorously proved by David, is to focus on  $O(3)$  invariant quantities [77, 78]. This is actually a natural way to proceed! From the Mermin-Wagner-Coleman theorem one knows that the ground state wave function respects the rotation symmetry of the Hamiltonian. Any expectation value of a non-rotational invariant quantity will vanish in the ground state, and only the symmetry-preserving observables are relevant. Elitzur's conjecture can be stated as follows<sup>4</sup>:

*In the  $O(3)$   $NL\sigma M$  the vacuum expectation value of any  $O(3)$  invariant observable is IR finite to any order in perturbation theory.*

The conjecture was built based on the IR finiteness of the two and four-point functions up to third and second order, respectively [77].

Given the mapping from the spin chain onto the  $NL\sigma M$ , the IR finiteness of rotationally-invariant quantities in the field theory and the extended perturbative regime for spin large enough and governed by asymptotic freedom, it is natural to ask whether perturbative expansions can be performed, using SWT, in the Heisenberg model directly and if meaningful expressions for the short distance behavior of the spin chain can be extracted. Adapting the perturbative expansions obtained by Elitzur in the  $NL\sigma M$  allows us to get good insight into the behavior of the spin chain, but the procedure fails at extracting accurately the physics at very short distance. This is due to the fact that the  $NL\sigma M$  needs to be regularized in the ultraviolet (UV). By contrast, the details of the lattice are implemented in SWT and the UV cutoff is thus incorporated naturally in the method. In the next sections we perform a second order analysis of the equal-time and dynamical correlation functions at zero and finite temperature using SWT and show that the relevant quantities are IR finite in the perturbative regime set up by asymptotic freedom.

## 2.2 Spin-wave theory

The material presented in this section has been exposed in great details in Ref. [55]. Here we follow closely this article, sometimes adapting the notations for more uniformity throughout the thesis. Additionally we present an alternative method to derive the equal-time correlation function from the ground state energy of a modified Hamiltonian.

---

<sup>4</sup>The conjecture actually applies to the  $O(n)$   $NL\sigma M$  where the order parameter  $\phi$  is an  $n$ -dimensional unit vector [77].

To perform perturbative expansions using SWT we first rewrite the Hamiltonian, using the HP transformation, in terms of bosonic operators – the HP bosons. To simplify the procedure we first operate a rotation of  $\pi$  along the  $x$  axis for all spins living on the  $B$  sublattice. Denoting by  $\tilde{\mathbf{S}}_i$  the rotated spins, with  $\tilde{\mathbf{S}}_i = \mathbf{S}_i$ ,  $i \in A$  for the spins of the  $A$  sublattice, the HP transformation reads

$$\tilde{S}_i^+ = \sqrt{2S} f_i(S) a_i, \quad (2.20)$$

$$\tilde{S}_i^- = \sqrt{2S} a_i^\dagger f_i(S), \quad (2.21)$$

$$\tilde{S}_i^z = S - a_i^\dagger a_i, \quad (2.22)$$

where

$$f_i(S) = \sqrt{1 - \frac{a_i^\dagger a_i}{2S}} \quad (2.23)$$

and where the bosonic operators  $a_i, a_i^\dagger$  satisfy

$$[a_i, a_j^\dagger] = \delta_{ij}. \quad (2.24)$$

Making the assumption of small fluctuations around the ordered Néel ground state  $f_i(S)$  can be expanded in powers of  $1/S$ . To first order we have

$$f_i(S) = 1 - \frac{a_i^\dagger a_i}{4S} + \mathcal{O}(S^{-2}). \quad (2.25)$$

Hamiltonian (2.1) then becomes

$$\mathcal{H} = \mathcal{H}^{(0)} + \mathcal{H}^{(2)} + \mathcal{V} \quad (2.26)$$

where

$$\mathcal{H}^{(0)} = -JN_s S^2 \quad (2.27)$$

is the classical ground state energy,  $\mathcal{H}^{(2)}$  is quadratic in bosonic operators

$$\mathcal{H}^{(2)} = JS \sum_{\langle ij \rangle} \left( a_i^\dagger a_i + a_j^\dagger a_j + a_i a_j + a_i^\dagger a_j^\dagger \right) \quad (2.28)$$

where  $\langle ij \rangle$  denotes nearest neighbor pairs of sites, while  $\mathcal{V}$  contains all interacting terms which are suppressed by higher orders in  $1/S$

$$\mathcal{V} = \mathcal{H}^{(4)} + \mathcal{H}^{(6)} + \dots \quad (2.29)$$

with  $\mathcal{H}^{(2k)}$  an interaction which contains  $2k$  bosonic operators and which is  $\mathcal{O}(S^{2-k})$ .

## Chapter 2. Asymptotic freedom in the $SU(2)$ Heisenberg chain

---

In particular, the first order interaction  $\mathcal{H}^{(4)} = \mathcal{O}(S^0)$  is given by

$$\mathcal{H}^{(4)} = -\frac{J}{2} \sum_{\langle ij \rangle} \left( a_i^\dagger a_i a_j + \text{h.c.} \right) - J \sum_{\langle ij \rangle} a_i^\dagger a_j^\dagger a_i a_j. \quad (2.30)$$

In what follows we neglect all higher order terms in  $1/S$ , namely we approximate

$$\mathcal{H} = \mathcal{H}^{(0)} + \mathcal{H}^{(2)} + \mathcal{H}^{(4)} + \mathcal{O}(S^{-1}) \simeq \mathcal{H}^{(0)} + \mathcal{H}^{(2)} + \mathcal{H}^{(4)}. \quad (2.31)$$

We thus treat the model to first order in nonlinear SWT (NLSWT).

The quadratic Hamiltonian  $\mathcal{H}^{(2)}$  can be diagonalized with Fourier and Bogoliubov transformations. The Fourier transformed HP bosons are given by

$$a_k = \frac{1}{\sqrt{N_s}} \sum_j e^{-ikr_j} a_j, \quad a_k^\dagger = \frac{1}{\sqrt{N_s}} \sum_j e^{ikr_j} a_j^\dagger \quad (2.32)$$

where  $r_j = j$  is the position of the  $j$ -th spin. After Fourier transformation the Hamiltonian reads

$$\mathcal{H}^{(2)} = \sum_k \left[ A_k a_k^\dagger a_k - \frac{1}{2} B_k \left( a_k^\dagger a_{-k}^\dagger + a_k a_{-k} \right) \right] \quad (2.33)$$

where

$$A_k = 2JS, \quad B_k = -2JS\gamma_k, \quad \gamma_k = \cos k \quad (2.34)$$

and

$$\begin{aligned} \mathcal{H}^{(4)} = \frac{1}{N_s} \sum_{k_1, k_2, k_3} \Xi_1(k_1) & \left( a_{k_1+k_2+k_3}^\dagger a_{k_1} a_{k_2} a_{k_3} + \text{h.c.} \right) \\ & + \frac{1}{N_s} \sum_{k_1, k_2, k_3} \Xi_2(k_1, k_3) a_{k_1}^\dagger a_{k_2}^\dagger a_{k_3} a_{k_1+k_2-k_3} \end{aligned} \quad (2.35)$$

with

$$\Xi_1(k_1) = -\frac{J}{2} \gamma_{k_1}, \quad \Xi_2(k_1, k_3) = -J\gamma_{k_1-k_3}. \quad (2.36)$$

Performing the Bogoliubov transformation

$$\begin{pmatrix} \alpha_k \\ \alpha_{-k}^\dagger \end{pmatrix} = \begin{pmatrix} u_k & v_k \\ v_k & u_k \end{pmatrix} \begin{pmatrix} a_k \\ a_{-k}^\dagger \end{pmatrix} \quad (2.37)$$

with coefficients  $u_k$  and  $v_k$  even functions of momentum  $k$  satisfying

$$u_k^2 - v_k^2 = 1 \quad (2.38)$$

in order to ensure the commutation relations of the Bogoliubov bosons  $[\alpha_k, \alpha_{k'}^\dagger] = \delta_{k,k'}$



one obtains

$$\mathcal{H}^{(2)} = \delta\mathcal{E}^{(2)} + \sum_k \epsilon_k \alpha_k^\dagger \alpha_k \quad (2.39)$$

where

$$\delta\mathcal{E}^{(2)} = -JN_s S + \frac{1}{2} \sum_k \epsilon_k \quad (2.40)$$

is the first order correction to the ground state energy and where

$$\epsilon_k = \sqrt{A_k^2 - B_k^2} = 2JS|\sin k| \quad (2.41)$$

is the linear SWT dispersion relation. The functions  $u_k$  and  $v_k$  read

$$u_k = \sqrt{\frac{A_k + \epsilon_k}{2\epsilon_k}}, \quad v_k = -\text{sign}(B_k) \sqrt{\frac{A_k - \epsilon_k}{2\epsilon_k}}. \quad (2.42)$$

To compute the first order correction to the dispersion relation one needs to rewrite the first order interaction  $\mathcal{H}^{(4)}$  in the Bogoliubov basis. First let us define the two following expectation values taken in the free theory

$$\Delta = \langle a_i a_j \rangle = -\frac{1}{N_s} \sum_k \gamma_k u_k v_k, \quad (2.43)$$

$$n = \langle a_i^\dagger a_i \rangle = \frac{1}{N_s} \sum_k v_k^2. \quad (2.44)$$

One sees that both  $\Delta$  (not to be confused with the gap) and  $n$  have IR divergences. When computing the corrections to the ground state energy and to the dispersion relation to first order, however,  $\Delta$  and  $n$  will always appear together as an IR finite combination

$$\kappa = \Delta + n = \frac{1}{N_s} \sum_k v_k (v_k - \gamma_k u_k) = \frac{1}{N_s} \sum_k \frac{|\sin k| - 1}{2} = \frac{1}{\pi} - \frac{1}{2} \quad (2.45)$$

where, in the last equality, we have taken the continuum limit to compute the sum.

Using Wick's theorem to decouple the interaction terms, the first order interaction  $\mathcal{H}^{(4)}$  then reads

$$\mathcal{H}^{(4)} = \delta\mathcal{E}^{(4)} + \sum_k \delta\mathcal{E}_k^{(4)} \alpha_k^\dagger \alpha_k + : (4\text{-bosons}) : \quad (2.46)$$

where

$$\delta\mathcal{E}^{(4)} = -JN_s \kappa^2 \quad (2.47)$$

is the correction to the ground state energy,

$$\delta\mathcal{E}_k^{(4)} = -2J\kappa \left[ (u_k^2 + v_k^2) - 2\gamma_k u_k v_k \right] = 2J|\kappa \sin k| \quad (2.48)$$

renormalizes the dispersion relation and  $:$  (4-bosons)  $:$  denotes all normal-ordered terms made of four Bogoliubov operators. Luckily, their exact expressions will not be needed, as we will show below. The NLSWT dispersion relation is thus given by

$$\mathcal{E}_k = \epsilon_k + \delta\mathcal{E}_k^{(4)} + \mathcal{O}(S^{-1}) \simeq 2JS \left(1 + \frac{|\kappa|}{S}\right) |\sin k|. \quad (2.49)$$

Two observations are in order. First we have encountered the first occurrences of cancellations of IR divergences as we computed the expectation value of the Hamiltonian and the spectrum of spin-waves. Secondly, in Eq. (2.46) there are no anomalous terms with two creation or two annihilation operators.

### 2.2.1 Equal-time correlation function

The equal-time (or instantaneous) spin-spin correlation function is defined by

$$C_{ij} = \frac{\langle \Psi_0 | \mathbf{S}_i \cdot \mathbf{S}_j | \Psi_0 \rangle}{\langle \Psi_0 | \Psi_0 \rangle} \quad (2.50)$$

where the expectation value is taken in the exact ground state  $|\Psi_0\rangle$ . Both this wave function and the operator  $\mathbf{S}_i \cdot \mathbf{S}_j$  can be expanded in powers of  $1/S$ . We thus write [55]

$$\mathcal{O}_{ij} = \mathbf{S}_i \cdot \mathbf{S}_j = S^2 \left( \mathcal{O}_{ij}^{(0)} + \frac{1}{S} \mathcal{O}_{ij}^{(1)} + \frac{1}{S^2} \mathcal{O}_{ij}^{(2)} + \mathcal{O}(S^{-3}) \right). \quad (2.51)$$

Using the HP transformation we obtain  $\mathcal{O}_{ij}^{(0)} = (-1)^{i-j}$ ,

$$\mathcal{O}_{ij}^{(1)} = \begin{cases} a_i^\dagger a_j + a_i a_j^\dagger - a_i^\dagger a_i - a_j^\dagger a_j & \text{for } i - j \text{ even} \\ a_i^\dagger a_j^\dagger + a_i a_j + a_i^\dagger a_i + a_j^\dagger a_j & \text{for } i - j \text{ odd,} \end{cases} \quad (2.52)$$

and

$$\mathcal{O}_{ij}^{(2)} = \begin{cases} a_i^\dagger a_i a_j^\dagger a_j - \frac{1}{4} \left( a_i a_j^\dagger a_j^\dagger a_j + a_i^\dagger a_i a_i a_j^\dagger + a_i^\dagger a_j^\dagger a_j a_j + a_i^\dagger a_i^\dagger a_i a_j \right) & \text{for } i - j \text{ even} \\ - a_i^\dagger a_i a_j^\dagger a_j - \frac{1}{4} \left( a_i^\dagger a_i a_i a_j + a_i a_j^\dagger a_j a_j + a_i^\dagger a_i^\dagger a_i a_j^\dagger + a_i^\dagger a_j^\dagger a_j^\dagger a_j \right) & \text{for } i - j \text{ odd.} \end{cases} \quad (2.53)$$

Similarly the ground-state wave function in Rayleigh-Schrödinger perturbation theory reads

$$|\Psi_0\rangle = |0\rangle + \frac{1}{S} |\Psi_0^{(1)}\rangle + \mathcal{O}(S^{-2}) \quad (2.54)$$

where  $|0\rangle$  is the Bogoliubov vacuum and we take the normalization  $\langle 0 | \Psi_0 \rangle = 1$  which implies  $\langle 0 | \Psi_0^{(i)} \rangle = 0 \forall i$ . We thus have  $\langle \Psi_0 | \Psi_0 \rangle = 1 + S^{-2} \langle \Psi_0^{(1)} | \Psi_0^{(1)} \rangle + \mathcal{O}(S^{-3})$ .

Developing the correlation function in powers of  $1/S$  one obtains

$$C_{ij} = S^2 \left( C_{ij}^{(0)} + \frac{1}{S} C_{ij}^{(1)} + \frac{1}{S^2} C_{ij}^{(2)} + \mathcal{O}(S^{-3}) \right) \quad (2.55)$$

where

$$C_{ij}^{(0)} = (-1)^{i-j} \quad (2.56)$$

$$C_{ij}^{(1)} = \langle 0 | \mathcal{O}_{ij}^{(1)} | 0 \rangle \quad (2.57)$$

$$C_{ij}^{(2)} = \langle 0 | \mathcal{O}_{ij}^{(2)} | 0 \rangle + \langle 0 | \mathcal{O}_{ij}^{(1)} | \Psi_0^{(1)} \rangle + \langle \Psi_0^{(1)} | \mathcal{O}_{ij}^{(1)} | 0 \rangle. \quad (2.58)$$

As we have mentioned above, the first order interaction  $\mathcal{H}^{(4)}$  in Eq. (2.46) does not have anomalous terms with two bosons. Thus the first order correction  $|\Psi_0^{(1)}\rangle$  is made of four bosons. As a consequence one has

$$\langle 0 | \mathcal{O}_{ij}^{(1)} | \Psi_0^{(1)} \rangle = \langle \Psi_0^{(1)} | \mathcal{O}_{ij}^{(1)} | 0 \rangle = 0 \quad (2.59)$$

leading to

$$C_{ij}^{(2)} = \langle 0 | \mathcal{O}_{ij}^{(2)} | 0 \rangle \quad (2.60)$$

greatly simplifying the calculation of the second order term of the correlation function. We have now presented all the necessary tools to extract the equal-time spin-spin correlation function of the Heisenberg model to second order in  $1/S$  using standard Rayleigh-Schrödinger perturbation theory. In Appendix B we present an alternative method relying on the Hellmann-Feynman theorem [79, 80] which allows us to extract the correlation function from the ground state energy of a modified Hamiltonian. We explicitly show in this appendix that the equal-time spin-spin correlation function is given by [55]

$$\langle \mathbf{S}_0 \cdot \mathbf{S}_n \rangle = (-1)^n S^2 \left[ 1 + \frac{1}{S} \left( 1 - \frac{2}{\pi} J_\alpha(n) \right) + \frac{1}{4S^2} \left( 1 - \frac{2}{\pi} J_\alpha(n) - \delta_{n,0} \right)^2 + \mathcal{O}(S^{-3}) \right] \quad (2.61)$$

where  $\alpha = |n| \pmod{2}$  and where the IR finite integrals  $J_0$  and  $J_1$  are given by

$$J_0(n) = \int_0^{\pi/2} dk \frac{1 - \cos(kn)}{\sin k}, \quad (2.62)$$

$$J_1(n) = \int_0^{\pi/2} dk \left( \frac{1}{\sin k} - \frac{\cos(kn)}{\tan k} \right). \quad (2.63)$$

Up to second order, the  $\mathcal{O}(3)$  invariant two-point function of spin operators is thus IR finite. Let us look now at the long distance behavior of the integrals  $J_0$  and  $J_1$ . We take  $1 \ll |n|$  but keep  $|n| \ll \xi$  in order to stay in the perturbative regime. One can show that

(see Appendix C or Ref. [55])

$$J_0(n) = \ln 2 + \gamma + \ln |n| + \mathcal{O}(n^{-4}) \quad n \text{ even}, \quad (2.64)$$

$$J_1(n) = \ln 2 + \gamma + \ln |n| - \frac{1}{2n^2} + \mathcal{O}(n^{-4}) \quad n \text{ odd} \quad (2.65)$$

where  $\gamma \simeq 0.577$  is the Euler-Mascheroni constant. In the “large distance” regime  $1 \ll |n| \ll \xi$  one thus has

$$\langle \mathbf{S}_0 \cdot \mathbf{S}_n \rangle \simeq (-1)^n S^2 \left[ 1 - \frac{2}{\pi S} \ln \left( \frac{|n|}{n_0} \right) + \frac{1}{2\pi S n^2} + \frac{1}{\pi^2 S^2} \ln^2 \left( \frac{|n|}{n_0} \right) \right] - \frac{S}{2\pi n^2} \quad (2.66)$$

where  $n_0 = e^{\pi/2-\gamma}/2 \simeq 1.35$  plays the role of a UV cutoff. One recovers the logarithmic term at first order occurring in the  $NL\sigma M$ , and the  $\ln^2$  term at second order [77]. The  $1/n^2$  term in the staggered part of Eq. (2.66) comes from the fact that SWT breaks Lorentz invariance away from  $k = 0, \pi$ . It is thus absent in the  $NL\sigma M$ . By contrast the  $1/n^2$  term of the uniform part corresponds to the two-point function of the  $l$  field in the  $NL\sigma M$ .

Equation (2.66) or, more precisely, Eq. (2.61), is expected to describe the short distance behavior of the spin- $S$  Heisenberg model, namely the behavior at distance  $|n| \ll \xi$ , for integer spin and half-odd integer spin, provided the perturbative regime is sufficiently extended. This is the case when the spin  $S$  is large enough. At length scale  $|n| \sim \xi$  the crossover between the weak and strong coupling regimes occurs and, for  $|n| \gg \xi$  the behavior of the correlation function reveals the nature of the spin: exponential decay for integer spin and power-law decay for half-odd integer spin.

Figure 2.2 shows the correlation function obtained in SWT and with QMC simulations for spin  $S = 2$  and  $S = 5/2$ . For  $S = 2$  where the correlation length is  $\xi \simeq 49$ , the perturbative regime is extremely restricted. However for  $S = 5/2$  one observes an extended regime where the perturbative calculation reproduces accurately the exact numerical results. Spin-wave theory calculations at finite temperature are presented in Appendix D.6.

### 2.2.2 Dynamical structure factor

More relevant to experimentalists than the equal-time spin-spin correlation function computed above is the dynamical structure factor  $S(k, \omega)$ , which provides information on the entire spectrum of the spin chain. The dynamical structure factor is essentially the double Fourier transform of the real time, real space correlation function

$$S^{ab}(k, \omega) = \sum_j e^{-ikr_j} \int_{-\infty}^{\infty} dt e^{i\omega t} \langle S_j^a(t) S_0^b(0) \rangle \quad (2.67)$$

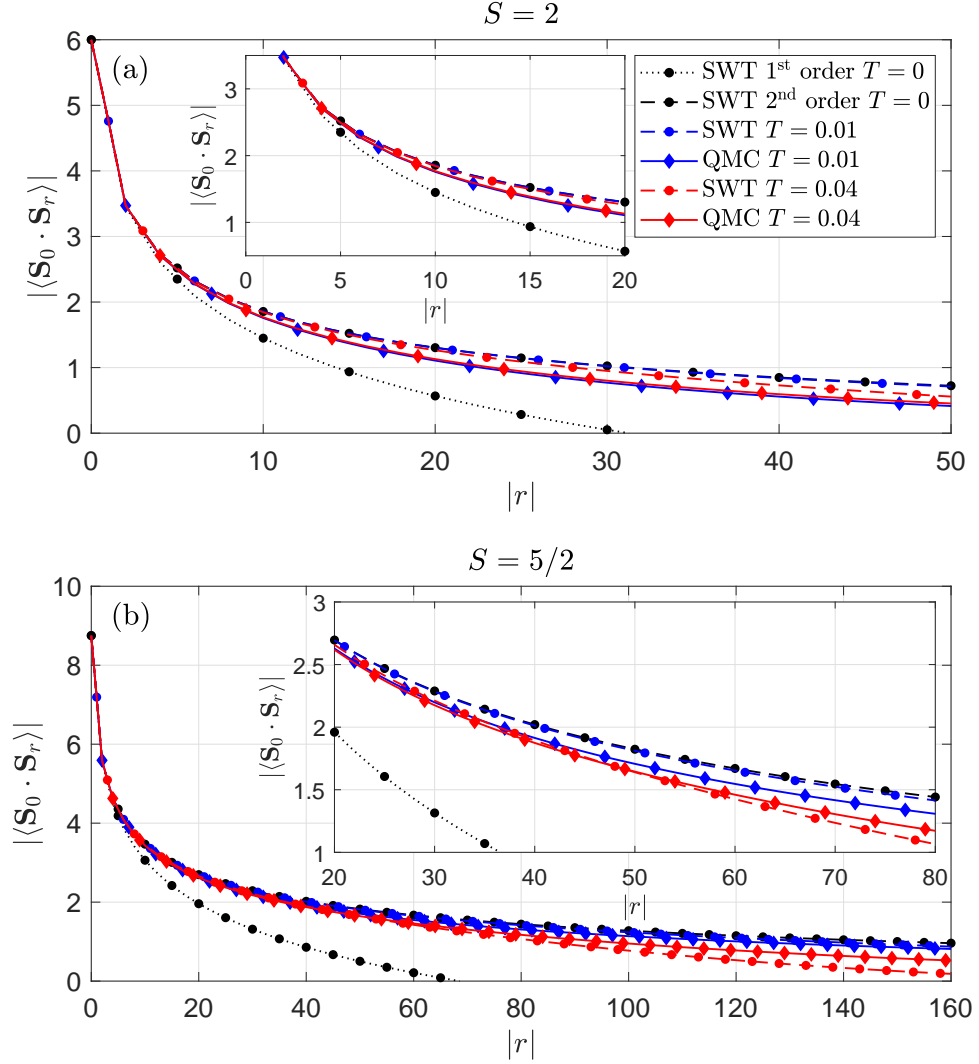


Figure 2.2: Equal-time spin-spin correlation function of the Heisenberg chain for spin (a)  $S = 2$  and (b)  $S = 5/2$  obtained with SWT and QMC. The dotted lines show that the first order SWT calculation breaks down well before the crossover length scale  $\xi \simeq 49, 160$  for  $S = 2, 5/2$ , respectively. Figure (b) adapted from Ref. [55] with the permission of the APS, © 2020 American Physical Society.

where the expectation value is taken in the exact ground state  $|0\rangle$  with energy  $E_0$  of the Hamiltonian. Going to the Lehmann representation and taking  $S^a = (S^b)^\dagger$  one obtains

$$S^{ab}(k, \omega) = \frac{2\pi}{N_s} \sum_{\alpha} |\langle \alpha | S_k^a | 0 \rangle|^2 \delta(\omega - E_{\alpha} + E_0) \quad (2.68)$$

where  $\{|\alpha\rangle\}$  is a complete set of excited states having energy  $E_\alpha$  and we have used

$$S_k^a = \sum_j e^{-ikr_j} S_j^a. \quad (2.69)$$

The dynamical structure factor is accessible with neutron scattering experiments: the energy-momentum transfer from an incident neutron to the sample is given by  $(\omega, k)$ . Experiments, however, usually run at finite temperature  $T = 1/\beta$ . The expectation value in Eq. (2.67) should then be understood by use of the density matrix  $\rho = e^{-\beta\mathcal{H}}/\text{Tr}(e^{-\beta\mathcal{H}})$ . The dynamical structure factor can then be reexpressed in terms of the retarded Green's function  $F^{ab,R}(k, \omega; \beta)$  as [81]

$$S^{ab}(k, \omega; \beta) = -\frac{2}{1 - e^{-\beta\omega}} \text{Im} \left[ F^{ab,R}(k, \omega; \beta) \right]. \quad (2.70)$$

At finite temperature it is convenient to compute Green's functions in imaginary time, and to perform an analytic continuation. One first computes the imaginary-time ordered Green's function of spin operators

$$F^{ab}(k, i\omega_n) = -\int_0^\beta d\tau e^{i\omega_n\tau} \langle T_\tau S_k^a(\tau) S_{-k}^b(0) \rangle \quad (2.71)$$

where  $\omega_n = 2n\pi/\beta$ ,  $n \in \mathbb{Z}$  are the bosonic Matsubara frequencies,  $\tau$  is the imaginary time and  $T_\tau$  is the time ordering operator. The analytic continuation of this Green's function simply reads

$$\lim_{i\omega_n \rightarrow \omega + i\eta} F^{ab}(k, i\omega_n) = F^{ab,R}(k, \omega; \beta). \quad (2.72)$$

In this section we compute the dynamical structure factor of the Heisenberg chain in NLSWT at finite temperature. To perform the calculation we first compute the imaginary-time ordered Green's functions of HP operators

$$\mathbb{G}(k, \tau) = -\langle T_\tau \begin{pmatrix} a_k(\tau) \\ a_{-k}^\dagger(\tau) \end{pmatrix} \begin{pmatrix} a_k^\dagger(0) & a_{-k}(0) \end{pmatrix} \rangle. \quad (2.73)$$

The free Green's function is given by

$$\mathbb{G}^0(k, i\omega_n) = \frac{1}{(i\omega_n)^2 - \epsilon_k^2} \begin{pmatrix} A_k + i\omega_n & B_k \\ B_k & A_k - i\omega_n \end{pmatrix} \quad (2.74)$$

where one goes from imaginary-time to imaginary frequency with

$$\mathbb{G}^0(k, i\omega_n) = \int_0^\beta d\tau e^{i\omega_n\tau} \mathbb{G}^0(k, \tau). \quad (2.75)$$

To first order in perturbation theory the Green's functions read (see Appendix D)

$$\mathbb{G}(k, i\omega_n) = \frac{1}{(i\omega_n)^2 - \xi_k^2} \begin{pmatrix} A_k \left(1 + \frac{|\kappa_\beta|}{S}\right) + i\omega_n & B_k \left(1 + \frac{|\kappa_\beta|}{S}\right) \\ B_k \left(1 + \frac{|\kappa_\beta|}{S}\right) & A_k \left(1 + \frac{|\kappa_\beta|}{S}\right) - i\omega_n \end{pmatrix} \quad (2.76)$$

where  $\xi_k$  is the NLSWT dispersion relation at finite temperature

$$\xi_k = 2JS \left(1 + \frac{|\kappa_\beta|}{S}\right) |\sin k| \quad (2.77)$$

with

$$\kappa_\beta = \frac{1}{N_s} \sum_k \frac{|\sin k| \coth\left(\frac{\beta \epsilon_k}{2}\right) - 1}{2} \quad (2.78)$$

which is IR finite and which satisfies  $\lim_{\beta \rightarrow \infty} \kappa_\beta = \kappa$ .

Having given the tools to compute the dynamical structure factor at inverse temperature  $\beta$  we now present the final results. The actual calculation being rather tedious we give some of its details in Appendix D. The longitudinal structure factor is given by [55]

$$S^{zz}(k, \omega; \beta) = \frac{2\pi}{1 - e^{-\beta\omega}} \frac{1}{N_s} \sum_{q>0} \left[ T_{k,q}^{(1)} \delta(\omega - \xi_q - \xi_{k+q}) + T_{k,q}^{(2)} \delta(\omega + \xi_q + \xi_{k+q}) \right. \\ \left. + T_{k,q}^{(3)} \delta(\omega - \xi_q + \xi_{k+q}) + T_{k,q}^{(4)} \delta(\omega + \xi_q - \xi_{k+q}) \right] \quad (2.79)$$

where

$$T_{k,q}^{(1)} = \frac{1}{4} \left[ \coth\left(\frac{\beta \xi_q}{2}\right) + \coth\left(\frac{\beta \xi_{k+q}}{2}\right) \right] \left[ \frac{1 - \cos q \cos(k+q) + \sin q - |\sin(k+q)|}{\sin q |\sin(k+q)|} - 1 \right], \quad (2.80)$$

$$T_{k,q}^{(2)} = -\frac{1}{4} \left[ \coth\left(\frac{\beta \xi_q}{2}\right) + \coth\left(\frac{\beta \xi_{k+q}}{2}\right) \right] \left[ \frac{1 - \cos q \cos(k+q) - \sin q + |\sin(k+q)|}{\sin q |\sin(k+q)|} - 1 \right], \quad (2.81)$$

$$T_{k,q}^{(3)} = -\frac{1}{4} \left[ \coth\left(\frac{\beta \xi_q}{2}\right) - \coth\left(\frac{\beta \xi_{k+q}}{2}\right) \right] \left[ \frac{1 - \cos q \cos(k+q) + \sin q + |\sin(k+q)|}{\sin q |\sin(k+q)|} + 1 \right], \quad (2.82)$$

$$T_{k,q}^{(4)} = \frac{1}{4} \left[ \coth\left(\frac{\beta \xi_q}{2}\right) - \coth\left(\frac{\beta \xi_{k+q}}{2}\right) \right] \left[ \frac{1 - \cos q \cos(k+q) - \sin q - |\sin(k+q)|}{\sin q |\sin(k+q)|} + 1 \right]. \quad (2.83)$$

and the transverse structure factor by

$$S^{xx}(k, \omega; \beta) = \frac{S\pi \text{sign}(\omega)}{1 - e^{-\beta\omega}} \left(1 - \frac{n_\beta}{S}\right) \left| \tan\left(\frac{k}{2}\right) \right| (\delta(\omega - \xi_k) + \delta(\omega + \xi_k)) \quad (2.84)$$

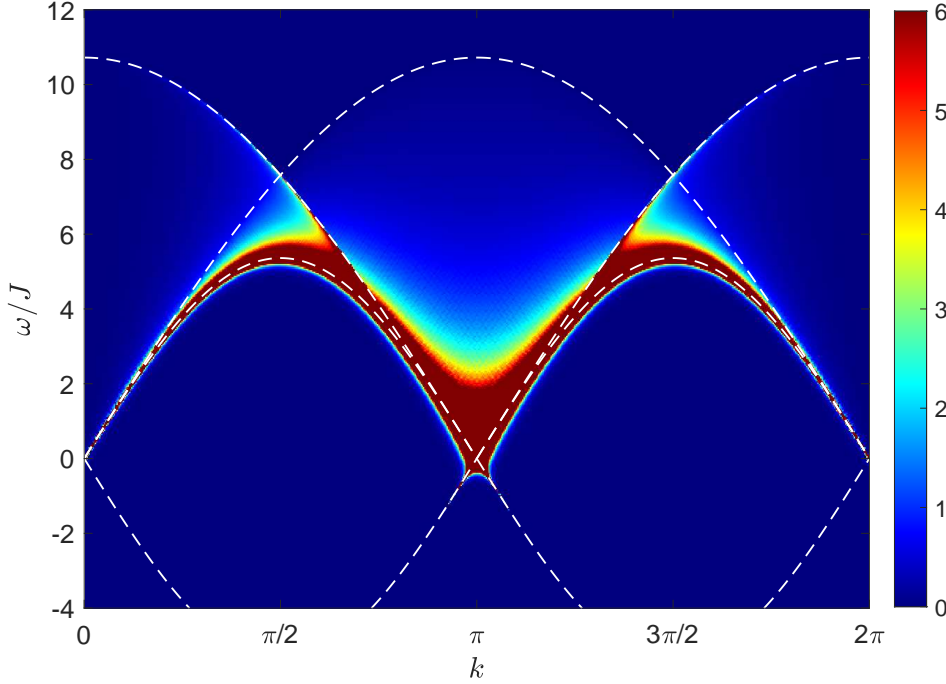


Figure 2.3: Dynamical structure factor of the Heisenberg chain at inverse temperature  $\beta = 10$ . The dashed lines represent the upper and lower thresholds obtained from the dispersion relation  $\xi_k$  at finite temperature. Figure adapted from Ref. [55] with the permission of the APS, © 2020 American Physical Society.

where

$$n_\beta = -\frac{1}{N_s} \sum_k \mathbb{G}_{22}^0(k, \tau = 0^+) = \frac{1}{N_s} \sum_k \frac{u_k^2 + v_k^2 e^{\beta \epsilon_k}}{e^{\beta \epsilon_k} - 1} \quad (2.85)$$

is positive and IR divergent.

Let us now analyze in details these results, which are illustrated in Fig. 2.3. First, at finite temperature there is spectral weight at negative energy. This weight however becomes exponentially small as the energy is lowered. Indeed, at finite temperature the ground state is defined by the density matrix and is not only made of the Bogoliubov vacuum. Transitions from a higher energy state to a lower energy state are thus possible.

More striking is the fact that the transverse structure factor in Eq. (2.84) is negative along the single-magnon branch. Indeed the first order correction turns the weight from finite and positive to infinite and negative. This is again a trace of the breakdown of perturbation theory in one dimension. However, there are several important points to recall. First,  $S^{xx}$  is not rotationally invariant and thus an IR divergence is expected to occur in this quantity. It should be compensated by the divergence of the longitudinal



part. We shall come back to this later. More importantly, we see that the transverse structure factor has spectral weight only along the one-magnon branch  $\omega = \pm \xi_k$ . Coming back to the notion of asymptotic freedom, we see that this spectral weight is not in this regime. We have insisted above that asymptotic freedom is encountered in the spin chain at length scale  $|x| \ll \xi$  in the equal time, real space correlation function. When treating energy-momentum-dependent quantities the relevant scale is the crossover energy scale  $\Delta = v/\xi$  and the two-momentum  $(\omega, k)$  must satisfy, in analogy with the NL $\sigma$ M,  $|\omega^2 - \epsilon_k^2| \gg \Delta^2$ . When  $|\omega^2 - \epsilon_k^2| \ll \Delta^2$ , the behavior of the spin chain is drastically different for integer and half-odd integer spin: for integer spin, there is an opening of the gap at momentum  $\pi$  while the spectrum remains gapless for half-odd integer spin. Spin-wave theory, however, is unable to describe these behaviors: it always predicts a gapless spectrum. But these predictions are not in the validity range of perturbation theory, and we shall completely ignore such results.

In the validity range of perturbation theory  $|\omega^2 - \epsilon_k^2| \gg \Delta^2$  the non-vanishing spectral weight comes from the longitudinal part of the structure factor. One sees from Eq. (2.79) that it is everywhere positive, and it is finite in the perturbative regime. The divergence of the longitudinal structure factor on the threshold  $\omega = \xi_k$  must cancel the divergence of the transverse structure factor discussed above. However we do not trust the results close to the threshold, but only sufficiently far away where  $S^{zz}$  is finite.

Finally let us now discuss the  $T \rightarrow 0$  limit of these results. For the transverse part in Eq. (2.84) the limit is taken straightforwardly and we end up with the contribution along the positive single-magnon branch  $\omega = \mathcal{E}_k$ , which, anyways, we do not trust. For the longitudinal part in Eq. (2.79) we observe that only the  $T_{k,q}^{(1)}$  term remains and the structure factor is thus given by

$$S^{zz}(k, \omega) = \frac{1}{2} \int_0^\pi dq \frac{1 - \cos q \cos(k+q)}{\sin q |\sin(k+q)|} \delta(\omega - \mathcal{E}_q - \mathcal{E}_{k+q}) \quad (2.86)$$

where we have taken the continuum limit. These results are consistent with Takahashi's expressions at first order [64, 65].

### 2.2.3 Equal-time structure factor

Another relevant quantity for experimentalists is the equal-time (or instantaneous) structure factor, obtained by integrating the dynamical structure factor over energy<sup>5</sup>

$$S^{aa}(k; \beta) = \int_{-\infty}^{\infty} \frac{d\omega}{2\pi} S^{aa}(k, \omega; \beta). \quad (2.87)$$

Alternatively it can be obtained by Fourier transforming the equal-time spin-spin correlation function. Since the rotationally invariant two-point function of spin operators

<sup>5</sup>At  $T = 0$  the integral can naturally be restricted to positive energy.

was IR finite and well defined, we can expect the structure factor  $S(k)$  to be well defined. There are a few subtleties that we should still discuss. To first order, for instance, the IR finiteness of the equal-time correlation function was obtained thanks to constant terms coming from the transverse part  $\langle S_i^x S_j^x + S_i^y S_j^y \rangle$ . This is traced back to the form of the integrals  $J_\alpha(n)$ ,  $\alpha = 0, 1$  in Eqs. (2.62)-(2.63). When Fourier transforming the equal-time correlation function, these constant terms give divergent contributions at  $k = \pi$ . As a consequence, the longitudinal part of the structure factor will also be divergent at  $k = \pi$ . This is again a minor problem since  $k = \pi$  is not in the validity range of perturbation theory set up by asymptotic freedom. To proceed, we shall simply ignore the contribution at  $k = \pi$ . The transverse structure factor is easily obtained,

$$S^{xx}(k) = \frac{S}{2} \left( 1 - \frac{n}{S} \right) \left| \tan \left( \frac{k}{2} \right) \right|. \quad (2.88)$$

Proceeding similarly for the longitudinal part we obtain

$$S^{zz}(k) = -\frac{1}{4} + \frac{1}{4\pi} \int_0^\pi dq \frac{1 - \cos(q) \cos(k+q)}{\sin(q) |\sin(k+q)|}. \quad (2.89)$$

The longitudinal part of the equal-time structure factor is thus divergent whenever the momentum  $k$  is different from zero. In Appendix E we show that the divergence of  $S^{zz}(k)$  is exactly canceled by the divergence of  $2S^{xx}(k)$  leading to an IR finite result for  $S(k)$ , thus providing a meaningful description of the structure factor in the appropriate window of momentum. The structure factor thus reads

$$\begin{aligned} S(k) &= 2S^{xx}(k) + S^{zz}(k) \\ &= \left( S + \frac{1}{2} \right) \left| \tan \left( \frac{k}{2} \right) \right| - \frac{1}{4} \\ &\quad + \frac{1}{4\pi} \int_0^\pi dq \frac{1}{\sin(q)} \left( \frac{1 - \cos(q) \cos(k+q)}{|\sin(k+q)|} - 2 \left| \tan(k/2) \right| \right) \end{aligned} \quad (2.90)$$

where we have used the definition of  $n$  in Eq. (2.44) and where the integral is convergent and can be computed numerically.

### 2.3 Conclusion

In this chapter we have shown that perturbative calculations can actually successfully be applied to the antiferromagnetic Heisenberg chain. There is indeed a subtle cancellation of IR divergences when considering  $O(3)$  invariant observables in SWT. This is analogous to “Elitzur’s conjecture” claiming the IR-finiteness of  $O(3)$  invariant quantities in perturbative calculations on the  $O(3)$  NL $\sigma$ M. To illustrate the situation we have computed the equal-time spin-spin correlation function to second order in perturbation theory and have compared it with QMC simulations. Spin-wave theory provides, when the spin is large enough, a surprisingly accurate description of the cor-

relation function at short distance, namely at distance  $|x| \ll \xi$ , where  $\xi$  is the crossover length scale of the model which scales exponentially with the spin. For  $S = 5/2$  we have found that the SWT results actually reproduce the QMC data over a significantly more extended region as the results remained very close up to distance  $|x| \sim \xi/3$ .

The extended perturbative regime observed in the spin chain is a consequence of the mapping of the model onto the NL $\sigma$ M and of an important property of its  $\beta$ -function. The coupling constant of the NL $\sigma$ M flows to large values at large length scales, which is commonly called asymptotic freedom. The length scale  $\xi$  is the length scale at which the coupling constant changes from the weak to the strong coupling regime. At distances much beyond  $\xi$ , the behavior of the spin chain is different for integer and half-odd integer spin. Conversely, at distances much below  $\xi$ , integer and half-odd integer spin chains behave similarly, as described by perturbation theory.

To provide a complete description of the physics of the Heisenberg chain with SWT, we have also computed the dynamical structure factor. We have shown that in the perturbative regime, namely far enough from the threshold of the spectral weight, the dynamical structure factor is well defined. This analysis was motivated by the new potential experimental studies of spin chains, in particular with neutron scattering. Spin-5/2 chains were studied experimentally in the 1970's, mainly focusing on the determination of the quantum renormalization factor, namely the correction to the dispersion relation of the lowest lying excitation with respect to SWT [82–84]. The lack of deeper experimental studies can find its origin in the Haldane conjecture: the large- $S$  spin chains being more classical than their small- $S$  counterparts, it was more important to investigate properties of the latter. With the improvement of the resolution of the neutron scattering experiments, illustrated for instance by the recent detailed experimental investigation of the dynamical structure factor of the spin-1/2 chain, showing the existence of the two- and four-spinon continua [15], we hope that the complete description of the equal-time and dynamical properties of the large- $S$  spin chain will motivate new experimental investigations to confirm the observation of the perturbative regime, and thus of asymptotic freedom, in the Heisenberg chain.



### 3 Elements of group theory

To proceed further into this thesis one needs to introduce some notions of group theory before we dive into the physics of  $SU(N)$  spin models. While the representation theory of the  $SU(2)$  group (or  $\mathfrak{su}(2)$  Lie algebra) is a standard topic in any introductory quantum mechanics course and can be grasped rather easily in a very limited amount of time<sup>1</sup>, it is not so true for  $SU(N > 2)$ . First the theory by itself is more complex, and is actually often misunderstood. For instance a common mistake is to associate the fundamental irreducible representation (irrep) of  $\mathfrak{su}(3)$  to the spin-1 irrep of  $\mathfrak{su}(2)$ , because both have dimension three. A quick look at their weight diagrams reveals that the structure of both irreps is actually completely different. It is quite remarkable, however, that almost all that a physicist interested only in practical applications needs to know about the representation theory of the  $\mathfrak{su}(N)$  Lie algebra is contained in the use of the Young diagrams, which are nothing but labels for the different irreps, including the rules for tensor products of irreps, the structure of the generalized Gell-Mann matrices and the notion of Clebsch-Gordan coefficients (CGCs), which are known to any physicists<sup>2</sup>. When the aim is to perform numerical calculations on  $SU(N)$  spin models it appears however that the algorithmic complexity caused by the large dimension of the local Hilbert space, as well as the structure of the algebra, prohibits any “non- $SU(N)$ -symmetric” approach and the actual implementation of the  $SU(N)$  symmetry is necessary. A possible route to incorporating the  $SU(N)$  symmetry in a numerical algorithm [86–89] then requires a number of additional notions, such as the standard Young tableaux [90]. In fact, the standard Young tableaux were firstly introduced in the study of the symmetric (or permutation) group and we shall follow the same path in this chapter. Indeed, the representation theory of the  $SU(N)$  group can be deduced from the representation theory of the permutation group thanks to the Schur-Weyl duality.

---

<sup>1</sup>We assume that the reader is familiar with the basic theory of the  $SU(2)$  group and associated  $\mathfrak{su}(2)$  Lie algebra.

<sup>2</sup>Unlike for  $SU(2)$  where the CGCs can be expressed in terms of other coefficients such as the Racah coefficients, the  $3j$ - or  $6j$ -symbols for which explicit formulas are known, the calculation of  $SU(N)$  CGCs in the general case is not a trivial problem, but it is a solved problem, see Section 3.3.5 and Ref. [85].

The chapter is thus structured as follows. In Section 3.1 we go through the basics of the representation theory of the permutation group. We follow Ref. [91] as well as the four first chapters of the excellent book of Chen, Ping and Wang, Ref. [92], and adopt the same definitions, notations and conventions. Although we try to keep it at a minimal level the material in this section is rather technical, in particular when it comes to the calculation of the subduction coefficients (SDCs). Section 3.1 is mainly useful for Chapter 5 and can be omitted by readers only interested in Chapter 4. In Section 3.2 we present briefly the Schur-Weyl duality which interrelates the permutation group and the  $SU(N)$  group. Section 3.2 thus gives a justification for our extensive discussion of the permutation group in Section 3.1 while our ultimate aim is at developing the theory of the  $SU(N)$  group and  $\mathfrak{su}(N)$  Lie algebra. Finally we turn to the representation theory of the Lie algebra  $\mathfrak{su}(N)$  in Section 3.3. We introduce again the notion of Young diagrams, discuss several choices of generators of the Lie algebra and present the Itzykson-Nauenberg (or Littlewood-Richardson) rules which explain how to decompose any tensor product of irreps into a direct sum of irreps. Section 3.3 is mainly inspired by Refs. [93, 94].

### 3.1 The permutation group

#### 3.1.1 Group definition

The permutation group (or symmetric group)  $\mathcal{S}_n = \mathcal{S}_n(1, 2, \dots, n)$  where  $n$  is an integer is the group of all permutations of the set  $\{1, 2, \dots, n\}$ . A permutation is a reordering of the integers. The cardinal of the permutation group  $\mathcal{S}_n$  is  $n!$ , corresponding to all possible permutations of the  $n$  integers. Among all permutations, the 2-cycles, or transpositions, are those which exchange only two elements. We denote them by  $(i, j)$ , namely  $i$  is exchanged with  $j$ . An *adjacent transposition* is a 2-cycle of adjacent numbers  $(i, i + 1)$ . The *generators* of  $\mathcal{S}_n$  are given by the  $n - 1$  adjacent transpositions  $(i, i + 1)$ ,  $i = 1, 2, \dots, n - 1$ . Indeed, any permutation can be rewritten as a product of adjacent transpositions. Notice that the inverse of a transposition  $(i, j)$  is the transposition itself.

The *2-cycle class operator* is the sum of all transpositions<sup>3</sup>

$$C_2(n) = \sum_{1 \leq i < j \leq n} (i, j). \quad (3.1)$$

This operator will be of major importance throughout the rest of the chapter. Indeed

---

<sup>3</sup>An element  $g_1$  of a group  $G$  is said to be conjugate to  $g_2 \in G$  if it exists  $u \in G$  such that  $g_1 = ug_2u^{-1}$ . A class is made of all group elements which are conjugate to each other. The set of transpositions forms a class. A class operator is obtained by summing all elements of the class.

one can show that the 2-cycle class operator commutes with all group elements,

$$[C_2(n), \sigma] = 0, \quad \forall \sigma \in \mathcal{S}_n. \quad (3.2)$$

The 2-cycle class operator  $C_2(n)$  thus corresponds to what physicists call a *Casimir operator*. By Schur's lemma, it is proportional to the identity and its eigenvalues can be used to label the different representations of the group. However, as we will see below, the sole eigenvalue of the 2-cycle class operator  $C_2(n)$  does not provide a satisfying label for the representations of the permutation group as different irreps can have the same eigenvalue (this is the case for conjugate representations). A *complete set of commuting operators* (CSCO) in a space  $L$  is a set of commuting operators  $C = (C_1, C_2, \dots, C_l)$  such that all eigenvalues of  $C$  in the space  $L$  are non-degenerate. In other words, the eigenvalues of  $C$  can be used to label uniquely all states of  $L$ :

$$C_i |\psi_\lambda\rangle = \lambda_i |\psi_\lambda\rangle, \quad i = 1, 2, \dots, l \quad \text{where } \lambda = (\lambda_1, \lambda_2, \dots, \lambda_l), \quad |\psi_\lambda\rangle \in L. \quad (3.3)$$

#### 3.1.2 Representations

The irreps of the permutation group can be labeled using either partitions or Young diagrams. A partition of  $n$  is a splitting of  $n$  into a sum of integers  $\nu_i$ ,

$$\begin{aligned} n &= \nu_1 + \nu_2 + \dots + \nu_n, \\ \nu_1 &\geq \nu_2 \geq \dots \geq \nu_n \geq 0. \end{aligned} \quad (3.4)$$

We use  $[\nu] = [\nu_1, \nu_2, \dots]$  to denote a partition of  $n$ , and we shall keep only the non-zero integers  $\nu_i$ . The number of different partitions of  $n$  thus corresponds to the number of irreps of  $\mathcal{S}_n$ . A *Young diagram* is a graphical representation of a partition. It is an array of boxes aligned on the left and containing  $\nu_i$  boxes in the  $i$ -th row. Examples are given in Fig. 3.1. Since  $\nu_i \geq \nu_{i+1}$  the number of boxes in each row is non-ascending from top to bottom. The eigenvalue of the 2-cycle class operator  $C_2(n)$  of  $\mathcal{S}_n$  of the irrep  $[\nu]$  is given by

$$\lambda_2^{[\nu]} = \frac{1}{2} \left( \sum_i \nu_i^2 - \sum_i (\nu_i^T)^2 \right) = \frac{1}{2} \sum_i \nu_i (\nu_i - 2i + 1) \quad (3.5)$$

where  $\nu_i^T$  is the length of the  $i$ -th column of the Young diagram  $[\nu]$ , or equivalently the length of the  $i$ -th row of the transposed shape  $[\nu^T]$  obtained by converting each row of  $[\nu]$  into a column. The second expression can be obtained easily from inspection of the Young diagram.

Before stating the key theorem which will allow us to classify states uniquely we shall introduce a few more technical notions. The group chain  $\mathcal{S}_n \supset \mathcal{S}_{n-1} \supset \dots \supset \mathcal{S}_2$  is called a canonical group chain because  $\mathcal{S}_2$  is abelian and because  $\mathcal{S}_{n-1}$  is a canonical subgroup of  $\mathcal{S}_n$ , namely for any irrep  $D^{[\nu]}$  of  $\mathcal{S}_n$ , the subduced representation  $D^{[\nu]} \downarrow \mathcal{S}_n$

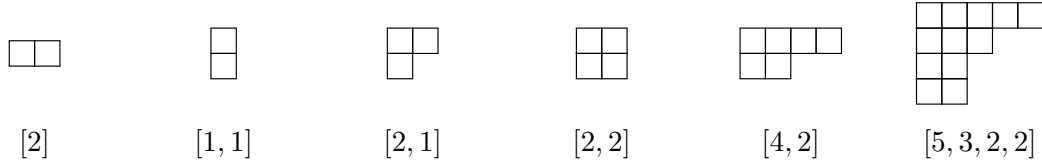


Figure 3.1: Examples of Young diagrams with the corresponding partition of  $\mathcal{S}_n$ .

of  $\mathcal{S}_{n-1}$  obtained by restricting the irrep  $[\nu]$  of  $\mathcal{S}_n$  to the elements of  $\mathcal{S}_{n-1}$  is a reducible representation of  $\mathcal{S}_{n-1}$ , meaning that any irrep  $[\mu]$  of  $\mathcal{S}_{n-1}$  appears at most once in the decomposition of  $D^{[\nu]} \downarrow \mathcal{S}_n$  into irreducible parts. We write this as

$$D^{[\nu]} \downarrow \mathcal{S}_n = \sum_{[\mu]} \oplus \tau_{[\mu]}^{[\nu]} D^{[\mu]}(\mathcal{S}_{n-1}) \quad (3.6)$$

where  $\tau_{[\mu]}^{[\nu]} = 0, 1$ . It is in practice very simple to obtain the decomposition of the subduced representation  $D^{[\nu]} \downarrow \mathcal{S}_n$  of an irrep  $[\nu]$  of  $\mathcal{S}_n$ . A bottom corner is defined as a box of a Young diagram which does not have any box below and does not have any box on its right. Then the subduced basis  $D^{[\nu]} \downarrow \mathcal{S}_n$  is simply obtained by following the *branching law of  $\mathcal{S}_n$*

$$D^{[\nu]} \downarrow \mathcal{S}_n = \sum_{[\nu']} \oplus D^{[\nu']}(\mathcal{S}_{n-1}) \quad (3.7)$$

where the sum in the right-hand side restricts to all irreps  $[\nu']$  of  $\mathcal{S}_{n-1}$  having  $n - 1$  boxes and obtained from  $[\nu]$  by removing a box in all possible bottom corners. For instance the irrep  $[\nu] = [3, 2]$  has two bottom corners,

$$\begin{array}{|c|c|c|} \hline \square & \square & \square \\ \hline \square & \square & \square \\ \hline \end{array} \longrightarrow \begin{array}{|c|c|c|} \hline \square & \square & \times \\ \hline \square & \times & \square \\ \hline \end{array} \quad (3.8)$$

and removing a box in these bottom corners leads to the following irreps,

$$\begin{array}{|c|c|c|} \hline \square & \square & \times \\ \hline \square & \times & \square \\ \hline \end{array} \longrightarrow \begin{array}{|c|c|} \hline \square & \square \\ \hline \square & \square \\ \hline \end{array} \quad \text{and} \quad \begin{array}{|c|c|c|} \hline \square & \square & \square \\ \hline \square & \square & \square \\ \hline \end{array}. \quad (3.9)$$

Thus the subduced representation of the irrep  $[\nu] = [3, 2]$  of  $\mathcal{S}_5$  is given by

$$D^{\square\square\square} \downarrow \mathcal{S}_5 = D^{\square\square} \oplus D^{\square\square\square}. \quad (3.10)$$

The following theorem is the key to the classification of all states of  $\mathcal{S}_n$ .

**Theorem<sup>4</sup>:** The  $(n - 1)$  2-cycle class operators  $C = (C_2(n), C_2(n - 1), \dots, C_2(2))$  of the group chain  $\mathcal{S}_n \supset \mathcal{S}_{n-1} \supset \dots \supset \mathcal{S}_2$  form a CSCO of  $\mathcal{S}_n$ .

---

<sup>4</sup>See Ref. [92] page 127.



Thus the eigenvalues of  $C$ , which can be easily computed using Eq. (3.5), can be used to label uniquely the different states of the irreps of  $\mathcal{S}_n$ .

#### 3.1.3 Littlewood-Richardson rules

The tensor product of an irrep  $[\nu_1]$  of  $\mathcal{S}_{n_1}$  with an irrep  $[\nu_2]$  of  $\mathcal{S}_{n_2}$  is an induced reducible representation of  $\mathcal{S}_n$  with  $n = n_1 + n_2$  denoted  $([\nu_1] \times [\nu_2]) \uparrow \mathcal{S}_n$ . The decomposition into irreps of  $\mathcal{S}_n$  reads

$$([\nu_1] \times [\nu_2]) = \sum_{[\nu]} \{\nu_1 \nu_2 \nu\} [\nu] \quad (3.11)$$

where  $\{\nu_1 \nu_2 \nu\}$  is the *outer multiplicity* of the irrep  $[\nu]$  in the tensor product of  $[\nu_1]$  and  $[\nu_2]$ . The Littlewood-Richardson rules allow us to determine all the irreps  $[\nu]$  for which  $\{\nu_1 \nu_2 \nu\}$  is non-zero [95]. The Littlewood-Richardson rules are as follows:

1. Select among  $[\nu_1]$  and  $[\nu_2]$  the most complicated Young diagram as the base<sup>5</sup>.
2. Fill the other Young diagram with  $a$ 's in the first row,  $b$ 's in the second row,  $c$ 's in the third row, etc...
3. Enlarge the base diagram by moving the  $a$ 's to all possible positions satisfying the two following constraints: i) two  $a$ 's should not stand in the same column; ii) the diagram obtained at each step should be a valid Young diagram.
4. Perform similarly for all  $b$ 's with the following additional constraint: iii) when going through the Young diagram from right to left and from top to bottom, the total number of  $b$ 's should never exceed the total number of  $a$ 's.
5. Proceed similarly for all  $c$ 's, ... until the resultant diagrams all contain  $n$  boxes.

For a Young diagram  $[\nu]$  appearing in the decomposition, the multiplicity  $\{\nu_1 \nu_2 \nu\}$  is given by the total number of obtained arrangements of the letters  $a, b, c, \dots$

#### 3.1.4 Standard Young tableaux

A *Standard Young Tableau* (SYT) is a Young diagram filled with integers from 1 to  $n$  in ascending order from left to right and from top to bottom. All SYTs of an irrep  $[\nu]$  can be obtained easily using the reducibility of the irrep  $[\nu]$  of  $\mathcal{S}_n$  with respect to its subgroup

<sup>5</sup>By “most complicated” Young diagram we mean either the one with the largest number of boxes, or the one with the shape which is far from being purely symmetric (thus several rows) and far from being purely antisymmetric (thus several columns). In any case, the tensor product of two irreps is abelian, and the sole aim of selecting the “most complicated” diagram is to reduce the number of operations in the Littlewood-Richardson rules. This could thus be used to define *a posteriori* what is the “most complicated” Young diagram.

$\mathcal{S}_{n-1}$  and by iterating the procedure up to  $\mathcal{S}_1$ . We denote by  $Y_m^{[\nu]}$ ,  $m = 1, \dots, h^{[\nu]}$  the SYTs associated to an irrep  $[\nu]$  of  $\mathcal{S}_n$ , where  $h^{[\nu]}$  is the dimension of the irrep  $[\nu]$ . For instance the five SYTs for the irrep  $[\nu] = [3, 2]$  of  $\mathcal{S}_5$  are given by

$$\begin{array}{|c|c|c|}, \\ \hline 1 & 2 & 3 \\ \hline 4 & 5 & \\ \hline \end{array}, \quad \begin{array}{|c|c|c|}, \\ \hline 1 & 2 & 4 \\ \hline 3 & 5 & \\ \hline \end{array}, \quad \begin{array}{|c|c|c|}, \\ \hline 1 & 3 & 4 \\ \hline 2 & 5 & \\ \hline \end{array}, \quad \begin{array}{|c|c|c|}, \\ \hline 1 & 2 & 5 \\ \hline 3 & 4 & \\ \hline \end{array}, \quad \begin{array}{|c|c|c|}, \\ \hline 1 & 3 & 5 \\ \hline 2 & 4 & \\ \hline \end{array}. \quad (3.12)$$

We have sorted the SYTs from left to right in a specific order called the ascending order of the last letter order sequence (LLOS) [96]. It is defined as follows. For two SYTs  $Y_m^{[\nu]}$  and  $Y_{m'}^{[\nu]}$  one looks at the location of the number  $n$ . If  $n$  appears in  $Y_m^{[\nu]}$  in a row below the one in which it appears in  $Y_{m'}^{[\nu]}$ , then  $Y_m^{[\nu]} < Y_{m'}^{[\nu]}$ . If  $n$  appears in the same row in both SYTs, then one looks at the row of number  $n - 1$  and proceed similarly, etc... Since all SYTs differ from each other by at least one interchange of numbers, then this defines an unambiguous order among SYTs<sup>6</sup>. We decide to label the SYTs with  $m = 1, \dots, h^{[\nu]}$  so as to correspond with the increasing order of the LLOS. This means that the SYT  $Y_1^{[\nu]}$  is the *smallest* SYT in the LLOS and  $Y_{h^{[\nu]}}^{[\nu]}$  is the *largest* SYT in the LLOS. One can also label SYTs using the Yamanouchi symbols. A Yamanouchi symbol  $\mathbf{r} = (r_n, r_{n-1}, \dots, r_2, r_1 = 1)$  is such that  $r_i$  is the row of number  $i$  in the SYT. For the shape  $[\nu] = [3, 2]$  the Yamanouchi symbols of the  $h^{[\nu]} = 5$  SYTs given in Eq. (3.12) are

$$(2, 2, 1, 1, 1), \quad (2, 1, 2, 1, 1), \quad (2, 1, 1, 2, 1), \quad (1, 2, 2, 1, 1), \quad (1, 2, 1, 2, 1). \quad (3.13)$$

We observe now that the ascending order of the LLOS corresponds to the descending page order of Yamanouchi symbols. What is meant here is that the Yamanouchi symbols define  $n$ -digit numbers when removing the separators between the different entries  $r_i$ , and the numbers are then in decreasing order. For our example, the sequence is  $22111 > 21211 > 21121 > 12211 > 12121$ .

The third labeling scheme for SYTs makes use of the last theorem of Section 3.1.2. We define the eigenvalue  $\lambda = (\lambda_n, \lambda_{n-1}, \dots, \lambda_2)$  of the CSCO of  $\mathcal{S}_n$  obtained using the canonical group chain  $\mathcal{S}_n \supset \mathcal{S}_{n-1} \supset \mathcal{S}_{n-2} \supset \dots \supset \mathcal{S}_2$ . The eigenvalues  $\lambda$  can then be obtained easily from the truncated branching diagram of the group  $\mathcal{S}_n$  and with the help of Eq. (3.5). An example for  $[\nu] = [3, 2]$  is shown in Fig. 3.2. We thus extract the eigenvalues  $\lambda$  (again the ordering of Eq. (3.12) is respected)

$$(2, 2, 3, 1), \quad (2, 2, 0, 1), \quad (2, 2, 0, -1), \quad (2, 0, 0, 1), \quad (2, 0, 0, -1). \quad (3.14)$$

We observe that the ascending order of the LLOS corresponds to the decreasing page order of the eigenvalues of the CSCO. Notice also that from the truncated branching diagram one can easily obtain the SYTs by following the group chain

<sup>6</sup>Notice how algorithmically simple it is to generate efficiently on a computer all SYTs for an irrep  $[\nu]$  of  $\mathcal{S}_n$  in the LLOS [97].

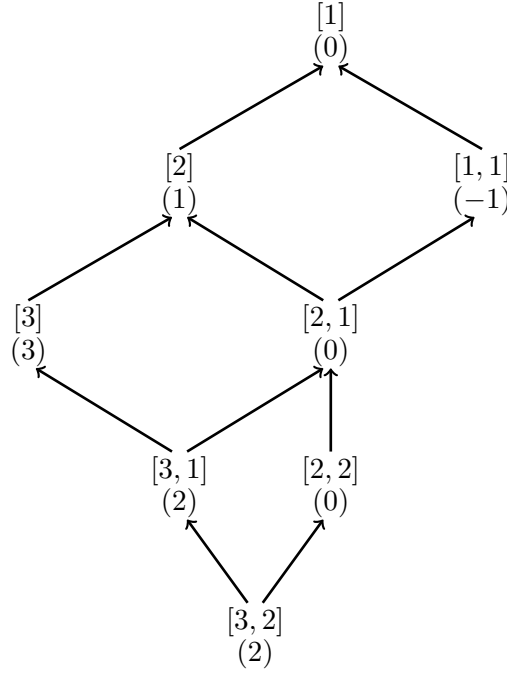
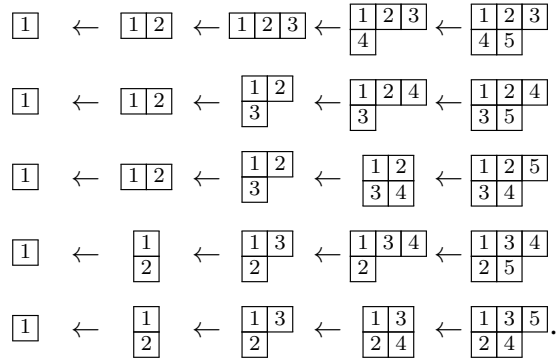


Figure 3.2: Truncated branching diagram of the group  $S_5$ . Only the relevant irreps for  $[\nu] = [3, 2]$  are shown. The number of possible paths to reach  $[1]$  from  $[\nu] = [3, 2]$  following the arrows corresponds to  $h^{[\nu]} = 5$ , the total number of SYTs for the irrep  $[\nu]$ . The eigenvalues  $\lambda_2$  of the 2-cycle class operator  $C_2(f)$  of  $S_f$  ( $f = n, n-1, \dots, 2, 1$ ) of each irrep along the paths are given in parenthesis.



Finally I shall mention that, from a numerical point of view, it is convenient to label a SYT  $Y_m^{[\nu]}$  by the *reversed Yamanouchi symbol*  $\mathbf{y}$  obtained by flipping the Yamanouchi symbol  $\mathbf{r}$  [86]. Thus  $\mathbf{y} = [y_1 = 1, y_2, \dots, y_n]$  is such that  $y_i = r_i$  is the row of number  $i$ . Table 3.1 summarizes all labeling schemes presented above.

The total number of SYTs  $h^{[\nu]}$  for an irrep  $[\nu]$  of  $S_n$  can be calculated easily from the Young diagram of the irrep. Let us introduce the hook length of a box as the number

$m$	1	2	3	4	5	Increasing page order
$Y_m^{[\nu]}$	$\begin{array}{ c c c } \hline 1 & 2 & 3 \\ \hline 4 & 5 & \\ \hline \end{array}$	$\begin{array}{ c c c } \hline 1 & 2 & 4 \\ \hline 3 & 5 & \\ \hline \end{array}$	$\begin{array}{ c c c } \hline 1 & 3 & 4 \\ \hline 2 & 5 & \\ \hline \end{array}$	$\begin{array}{ c c c } \hline 1 & 2 & 5 \\ \hline 3 & 4 & \\ \hline \end{array}$	$\begin{array}{ c c c } \hline 1 & 3 & 5 \\ \hline 2 & 4 & \\ \hline \end{array}$	Increasing order of LLOS
$\mathbf{r}$	(2, 2, 1, 1, 1)	(2, 1, 2, 1, 1)	(2, 1, 1, 2, 1)	(1, 2, 2, 1, 1)	(1, 2, 1, 2, 1)	Decreasing page order
$\mathbf{y}$	[1, 1, 1, 2, 2]	[1, 1, 2, 1, 2]	[1, 2, 1, 1, 2]	[1, 1, 2, 2, 1]	[1, 2, 1, 2, 1]	
$\lambda$	(2, 2, 3, 1)	(2, 2, 0, 1)	(2, 2, 0, -1)	(2, 0, 0, 1)	(2, 0, 0, -1)	Decreasing page order

Table 3.1: Different labeling schemes for the SYTs of the irrep  $[\nu] = [3, 2]$ .

of boxes in the same row on the right of this box, plus the number of boxes below in the same column, plus one for the box itself. Then the dimension of an irrep (Young diagram) of  $\mathcal{S}_n$  is given by,

$$h^{[\nu]} = \frac{n!}{\prod_i l_i} \quad (3.15)$$

where the denominator is the product of the hook lengths of all boxes in the Young diagram  $[\nu]$ .

### 3.1.5 The Yamanouchi basis and the Young rules

To each SYT  $Y_m^{[\nu]}$  we associate a Yamanouchi basis vector  $|Y_m^{[\nu]}\rangle$ ,  $m = 1, 2, \dots, h^{[\nu]}$ . As defined by Chen *et al.* (Ref. [92] page 121) “the symbol  $|Y_m^{[\nu]}\rangle$  stands for an irreducible basis vector belonging to the irrep  $[\nu], [\nu'], [\nu''], \dots, [1]$  of the group  $\mathcal{S}_n, \mathcal{S}_{n-1}, \mathcal{S}_{n-2}, \dots, \mathcal{S}_1$ .” The chain is obtained by successively removing the largest number in the SYT. The SYT for the irrep  $[\nu^{(p)}]$  is denoted  $Y_{m^{(p)}}^{[\nu^{(p)}]}$ . For instance,

$$\begin{aligned}
Y_m^{[\nu]} &= \begin{array}{|c|c|c|c|} \hline 1 & 2 & 4 & 6 \\ \hline 3 & 7 & & \\ \hline 5 & 8 & & \\ \hline \end{array} \rightarrow Y_{m'}^{[\nu']} = \begin{array}{|c|c|c|c|} \hline 1 & 2 & 4 & 6 \\ \hline 3 & 7 & & \\ \hline 5 & & & \\ \hline \end{array} \rightarrow Y_{m''}^{[\nu'']} = \begin{array}{|c|c|c|c|} \hline 1 & 2 & 4 & 6 \\ \hline 3 & & & \\ \hline 5 & & & \\ \hline \end{array} \rightarrow Y_{m^{(3)}}^{[\nu^{(3)}]} = \begin{array}{|c|c|c|} \hline 1 & 2 & 4 \\ \hline 3 & & \\ \hline 5 & & \\ \hline \end{array} \\
&\rightarrow Y_{m^{(4)}}^{[\nu^{(4)}]} = \begin{array}{|c|c|c|} \hline 1 & 2 & 4 \\ \hline 3 & & \\ \hline & & \\ \hline \end{array} \rightarrow Y_{m^{(5)}}^{[\nu^{(5)}]} = \begin{array}{|c|c|} \hline 1 & 2 \\ \hline 3 & \\ \hline & \\ \hline \end{array} \rightarrow Y_{m^{(6)}}^{[\nu^{(6)}]} = \begin{array}{|c|c|} \hline 1 & 2 \\ \hline & \\ \hline & \\ \hline \end{array} \rightarrow Y_{m^{(7)}}^{[\nu^{(7)}]} = \begin{array}{|c|} \hline 1 \\ \hline \\ \hline \\ \hline \end{array}.
\end{aligned} \tag{3.16}$$

Assume now that  $Y_{m'}^{[\nu]} = (i, i+1)Y_m^{[\nu]}$ , namely the Young tableau  $Y_{m'}^{[\nu]}$  (not to be confused with  $Y_{m'}^{[\nu']}$ ) is obtained from the Young tableau  $Y_m^{[\nu]}$  by exchanging  $i$  and  $i+1$ . Then the

following important relation holds [98–100]

$$(i, i+1) |Y_m^{[\nu]}\rangle = -\rho |Y_m^{[\nu]}\rangle + \sqrt{1-\rho^2} |Y_{m'}^{[\nu]}\rangle \quad (3.17)$$

where  $\rho$  is the inverse of the axial distance to reach  $i+1$  from  $i$  in the Young tableau  $Y_m^{[\nu]}$ . The axial distance from  $i$  to  $i+1$  is obtained by counting  $+1$  (respectively  $-1$ ) for each step made downwards or to the left (respectively upwards or to the right) along any rectangular path from  $i$  to  $i+1$ <sup>7</sup>. A crucial corollary of Eq. (3.17) is that one should take care of distinguishing a SYT from a Yamanouchi basis vector. Indeed as shown above  $(i, i+1)Y_m^{[\nu]} = Y_{m'}^{[\nu]}$  but  $(i, i+1) |Y_m^{[\nu]}\rangle \neq |Y_{m'}^{[\nu]}\rangle$ . Now assume that  $Y_m^{[\nu]}$  has numbers  $i$  and  $i+1$  located in the same row ( $i$  and  $i+1$  are then necessarily adjacent to each other). Then

$$(i, i+1) |Y_m^{[\nu]}\rangle = |Y_m^{[\nu]}\rangle. \quad (3.18)$$

Conversely, if  $i$  and  $i+1$  are in the same column of  $Y_m^{[\nu]}$  (thus  $i+1$  appears directly below  $i$ ) then

$$(i, i+1) |Y_m^{[\nu]}\rangle = -|Y_m^{[\nu]}\rangle. \quad (3.19)$$

Equations (3.17)-(3.19) are the *Young rules*<sup>8</sup>.

The Yamanouchi basis is also called the *standard basis* and the Yamanouchi basis vectors are also denoted as

$$\left| \begin{array}{c} [\nu] \\ m \end{array} \right\rangle \equiv |Y_m^{[\nu]}\rangle. \quad (3.20)$$

This notation will be used when computing SDCs of the permutation group. As we will see below, the SDCs are merely a unitary change of basis from the so-called *non-standard basis* (to be introduced in the next section) to the standard (Yamanouchi) basis.

#### 3.1.6 The non-standard basis and the subduction coefficients

The basis vectors of the *non-standard* basis of  $\mathcal{S}_n$  are denoted by

$$\left| \begin{array}{c} [\nu] \\ \tau \end{array} \right\rangle, \quad \tau = 1, \dots, \{\nu_1 \nu_2 \nu\}, \quad m_1 = 1, \dots, h^{[\nu_1]}, \quad m_2 = 1, \dots, h^{[\nu_2]}. \quad (3.21)$$

<sup>7</sup>Notice the different convention between Ref. [92] (Section 4.4 page 122) and the convention adopted in Refs. [57, 86–89], which corresponds to the one of Refs. [98–100]. In Refs. [92, 94], the axial distance is counted positively when going upwards or to the right and negatively when going downwards or to the left, leading to a positive sign in the first term of Eq. (3.17).

<sup>8</sup>One should now mention that the Young rules together with the decomposition of any permutation into a product of adjacent transpositions and the Schur-Weyl duality is, in practical calculations, *all* what is required to diagonalize the  $SU(N)$  Heisenberg model in specific  $SU(N)$  irreps [86].

### Chapter 3. Elements of group theory

---

The number  $\{\nu_1\nu_2\nu\}$  is equal to the multiplicity (or number of occurrences) of the irrep  $[\nu]$  in the tensor product of the irreps  $[\nu_1]$  and  $[\nu_2]$ , thanks to the Frobenius reciprocity theorem [101].  $\{\nu_1\nu_2\nu\}$  can thus easily be computed by using the Littlewood-Richardson rules for the permutation group given in Section 3.1.3.

The non-standard basis corresponds to the subduced basis belonging to the irrep  $[\nu]$  of  $\mathcal{S}_n \supset \mathcal{S}_{n_1} \otimes \mathcal{S}_{n_2}$ ,  $n_1 + n_2 = n$ , where the subduction is denoted by

$$[\nu] \downarrow (\mathcal{S}_{n_1} \otimes \mathcal{S}_{n_2}) = \sum_{\nu} \{\nu_1\nu_2\nu\} ([\nu_1], [\nu_2]). \quad (3.22)$$

The  $[\nu] \downarrow ([\nu_1], [\nu_2])$  *subduction coefficients* (SDCs) of  $\mathcal{S}_n$  are the transformation coefficients of the permutation group between the standard basis and the non-standard basis of  $\mathcal{S}_n$

$$\left| [\nu], \tau \begin{array}{cc} [\nu_1] & [\nu_2] \\ m_1 & m_2 \end{array} \right\rangle = \sum_m \left| \begin{array}{c} [\nu] \\ m \end{array} \right\rangle \left\langle \begin{array}{c} [\nu] \\ m \end{array} \left| [\nu], \tau \begin{array}{cc} [\nu_1] & [\nu_2] \\ m_1 & m_2 \end{array} \right\rangle. \quad (3.23)$$

In the previous equation the summation is restricted to the Yamanouchi basis vectors  $|Y_m^{[\nu]}\rangle$  such that the first  $n_1$  particles of  $Y_m^{[\nu]}$  are located in the same positions as the particles of  $Y_{m_1}^{[\nu_1]}$ . This is natural since, as we have explained above, the Yamanouchi basis vector  $|Y_m^{[\nu]}\rangle$  of  $\mathcal{S}_n$  is also an irreducible basis vector of the subgroup  $\mathcal{S}_{n_1}$ . Now one can easily convince oneself that the SDCs are independent of  $m_1$ , and that  $[\nu_1]$  can be determined from  $[\nu]$ ,  $m$  and  $n_2$ . In what follows, we shall nevertheless use the notation

$$\left\langle \begin{array}{c} [\nu] \\ m \end{array} \left| [\nu], \tau \begin{array}{cc} [\nu_1] & [\nu_2] \\ m_1 & m_2 \end{array} \right\rangle \quad (3.24)$$

but we keep in mind that a “minimalist” notation would make use only of  $[\nu]$ ,  $m$ ,  $\tau$ ,  $[\nu_2]$ ,  $m_2$ . The SDCs should be chosen in order to satisfy the following orthogonality relations

$$\sum_{\tau, [\nu_2], m_2} \left\langle \begin{array}{c} [\nu] \\ m \end{array} \left| [\nu], \tau \begin{array}{cc} [\nu_1] & [\nu_2] \\ m_1 & m_2 \end{array} \right\rangle \left\langle \begin{array}{c} [\nu] \\ m' \end{array} \left| [\nu], \tau \begin{array}{cc} [\nu_1] & [\nu_2] \\ m_1 & m_2 \end{array} \right\rangle = \delta_{m, m'}, \quad (3.25)$$

$$\sum_m \left\langle \begin{array}{c} [\nu] \\ m \end{array} \left| [\nu], \tau \begin{array}{cc} [\nu_1] & [\nu_2] \\ m_1 & m_2 \end{array} \right\rangle \left\langle \begin{array}{c} [\nu] \\ m \end{array} \left| [\nu], \tau' \begin{array}{cc} [\nu_1] & [\nu'_2] \\ m_1 & m'_2 \end{array} \right\rangle = \delta_{[\nu_2], [\nu'_2]} \delta_{m_2, m'_2} \delta_{\tau, \tau'}. \quad (3.26)$$

The subduced basis is thus an orthonormal basis of  $\mathcal{S}_n$ .

### 3.1.7 Calculation of SDCs – the multiplicity-free case

In this section we focus on the case where the multiplicity index  $\tau$  can take a single value  $\tau = 1 = \{\nu_1 \nu_2 \nu\}$ , namely the problem is multiplicity-free.

#### Calculation of SDCs using the eigenfunction method

We follow Chen *et al.* and use the eigenfunction method to compute the SDCs [91, 92]. The calculation is easily done by diagonalizing the CSCO of  $\mathcal{S}_{n_2}$  in the Yamanouchi basis  $|Y_m^{[\nu]}\rangle$ . In practice, we compute the kernel of an operator (see Eq. (8) of Ref. [91] or Eq. (4-172) of Ref. [92])

$$\sum_{m'} \left[ \left\langle \begin{matrix} [\nu] \\ m \end{matrix} \middle| \begin{matrix} C'(n_2) \\ C'(s_2) \end{matrix} \middle| \begin{matrix} [\nu] \\ m' \end{matrix} \right\rangle - \binom{\nu_2}{m_2} \delta_{m,m'} \right] \left\langle \begin{matrix} [\nu] \\ m' \end{matrix} \middle| \begin{matrix} [\nu] \\ \tau \end{matrix} \begin{matrix} [\nu_1] \\ m_1 \end{matrix} \begin{matrix} [\nu_2] \\ m_2 \end{matrix} \right\rangle = 0 \quad (3.27)$$

where  $(C'(n_2), C'(s_2)) = (C'_2(n_2), C'_2(n_2 - 1), \dots, C'_2(2))$  is the CSCO of  $\mathcal{S}_{n_2}(n_1 + 1, \dots, n)$ . More precisely  $C'_2(n_2)$  is the 2-cycle class operator of  $\mathcal{S}_{n_2}(n_1 + 1, \dots, n)$  given by

$$C'_2(n_2) = \sum_{n_1 < i < j \leq n} (i, j) \quad (3.28)$$

and similarly for  $C'_2(s_2)$ ,  $s_2 = n - 1, \dots, 2$ . There are two sorts of phases that we need to fix. First, there is an overall phase convention. If

$$\left\langle \begin{matrix} [\nu] \\ m \end{matrix} \middle| \begin{matrix} [\nu] \\ \tau \end{matrix} \begin{matrix} [\nu_1] \\ m_1 \end{matrix} \begin{matrix} [\nu_2] \\ m_2 \end{matrix} \right\rangle \quad (3.29)$$

solves Eq. (3.27) then so does

$$-\left\langle \begin{matrix} [\nu] \\ m \end{matrix} \middle| \begin{matrix} [\nu] \\ \tau \end{matrix} \begin{matrix} [\nu_1] \\ m_1 \end{matrix} \begin{matrix} [\nu_2] \\ m_2 \end{matrix} \right\rangle. \quad (3.30)$$

Second, we should fix the relative phase convention between SDCs with different  $m_2$ 's.

#### Phase conventions

The developments in this section correspond to Eq. (12)-(14) of Ref. [91] or equivalently Eq. (4-173)-(4-174) of Ref. [92]<sup>9</sup>.

The Yamanouchi relative phase between SDCs with different  $m_2$ 's is easily fixed thanks

<sup>9</sup>Notice that the definitions of  $T_2$  and  $T'_2$  are exchanged between Ref. [91] and Ref. [92].

to the following equation [91],

$$\left| \begin{array}{c} [\nu], \tau \\ m_1 \end{array} \begin{array}{c} [\nu_1] \\ m'_2 \end{array} \begin{array}{c} [\nu_2] \\ m_2 \end{array} \right\rangle = \frac{1}{D_{m'_2, m_2}^{[\nu_2]}(T_2)} \left( T'_2 - D_{m_2, m_2}^{[\nu_2]}(T_2) \right) \left| \begin{array}{c} [\nu], \tau \\ m_1 \end{array} \begin{array}{c} [\nu_1] \\ m_2 \end{array} \begin{array}{c} [\nu_2] \\ m_2 \end{array} \right\rangle \quad (3.31)$$

where  $T'_2 = (i, i+1) \in \mathcal{S}_{n_2}(n_1+1, \dots, n)$ ,  $T_2 = (i-n_1, i-n_1+1) \in \mathcal{S}_{n_2}(1, 2, \dots, n_2)$ ,  $D^{[\nu_2]}(T_2)$  is the representation of  $T_2$  in irrep  $[\nu_2]$  of  $\mathcal{S}_{n_2}$  and

$$T_2 Y_{m'_2}^{[\nu_2]} = Y_{m'_2}^{[\nu_2]}. \quad (3.32)$$

Then the SDCs with different  $m_2$ 's are simply related with,

$$\begin{aligned} \left\langle \begin{array}{c} [\nu] \\ m \end{array} \left| \begin{array}{c} [\nu], \tau \\ m_1 \end{array} \begin{array}{c} [\nu_1] \\ m'_2 \end{array} \begin{array}{c} [\nu_2] \\ m_2 \end{array} \right\rangle = \frac{1}{D_{m'_2, m_2}^{[\nu_2]}(T_2)} \times \\ \sum_{m'} \left( D_{m', m}^{[\nu]}(T'_2) - D_{m_2, m_2}^{[\nu_2]}(T_2) \delta_{m, m'} \right) \left\langle \begin{array}{c} [\nu] \\ m' \end{array} \left| \begin{array}{c} [\nu], \tau \\ m_1 \end{array} \begin{array}{c} [\nu_1] \\ m_2 \end{array} \begin{array}{c} [\nu_2] \\ m_2 \end{array} \right\rangle. \end{aligned} \quad (3.33)$$

The overall phase convention is fixed as follows (Chen *et al.*, Ref. [91]):

*“We remove all sign arbitrariness by requiring the absolute phase convention that the first nonvanishing coefficient of a nonstandard basis vector (where the Yamanouchi basis vectors are enumerated in decreasing page order) with  $m_2 = 1$  be positive.”*

In other words, we first compute the SDCs for the state  $m_2 = 1$  (smallest in the LLOS) and fix the phase by setting to positive value the first (in ascending order of the LLOS – decreasing page order of Yamanouchi symbols) non-vanishing coefficient, namely the coefficient of the smallest  $m$ . Then one computes the SDCs for the state  $m'_2$  using Eq. (3.33). A complete example of calculation of SDCs is given in Appendix G.

#### 3.1.8 Calculation of SDCs – the non-multiplicity-free case

We now treat the case where the multiplicity is  $\{\nu_1 \nu_2 \nu\} = 2$ . The case of multiplicity  $\{\nu_1 \nu_2 \nu\} > 2$  is a straightforward extension. We note that we could not find any details on how to deal with non-trivial multiplicities in Chen *et al.*'s work [91, 92]. However Table II.23 of Ref. [91] shows that the problem of multiplicity was actually handled by the authors, and we shall explain here the method that we induced from these results.

##### Phase convention

Assume that we proceed to the calculation for the *smallest* SYT in the LLOS for the irrep  $[\nu_2]$ , thus  $m_2 = 1$ . This SYT is the “reference” SYT which will be used to set the Yamanouchi relative phases among the SDCs for the other  $m_2$ 's, as we have done in the



case where  $\{\nu_1 \nu_2 \nu\} = 1$ .

We proceed similarly to the multiplicity-free case. When solving Eq. (3.27) one obtains two sets of SDCs which we label with  $\tau = 1, 2$  (the kernel of the operator in the square bracket is two-dimensional). The SDCs must satisfy the following orthogonality relation (see Eq. (3.26) or Eq. (4) of Ref. [91])

$$\sum_m \left\langle \begin{array}{c} [\nu] \\ m \end{array} \middle| \begin{array}{c} [\nu], \tau \end{array} \begin{array}{cc} [\nu_1] & [\nu_2] \\ m_1 & m_2 \end{array} \right\rangle \left\langle \begin{array}{c} [\nu] \\ m \end{array} \middle| \begin{array}{c} [\nu], \tau' \end{array} \begin{array}{cc} [\nu_1] & [\nu_2] \\ m_1 & m_2 \end{array} \right\rangle = \delta_{\tau, \tau'}. \quad (3.34)$$

Any orthonormal basis of the span of the two sets of SDCs will be a valid set of SDCs. We fix the relative phase between  $\tau = 1$  and  $\tau = 2$  as follows. One finds a rotation which sets to zero the coefficient of the *last* non-zero coefficient (where the Yamanouchi basis vectors are enumerated in decreasing page order) of the SDCs with  $\tau = 1$ . One then applies the same rotation to the SDCs with  $\tau = 2$ . The *overall* phase of each set is then fixed using the same convention as above: one ensures that the first non-zero coefficient is positive, where again the Yamanouchi basis vectors are enumerated in decreasing page order of Yamanouchi symbols.

Once this is done, the calculation of the SDCs for  $m_2 > 1$  follows from Eq. (3.33) without any ambiguity, since each  $\tau$  now defines an independent set of SDCs.

#### Example

We consider the case given by Chen *et al.* in Table II.23 of Ref. [91]:  $[\nu] = [3, 2, 1]$ ,  $[\nu_1] = [\nu_2] = [2, 1]$ . We begin with the “reference” SYT  $Y_{m_2=1}^{[\nu_2]}$  corresponding to the *smallest* in the LLOS:

$$Y_{m_2=1}^{[\nu_2]} \Leftrightarrow \begin{array}{|c|c|} \hline 1 & 2 \\ \hline 3 & \\ \hline \end{array} \Leftrightarrow \mathbf{r} = (2, 1, 1) \Leftrightarrow \mathbf{y} = [1, 1, 2] \Leftrightarrow \boldsymbol{\lambda} = (0, 1). \quad (3.35)$$

Computing the kernel as in Eq. (3.27) one obtains two states. To simplify the notation one defines two 6-dimensional vectors  $\mathbf{a}$  and  $\mathbf{b}$  such that

$$a_m = \left\langle \begin{array}{c} [\nu] \\ m \end{array} \middle| \begin{array}{c} [\nu], 1 \end{array} \begin{array}{cc} [\nu_1] & [\nu_2] \\ m_1 & 1 \end{array} \right\rangle, \quad m = 1, \dots, 6 \quad (3.36)$$

$$b_m = \left\langle \begin{array}{c} [\nu] \\ m \end{array} \middle| \begin{array}{c} [\nu], 2 \end{array} \begin{array}{cc} [\nu_1] & [\nu_2] \\ m_1 & 1 \end{array} \right\rangle, \quad m = 1, \dots, 6. \quad (3.37)$$

### Chapter 3. Elements of group theory

---

One has for instance:

$$\mathbf{a} = \begin{pmatrix} 0.4456... \\ 0.7719... \\ 0.0468... \\ 0.0605... \\ -0.2235... \\ -0.3871... \end{pmatrix}, \quad \mathbf{b} = \begin{pmatrix} -0.1420... \\ -0.2459... \\ 0.5283... \\ 0.6820... \\ -0.2093... \\ -0.3625... \end{pmatrix}. \quad (3.38)$$

Observe that

$$\mathbf{a}^T \mathbf{a} = 1, \quad \mathbf{b}^T \mathbf{b} = 1, \quad \mathbf{a}^T \mathbf{b} = 0 \quad (3.39)$$

namely the SDCs already satisfy the orthogonality relations. However no specific relative phase is chosen. The two vectors  $\mathbf{a}$  and  $\mathbf{b}$  are merely two orthogonal random vectors living in a specific plane embedded in  $\mathbb{R}^6$ .

We observe that  $a_6 \neq 0$  and  $b_6 \neq 0$ . We will thus define a unitary transformation  $U$  such that the last component of  $\mathbf{a}' = U\mathbf{a}$  is  $a'_6 = 0$ . This rotation is trivial to obtain. Applying the same rotation on  $\mathbf{b}$  one ends up with

$$\mathbf{a}' = U\mathbf{a} = \begin{pmatrix} \frac{1}{\sqrt{6}} \\ \frac{1}{\sqrt{2}} \\ -\frac{1}{\sqrt{8}} \\ -\sqrt{\frac{5}{24}} \\ 0 \\ 0 \end{pmatrix}, \quad \mathbf{b}' = U\mathbf{b} = \begin{pmatrix} \sqrt{\frac{5}{96}} \\ \sqrt{\frac{5}{32}} \\ \sqrt{\frac{5}{32}} \\ \sqrt{\frac{25}{96}} \\ -\sqrt{\frac{3}{32}} \\ -\sqrt{\frac{9}{32}} \end{pmatrix}. \quad (3.40)$$

Now we note that  $a'_1 > 0$  and  $b'_1 > 0$ , thus the overall phase for each set of SDCs is already satisfied and no more unitary transformation needs to be operated. We thus replace the SDCs in Eq. (3.38) by,

$$\left\langle \begin{matrix} [\nu] \\ m \end{matrix} \middle| \begin{matrix} [\nu], 1 \\ m_1 \end{matrix} \begin{matrix} [\nu_1] & [\nu_2] \\ m_1 & 1 \end{matrix} \right\rangle = a'_m, \quad m = 1, \dots, 6, \quad (3.41)$$

$$\left\langle \begin{matrix} [\nu] \\ m \end{matrix} \middle| \begin{matrix} [\nu], 2 \\ m_1 \end{matrix} \begin{matrix} [\nu_1] & [\nu_2] \\ m_1 & 1 \end{matrix} \right\rangle = b'_m, \quad m = 1, \dots, 6. \quad (3.42)$$

Now we compute the SDCs for  $m_2 = 2$  by proceeding independently for each  $\tau$ , starting from the SDCs given in Eqs. (3.41)-(3.42) and using Eq. (3.33). All phases are already fixed: the overall phase for each set ( $\tau$ ) and the relative phase between both sets.

We can thus state the following rule to fix the relative phase convention between

different sets of SDCs:

*We fix the phase such that the SDCs with  $\tau = 1$  have a vanishing coefficient for the largest possible  $m$ .*

If the multiplicity  $\{\nu_1 \nu_2 \nu\} > 2$  we proceed in the exact same way as above, but fixing the largest possible  $(\{\nu_1 \nu_2 \nu\} - 1)$  coefficients of the SDCs with  $\tau = 1$  to zero, then fixing the largest possible  $(\{\nu_1 \nu_2 \nu\} - 2)$  coefficients of the SDCs with  $\tau = 2$  to zero, etc ...

## 3.2 The Schur-Weyl duality

It is far beyond the scope of this thesis to discuss in full details the Schur-Weyl duality [96, 101]<sup>10</sup>. Here we adopt a very superficial description. The Schur-Weyl duality essentially states that irreps of the symmetric group  $\mathcal{S}_n$  are related to the irreps of the special unitary group  $SU(N)$ , which itself is closely related to the Lie algebra  $\mathfrak{su}(N)$ , as is described in Section 3.3.6. From a practical point of view, it follows that irreps of the Lie algebra  $\mathfrak{su}(N)$  can be labeled by Young diagrams exactly as it was the case for the symmetric group, but with the additional constraint that a Young diagram cannot have more than  $N$  rows. Once this condition is imposed, the machinery developed for the symmetric group applies directly to  $\mathfrak{su}(N)$ . As we will see below, in a Young diagram of an  $\mathfrak{su}(N)$  irrep, any column with  $N$  boxes can be removed. For  $\mathfrak{su}(2)$  for instance, the irrep  $\begin{array}{|c|} \hline \square \\ \hline \end{array}$  corresponding to a totally antisymmetric wave function made of two particles, a singlet state such as  $|\uparrow\downarrow\rangle - |\downarrow\uparrow\rangle$  where  $\{\uparrow, \downarrow\}$  are the two colors of  $\mathfrak{su}(2)$ , is simply represented as  $\bullet$  since the column with 2 boxes can be removed from the Young diagram. Thus, in compact form an irrep  $[\nu]$  of  $\mathfrak{su}(N)$  is actually a set of  $1 \leq k \leq N - 1$  non-ascending integers  $[\nu] = [\nu_1, \nu_2, \dots, \nu_k]$ .

However when using the technology of the symmetric group to study the representation theory of the  $SU(N)$  group (or  $\mathfrak{su}(N)$  Lie algebra) it is often useful to preserve the columns of  $N$  boxes in the Young diagrams. Keeping these “totally antisymmetric columns” corresponds actually to particle conservation. In a tensor product of two irreps, for instance, one forces the conservation of the total number of boxes in the decomposition. This is only necessary when interpreting an  $\mathfrak{su}(N)$  irrep as an irrep of the symmetric group. In Chapter 5, while we will be treating the case of  $N = 3$ , we will often encounter irreps  $[\nu_1, \nu_2, \nu_3]$  with row lengths  $\nu_1 \geq \nu_2 \geq \nu_3 > 0$ . This corresponds to an irrep of  $\mathcal{S}_n$  with  $n = \nu_1 + \nu_2 + \nu_3$  having  $\nu_3$  columns of three boxes, which is reduced to  $[\nu_1 - \nu_3, \nu_2 - \nu_3]$  in the  $\mathfrak{su}(3)$  language. The Dynkin labels (to be introduced below) in the  $\mathfrak{su}(3)$  language are then  $(\nu_1 - \nu_2, \nu_2 - \nu_3)$ .

To convince the reader of the usefulness of preserving the columns of  $N$  boxes, let us provide a simple example. Let us consider a chain (or actually any arrangement on a

<sup>10</sup>And even further beyond my abilities.

### Chapter 3. Elements of group theory

lattice) of 6 spin-1/2 degrees of freedom, and ask the question: what is the dimension of the singlet sector and the dimension of the quintuplet sector? In other words, how many singlets and how many quintuplets are there when decomposing the product  $(S = 1/2)^{\otimes 6}$  as a direct sum of irreps? These questions are of major interest in physics because if the Hamiltonian of the 6 spins is  $SU(2)$  invariant and if one knows *a priori* that the ground state lives in the singlet sector, for instance, then the Hamiltonian only needs to be diagonalized in this specific symmetry sector. The real difficulty is then to find out what is the form of the Hamiltonian in this sector, and the answer to the first question above simply provides the dimension of the effective Hamiltonian in the singlet sector. The first route to answering the questions consists in performing explicitly the tensor product  $(S = 1/2)^{\otimes 6}$  and reading the multiplicities. This method actually answers a more general question since it provides the dimension of every sector  $S = 0, 1, 2, 3$ . We indeed obtain

$$2^{\otimes 6} = 5 \times \mathbf{1} \oplus 9 \times \mathbf{3} \oplus 5 \times \mathbf{5} \oplus \mathbf{7} \quad (3.43)$$

where a spin- $S$  has been denoted by its dimension  $2S + 1$ . One reads out that there are 5 singlets and 5 quintuplets in the tensor product of 6 spin-1/2's. The complete decomposition above, that we will call a Clebsch-Gordan series, can be checked by dimensional-counting:  $2^6 = 5 + 9 \times 3 + 5 \times 5 + 7$ . Another technique which answers the questions above, and *solely* the questions above, is the following one. The total number of singlets, respectively of quintuplets, in the tensor product of 6 spin-1/2 corresponds to the total number of SYTs for the irrep  $[3, 3]$ , respectively the irrep  $[5, 1]$  [86]. The SYTs in each of these cases are given by

$$\begin{array}{|c|c|c|} \hline 1 & 2 & 3 \\ \hline 4 & 5 & 6 \\ \hline \end{array}, \quad \begin{array}{|c|c|c|} \hline 1 & 2 & 4 \\ \hline 3 & 5 & 6 \\ \hline \end{array}, \quad \begin{array}{|c|c|c|} \hline 1 & 3 & 4 \\ \hline 2 & 5 & 6 \\ \hline \end{array}, \quad \begin{array}{|c|c|c|} \hline 1 & 2 & 5 \\ \hline 3 & 4 & 6 \\ \hline \end{array}, \quad \begin{array}{|c|c|c|} \hline 1 & 3 & 5 \\ \hline 2 & 4 & 6 \\ \hline \end{array} \quad (3.44)$$

and

$$\begin{array}{|c|c|c|c|c|} \hline 1 & 2 & 3 & 4 & 5 \\ \hline 6 & & & & \\ \hline \end{array}, \quad \begin{array}{|c|c|c|c|c|} \hline 1 & 2 & 3 & 4 & 6 \\ \hline 5 & & & & \\ \hline \end{array}, \quad \begin{array}{|c|c|c|c|c|} \hline 1 & 2 & 3 & 5 & 6 \\ \hline 4 & & & & \\ \hline \end{array}, \quad \begin{array}{|c|c|c|c|c|} \hline 1 & 2 & 4 & 5 & 6 \\ \hline 3 & & & & \\ \hline \end{array}, \quad \begin{array}{|c|c|c|c|c|} \hline 1 & 3 & 4 & 5 & 6 \\ \hline 2 & & & & \\ \hline \end{array}. \quad (3.45)$$

Notice that the irrep  $[3, 3]$  is the singlet irrep since each column of 2 boxes could be removed

$$\begin{array}{|c|c|} \hline & \\ \hline & \\ \hline \end{array} \equiv \bullet \rightarrow S = 0. \quad (3.46)$$

In fact, for  $\mathfrak{su}(2)$ , the spin  $S$  can be obtained from the Young diagram as  $S = (\nu_1 - \nu_2)/2$  where  $\nu_1$  and  $\nu_2$  are the lengths of the first and second rows, respectively, in the Young diagram. It follows that the irrep  $[5, 1]$  is actually the quintuplet irrep,

$$\begin{array}{|c|c|c|c|} \hline & & & \\ \hline & & & \\ \hline \end{array} \equiv \begin{array}{|c|c|c|c|} \hline & & & \\ \hline & & & \\ \hline \end{array} \rightarrow S = 2. \quad (3.47)$$

One thus concludes that one *needs* to preserve the total number of boxes between the Kronecker product representation  $2^{\otimes 6}$  and the decomposition into irreps to obtain sensible results, in particular one needs to keep columns of  $N$  boxes in the Young

diagram if one aims at performing calculations related to the theory of the symmetric group. This conservation of boxes is a key aspect of the implementation of the  $SU(N)$  symmetry in ED and DMRG codes [57, 86–89].

## 3.3 The $\mathfrak{su}(N)$ Lie algebra

### 3.3.1 Preliminary definitions

A *Lie algebra*  $\mathcal{L}$  (over a field  $K$ ) is a  $K$ -vector space  $\mathfrak{g}$  with a bilinear operator  $[\cdot, \cdot] : \mathfrak{g} \times \mathfrak{g} \rightarrow \mathfrak{g}$  such that:

1.  $[x, x] = 0, \forall x \in \mathfrak{g}$ ,
2. the Jacobi identity is satisfied:  $[x, [y, z]] + [y, [z, x]] + [z, [x, y]] = 0, \forall x, y, z \in \mathfrak{g}$ .

The bilinear operator  $[\cdot, \cdot]$  is called a *Lie product*, a *Lie bracket* or a *commutator*. A Lie algebra is said to be *abelian* if  $[x, y] = 0 \forall x, y \in \mathcal{L}$ . A non-empty subalgebra  $\mathcal{L}'$  of  $\mathcal{L}$  is said to be *proper* if  $\mathcal{L} \setminus \mathcal{L}'$  is not empty and it is said to be *invariant* if  $[x, y] \in \mathcal{L}' \forall x \in \mathcal{L}', y \in \mathcal{L}$ . Finally a Lie algebra is said to be *simple* if it is not Abelian and if it does not possess a proper invariant Lie subalgebra. The Lie algebra  $\mathfrak{su}(N)$ , on which we should focus later on, is a simple Lie algebra<sup>11</sup>.

Here we will specialize to finite-dimensional Lie algebras, for which Ado's theorem holds.

**Ado's theorem:** Every finite-dimensional Lie algebra  $\mathcal{L}$  over a field  $K$  is isomorphic to a Lie algebra of matrices with the Lie bracket being the usual matrix commutator.

Thus, in what follows one should simply study the matrix Lie algebra, for which explicit calculations can be performed easily.

Let us introduce two more important concepts. A  $d$ -dimensional *representation* of a Lie algebra  $\mathcal{L}$  is a matrix representation  $R : \mathcal{L} \rightarrow K^{d \times d}$  such that  $R(\cdot)$  itself forms a Lie algebra. A representation  $R$  of a Lie algebra is said to be *irreducible* if it cannot be decomposed into a direct sum of representations. One can now state one of Weyl's theorems.

**Weyl's theorem on complete reducibility:** Every finite-dimensional representation of a semi-simple Lie algebra can be decomposed into a direct sum of irreps.

We are now equipped with the very basics required to understand sufficiently deeply the structure of the  $\mathfrak{su}(N)$  Lie algebra.

<sup>11</sup>The Lie algebra  $\mathfrak{su}(N)$  is actually a semi-simple Lie algebra, meaning that it is a direct sum of simple algebras.

### 3.3.2 The $\mathfrak{su}(N)$ Lie algebra

The  $\mathfrak{su}(N)$  Lie algebra is the real algebra of  $N \times N$  anti-hermitian matrices with vanishing trace. Clearly the set of anti-hermitian matrices is a  $\mathbb{R}$ -vector space, the commutator is closed under the Lie bracket and the Jacobi identity is satisfied. It is easy to see that any traceless anti-hermitian matrix can be written as a linear combination (with real coefficients) of  $N^2 - 1$  basis elements. Thus the Lie algebra  $\mathfrak{su}(N)$  has dimension  $N^2 - 1$ . The Lie algebra  $\mathfrak{su}(N)$  is a subgroup of the  $N^2$ -dimensional Lie algebra  $\mathfrak{u}(N)$  which does not have the condition of vanishing trace. Let us use  $E_{ij}$  to denote the canonical basis of square  $N$ -dimensional real matrices, which form a  $N^2$ -dimensional real Lie algebra, defined as

$$(E_{ij})_{k,l} = \delta_{ik}\delta_{jl}, \quad i, j, k, l = 1, \dots, N. \quad (3.48)$$

The matrix  $E_{ij}$  has zeros everywhere except at row  $i$  and column  $j$  where it is  $(E_{ij})_{i,j} = 1$ . Then a possible basis for  $\mathfrak{su}(N)$  is given by the following matrices:

$$E_{ij} + E_{ji}, \quad 1 \leq i < j \leq N, \quad (3.49)$$

$$-i(E_{ij} - E_{ji}), \quad 1 \leq i < j \leq N, \quad (3.50)$$

and

$$E_{ii} - E_{i+1,i+1}, \quad 1 \leq i < N. \quad (3.51)$$

This indeed defines  $N^2 - 1$  independent elements of the Lie algebra. Notice that  $N - 1$  of them are diagonal, and we shall call this the rank of  $\mathfrak{su}(N)$  [102]. The diagonal elements form the so-called *Cartan subalgebra* and are at the root of the weight diagrams often used in high-energy physics to classify hadrons. Let us now denote by  $\{e_i\}_{i=1}^{N^2-1}$  a generic basis of  $\mathfrak{su}(N)$ . We then define the following matrices,

$$\lambda_i = 2ie_i, \quad i = 1, \dots, N^2 - 1. \quad (3.52)$$

The  $\lambda_i$ 's are hermitian matrices, and, as such, they do not form a Lie algebra. We then define the *generators* of  $\mathfrak{su}(N)$  as

$$t_i = \frac{1}{2}\lambda_i = ie_i, \quad i = 1, \dots, N^2 - 1. \quad (3.53)$$

The *structure constants*  $f_{ijk}$  are real coefficients which define the Lie algebra<sup>12</sup>,

$$[e_i, e_j] = f_{ijk}e_k \quad (3.54)$$

---

<sup>12</sup>The structure constants are real since the Lie algebra is closed under the Lie bracket.

where a sum over the repeated index is implicit. This equation can be reexpressed in terms of the generators of the Lie algebra as

$$[t_i, t_j] = if_{ijk}t_k \quad (3.55)$$

which is the usual form known by physicists for the commutation relations of the generators of the  $\mathfrak{su}(N)$  Lie algebra. Observe that for  $\mathfrak{su}(2)$  the basis elements in Eq. (3.49)-(3.51) indeed correspond to the usual Pauli matrices,

$$\begin{pmatrix} 0 & 1 \\ 1 & 0 \end{pmatrix}, \quad \begin{pmatrix} 0 & -i \\ i & 0 \end{pmatrix}, \quad \begin{pmatrix} 1 & 0 \\ 0 & -1 \end{pmatrix}. \quad (3.56)$$

For  $\mathfrak{su}(N)$  we shall replace the diagonal basis elements in Eq. (3.51) in order the following trace condition to be satisfied,

$$\text{Tr}(\lambda_i \lambda_j) = 2\delta_{ij}, \quad \forall i, j = 1, \dots, N^2 - 1. \quad (3.57)$$

Indeed a convenient consequence of this trace condition is that the new structure constants are totally anti-symmetric in all indices. For  $\mathfrak{su}(3)$  an appropriate set of hermitian matrices  $\lambda_i = 2ie_i$  is given by the Gell-Mann matrices [93],

$$\lambda_1 = \begin{pmatrix} 0 & 1 & 0 \\ 1 & 0 & 0 \\ 0 & 0 & 0 \end{pmatrix}, \quad \lambda_2 = \begin{pmatrix} 0 & -i & 0 \\ i & 0 & 0 \\ 0 & 0 & 0 \end{pmatrix}, \quad \lambda_3 = \begin{pmatrix} 1 & 0 & 0 \\ 0 & -1 & 0 \\ 0 & 0 & 0 \end{pmatrix}, \quad (3.58)$$

$$\lambda_4 = \begin{pmatrix} 0 & 0 & 1 \\ 0 & 0 & 0 \\ 1 & 0 & 0 \end{pmatrix}, \quad \lambda_5 = \begin{pmatrix} 0 & 0 & -i \\ 0 & 0 & 0 \\ i & 0 & 0 \end{pmatrix}, \quad \lambda_6 = \begin{pmatrix} 0 & 0 & 0 \\ 0 & 0 & 1 \\ 0 & 1 & 0 \end{pmatrix}, \quad \lambda_7 = \begin{pmatrix} 0 & 0 & 0 \\ 0 & 0 & -i \\ 0 & i & 0 \end{pmatrix}, \quad (3.59)$$

$$\lambda_8 = \frac{1}{\sqrt{3}} \begin{pmatrix} 1 & 0 & 0 \\ 0 & 1 & 0 \\ 0 & 0 & -2 \end{pmatrix}. \quad (3.60)$$

The matrices  $\lambda_i$ ,  $i = 1, 2, 3$  are simply obtained by embedding the Pauli matrices in  $3 \times 3$  matrices. The matrices  $\lambda_i$ ,  $i = 4, \dots, 7$  are obtained by putting 1 or  $-i$  at all possible locations in the third column, except in the last row. Finally  $\lambda_8$  is simply obtained by imposing the trace condition in Eq. (3.57). The same procedure can be followed to derive the generalized  $\mathfrak{su}(N)$  Gell-Mann matrices from the  $\mathfrak{su}(N-1)$  Gell-Mann matrices when  $N > 3$  [93]. The  $N$ -dimensional matrix representation  $e_i = -i\lambda_i/2$  where  $\lambda_i$  are the Gell-Mann matrices is called the *defining* representation, or the fundamental representation of  $\mathfrak{su}(N)$ . Thanks to the trace condition in Eq. (3.57) the structure constants are totally antisymmetric in all indices and can be easily computed

### Chapter 3. Elements of group theory

---

as follows

$$f_{ijk} = \frac{1}{4i} \text{Tr}([\lambda_i, \lambda_j] \lambda_k). \quad (3.61)$$

Another important representation that we can introduce without further notions is the adjoint representation. It is the representation for which the generators are the structure constants themselves,

$$(t_i^{\text{adj}})_{j,k} = -if_{ijk}. \quad (3.62)$$

Obviously the dimension of the adjoint representation corresponds to the dimension of the underlying Lie algebra, namely  $N^2 - 1$ .

From the  $\mathfrak{su}(3)$  generators  $t_i$  in the fundamental representation one can build three sets of raising and lowering operators,

$$u^\pm = t_1 \pm it_2, \quad v^\pm = t_4 \pm it_5, \quad w^\pm = t_6 \pm it_7 \quad (3.63)$$

where  $u^- = (u^+)^\dagger$ ,  $v^- = (v^+)^\dagger$  and  $w^- = (w^+)^\dagger$ . For  $\mathfrak{su}(N)$  in general one defines  $N(N-1)/2$  sets of raising and lowering operators by proceeding similarly. The remaining operators are the  $N-1$  diagonal operators. We define the Cartan operators as,

$$h_1 = t_3, \quad h_2 = \frac{2}{\sqrt{3}} t_8. \quad (3.64)$$

The definition of raising and lowering operators allows us to circulate from one state to the other, exactly as one circulates from one state to the other by applying  $S^\pm$  in the case of  $\mathfrak{su}(2)$ . Moreover, since there are  $N-1$  diagonal generators one can illustrate how the operators act in the Hilbert space of states using a weight diagram. Figure 3.3(a) shows the weight diagram of  $\mathfrak{su}(3)$  in the defining representation where we have used the three “colors”  $A$ ,  $B$  and  $C$  to denote the states of the irrep. The state  $A$  is called the highest weight state since the application of any raising operator on  $A$  vanishes.

Now we will define a new set of generators widely used in physics and which will appear to be “maximally symmetric”. Let us introduce the operators  $\mathcal{S}^{\alpha\beta}$  where  $\alpha, \beta = 1, \dots, N$  are the  $\mathfrak{su}(N)$  color indices. For the case of  $\mathfrak{su}(3)$  developed above we take  $\mathcal{S}^{12} = u^+$ ,  $\mathcal{S}^{13} = v^+$ ,  $\mathcal{S}^{23} = w^+$  as well as  $\mathcal{S}^{\beta\alpha} = (\mathcal{S}^{\alpha\beta})^\dagger$ . We further define the diagonal elements  $\mathcal{S}^{\alpha\alpha}$ ,  $\alpha = 1, \dots, N$  using the Cartan generators,

$$h_a = \sum_{\alpha=1}^N (h_a)_{\alpha,\alpha} \mathcal{S}^{\alpha\alpha}, \quad a = 1, \dots, N-1. \quad (3.65)$$

Moreover, in order  $\mathcal{S}^{\alpha\beta}$ ,  $\alpha, \beta = 1, \dots, N$  to have the good number of elements we impose the overall trace condition,

$$\sum_{\alpha=1}^N \mathcal{S}^{\alpha\alpha} = 0. \quad (3.66)$$



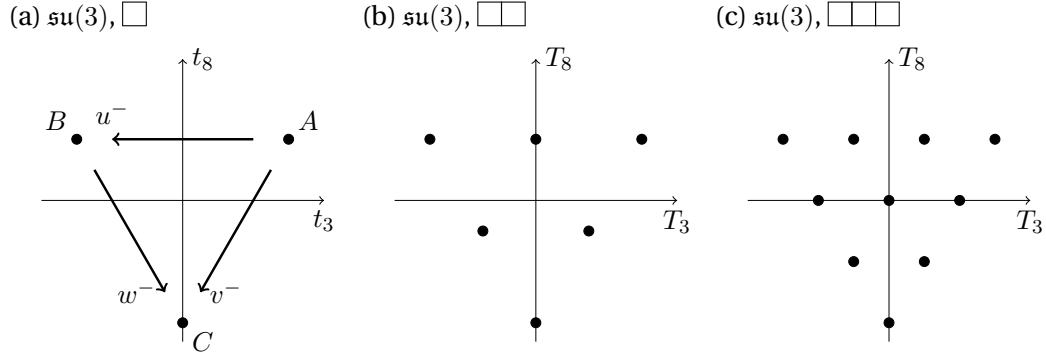


Figure 3.3:  $\mathfrak{su}(3)$  weight diagrams of (a) the fundamental irrep, (b) the 2-box symmetric irrep and (c) the 3-box symmetric irrep. The generators for (b) and (c) are given in Appendix F.

Inverting Eq. (3.65)-(3.66) one ends up with explicit expressions for the diagonal operators  $S^{\alpha\alpha}$ . For  $N = 3$  for instance one has,

$$S^{11} = h_1 + \frac{1}{2}h_2, \quad S^{22} = -h_1 + \frac{1}{2}h_2, \quad S^{33} = -h_2. \quad (3.67)$$

The commutation relations satisfied by the generators  $S^{\alpha\beta}$  are easily obtained by direct calculation and are given by

$$[S^{\alpha\beta}, S^{\mu\nu}] = \delta^{\mu\beta} S^{\alpha\nu} - \delta^{\alpha\nu} S^{\mu\beta}. \quad (3.68)$$

These commutation relations are called the  $\mathfrak{su}(N)$ -commutation relations as they are true for any  $N$ . Because of the structure of  $S^{\alpha\beta}$  one observes also that the bilinear operator is written as,

$$2\mathbf{t} \cdot \mathbf{t} \equiv 2 \sum_{i=1}^{N^2-1} t_i t_i = S^{\alpha\beta} S^{\beta\alpha} \equiv \text{Tr}(SS) \quad (3.69)$$


where a sum over the color indices is implicit in the next to last expression.

### 3.3.3 Irreducible representations

The other irreps of the  $\mathfrak{su}(N)$  Lie algebra can be labeled with Young diagrams with no more than  $N$  rows. This constraint comes from the fact that a column of  $p$  boxes corresponds to  $p$ -particle states which are antisymmetric in the  $N$  colors. Thus, any column of  $N$  boxes in a Young diagram can be safely removed since it corresponds to a singlet state, a totally antisymmetric combination of  $N$  colors. We have already encountered the fundamental irrep, which is denoted by a Young diagram with a single box  $\square$  as well as the adjoint irrep. The Young diagram of the adjoint irrep is made of

### Chapter 3. Elements of group theory

---

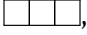
two columns, one with  $N - 1$  boxes and one with a single box. For instance for  $\mathfrak{su}(3)$  it is .

The dimension of an irrep can be obtained from the shape of the Young diagram. We have already introduced the hook length  $l_i$  of a box defined as the number of boxes in the Young diagram situated to the right of that box, plus the number of boxes situated below that box, plus one for the box itself. We also define the algebraic distance  $\gamma_i$  of a box as the distance from the main diagonal to that box, counted positively when going to the right and negatively when going downwards [86]. Then, the dimension of an  $\mathfrak{su}(N)$  irrep is given by

$$D = \prod_i \frac{N + \gamma_i}{l_i} \quad (3.70)$$

where the product is over all boxes of the Young diagram. For instance, the dimension of the fundamental irrep is  $D = N/1 = N$  as expected while the dimension of the adjoint irrep is

$$D = \frac{N!(N+1)}{N(N-2)!} = N^2 - 1 \quad (3.71)$$

as expected. In fact, the  $D$  states of a given irrep can be constructed explicitly using the fact that boxes in the same row of the Young diagram are symmetrized while boxes in the same column are antisymmetrized. For instance, the states of the 3-box symmetric irrep of  $\mathfrak{su}(3)$  corresponding to a Young diagram with three boxes in the first row, , are given by

$$\begin{aligned} &|AAA\rangle \\ &|BBB\rangle \\ &|CCC\rangle \\ &\frac{1}{\sqrt{3}} (|AAB\rangle + |ABA\rangle + |BAA\rangle) \\ &\frac{1}{\sqrt{3}} (|ABB\rangle + |BAB\rangle + |BBA\rangle) \\ &\frac{1}{\sqrt{3}} (|AAC\rangle + |ACA\rangle + |CAA\rangle) \\ &\frac{1}{\sqrt{3}} (|ACC\rangle + |CAC\rangle + |CCA\rangle) \\ &\frac{1}{\sqrt{3}} (|BBC\rangle + |BCB\rangle + |CBB\rangle) \\ &\frac{1}{\sqrt{3}} (|BCC\rangle + |CBC\rangle + |CCB\rangle) \\ &\frac{1}{\sqrt{6}} (|ABC\rangle + |ACB\rangle + |BAC\rangle + |BCA\rangle + |CAB\rangle + |CBA\rangle). \end{aligned} \quad (3.72)$$

These states indeed correspond to all possible fully symmetric states with three particles (boxes) and three colors. From Eq. (3.70) we obtain the dimension of the 3-box symmetric irrep,

$$D = \frac{\begin{array}{|c|c|c|} \hline 3 & 4 & 5 \\ \hline \end{array}}{\begin{array}{|c|c|c|} \hline 3 & 2 & 1 \\ \hline \end{array}} = \frac{3 \times 4 \times 5}{3 \times 2 \times 1} = 10 \quad (3.73)$$

in agreement with the above wave functions. It is sometimes convenient to denote an irrep by its dimension, which we write in boldface characters. For instance  $\mathbf{10} \equiv \begin{array}{|c|c|c|} \hline & & \\ \hline \end{array}$ . However this notation is not ideal as different irreps can have the same dimension. For instance, the (complex) conjugate irrep of an irrep has the same dimension<sup>13</sup>. The Young diagram of the (complex) conjugate irrep of a given irrep is obtained as follows: replace each column of length  $\nu_i^T$  of the irrep  $[\nu]$  by a column with  $N - \nu_i^T$  boxes. Then flip the obtained diagram around the vertical axis to obtain a valid Young diagram. For instance one has, for  $\mathfrak{su}(3)$ ,

$$\overline{\mathbf{10}} = \begin{array}{|c|c|c|} \hline & & \\ \hline \end{array}. \quad (3.74)$$

An irrep is said to be self-conjugate if it is conjugate to itself. The adjoint irrep, in particular, is self-conjugate. For  $\mathfrak{su}(3)$ , a self-conjugate irrep has as many columns with two boxes as columns with one box. An alternative and convenient notation for irreps of  $\mathfrak{su}(N)$  is through the *Dynkin label*, which counts the number of columns with  $i$  boxes in the Young diagram. For an irrep  $[\nu]$  the Dynkin label is thus given by  $(\nu_1 - \nu_2, \nu_2 - \nu_3, \dots, \nu_{N-1})$ . For instance  $\mathbf{10} \equiv \begin{array}{|c|c|c|} \hline & & \\ \hline \end{array} \equiv (3, 0)$ . The Dynkin label of the conjugate irrep of an irrep is thus simply obtained by reversing the Dynkin label:

$$\begin{array}{|c|c|c|} \hline & & \\ \hline \end{array} = (3, 0) \longrightarrow \begin{array}{|c|c|c|} \hline & & \\ \hline \end{array} = (0, 3) \quad (3.75)$$

and a self-conjugate irrep must then be invariant under this transformation of the Dynkin label,

$$\begin{array}{|c|c|} \hline & \\ \hline \end{array} = (1, 1). \quad (3.76)$$

To each irrep  $[\nu]$  we associate a set of generators  $T_i$ ,  $i = 1, \dots, N^2 - 1$  which are  $D$ -dimensional hermitian traceless matrices and which satisfy the same algebra as the generators in the fundamental irrep, namely they satisfy Eq. (3.55) with the structure constants given in Eq. (3.61). Moreover we impose the following normalization condition [103],

$$\text{Tr}(T_i T_j) = \frac{DC_2}{N^2 - 1} \delta_{ij} \quad (3.77)$$

where  $C_2$  is the eigenvalue of the quadratic Casimir operator [104]

$$C_2 = \mathbf{T} \cdot \mathbf{T} = \frac{1}{2} \left( n \left( N - \frac{n}{N} \right) + \sum_i \nu_i^2 - \sum_j (\nu_j^T)^2 \right) \quad (3.78)$$

<sup>13</sup>For  $\mathfrak{su}(N > 3)$  there are irreps not related by complex conjugation which do have the same dimension.

### Chapter 3. Elements of group theory

---

and  $n$  is the total number of boxes in the the Young diagram of the irrep  $[\nu]$ . The normalization factor in Eq. (3.77) is called the Dynkin index of the irrep  $[\nu]$  of  $\mathfrak{su}(N)$ .

The  $D$  states of the irrep  $[\nu]$  can be placed on a  $(N - 1)$ -dimensional weight diagram according to the eigenvalues of the diagonal generators. For instance Fig. 3.3(c) shows the 10 states of the irrep  $\square\square\square$  of  $\mathfrak{su}(3)$  given in Eq. (3.72) in their weight diagram. One can again circulate from one state to the other by acting with the raising and lowering operators  $U^\pm$ ,  $V^\pm$  and  $W^\pm$  defined in the same fashion as in the fundamental irrep (see Eq. (3.63)). Moreover one follows the same steps as in the fundamental irrep to define the operators  $\mathcal{S}^{\alpha\beta}$ . One thus has  $\mathcal{S}^{12} = U^+$ ,  $\mathcal{S}^{13} = V^+$ ,  $\mathcal{S}^{23} = W^+$  and one should replace Eq. (3.65) by

$$H_a = \sum_{\alpha=1}^N (h_a)_{\alpha,\alpha} \mathcal{S}^{\alpha\alpha}, \quad a = 1, \dots, N - 1 \quad (3.79)$$

where  $H_a$  is the Cartan generator defined as in the fundamental irrep. Explicit expressions of the generators  $T_i$ ,  $i = 1, \dots, 8$  of  $\mathfrak{su}(3)$  in the 2-box and 3-box symmetric irreps  $\square\square$  and  $\square\square\square$ , respectively, are given in Appendix F.

#### 3.3.4 The Itzykson-Nauenberg rules

Starting from the fundamental irrep, any irrep of  $\mathfrak{su}(N)$  can be constructed by adding one box at a time until the obtained Young diagram has the right shape. For instance, taking the tensor product of two fundamental irreps of  $\mathfrak{su}(3)$  one obtains two different irreps,

$$\square \otimes \square = \begin{array}{|c|} \hline \square \\ \hline \end{array} \oplus \square\square. \quad (3.80)$$

One can then obtain all irreps of  $\mathfrak{su}(3)$  with three boxes by multiplying the result with another fundamental irrep,

$$\square \otimes \square \otimes \square = \left( \begin{array}{|c|} \hline \square \\ \hline \end{array} \oplus \square\square \right) \otimes \square = \bullet \oplus 2 \begin{array}{|c|c|} \hline \square & \square \\ \hline \end{array} \oplus \square\square\square \quad (3.81)$$

where  $\bullet$  denotes the singlet irrep of  $\mathfrak{su}(3)$  and corresponds to a Young diagram with three boxes in a single column. Equation (3.81) can be checked with the use of Eq. (3.70). We indeed have  $3 \times 3 \times 3 = 1 + 2 \times 8 + 10$ . We observe that the adjoint irrep appears twice in the product of three fundamental irreps. In fact, the number of times that an irrep  $[\nu]$  with  $n$  boxes appears in the tensor product of  $n$  fundamental irreps corresponds to  $h^{[\nu]}$  given in Eq. (3.15), the total number of SYTs for the irrep  $[\nu]$  of  $\mathcal{S}_n$  [86].

More generally, two arbitrary irreps  $[\nu_1]$  and  $[\nu_2]$  of  $\mathfrak{su}(N)$  can be multiplied and decom-

posed into a direct sum of irreps

$$[\nu_1] \otimes [\nu_2] = \sum_{[\nu]} (\nu_1 \nu_2 \nu) [\nu] \quad (3.82)$$

where  $(\nu_1 \nu_2 \nu)$  is the *outer multiplicity* of the irrep  $[\nu]$  in the tensor product of  $[\nu_1]$  and  $[\nu_2]$  [92]. The decomposition is called the Clebsch-Gordan series and is obtained by following the Itzykson-Nauenberg rules, which are slightly different from the Littlewood-Richardson rules of the permutation group [105].

1. Select among  $[\nu_1]$  and  $[\nu_2]$  the most complicated Young diagram as the base.
2. Fill the other Young diagram with  $a$ 's in the first row,  $b$ 's in the second row,  $c$ 's in the third row, etc...
3. Enlarge the base diagram by moving the  $a$ 's to all possible positions satisfying the two following constraints: i) two  $a$ 's should not stand in the same column; ii) the diagram obtained at each step should be a valid Young diagram for  $\mathfrak{su}(N)$ , namely it should have at most  $N$  rows, and row lengths are non-ascending from top to bottom.
4. Perform similarly for all  $b$ 's with the following additional constraint: iii) when going through the Young diagram from right to left and from top to bottom, the total number of  $b$ 's should never exceed the total number of  $a$ 's.
5. If two diagrams are identical (same shape and same letters placed at the same locations), then only one instance should be kept.
6. Proceed again to steps 4 and 5 for all  $c$ 's,  $d$ 's etc ... until the resultant diagrams all contain  $n$  boxes. At each step, when counting from right to left and from top to bottom, the total number of  $c$ 's should not exceed the total number of  $b$ 's, the total number of  $d$ 's should no exceed the total number of  $c$ 's etc ...
7. Once all boxes containing letters are placed, keep all diagrams for which the pattern of letters is different (if two Young diagrams have the same shape but the pattern of letters is different, then both instances should be kept).
8. Remove all letters and remove all columns with  $N$  boxes.

When  $N = 2$  the Itzykson-Nauenberg rules reduce to the simple rules for the multiplication of angular momenta,  $j_1 \otimes j_2 = |j_1 - j_2| \oplus \dots \oplus (j_1 + j_2)$  where angular momentum  $j$  corresponds to a Young diagram made of a single row with  $2j$  boxes. When  $N > 2$  however the rules are more sophisticated and, in particular, they allow for a non-trivial

outer multiplicity: a given irrep  $[\nu]$  can appear more than once in the tensor product of two irreps  $[\nu_1]$  and  $[\nu_2]$ . For instance in  $\mathfrak{su}(3)$  one has

$$\begin{array}{|c|c|} \hline & \\ \hline \end{array} \otimes \begin{array}{|c|c|} \hline & \\ \hline \end{array} = \bullet \oplus 2 \begin{array}{|c|c|} \hline & \\ \hline \end{array} \oplus \begin{array}{|c|c|c|} \hline & & \\ \hline \end{array} \oplus \begin{array}{|c|c|c|} \hline & & \\ \hline \end{array} \oplus \begin{array}{|c|c|c|c|} \hline & & & \\ \hline \end{array}. \quad (3.83)$$

The adjoint irrep of  $\mathfrak{su}(3)$  appears twice in the tensor product of two adjoint irreps.

#### 3.3.5 The Clebsch-Gordan coefficients

The CGCs are closely related to the Clebsch-Gordan series. Indeed according to Eq. (3.82) the Kronecker product (or tensor product, or direct product) representation  $[\nu_1] \otimes [\nu_2]$  is a reducible representation of  $\mathfrak{su}(N)$ . The CGCs are thus the recombination coefficients which allow us to pass from the tensor product representation to the different irreps. Denoting by  $|\nu_i, m_i\rangle$ ,  $m_i = 1, \dots, \dim([\nu_i])$  for  $i = 1, 2$  the states of the irrep  $[\nu_i]$  then the states  $|\nu, m, \tau\rangle$  of the  $\tau$ -th irrep  $[\nu]$  appearing in the decomposition (3.82),  $\tau = 1, \dots, (\nu_1 \nu_2 \nu)$ , and  $m = 1, \dots, \dim([\nu])$ , are given by<sup>14</sup>

$$|\nu, m, \tau\rangle = \sum_{m_1, m_2} C_{[\nu_1], m_1, [\nu_2], m_2}^{[\nu], m, \tau} |[\nu_1], m_1; [\nu_2], m_2\rangle \quad (3.84)$$

where  $|\nu_1, m_1; [\nu_2], m_2\rangle \equiv |[\nu_1], m_1\rangle \otimes |[\nu_2], m_2\rangle$  and where  $C_{[\nu_1], m_1, [\nu_2], m_2}^{[\nu], m, \tau}$  are the CGCs. The CGCs are merely a change of basis from the tensor-product basis to the irreducible basis and one shall take the following normalization conditions,

$$\sum_{m_1, m_2} (C_{[\nu_1], m_1, [\nu_2], m_2}^{[\nu], m, \tau})^* C_{[\nu_1], m_1, [\nu_2], m_2}^{[\nu'], m', \tau'} = \delta_{[\nu], [\nu']} \delta_{m, m'} \delta_{\tau, \tau'}, \quad (3.85)$$

$$\sum_{[\nu], m, \tau} (C_{[\nu_1], m_1, [\nu_2], m_2}^{[\nu], m, \tau})^* C_{[\nu_1], m'_1, [\nu_2], m'_2}^{[\nu], m, \tau} = \delta_{m_1, m'_1} \delta_{m_2, m'_2}. \quad (3.86)$$

Moreover, for  $\mathfrak{su}(N)$  the CGCs can be chosen to be real and we shall do so in what follows. The explicit calculation of CGCs being a standard exercise for  $\mathfrak{su}(2)$  and being well-documented for  $\mathfrak{su}(N \geq 2)$  we shall not provide further details [92, 106–113]. We should also point out Ref. [85] which provides an efficient computer implementation of the calculation of the CGCs for  $\mathfrak{su}(N)$ .

Let us now shortly come back to the generators of  $\mathfrak{su}(N)$  in a specific irrep. Denoting by  $T_j^{[\nu_i]}$ ,  $j = 1, \dots, N^2 - 1$  the generators in the irrep  $[\nu_i]$ ,  $i = 1, 2$  of  $\mathfrak{su}(N)$ , and assuming that condition (3.77) is satisfied, the generators in the Kronecker product representation  $[\nu_1] \otimes [\nu_2]$  can simply be obtained as

$$T_j^{[\nu_1] \otimes [\nu_2]} = T_j^{[\nu_1]} \otimes \mathbb{1} + \mathbb{1} \otimes T_j^{[\nu_2]}, \quad j = 1, \dots, N^2 - 1. \quad (3.87)$$

<sup>14</sup>If  $(\nu_1 \nu_2 \nu) = 1$  for a given irrep  $[\nu]$  one often omits the index  $\tau$  which can take a single value.

The generators  $T_j^{[\nu]}$  in the different irreps  $[\nu]$  appearing in the tensor product of  $[\nu_1]$  with  $[\nu_2]$  are then extracted by performing the change of basis using the CGCs. This method ensures that the new generators satisfy Eq. (3.77). As a consequence, a straightforward procedure to obtain the generators of  $\mathfrak{su}(N)$  in a given irrep  $[\nu]$  having  $n$  boxes in the Young diagram with the good normalization convention in Eq. (3.77) is to start from the generators in the fundamental irrep, which are obtained from the generalized Gell-Mann matrices, and to perform  $n - 1$  successive Kronecker products with a fundamental irrep followed by a rotation given by the CGCs, and keeping only the irreps in the chain leading from  $\square$  to  $[\nu]$ .

#### 3.3.6 The relationship to the Lie group $SU(N)$

All over this section we have discussed the representation theory of the Lie algebra  $\mathfrak{su}(N)$ . However, physicists mainly talk about  $SU(N)$  Heisenberg models, for instance, rather than  $\mathfrak{su}(N)$  Heisenberg models, so what is the relationship? The special unitary group  $SU(N)$  is the Lie group of  $N$ -dimensional unitary matrices with unit determinant<sup>15</sup>. It is a group as it satisfies all properties of a group: closed under matrix multiplication, associative, existence of an identity element (the unit matrix), and existence of an inverse element for any element of the group. It is a *Lie* group because it is a smooth manifold [101, 114]. It appears that the elements of  $SU(N)$  are then smooth functions of  $N^2 - 1$  real parameters  $\mathbf{x} = (x_1, \dots, x_{N^2-1})$ , the origin  $\mathbf{x} = 0$  corresponding to the identity element  $U(\mathbf{x} = 0) = \mathbb{1}$ . For any matrix  $U \in SU(N)$  one then has [93]

$$\left. \frac{\partial}{\partial x_k} \right|_{\mathbf{x}=0} U_{i,j}(\mathbf{x}) = -i(t_k)_{i,j}, \quad k = 1, \dots, N^2 - 1, \quad i, j = 1, \dots, N \quad (3.88)$$

where  $t_k$ ,  $k = 1, \dots, N^2 - 1$  are the generators of the Lie algebra  $\mathfrak{su}(N)$  in the fundamental irrep, and we recall that  $-it_k = e_k$  forms the Lie algebra  $\mathfrak{su}(N)$  as defined in the above sections. The generators of the Lie algebra thus span, or *generate*, the tangent space of  $SU(N)$  at the identity<sup>16</sup>.

When looking at a spin Hamiltonian such as the standard Heisenberg model, one writes the Hamiltonian in terms of the spin operators  $S^x$ ,  $S^y$  and  $S^z$  which are the generators of the Lie algebra  $\mathfrak{su}(2)$  in the spin- $S$  irrep and which, through the exponential map, generate infinitesimal  $SU(2)$  rotations. The Hamiltonian, denoted

$$\mathcal{H} = \mathbf{S}_1 \cdot \mathbf{S}_2 \equiv \sum_{\alpha=x,y,z} S_1^\alpha S_2^\alpha \quad (3.89)$$

is then invariant under  $SU(2)$  rotations, and it sounds reasonable to call this model the  $SU(2)$  Heisenberg model. We shall extend this model to  $\mathfrak{su}(N)$  (or  $SU(N)$ ) by using the

<sup>15</sup> $SU(N)$  is thus the subgroup of  $U(N)$  which is connected to the identity.

<sup>16</sup>The tangent space at the identity,  $T_e SU(N) = \text{Lie}(SU(N))$  actually *defines* a Lie algebra  $\text{Lie}(SU(N))$  called the Lie algebra of  $SU(N)$  and denoted  $\mathfrak{su}(N)$ .

### Chapter 3. Elements of group theory

---

generators of  $\mathfrak{su}(N)$  in a given irrep  $[\nu]$  and define the  $SU(N)$  Heisenberg model as

$$\mathcal{H} = 2\mathbf{T}_1 \cdot \mathbf{T}_2 = \mathcal{S}_1^{\alpha\beta} \mathcal{S}_2^{\beta\alpha} = \text{Tr}(\mathcal{S}_1 \mathcal{S}_2). \quad (3.90)$$



## 4 $SU(N)$ AKLT models

The Affleck-Kennedy-Lieb-Tasaki (AKLT) model derived in 1987 has been of great importance to understanding more deeply the structure of the spin-1 Heisenberg chain, in particular the gapped spectrum and the topologically protected edge states [115, 116]. It was the first exactly solvable point in the phase diagram of the bilinear-biquadratic spin-1 chain for which the existence of a finite gap could be rigorously demonstrated, and as such was a key model to confirm Haldane’s conjecture on spin- $S$  Heisenberg chains [31, 32].

With the advent of the matrix product state (MPS) formalism, the AKLT wave function could be reinterpreted in a very convenient fashion, making use of matrices of CGCs. In particular, the existence of a finite gap follows from the finite correlation length which can be extracted from the transfer matrix of the MPS, and the spin-1/2 edge states in an open chain are nothing but traces of the building blocks of the wave function.

Given the usefulness of the AKLT wave function, it was extended in many different directions, either by adapting the spin values, upgrading the lattice to higher dimensions or changing the symmetry group of the local degrees of freedom. In this respect, and motivated by the possible experimental realizations with ultracold atoms loaded in optical lattices, the extension to the  $SU(N)$  group has been an active field of research for several years [45, 117–121]. The protection of the edge states was studied and it was shown that, on a one-dimensional chain, there are  $N - 1$  gapped topological phases, generalizing the “Haldane phase” in the  $SU(2)$  spin-1 chain [122]. More generally the presence of an AKLT model gives insights on a possible gapped spectrum at the corresponding Heisenberg point, provided the AKLT and Heisenberg points are close enough. Deriving AKLT models for  $SU(N)$  spin chains is thus an excellent starting point to understand the extension of Haldane’s conjecture to  $SU(N)$  chains [123].

In this chapter we present a practical method to construct  $SU(N)$  AKLT wave functions and their parent Hamiltonians. We show that the variety of AKLT models is much wider than what has been studied so far. In particular we demonstrate that for the

same physical spin on each site one can derive several AKLT wave functions possessing different types of edge modes. To provide an illustrative example we study in Section 4.2 a spin-1 AKLT chain having spin-1 edge states, and we show that it belongs to a trivial phase separated from the Haldane phase by a continuous phase transition. We then turn to the case of  $SU(N)$  and, in anticipation of Chapter 5 we look at an  $SU(3)$  AKLT Hamiltonian for the 3-box symmetric irrep at each site. This model was first derived in Refs. [117, 118] but we present here an optimal and useful representation of the wave function. The new construction of the AKLT wave function will be key to the understanding of the structure of the spectrum of the 3-box symmetric Heisenberg chain in Chapter 5.

The material covered in this chapter was published in Ref. [56].

### 4.1 Generic construction of $SU(N)$ AKLT models

#### 4.1.1 AKLT states

An AKLT wave function is a valence-bond solid (VBS) state: the wave function is made of singlets on every bond of the lattice. From now on, we focus on the one-dimensional case, but most of the results can be extended to higher dimensions. To construct an AKLT wave function with a physical irrep  $\mathcal{P}$  on each site of the lattice, we select two virtual irreps  $\mathcal{V}_L$  and  $\mathcal{V}_R$  such that the physical irrep belongs to the tensor product of  $\mathcal{V}_L$  with  $\mathcal{V}_R$ . This ensures that, if one puts two virtual irreps  $\mathcal{V}_L, \mathcal{V}_R$  on each physical site, one is able to project them onto the physical irrep. To impose the formation of singlets on every bond, one must also ensure that the singlet irrep belongs to the tensor product of  $\mathcal{V}_L$  with  $\mathcal{V}_R$ . This is indeed the case provided that  $\mathcal{V}_L$  and  $\mathcal{V}_R$  are conjugate to each other. If the two virtual irreps  $\mathcal{V}_L, \mathcal{V}_R$  are not the same, then there are two ways of combining the virtual irreps on neighboring sites into a singlet bond, as shown in Fig. 4.1(a). This leads to two AKLT wave functions which break reflection symmetry. In what follows we focus on the case where the virtual irrep is self-conjugate,  $\mathcal{V} \equiv \mathcal{V}_L = \mathcal{V}_R$  which ensures that the AKLT wave function does not break reflection symmetry. The unique AKLT state with physical irrep  $\mathcal{P}$  and virtual irrep  $\mathcal{V}$  shown in Fig. 4.1(b) is denoted

$$|\text{AKLT}\rangle = |\mathcal{P}, \mathcal{V}\rangle. \quad (4.1)$$

There is an important subtlety, however, when considering the  $SU(N)$  group with  $N > 2$ . Some irreps might occur with a nontrivial outer multiplicity in the tensor product of the virtual irreps. Denoting by  $\mu^{\mathcal{P}}$  the outer multiplicity of the irrep  $\mathcal{P}$  in the tensor product of  $\mathcal{V} \otimes \mathcal{V}$ , one can actually build  $\mu^{\mathcal{P}}$  AKLT states which we denote by

$$|\mathcal{P}, \mathcal{V}, \tau\rangle, \quad \tau = 1, \dots, \mu^{\mathcal{P}}. \quad (4.2)$$

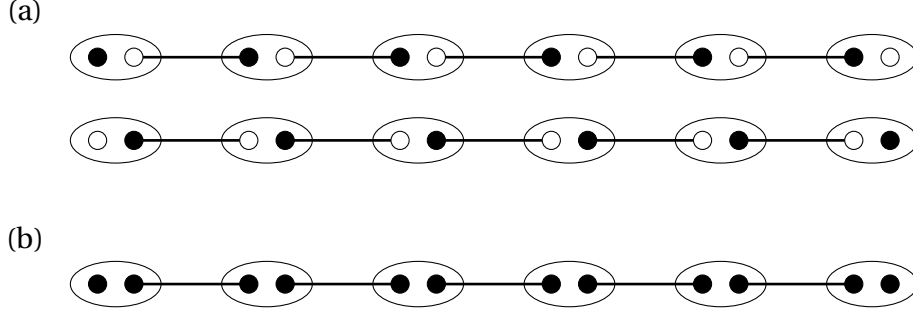


Figure 4.1: (a) Two AKLT states which break reflection symmetry when the virtual irreps  $\mathcal{V}_L, \mathcal{V}_R$ , denoted by filled and empty circles, are different. (b) Unique AKLT state  $|\mathcal{P}, \mathcal{V}\rangle$  for a self-conjugate virtual irrep  $\mathcal{V}$ , here denoted by a filled circle. The ellipses denote the projection of two virtual irreps onto the physical irrep  $\mathcal{P}$ , and the thick lines joining adjacent sites are singlets. Figure (b) taken and adapted from Ref. [56], © 2019 Elsevier, under CC BY license.

All AKLT states  $|\mathcal{P}, \mathcal{V}, \tau\rangle$  can be constructed explicitly using the CGCs associated to the singlet and physical irreps in the tensor product of two virtual irreps. Let us denote by  $[\mathcal{P}]$  the Young diagram of the physical irrep  $\mathcal{P}$ ,  $[\mathcal{V}]$  the Young diagram of the virtual irrep  $\mathcal{V}$  and  $[0]$  the Young diagram of the singlet irrep. To lighten the notations we define the following matrices of CGCs (see Section 3.3.5),

$$S_{a,b} = C_{[\mathcal{V}],a,[\mathcal{V}],b}^{[0]}, \quad a, b = 1, \dots, \dim(\mathcal{V}) \quad (4.3)$$

and

$$M_{a,b}^{m,\tau} = C_{[\mathcal{V}],a,[\mathcal{V}],b}^{[\mathcal{P}],m,\tau}, \quad m = 1, \dots, \dim(\mathcal{P}), \quad a, b = 1, \dots, \dim(\mathcal{V}), \quad \tau = 1, \dots, \mu^{\mathcal{P}}. \quad (4.4)$$

The AKLT wave functions can now be explicitly written in terms of the matrices  $S$  and  $M^{m,\tau}$  of CGCs for the singlet and physical states. We have

$$|\mathcal{P}, \mathcal{V}, \tau\rangle = \sum_{\mathbf{m}} \text{Tr} (M^{m_1,\tau} S M^{m_2,\tau} S \dots M^{m_L,\tau} S) |m_1, m_2, \dots, m_L\rangle \quad (4.5)$$

for a periodic chain of length  $L$ , where  $\sum_{\mathbf{m}}$  denotes a summation over all states of the tensor product basis  $|m_1, m_2, \dots, m_L\rangle \in \mathcal{P}^{\otimes L}$ . The AKLT wave functions are thus written as MPS with virtual (or auxiliary) bond dimension  $D = \dim(\mathcal{V})$  and physical dimension  $d = \dim(\mathcal{P})$ . Notice that the wave functions in Eq. (4.5) are neither normalized, nor orthogonal to each other.

The correlation length of the MPS can be directly extracted from the MPS tensors. Defining the matrices

$$A^{m,\tau} = M^{m,\tau} S \quad (4.6)$$

and the transfer matrix

$$\mathcal{T}^\tau = \sum_m A^{m,\tau} \otimes A^{m,\tau} \quad (4.7)$$

as well as its eigenvalues  $\lambda_i^\tau$  sorted in descending order of real parts,  $\text{Re}\lambda_1^\tau > \text{Re}\lambda_2^\tau \geq \text{Re}\lambda_3^\tau \geq \dots$  the correlation length is given by

$$\xi^\tau = \frac{1}{\ln \left| \frac{\lambda_1^\tau}{\text{Re}\lambda_2^\tau} \right|}. \quad (4.8)$$

For  $SU(2)$  spin chains the construction described above goes beyond the widely known AKLT states with physical spin  $S$  and virtual spin  $s = S/2$  [115, 116, 124]. Indeed, for a physical integer spin  $S$  one is now able to construct AKLT states with any virtual spin  $s \geq S/2$  [125]. In a similar fashion the construction of  $SU(N)$  AKLT states becomes much richer than what has been done so far. Indeed, the usual construction consisted in stacking fundamental irreps (or more generally antisymmetric irreps) and forming several singlet bonds, if necessary, to achieve a given physical irrep. The construction introduced here will prove to be very useful to characterize the structure of the edge states on open chains, which remains unclear in the usual construction.

#### 4.1.2 Parent Hamiltonians

Once the AKLT state is defined, the next step is to derive the associated parent Hamiltonian: an Hamiltonian for which the AKLT state is the unique ground state for periodic boundary conditions (PBC), and such that the ground state degeneracy is  $D^2$  for open boundary conditions (OBC). For instance the simplest parent Hamiltonian of the original  $SU(2)$  spin-1 AKLT state is the following bilinear-biquadratic form<sup>1</sup>

$$\mathcal{H}_{\text{AKLT}} = \sum_i \left( \mathbf{S}_i \cdot \mathbf{S}_{i+1} + \frac{1}{3}(\mathbf{S}_i \cdot \mathbf{S}_{i+1})^2 + \frac{2}{3} \right) \quad (4.9)$$

where the constant term simply sets the ground state energy to zero [115, 116]. One obtains this form very simply by inspection of the AKLT wave function on two neighboring sites. Since there is a singlet between sites  $i$  and  $i+1$ , the total spin of the AKLT wave function on these sites can be either zero or one, but not two. The kernel of a valid parent Hamiltonian must thus be the set of all wave functions satisfying this constraint of being either a singlet or a triplet on any pair of neighboring sites. The sum of the projectors onto the spin-2 subspace on two neighboring sites clearly satisfies this condition, and we write

$$\mathcal{H}_{\text{AKLT}} = 2 \sum_i \mathbb{P}_{i,i+1}^{S=2} \quad (4.10)$$

where the factor 2 is conventional and ensures the equivalence with Eq. (4.9).

---

<sup>1</sup>Throughout this chapter and for ease of notation, we remove the energy scale  $J$  from all Hamiltonians.

#### 4.1. Generic construction of $SU(N)$ AKLT models

This method to derive a valid AKLT Hamiltonian is not convenient for the more general framework introduced in Section 4.1.1, and actually does not lead to any meaningful result in many cases. For instance, let us consider again the spin-1 chain, but with virtual spin-1. Obviously the two-site approach used for the original AKLT state does not work here: since the physical and virtual irreps are the same, one would obtain  $\mathcal{H} = 0$ . The only way to solve this issue is to look at a three-site Hamiltonian. By analogy with Eq. (4.10) a naive expression would be

$$\mathcal{H} = \sum_i \mathbb{P}_{i,i+1,i+2}^{S=3} \quad (4.11)$$

where  $\mathbb{P}_{i,i+1,i+2}^{S=3}$  is the projector onto the spin-3 subspace on three neighboring sites. Indeed, the spin  $S = 3$  cannot be obtained from the tensor product of the two virtual irreps, while it can be obtained from the tensor product of three physical irreps. In fact, Hamiltonian (4.11) is not a valid parent Hamiltonian because its kernel is not only made of the AKLT wave function. The origin of this larger ground state degeneracy is the outer multiplicities of the spin-1 and spin-2 irreps in the tensor product of three physical irreps.

We will now describe a generic method to find valid parent Hamiltonians for the  $SU(N)$  AKLT states described in Section 4.1.1. We will then come back to the example above and derive the complete family of valid parent Hamiltonians.

To begin, let us define a few useful sets. First we define the tensor product of two virtual irreps

$$\mathcal{U} = \mathcal{V} \otimes \mathcal{V} \quad (4.12)$$

and the decomposition of its content in terms of spaces transforming according to the symmetry properties of Young diagrams

$$\mathcal{U} = \bigoplus_{[\nu] \in \mathcal{U}} U^{[\nu]} \quad (4.13)$$

where  $\mathcal{U}$  is the set of Young diagrams involved in the tensor product of the virtual irreps. We also define the tensor product space of  $l$  physical spins and decompose it in a similar fashion,

$$\mathcal{P}^{\otimes l} = \bigoplus_{[\nu] \in \mathcal{A}} V^{[\nu]}. \quad (4.14)$$

The space  $V^{[\nu]}$  can itself be decomposed into a direct sum of  $\mu^{[\nu]}$  copies  $V_i^{[\nu]}$ ,  $i = 1, \dots, \mu^{[\nu]}$  if the irrep  $[\nu]$  appears  $\mu^{[\nu]} > 1$  times in the tensor product of  $l$  physical irreps.

Given the spaces  $\mathcal{U}$  and  $\mathcal{P}^{\otimes l}$  one further defines their intersection

$$\mathcal{K} = \mathcal{U} \cap \mathcal{P}^{\otimes l} \quad (4.15)$$

## Chapter 4. $SU(N)$ AKLT models

---

as well as the complement of  $\mathcal{U}$  in  $\mathcal{P}^{\otimes l}$ ,

$$\mathcal{Q} = \mathcal{P}^{\otimes l} \setminus \mathcal{U}. \quad (4.16)$$

The spaces  $\mathcal{K}$  and  $\mathcal{Q}$  can also be decomposed as direct sums of spaces transforming according to irreps of the group,

$$\mathcal{K} = \bigoplus_{[\nu] \in \mathbf{K}} K^{[\nu]}, \quad \mathcal{Q} = \bigoplus_{[\nu] \in \mathbf{Q}} Q^{[\nu]} \quad (4.17)$$

and the spaces  $K^{[\nu]}$  and  $Q^{[\nu]}$  can be further decomposed into direct sums of  $\mu_{\mathcal{K}}^{[\nu]}$  and  $\mu_{\mathcal{Q}}^{[\nu]}$  copies of spaces if the irrep  $[\nu]$  appears  $\mu_{\mathcal{K}}^{[\nu]} > 1$  or  $\mu_{\mathcal{Q}}^{[\nu]} > 1$  times in the space  $\mathcal{K}$  or  $\mathcal{Q}$ , respectively.

From now on, we assume that the space  $\mathcal{Q}$  is not empty. In other words we assume that  $l$  is large enough in order for  $\mathcal{Q}$  to be non empty.

Before introducing the most general construction of the family of parent Hamiltonians we discuss the construction of one particular parent Hamiltonian, which we call the “MPS Hamiltonian”. Since we know the wave function of the AKLT state through its exact expression in terms of an MPS with finite auxiliary bond dimension, one can build a parent Hamiltonian as

$$h = \mathbb{1} - \mathbb{P}_{\text{MPS}} \quad (4.18)$$

where  $\mathbb{P}_{\text{MPS}}$  is a projector onto the MPS manifold of AKLT wave functions. Dealing with the entire wave function, however, is not so convenient and we aim at finding a local Hamiltonian. To do so, we consider the MPS of the AKLT states on  $l$  sites with OBC,

$$|\mathcal{P}, \mathcal{V}, \tau; a, b\rangle = \sum_m (M^{m_1, \tau} S M^{m_2, \tau} S \dots M^{m_l, \tau})_{a, b} |m_1, \dots, m_l\rangle. \quad (4.19)$$

The labels  $a, b = 1, \dots, D$  of the unpaired virtual states at sites 1 and  $l$ , respectively, now label the  $D^2$  AKLT states with OBC on  $l$  sites.

We choose  $l$  in such a way that all states  $|\mathcal{P}, \mathcal{V}, \tau; a, b\rangle$  are linearly independent. One then says that the MPS is injective on  $l$  sites<sup>2</sup>. The non-orthogonality of the  $D^2$  AKLT states prevents us from using them straight away to build a local projector. Orthogonalization

---

<sup>2</sup>The injectivity length is the smallest length  $l$  such that the MPS is injective on  $l$  sites. There is a criteria to find a length  $l$  such that the MPS is injective. Find the smallest  $l$  such that  $D^2 < d^l$ . Then the MPS is injective on  $l + 1$  sites [126–130]. The injectivity length, however, can be smaller, as is illustrated by the original AKLT model.

can be obtained easily using the CGCs as

$$|\mathcal{P}, \mathcal{V}, \tau; [\nu], m, \omega\rangle = \frac{1}{\text{Norm}} \sum_{a,b=1}^D C_{[\mathcal{V}],a,[\mathcal{V}],b}^{[\nu],m,\omega} |\mathcal{P}, \mathcal{V}, \tau; a, b\rangle, \quad [\nu] \in \mathcal{U}, \quad m = 1, \dots, \dim(U_{\omega}^{[\nu]}),$$

$$\omega = 1, \dots, \mu_{\mathcal{U}}^{[\nu]} \quad (4.20)$$

where  $\mu_{\mathcal{U}}^{[\nu]}$  is the multiplicity of the irrep  $[\nu]$  in the space  $\mathcal{U} = \mathcal{V} \otimes \mathcal{V}$  and  $U_{\omega}^{[\nu]}$  is the  $\omega$ -th copy of the invariant space with symmetry  $[\nu]$  in  $\mathcal{U}$ .

From the states in Eq. (4.20) one can form projectors onto the different components of  $\mathcal{K}$ ,

$$\mathbb{P}_{K_{\omega}^{[\nu]}}^{\tau} = \sum_{m=1}^{\dim([\nu])} |\mathcal{P}, \mathcal{V}, \tau; [\nu], m, \omega\rangle \langle \mathcal{P}, \mathcal{V}, \tau; [\nu], m, \omega|. \quad (4.21)$$

The  $l$ -site local MPS Hamiltonian is then given by

$$h_{\text{MPS}}^{\tau} = \mathbb{1} - \mathbb{P}_{\text{MPS}}^{\tau} \quad (4.22)$$

where

$$\mathbb{P}_{\text{MPS}}^{\tau} = \sum_{[\nu] \in \mathcal{K}} \sum_{\omega=1}^{\mu_{\mathcal{K}}^{[\nu]}} \mathbb{P}_{K_{\omega}^{[\nu]}}^{\tau}. \quad (4.23)$$

The Hamiltonian on a chain of length  $L$  is obtained as

$$\mathcal{H}_{\text{MPS}}^{\tau} = \sum_i \tau_i(h_{\text{MPS}}^{\tau}) \quad (4.24)$$

where  $\tau_i(h_{\text{MPS}}^{\tau})$  is the local MPS Hamiltonian in Eq. (4.22) acting on sites  $(i, i+1, \dots, i+l-1)$ .

So far we have found how to derive one particular parent Hamiltonian. However, parent Hamiltonians of AKLT states are not unique and we shall find the entire family of parent Hamiltonians acting on  $l$  sites, where  $l$  is the injectivity length defined above. To do so we first compute, using the CGCs, all states of the tensor product of  $l$  physical spins in definite symmetry sectors. The states are thus labeled by an  $SU(N)$  irrep  $[\nu]$ , a state index  $m$  and a multiplicity index  $\omega$ ,

$$|[\nu], m, \omega\rangle \in \mathcal{P}^{\otimes l}. \quad (4.25)$$

The key point is to ensure that the MPS states defined in Eq. (4.20) form a subset of these states. One obtains this property using the gauge freedom in the CGCs: within an irrep  $[\nu]$  one can perform a rotation which ensures that the AKLT states labeled by the irrep  $[\nu]$  correspond precisely to the states  $|[\nu], m, \omega\rangle$ . One can now define projectors

on all sectors belonging to  $\mathcal{P}^{\otimes l}$

$$\mathbb{P}_\omega^{[\nu]} = \sum_m |[\nu], m, \omega\rangle \langle [\nu], m, \tau|. \quad (4.26)$$

Moreover one can define additional operators which swap the states of different copies of the same irrep,

$$\mathbb{X}_{\omega,\kappa}^{[\nu]} = \sum_m |[\nu], m, \omega\rangle \langle [\nu], m, \kappa|, \quad 1 \leq \omega, \kappa \leq \mu^{[\nu]}, \omega \neq \kappa. \quad (4.27)$$

We call these operators the “intertwiners”.

The most general  $l$ -site local parent Hamiltonian is then given by

$$h = \sum_{[\nu] \in \mathcal{Q}} \sum_{\omega=1}^{\mu_{\mathcal{Q}}^{[\nu]}} \left( c_{\omega,\omega}^{[\nu]} \mathbb{P}_\omega^{[\nu]} + \sum_{\kappa \neq \omega} c_{\omega,\kappa}^{[\nu]} \mathbb{X}_{\omega,\kappa}^{[\nu]} \right) \quad (4.28)$$

where  $c^{[\nu]}$  is a symmetric positive definite matrix.

When taking  $c^{[\nu]} = \mathbb{1}$ ,  $\forall [\nu] \in \mathcal{Q}$ , the Hamiltonian in Eq. (4.28) reduces to a projector onto the space  $\mathcal{Q}$ , and we recover the MPS Hamiltonian in Eq. (4.22). Tuning the parameters  $c^{[\nu]}$  away, the Hamiltonian is not a projector anymore, but its kernel is still the space  $\mathcal{K}$ .

## 4.2 $SU(2)$ AKLT model with spin-1 edge states

In this section we provide an illustrative example of the construction of AKLT states and parent Hamiltonians discussed above: an  $SU(2)$  spin-1 AKLT state possessing spin-1 edge states. This model was initially introduced in Ref. [125] but in a somehow less general framework.

### 4.2.1 Construction of the state

From the standard rules for the tensor product of two  $SU(2)$  irreps one has

$$\mathbf{3} \otimes \mathbf{3} = \mathbf{1} \oplus \mathbf{3} \oplus \mathbf{5}. \quad (4.29)$$

One can thus use the CGCs to write the state of the singlet in terms of the spin-1 spins. Taking  $\{|1\rangle, |0\rangle, |-1\rangle\}$  as the basis of states of a spin-1 irrep the singlet reads

$$\frac{1}{\sqrt{3}} (|1\rangle \otimes |-1\rangle - |0\rangle \otimes |0\rangle + |-1\rangle \otimes |1\rangle). \quad (4.30)$$



One then translates this onto the following singlet matrix

$$S = \frac{1}{\sqrt{3}} \begin{pmatrix} 0 & 0 & 1 \\ 0 & -1 & 0 \\ 1 & 0 & 0 \end{pmatrix}. \quad (4.31)$$

Similarly the triplet states are given by

$$\begin{aligned} & \frac{1}{\sqrt{2}} (|0\rangle \otimes |1\rangle - |1\rangle \otimes |0\rangle) \\ & \frac{1}{\sqrt{2}} (|-1\rangle \otimes |1\rangle - |1\rangle \otimes |-1\rangle) \\ & \frac{1}{\sqrt{2}} (|-1\rangle \otimes |0\rangle - |0\rangle \otimes |-1\rangle) \end{aligned} \quad (4.32)$$

and the triplet matrices are thus

$$M^1 = \frac{1}{\sqrt{2}} \begin{pmatrix} 0 & -1 & 0 \\ 1 & 0 & 0 \\ 0 & 0 & 0 \end{pmatrix}, \quad M^2 = \frac{1}{\sqrt{2}} \begin{pmatrix} 0 & 0 & -1 \\ 0 & 0 & 0 \\ 1 & 0 & 0 \end{pmatrix}, \quad M^3 = \frac{1}{\sqrt{2}} \begin{pmatrix} 0 & 0 & 0 \\ 0 & 0 & -1 \\ 0 & 1 & 0 \end{pmatrix}. \quad (4.33)$$

Notice that we have removed the multiplicity index  $\tau$  from Eq. (4.4) since no nontrivial multiplicity occurs in the tensor product of two SU(2) irreps.

From these matrices one can build the AKLT wave function and extract its correlation length  $\xi = 1/\ln 2$  [125]. This is longer than the correlation length  $\xi = 1/\ln 3$  of the original AKLT state.

### 4.2.2 Parent Hamiltonians

Using Eq. (4.22) one easily derives an MPS parent Hamiltonian on  $l = 3$  sites, which is the injectivity length of the MPS.

While the Hamiltonian is written as a tensor it can be explicitly rewritten in terms of SU(2)-invariant operators. There are three reflection-antisymmetric and eight reflection-symmetric SU(2)-invariant operators which are invariant under time-reversal and are purely real. A possible choice for these operators is [56]

$$\begin{aligned} \mathcal{A}^1 &= \frac{1}{2} (\mathbf{S}_1 \cdot \mathbf{S}_2 - \mathbf{S}_2 \cdot \mathbf{S}_3), \\ \mathcal{A}^2 &= \frac{1}{2} ((\mathbf{S}_1 \cdot \mathbf{S}_2)^2 - (\mathbf{S}_2 \cdot \mathbf{S}_3)^2), \\ \mathcal{A}^3 &= ((\mathbf{S}_1 \cdot \mathbf{S}_3)(\mathbf{S}_2 \cdot \mathbf{S}_3) - (\mathbf{S}_1 \cdot \mathbf{S}_2)(\mathbf{S}_1 \cdot \mathbf{S}_3)) + \text{h.c.} \end{aligned} \quad (4.34)$$

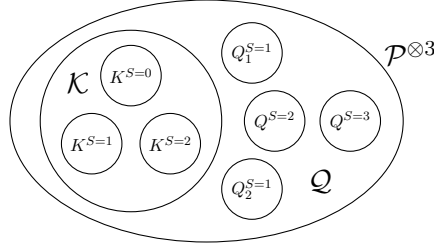


Figure 4.2: Decomposition of the physical space  $\mathcal{P}^{\otimes 3} \equiv \mathbf{3}^{\otimes 3}$  in irreps of  $SU(2)$ , and identification of the different sets  $\mathcal{K} \equiv \mathcal{U}$  and  $\mathcal{Q}$ . Figure taken from Ref. [56], © 2019 Elsevier, under CC BY license.

and

$$\begin{aligned}
 \mathcal{R}^1 &= \mathbb{1}, \\
 \mathcal{R}^2 &= \frac{1}{2} (\mathbf{S}_1 \cdot \mathbf{S}_2 + \mathbf{S}_2 \cdot \mathbf{S}_3), \\
 \mathcal{R}^3 &= \mathbf{S}_1 \cdot \mathbf{S}_3, \\
 \mathcal{R}^4 &= \frac{1}{2} ((\mathbf{S}_1 \cdot \mathbf{S}_2)^2 + (\mathbf{S}_2 \cdot \mathbf{S}_3)^2), \\
 \mathcal{R}^5 &= (\mathbf{S}_1 \cdot \mathbf{S}_3)^2, \\
 \mathcal{R}^6 &= (\mathbf{S}_1 \cdot \mathbf{S}_2)(\mathbf{S}_1 \cdot \mathbf{S}_3)(\mathbf{S}_2 \cdot \mathbf{S}_3) + \text{h.c.}, \\
 \mathcal{R}^7 &= (\mathbf{S}_1 \cdot \mathbf{S}_2)(\mathbf{S}_2 \cdot \mathbf{S}_3) + \text{h.c.}, \\
 \mathcal{R}^8 &= ((\mathbf{S}_1 \cdot \mathbf{S}_3)(\mathbf{S}_2 \cdot \mathbf{S}_3) + (\mathbf{S}_1 \cdot \mathbf{S}_2)(\mathbf{S}_1 \cdot \mathbf{S}_3)) + \text{h.c.}
 \end{aligned} \tag{4.35}$$

Expanding the MPS Hamiltonian on these operators one obtains [56]

$$\begin{aligned}
 h_{\text{MPS}} &= 2 - \frac{1}{4} \mathbf{S}_1 \cdot \mathbf{S}_3 - \frac{1}{4} (\mathbf{S}_1 \cdot \mathbf{S}_3)^2 - \frac{5}{8} ((\mathbf{S}_1 \cdot \mathbf{S}_2)^2 + (\mathbf{S}_2 \cdot \mathbf{S}_3)^2) \\
 &\quad + \frac{3}{8} ((\mathbf{S}_1 \cdot \mathbf{S}_2)(\mathbf{S}_1 \cdot \mathbf{S}_3)(\mathbf{S}_2 \cdot \mathbf{S}_3) + \text{h.c.}).
 \end{aligned} \tag{4.36}$$

Let us turn now to the construction of the entire family of parent Hamiltonians. It is useful to visualize the different spaces  $\mathcal{U}$ ,  $\mathcal{K}$  and  $\mathcal{Q}$  in a Venn diagram, as in Fig. 4.2. In this case where  $\mathcal{P} \equiv \mathcal{V} = \text{spin-1}$  one has  $\mathcal{U} \equiv \mathcal{K}$ . The most general expression for a hermitian parent Hamiltonian is then given by

$$h = c_{1,1}^{S=1} \mathbb{P}_1^{S=1} + c_{2,2}^{S=1} \mathbb{P}_2^{S=1} + c_{1,2}^{S=1} \mathbb{S} + c^{S=2} \mathbb{P}^{S=2} + c^{S=3} \mathbb{P}^{S=3} \tag{4.37}$$

where  $\mathbb{S} \equiv \mathbb{X}_{1,2}^{S=1} + \mathbb{X}_{2,1}^{S=1}$  is the reciprocal (or hermitian) intertwiner acting on the spin-1 irreps of  $\mathcal{Q}$  and where the coefficients  $c^{S=2} > 0$ ,  $c^{S=3} > 0$  and  $c^{S=1}$  is symmetric positive definite. Obviously Hamiltonian (4.37) is very different from the simple projector onto the spin-3 subspace. In particular, its kernel is restricted to the space  $\mathcal{K}$ , which is generated by the MPS wave functions in Eq. (4.20).

Building explicitly the states of the physical space on  $l = 3$  sites one can construct the different operators appearing in Eq. (4.37) and then re-express them in terms of the SU(2)-invariant operators in Eq. (4.34)-(4.35). Choosing the phases of the states such that  $\mathbb{P}_{\text{MPS}}^{S=1} \equiv \mathbb{P}_3^{S=1}$  and  $\mathbb{P}_{\text{MPS}}^{S=2} \equiv \mathbb{P}_2^{S=2}$  one gets

$$\begin{aligned}
 \mathbb{P}^{S=0} &= -\frac{1}{3} \left( \mathcal{R}^1 + \mathcal{R}^2 - \frac{1}{2}\mathcal{R}^3 - \mathcal{R}^4 - \frac{1}{2}\mathcal{R}^5 + \frac{1}{2}\mathcal{R}^6 - \frac{1}{4}\mathcal{R}^8 \right), \\
 \mathbb{P}_1^{S=1} &= \frac{1}{7} \left( 5\mathcal{R}^1 - \frac{11}{4}\mathcal{R}^3 - \frac{17}{4}\mathcal{R}^4 - \frac{3}{4}\mathcal{R}^5 + \frac{11}{8}\mathcal{R}^6 + \frac{1}{2}\mathcal{R}^7 - \frac{1}{4}\mathcal{R}^8 \right) - \frac{1}{7} \left( \mathcal{A}^2 + \frac{1}{2}\mathcal{A}^3 \right), \\
 \mathbb{P}_2^{S=1} &= \frac{1}{35} \left( 31\mathcal{R}^1 - 16\mathcal{R}^3 - 19\mathcal{R}^4 - 12\mathcal{R}^5 + 8\mathcal{R}^6 + \mathcal{R}^7 - \frac{1}{2}\mathcal{R}^8 \right) + \frac{1}{7} \left( \mathcal{A}^2 + \frac{1}{2}\mathcal{A}^3 \right), \\
 \mathbb{P}_3^{S=1} &= -\mathcal{R}^1 + \frac{1}{4}\mathcal{R}^3 + \frac{3}{4}\mathcal{R}^4 + \frac{1}{4}\mathcal{R}^5 - \frac{1}{8}\mathcal{R}^6, \\
 \mathbb{P}_1^{S=2} &= \frac{1}{3}\mathcal{R}^1 - \frac{1}{3}\mathcal{R}^2 + \frac{1}{2}\mathcal{R}^3 - \frac{1}{6}\mathcal{R}^4 + \frac{1}{6}\mathcal{R}^5 - \frac{1}{12}\mathcal{R}^6 - \frac{1}{6}\mathcal{R}^7, \\
 \mathbb{P}_2^{S=2} &= \frac{1}{3} \left( \mathcal{R}^1 + \mathcal{R}^2 - \frac{1}{2}\mathcal{R}^3 + \frac{1}{2}\mathcal{R}^4 - \frac{1}{2}\mathcal{R}^5 - \frac{1}{4}\mathcal{R}^6 - \frac{1}{4}\mathcal{R}^8 \right), \\
 \mathbb{P}^{S=3} &= \frac{1}{15}\mathcal{R}^1 + \frac{1}{3}\mathcal{R}^2 + \frac{1}{10}\mathcal{R}^3 + \frac{1}{15}\mathcal{R}^4 + \frac{1}{30}\mathcal{R}^5 + \frac{1}{30}\mathcal{R}^6 + \frac{1}{15}\mathcal{R}^7 + \frac{1}{20}\mathcal{R}^8.
 \end{aligned} \tag{4.38}$$

Similarly

$$\mathbb{S} = \frac{1}{7\sqrt{10}} \left( -8\mathcal{R}^1 + 3\mathcal{R}^3 - 3\mathcal{R}^4 + 11\mathcal{R}^5 - \frac{3}{2}\mathcal{R}^6 + 2\mathcal{R}^7 - \mathcal{R}^8 \right) + \frac{3}{7\sqrt{10}} \left( \mathcal{A}^2 + \frac{1}{2}\mathcal{A}^3 \right). \tag{4.39}$$

With Eq. (4.37)-(4.39) one can build explicit expressions of the entire family of three-site local parent Hamiltonians of the spin-1 AKLT state with spin-1 edge states. There are five parameters in total, but one of them is a scaling factor, and there is the additional constraint on the positive definiteness of  $c^{S=1}$ . Tuning the parameters one can thus search for particularly simple parent Hamiltonians. It is possible for instance to derive a parent Hamiltonian which does not have a 6-spin interaction, at the price of introducing 4-spin interactions. In what follows, however, we shall focus on the MPS Hamiltonian which can simply be obtained by setting  $c^{S=2} = c^{S=3} = 1$  and  $c^{S=1} = \mathbb{1}$  in Eq. (4.37).

### 4.2.3 Topological phase transition

The Haldane phase, in which the original AKLT Hamiltonian (4.9) lies, is a symmetry-protected topological (SPT) phase. The spin-1/2 edge states on an open chain are protected by  $\mathbb{Z}_2 \times \mathbb{Z}_2$  symmetry, there is a string order parameter, and a bulk-boundary correspondence [131–134].

By contrast, the AKLT Hamiltonian (4.36) is expected to lie in a trivial phase since the edge states have integer spin. Since both Hamiltonians respect the translation

and rotation symmetries they should be separated by a phase transition. The phase transitions between  $\mathbb{Z}_n \times \mathbb{Z}_n$  bosonic SPT phases has been extensively studied in Ref. [135]. When  $n = 2$  the transition has been predicted to be described by a critical theory with central charge  $c = 1$ .

To study the phase transition from the SPT phase of the original AKLT model to the trivial phase of the spin-1 AKLT model with spin-1 edge states we define the interpolating Hamiltonian

$$\mathcal{H}_\lambda = (1 - \lambda)\mathcal{H}_{\text{AKLT}} + \lambda\mathcal{H}_{\text{MPS}}, \quad \lambda \in [0, 1] \quad (4.40)$$

and study numerically the low-energy eigenstates on short chains. Figure 4.3 shows the spectrum of Hamiltonian (4.40) for  $N_s = 15$  sites. We find that the finite-size gap extrapolates in the thermodynamic limit to zero when  $\lambda$  is tuned to  $\lambda_c \simeq 0.8259(1)$ , an indication that the transition is continuous. We further characterize the phase transition using the standard approach based on conformal field theory (CFT). In Fig. 4.4(a) we show the scaling of the ground state energy per site which we fit as

$$\frac{E_0(N_s)}{N_s} = \epsilon_0(\infty) - \frac{\pi c v}{6N_s^2} + o(N_s^{-2}) \quad (4.41)$$

where  $\epsilon_0(\infty)$  is the thermodynamic ground state energy per site,  $c$  is the central charge of the CFT and  $v$  is the speed of light. To extract the central charge we further need to determine the speed of light. We thus look at the excited state energy of the first state having momentum  $2\pi/N_s$  and non-vanishing Casimir which should satisfy the following scaling formula for a critical theory

$$\Delta E_1(N_s) = E_1(N_s) - E_0(N_s) = \frac{2\pi v}{N_s} + o(N_s^{-1}). \quad (4.42)$$

The velocity  $v$  is extracted using this formula in Fig. 4.4(b). We then obtain the central charge  $c \simeq 1.00$ , in excellent agreement with a continuous phase transition described by the  $SU(2)_1$  Wess-Zumino-Witten (WZW) CFT. This is further confirmed by the analysis of the scaling dimensions of the primary fields associated to the singlet and triplet excited states in Fig. 4.4(c). To come back to Ref. [135], the  $SU(2)_1$  WZW CFT is indeed the most natural theory with central charge  $c = 1$  to describe the transition given the symmetry of the Hamiltonian  $\mathcal{H}_\lambda$ .

## 4.3 $SU(3)$ AKLT model with 3-box symmetric irrep

### 4.3.1 Original formulation with fundamental irreps

We now turn to the case of  $SU(3)$  and, more particularly, to the physical 3-box symmetric irrep 10 represented by a Young diagram with three boxes in its single row  $\square\square\square$ . The AKLT model for this irrep will be of significant help when studying the

### 4.3. $SU(3)$ AKLT model with 3-box symmetric irrep

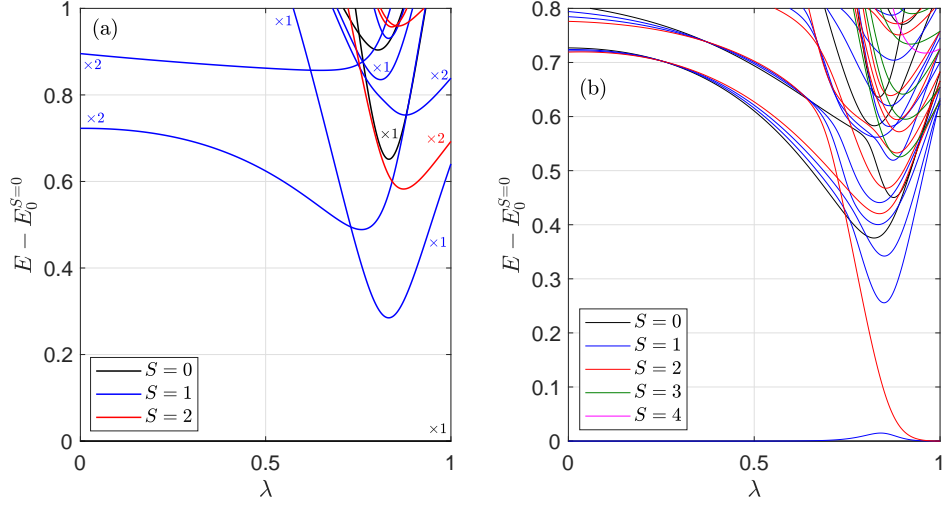


Figure 4.3: Finite-size spectrum of the interpolation Hamiltonian  $\mathcal{H}_\lambda$  for (a) PBC and (b) OBC on  $N_s = 15$  sites. In (a), the ground state is unique and is a singlet state. In (b) the ground state is four-fold degenerate at  $\lambda = 0$  and nine-fold degenerate at  $\lambda = 1$ , corresponding to spin-1/2 and spin-1 edge states, respectively. Figure taken and adapted from Ref. [56], © 2019 Elsevier, under CC BY license.

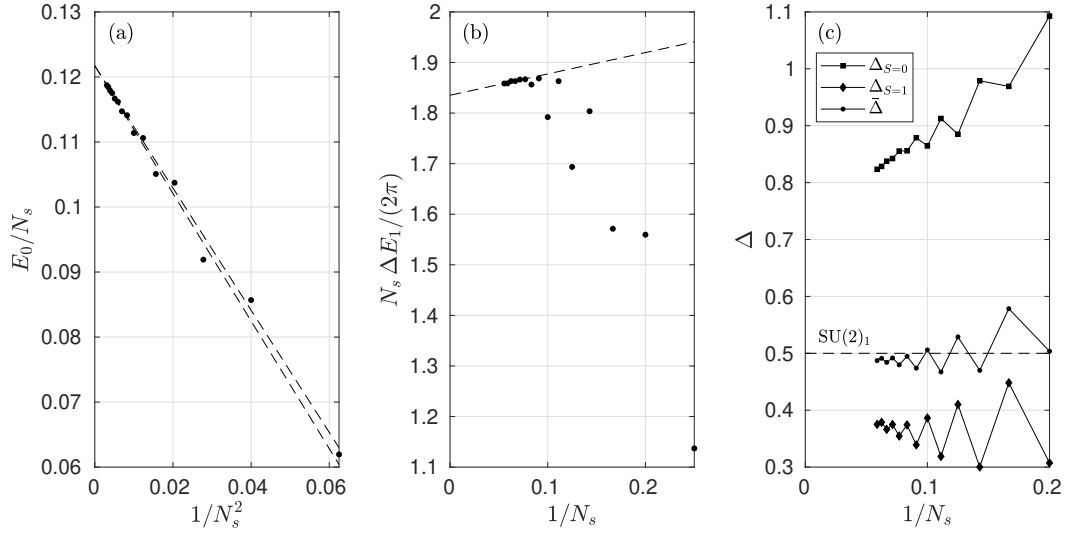
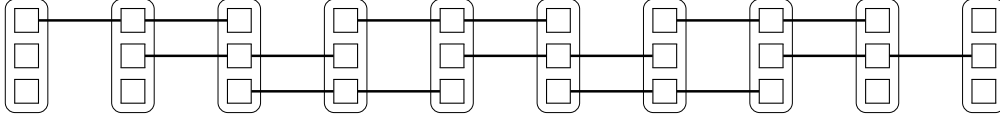


Figure 4.4: (a) Scaling of the ground state energy per site of the interpolation Hamiltonian  $\mathcal{H}_\lambda$  at  $\lambda = 0.8259$ . (b) Speed of light obtained from the first excited state at momentum  $2\pi/N_s$  and non-vanishing Casimir. (c) Scaling dimensions of the primary fields corresponding to the singlet and triplet excited states, as well as  $\bar{\Delta} = (3\Delta_{S=1} + \Delta_{S=0})/4$  which is free of logarithmic corrections [136, 137]. Figure taken and adapted from Ref. [56], © 2019 Elsevier, under CC BY license.

(a)



(b)

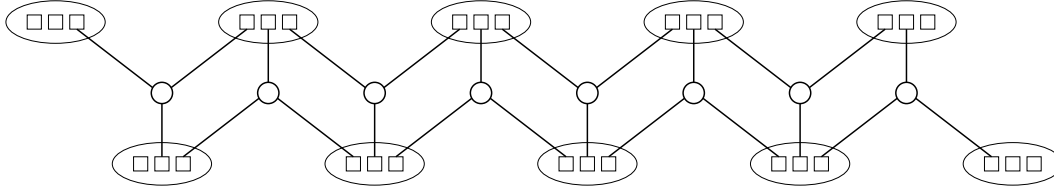


Figure 4.5: (a)  $SU(3)$  AKLT state of Greiter *et al.* for the 3-box symmetric irrep at each site [117, 118]. The rectangles containing three fundamental irreps denote a projection onto the physical irrep  $\square\square\square$  while the thick lines joining three neighboring sites denote extended singlet bonds. (b) Reinterpretation of the AKLT state in (a) as an MPS with bond dimension 9. The local projection onto the physical irrep is now denoted by an ellipse. The singlets are obtained with Levi-Civita tensors which antisymmetrize three fundamental irreps from three neighboring sites. Figure (b) is adapted from Ref. [56], © 2019 Elsevier, under CC BY license.

corresponding Heisenberg model in Chapter 5.

The model was first introduced in Refs. [117, 118] by Greiter *et al.*, who built the wave function out of fundamental irreps. On each site, three fundamental irreps are projected onto the physical 3-box symmetric irrep while extended singlets are made on three neighboring sites, as illustrated in Fig. 4.5(a). To rewrite this VBS state as an MPS one uses the expressions of the fully symmetric combinations of three colors given in Eq. (3.72). This allows us to build the local projector onto the physical irrep. Moreover, to obtain a singlet out of three fundamental irreps we need to fully antisymmetrize the three particles. The Levi-Civita tensor acts in the appropriate way, and a representation of the MPS is given in Fig. 4.5(b). The local MPS tensor is obtained through the contraction of the vertical auxiliary leg joining a Levi-Civita tensor to the tensor of the projector onto  $\mathbf{10}$ . One thus ends up with an MPS having auxiliary bond dimension  $D = 9$ , and correlation length  $\xi = 1/\ln 5$ .

Although the MPS structure is now clearly exhibited, the nature of the edge states on an open chain remains unrevealed. The auxiliary bond dimension of the MPS is  $D = 9$ . This corresponds to the tensor product of a fundamental irrep  $\mathbf{3}$  and a conjugate irrep  $\bar{\mathbf{3}}$  for which the Young diagram is made of a single column with two boxes. This tells us

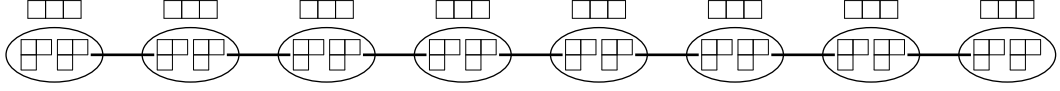


Figure 4.6: SU(3) AKLT state  $|\square\square\square, \begin{smallmatrix} \square & \square \\ \square & \end{smallmatrix}\rangle$ . The edge degrees of freedom on an open chain are, by construction, adjoint edge states. Figure adapted from Ref. [57] with the permission of the APS, © 2020 American Physical Society.

that the edge states are potentially made of a direct sum of an adjoint and a singlet,

$$\square \otimes \begin{smallmatrix} \square & \square \\ \square & \end{smallmatrix} = \bullet \oplus \begin{smallmatrix} \square & \square \\ \square & \square \end{smallmatrix}. \quad (4.43)$$

To shine light on the exact structure of these edge states, we compute the reduced density matrix  $\rho$  and obtain a characteristic spectrum  $\lambda_i = 1/\sqrt{8}$ ,  $1 \leq i \leq 8$  and  $\lambda_9 = 0$ . The singlet irrep at the edge thus does not carry any weight in the reduced density matrix. It should then be possible to rewrite the wave function of the AKLT state as an MPS with bond dimension  $D = 8$ , showing that the MPS in Fig. 4.5(b) is not optimal.

### 4.3.2 AKLT state with adjoint edge irreps

Since the physical irrep 10 appears in the tensor product of two adjoint irreps given by

$$\begin{smallmatrix} \square & \square \\ \square & \end{smallmatrix} \otimes \begin{smallmatrix} \square & \square \\ \square & \end{smallmatrix} = \bullet \oplus 2 \begin{smallmatrix} \square & \square \\ \square & \end{smallmatrix} \oplus \square\square\square \oplus \begin{smallmatrix} \square & \square & \square \\ \square & \square & \end{smallmatrix} \oplus \begin{smallmatrix} \square & \square & \square & \square \\ \square & \square & \square & \end{smallmatrix} \quad (4.44)$$

one can use the general method developed in Section 4.1.1 to construct an AKLT state for the 3-box symmetric irrep made of adjoint virtual spins, as pictured in Fig. 4.6. The correlation length of this state is readily obtained and corresponds to the one obtained in the construction of Greiter *et al.*,  $\xi = 1/\ln 5$ . The fact that the state  $|\square\square\square, \begin{smallmatrix} \square & \square \\ \square & \end{smallmatrix}\rangle$  is exactly identical to the state in Fig. 4.5(a) can further be exhibited by the spectrum of the reduced density matrix which is the same, except for the vanishing eigenvalue which is obviously absent in the spectrum associated to  $|\square\square\square, \begin{smallmatrix} \square & \square \\ \square & \end{smallmatrix}\rangle$ . The MPS representation of the state  $|\square\square\square, \begin{smallmatrix} \square & \square \\ \square & \end{smallmatrix}\rangle$  given in Fig. 4.6 having bond dimension  $D = 8$  with a flat spectrum of the reduced density matrix, it is optimal in the MPS sense.

### 4.3.3 Parent Hamiltonian

The parent Hamiltonian of the AKLT state above was first computed in Refs. [117, 118] based on the construction of the wave function out of fundamental irreps (Fig. 4.5). Here we derive the same Hamiltonian using the reinterpretation of the AKLT wave function as a VBS with adjoint edge states (Fig. 4.6). The Hamiltonian can be derived using the quadratic Casimir operator of SU(3). Indeed, the MPS is injective on two sites,

and the virtual and physical irreps are different. The tensor product of two physical irreps is given by

$$\begin{array}{|c|c|c|} \hline & & \\ \hline \end{array} \otimes \begin{array}{|c|c|c|} \hline & & \\ \hline \end{array} = \begin{array}{|c|c|c|} \hline & & \\ \hline \end{array} \oplus \begin{array}{|c|c|c|c|} \hline & & & \\ \hline \end{array} \oplus \begin{array}{|c|c|c|c|c|} \hline & & & & \\ \hline \end{array} \oplus \begin{array}{|c|c|c|c|c|c|} \hline & & & & & \\ \hline \end{array}. \quad (4.45)$$

Combining this decomposition with the tensor product of two virtual adjoint irreps in Eq. (4.44) one sees that, on two neighboring sites, the state can be either a  $\overline{10} \equiv [3, 3]$  or a  $27 \equiv [4, 2]$  irrep (these irreps appear both in Eq. (4.44) and in Eq. (4.45)). Thus a valid local parent Hamiltonian must annihilate the states of the  $\overline{10}$  and  $27$  irreps. One takes

$$h = \frac{1}{4} \left( (\mathbf{T}_1 + \mathbf{T}_2)^2 - C_2(\overline{10}) \right) \left( (\mathbf{T}_1 + \mathbf{T}_2)^2 - C_2(27) \right) \quad (4.46)$$

where the eigenvalues of the quadratic Casimir  $C_2$  are obtained with Eq. (3.78). The Hamiltonian in Eq. (4.46) has the right kernel and the spectrum is positive since the eigenvalues of  $C_2$  are larger for the irreps  $[5, 1] \equiv 35$  and  $[6] \equiv 28$  than for the irreps  $\overline{10}$  and  $27$ . As a side remark we emphasize that  $h$  given in Eq. (4.46) is not strictly speaking a projector, but rather a realization of Eq. (4.28). Developing Eq. (4.46) and using the fact that  $C_2(10) = 6$  one obtains

$$h = (\mathbf{T}_1 \cdot \mathbf{T}_2)^2 + 5\mathbf{T}_1 \cdot \mathbf{T}_2 + 6 \quad (4.47)$$

where  $\mathbf{T}$  are the generators in the physical irrep  $[3] \equiv 10$ . The Hamiltonian on a chain is then given by

$$\mathcal{H} = \sum_i \left( (\mathbf{T}_i \cdot \mathbf{T}_{i+1})^2 + 5\mathbf{T}_i \cdot \mathbf{T}_{i+1} + 6 \right). \quad (4.48)$$

A quick numerical study of Hamiltonian (4.48) shows that, on a periodic chain, the ground state is unique with a finite gap to the first excited states and for OBC the ground state is 64-fold degenerate. In that case the ground state wave functions live in all irreps occurring in the right-hand side of Eq. (4.44), which further confirms the equivalence of both formulations (Fig. 4.5 and 4.6) for the AKLT wave function.

#### 4.3.4 Perspective on the $p$ -box symmetric irrep of $SU(3)$

Let us now consider fully symmetric irreps of  $SU(3)$  represented by a Young diagram with  $p$  boxes in the first row. The AKLT model discussed in the previous section is thus the  $p = 3$  AKLT model. One can obviously generalize this construction to any symmetric irrep with  $p = 3n$ ,  $n$  being an integer. For instance one can build a unique AKLT model

$$\left| \begin{array}{|c|c|c|c|c|} \hline & & & & \\ \hline \end{array}, \begin{array}{|c|c|c|} \hline & & \\ \hline \end{array} \right\rangle \quad (4.49)$$

for the 6-box symmetric irrep made of virtual self-conjugate  $[4, 2]$  irreps.



On the contrary, one is not able to build AKLT models when  $p = 3n + q$  with  $q = 1, 2$ . This actually follows from a simple counting argument. Self-conjugate irreps of  $SU(3)$  have a number of boxes which is a multiple of 3. Consequently all irreps appearing in the tensor product of two virtual irreps have a number of boxes which is incompatible with  $p = 3n + q$  when  $q = 1, 2$ .

From a conceptual point of view, this has deep consequences. When  $p = 3n$ , one is able to show rigorously the existence of a gapped VBS phase. When  $p = 3$ , the exactly solvable AKLT model (Eq. (4.48)) has only an additional biquadratic term compared to the pure Heisenberg model. Keeping apart any rigorous treatment for now, it is already reasonable to guess that the 3-box symmetric, and more generally the  $3n$ -box symmetric  $SU(3)$  Heisenberg model is gapped. Moreover, from the absence of AKLT models for  $p = 3n + q$  when  $q = 1, 2$ , and from the Bethe ansatz solution of Sutherland on the  $p = 1$  model [35], one can conjecture a gapless phase of the  $SU(3)$  Heisenberg model when  $p$  is not a multiple of three. This is nothing but a Haldane conjecture for the  $SU(3)$  chain with  $p$ -box symmetric irrep. In Chapter 5 we will discuss more deeply the different arguments leading to this conjecture, and will provide a numerical confirmation when  $p = 3$ .

## 4.4 Conclusion

Since the derivation of the AKLT model realizing an exactly solvable gapped point in the phase diagram of the bilinear-biquadratic spin-1 chain, and providing a strong argument in favor of the gapped phase at the Heisenberg point conjectured by Haldane, AKLT models have been recurrently used as a very useful tool to analyze phases of spin chains. With the recent advent of experiments which engineer  $SU(N)$  spin models using ultracold atoms tuned to the Mott insulating phase of the Hubbard model, the AKLT models have been naturally generalized to the  $SU(N)$  group. From a theoretical point of view the  $SU(N)$  AKLT models are of particular interest. They provide a first indication of the existence of a gapped phase of the spin chain. Alternatively, if no AKLT state is found for a given physical local irrep of  $SU(N)$  this potentially indicates a gapless phase. The  $SU(N)$  AKLT models are thus valuable guides for elaborating a Haldane-type argument for  $SU(N)$  Heisenberg chains [118]. They further give access to a point in the phase diagram which is computationally easily accessible, despite the generally large local Hilbert space dimension, thanks to their short correlation lengths.

In this chapter we have described a generic method to construct reflection-symmetric AKLT states with  $SU(N)$  symmetry and their parent Hamiltonians. To impose the reflection symmetry we work with “building blocks”, the virtual irreps, which are self-conjugate. These irreps become the edge states on finite open chains, and thus dictate the ground state degeneracy in this case. Moreover they allow us to argue if the AKLT model lies in a SPT phase or in a trivial phase, by analyzing if the edge spins can

merge with bulk excitations. The MPS form of the AKLT wave function proved to be particularly useful both for visualizing the structure of the state and to construct parent Hamiltonians. We have discussed how to actually build the entire family of local parent Hamiltonians acting on  $l$  adjacent sites where  $l$  is greater than or equal to the injectivity length of the MPS, namely the smallest length for which the MPS is an injective map from the auxiliary degrees of freedom onto the physical space. This condition is the most critical one: if one selects edge spins with a large dimension, the injectivity length increases and the Hamiltonian becomes longer-ranged. Rewriting the Hamiltonian in a compact form using spin operators becomes quickly intractable due to the large number of rotation invariant operators on  $l$  sites.

As an example we have constructed a spin-1 AKLT model for which the ground state wave function possesses spin-1 edge states. The entire family of parent Hamiltonians has been derived. Thanks to the relatively small number of reflection-symmetric  $SU(2)$  invariant operators we have rewritten these Hamiltonians in a compact form with spin operators. Since the edge states of the wave function are of the same nature as the bulk excitations, namely integer spin states, the model was expected to lie in a trivial gapped phase. This was demonstrated by exhibiting a continuous phase transition between that model and the original AKLT model which lies in the Haldane phase. The topological phase transition was shown to be governed by the  $SU(2)_1$  WZW CFT, in agreement with previous analytical predictions for such transitions [135].

Finally we revisited an  $SU(3)$  AKLT model for the physical 3-box symmetric irrep of dimension 10 initially introduced in Refs. [117, 118]. Building on the spectrum of the reduced density matrix we showed that the wave function has edge states belonging to the adjoint irrep. These edge states are not expected to be protected by symmetry as they are indistinguishable from bulk excitations. One possible parent Hamiltonian of this AKLT state being simply made of bilinear and biquadratic interactions on two neighboring sites it will be used in the next chapter to guide our study of the corresponding pure Heisenberg model.

## 5 The 3-box symmetric $SU(3)$ chain

In 1975, Sutherland extended the Bethe ansatz to the  $SU(N > 2)$  Heisenberg model with the fundamental irrep at each site, thus implicitly showing that, as is the case for  $SU(2)$ , the model is gapless [35]. This paved the way to an increasing interest of the condensed matter community in the physics of  $SU(N)$  models. Indeed, before this paper the  $SU(N)$  group appeared mainly as a playground for mathematical physics or high-energy physics. It is well-known that the hadrons can be described to some extent as  $SU(3)$  particles forming different irreps<sup>1</sup>. The excitement of the condensed matter community, however, stayed rather limited in the beginning. The topic was quite remote and the absence of obvious experimental realizations of such models at low energy refrained the community from giving all the attention that these models deserve. The situation has considerably changed since then, with the advent of experiments with ultracold atoms loaded in optical lattices which can realize Mott insulating phases of the Hubbard model, thus giving access to the physics of the  $SU(N)$  models [40–51]. With the increasing interest, both experimental and theoretical, in the  $SU(N)$  models the question of whether an  $SU(N)$  Heisenberg spin chain is gapped or gapless becomes natural, and the situation is essentially the same as 37 years ago when considering  $SU(2)$  spin chains: on the one hand, performing numerics on  $SU(N)$  models with non-trivial irreps is a difficult task, in particular because of the large local Hilbert space dimension associated to these systems. On the other hand, although progress has been made constantly in the experimental realizations of  $SU(N)$  models with ultracold atoms, they are still restricted to simple irreps, those with a Young diagram made of two columns, and quite far from being able to extract thermodynamic quantities and thus discriminate between gapped and gapless models. On top of this, asserting which models are gapped or gapless for  $SU(N)$  looks a priori more complicated since  $SU(N)$  irreps are labeled by  $N - 1$  integers. The variety of irreps is thus bigger, and a general claim about gaplessness must be less simple than for  $SU(2)$ . Unlike in the 80's where the AKLT model was developed after the Haldane conjecture and could bring

---

<sup>1</sup>For instance the family of mesons can be described as the combination of an  $SU(3)$  quark corresponding to the fundamental irrep with an  $SU(3)$  anti-quark corresponding to the conjugate irrep.

it additional credit, the chronology was different for  $SU(N > 2)$ . AKLT models were developed first, providing hints on what would be a possible Haldane conjecture for the corresponding Heisenberg chains [123]. Alternatively, for some irreps AKLT models cannot be constructed, and this hints at a gapless spectrum. The path followed by Haldane in 1983 [31, 32] was finally reproduced very recently for  $SU(3)$  and  $SU(N)$  models in some specific irreps [138–141]. In particular, in Ref. [138], based on a mapping onto a  $NL\sigma M$ , it was argued that the  $SU(3)$  Heisenberg model in the symmetric irrep with  $p$  boxes should be gapped when  $p$  is a multiple of three, and gapless otherwise, the case  $p = 1$  being in agreement with Sutherland's result. From a numerical point of view, results in favor of a finite gap in the  $p = 3$  case were inconclusive for several years. The model was claimed to be gapped in 2009 based on the saturation of the entanglement entropy on a periodic chain of length 48 studied using DMRG [123]. The saturation being observed over a very short characteristic length, it could be argued from these results that the associated correlation length is rather short, of order  $6 - 8$  sites, and thus that the gap is rather large. Later on, the model was studied using ED on a 12-site periodic chain, and the results were in contradiction with the existence of a short correlation length [87]. Moreover the calculated central charge was surprisingly in agreement with a critical  $SU(3)_3$  WZW CFT universality class. However it had been demonstrated that the  $SU(N)$  Heisenberg models should flow in the IR towards the stable  $SU(N)_1$  WZW CFT, except if finely tuned to some unstable integrable points where the  $SU(N)_k$  WZW CFT can be realized [142, 143]. These special points are actually the generalization of the well known Takhtajan-Babudjian integrable points for  $SU(2)$  spin chains [144, 145]. Although the results on the central charge reported in Ref. [87] seemed in contradiction with the existence of a gap in the model, it was pointed out that the thermodynamic regime was not achieved on a 12-site chain. This observation was crucial in two respects. First, and most importantly, the critical behavior observed at short length scale does not rule out the possibility of a gapped spectrum. The IR behavior of the spin chain, namely the low-energy, or long-distance behavior must be probed to determine the existence or absence of a gap<sup>2</sup>. Secondly, a critical reading of the early DMRG results could be inferred. The correlation length that could be extracted from the saturation of the entanglement entropy seemed significantly underestimated, and it was argued that this saturation was actually due to a too severe truncation of the Hilbert space in DMRG. The 3-box symmetric  $SU(3)$  chain, if gapped, must then have a large correlation length which prevents the observation of the IR behavior with ED. Quantum Monte Carlo being affected by the sign problem for  $p$ -box symmetric irreps when  $p > 1$ , the only numerical technique which could possibly probe the thermodynamic properties of the model is the DMRG, but the large local Hilbert space dimension sounds prohibitive<sup>3</sup>. The confirmation of the Haldane

<sup>2</sup>This can be related to the material covered in Chapter 2, where the physics in the IR and in the UV are, as often, drastically different, and where the characteristic length scale which specifies the transition from one behavior to the other is a key parameter.

<sup>3</sup>Other tensor network based methods which probe directly the model in the thermodynamic limit, such as the variational uniform matrix product state (VUMPS) algorithm are also promising, see Sec-

---

conjecture, however, relies almost entirely on the demonstration that the  $p = 3$  case is gapped. It is indeed the “most quantum” case for which the conjecture predicts a gap. As it is the case for  $SU(2)$  where the mapping from the spin chain onto the  $NL\sigma M$  is exact in the limit of infinite spin, and where the spin-1 chain is the most quantum gapped spin chain, the mapping from the  $SU(3)$  spin chain becomes exact in the limit of infinite  $p$ . One can thus trust more safely Haldane’s conjecture at large  $p$  than at small  $p$ .

Not to our disappointment, and in a similar fashion as for  $SU(2)$  where it was shown that the characteristic length scale of the spin- $S$  Heisenberg chain scales as  $e^{\pi S}/S$ , it is expected that the characteristic length scale of the  $p$ -box symmetric  $SU(3)$  chain scales as  $e^{\alpha p}/p$ ,  $\alpha > 0$ . The simplest model, meaning the model with the shortest characteristic length scale, which is thought to be gapped is thus the  $p = 3$  one, and the attempt at demonstrating the presence of a finite gap in the  $p = 3$   $SU(3)$  spin chain is the exact analogue of the search for a finite gap in the spin-1 chain in the early 80’s. For the reason mentioned above, showing numerically rigorously the existence of a finite gap in the 3-box symmetric  $SU(3)$  chain would be a very strong indication that the Haldane conjecture for  $SU(3)$  spin chains in the  $p$ -box symmetric irrep applies when  $p$  is any multiple of 3. The next step to strengthen Haldane’s conjecture would be to probe the 2-box symmetric chain and to show the gaplessness of the spectrum.

The aim of this chapter is to present a numerical study of the  $p = 3$  Heisenberg model, using the group theory machinery developed in Chapter 3 to implement a DMRG algorithm taking advantage of the full  $SU(3)$  symmetry, and to show evidence for the existence of a finite gap in the model. The AKLT model and wave function presented in Chapter 4 will prove to be valuable guides in our search for a tiny gap.

The chapter is organized as follows. In Section 5.1 we present Haldane’s conjecture for the  $p$ -box symmetric  $SU(3)$  Heisenberg chain as developed in Refs. [138, 139]. We then turn to the description of the numerical tool used for our analysis, a DMRG algorithm with the implementation of the full  $SU(3)$  symmetry, making use of the SDCs introduced in Chapter 3. We then numerically study the AKLT model with a biquadratic interaction introduced in Refs. [117, 118] and extensively discussed in Section 4.3. We then turn to the numerical investigation of the pure Heisenberg model in Section 5.6. Finally, Section 5.7 gives some concluding remarks and an outlook of this chapter.

Part of the material presented in this chapter has been the object of Ref. [57]. More precisely: Section 5.1 is mainly inspired from Ref. [138]. Sections 5.2 and 5.3 have been presented in Ref. [57]. Section 5.4 goes beyond what has been provided in Ref. [57] and gives a number of additional details adapted from Ref. [89] for the case of the 3-box symmetric irrep. Finally, the results presented in Secs. 5.5 and 5.6 are the core of Ref. [57].

---

tion 5.7 [146].

## 5.1 Haldane's conjecture for symmetric SU(3) chains

### 5.1.1 Statement of the conjecture

Let us consider the antiferromagnetic SU(3) Heisenberg model with  $p$ -box symmetric irrep at each site

$$\mathcal{H} = 2J \sum_i \mathbf{T}_i \cdot \mathbf{T}_{i+1} \quad (5.1)$$

where  $J > 0$  is the antiferromagnetic coupling and  $\mathbf{T}_i$  are the generators in the  $p$ -box symmetric irrep. When  $p = 2, 3$  the generators are given in Appendix F. This Hamiltonian can be rewritten in terms of the operators  $\mathcal{S}^{\alpha\beta}$  as

$$\mathcal{H} = J \sum_i \mathcal{S}_i^{\alpha\beta} \mathcal{S}_{i+1}^{\beta\alpha} \quad (5.2)$$

where a sum over the color indices is implicit. The Haldane conjecture is as follows [138]:

- when  $p$  is a multiple of three, the spectrum of Hamiltonian (5.1) is gapped;
- when  $p$  is not a multiple of three, the spectrum of Hamiltonian (5.1) is gapless.

### 5.1.2 Hints from AKLT construction and Lieb-Schultz-Mattis-Affleck theorem

In Section 4.3 we have shown the existence of AKLT models for the  $p$ -box symmetric chain when  $p$  is a multiple of three. In particular, when  $p = 3$  the AKLT parent Hamiltonian was a bilinear-biquadratic form [117, 118]. When  $p$  is not a multiple of three, however, we showed that no AKLT model can be constructed. This is a first hint of the existence of a gapped phase for  $p = 3n$  and a gapless phase otherwise.

The case of  $p = 3n + q$  when  $q = 1, 2$  can be treated with the Lieb-Schultz-Mattis-Affleck (LSMA) theorem [147, 148]. In this case one can indeed show that either the ground state is degenerate or the spectrum is gapless [138]. When  $p = 3n$ , however, nothing can be extracted from the LSMA theorem. Finally, the case of  $p = 1$ , which is Bethe ansatz solvable, corresponds to the gapless realization of the LSMA theorem.

The three arguments above (existence or absence of AKLT models, LSMA theorem, gapless spectrum for  $p = 1$ ) already shape Haldane's conjecture as stated in Section 5.1.1. To complete and to fully ground the conjecture for symmetric SU(3) chains, it is necessary to follow Haldane's procedure for SU(2) chains, namely to map the spin chain onto a low-energy theory and to derive consequences based on the structure of this field theory [31, 32]. In the next section, we summarize this procedure which was carried out in Refs. [138, 139].

### 5.1.3 Mapping onto a nonlinear sigma model

This section summarizes step by step the mapping of the spin chain onto the NL $\sigma$ M introduced in Ref. [138].

Following Haldane who mapped the SU(2) Heisenberg spin chain onto the O(3) NL $\sigma$ M in the limit of large spin  $S$ , the idea is to look at the large- $p$  limit. Examining the classical limit one faces a first problem: the ground state of the Heisenberg Hamiltonian (5.2) is degenerate. This is a major issue for developing a large- $p$  semi-classical limit where fluctuations are introduced around a unique classical ground state. The solution consists in lifting this degeneracy by introducing further-neighbor couplings,

$$\mathcal{H}' = J \sum_i \mathcal{S}_i^{\alpha\beta} \mathcal{S}_{i+1}^{\beta\alpha} + J_2 \sum_i \mathcal{S}_i^{\alpha\beta} \mathcal{S}_{i+2}^{\beta\alpha} - J_3 \sum_i \mathcal{S}_i^{\alpha\beta} \mathcal{S}_{i+3}^{\beta\alpha}. \quad (5.3)$$

The antiferromagnetic and ferromagnetic couplings  $J_2$  and  $J_3$ , respectively, are both decreasing as  $p$  increases and are generated by quantum fluctuations in the Heisenberg model, selecting one particular ground state, the three-sublattice state which is made of the alternation of the three colors of SU(3),  $ABCABC\dots$ . It is thus  $\mathcal{H}'$ , not  $\mathcal{H}$ , which will be mapped onto a NL $\sigma$ M. In fact, it would be sufficient to take only  $J_2$  or  $J_3$  to lift the degeneracy, but for consistency with Ref. [138] we also keep both couplings here.

The mapping onto the field theory can be conveniently derived by writing the action as a path integral over spin-coherent states at inverse temperature  $\beta$  as

$$S[\vec{\Phi}, \vec{\Phi}^\dagger] = \int_0^\beta d\tau \left( \langle \vec{\Phi}(\tau) | \mathcal{H}' | \vec{\Phi}(\tau) \rangle + p \sum_j \vec{\Phi}(j, \tau)^\dagger \partial_\tau \vec{\Phi}(j, \tau) \right) \quad (5.4)$$

where  $\vec{\Phi}(j, \tau)$  is a 3-dimensional unit complex vector at site  $j$  and imaginary time  $\tau$ ,  $\vec{\Phi}(j, \tau)^\dagger \vec{\Phi}(j, \tau) \equiv \vec{\Phi}(j, \tau)^* \cdot \vec{\Phi}(j, \tau) = 1$ ,  $\forall j, \tau$ , and where  $|\vec{\Phi}(\tau)\rangle$  is the spin-coherent state of the entire chain at time  $\tau$ ,

$$|\vec{\Phi}(\tau)\rangle = \bigotimes_j |\vec{\Phi}(j, \tau)\rangle \quad (5.5)$$

where

$$|\vec{\Phi}(j, \tau)\rangle = \frac{1}{\sqrt{p!}} \left( \Phi_\mu(j, \tau) b_\mu^\dagger(j) \right)^p |0\rangle \quad (5.6)$$

and there is an implicit sum over the index  $\mu = 1, 2, 3$ ,  $\Phi_\mu(j, \tau)$  being the  $\mu$ -th component of  $\vec{\Phi}(j, \tau)$ . In Eq. (5.6)  $|0\rangle$  is the vacuum and the operator  $b_\mu^\dagger(j)$  creates a boson of color  $\mu$  at site  $j$ .

After some algebra, which essentially consists in introducing some quantum fluctuations around the three-sublattice classical ground state (when  $J_1, J_2, J_3 > 0$ ) by decomposing the  $\vec{\Phi}(j, \tau)$  fields into the combination of a field describing the fluctua-

tions inside a unit cell and a field describing the fluctuations between the unit cells, taking the continuum limit and integrating out the slow motion within the unit cell one ends up with (see Eq. (4.14) of Ref. [138])

$$\begin{aligned}
 S[\{\vec{\phi}_n\}, \{\vec{\phi}_n^\dagger\}] &= \sum_{n=1}^3 \int dx d\tau \frac{1}{2g} \left( |\partial_\mu \vec{\phi}_n|^2 - |\vec{\phi}_n^* \cdot \partial_\mu \vec{\phi}_n|^2 \right) \\
 &+ i \sum_{n=1}^3 \frac{\theta_n}{2\pi i} \int dx d\tau \epsilon^{\mu\nu} \partial_\mu \vec{\phi}_n \cdot \partial_\nu \vec{\phi}_n^* \\
 &+ i \frac{\lambda}{2\pi i} \sum_{n=1}^3 \int dx d\tau \epsilon^{\mu\nu} \left( \vec{\phi}_{n+1}^* \cdot \partial_\mu \vec{\phi}_n \right) \left( \vec{\phi}_{n+1} \cdot \partial_\nu \vec{\phi}_n^* \right).
 \end{aligned} \tag{5.7}$$

The fields  $\vec{\phi}_n$ ,  $n = 1, 2, 3$  are 3-dimensional unit complex vectors satisfying the unitarity condition<sup>4</sup>

$$\vec{\phi}_m^\dagger \vec{\phi}_n \equiv \vec{\phi}_m^* \cdot \vec{\phi}_n = \delta_{mn}, \quad m, n = 1, 2, 3 \tag{5.8}$$

and, in the third line of Eq. (5.7), we take  $\vec{\phi}_4 \equiv \vec{\phi}_1$ . Notice that all over Eq. (5.7) we have omitted the space-time variables  $(x, \tau)$  on which the fields depend,  $\vec{\phi}_n \equiv \vec{\phi}_n(x, \tau)$ . Although the first line of the action (5.4) looks like three independent field theories, they are actually interacting through the unitarity condition. Each field theory in the first line of (5.4) is called a  $\mathbb{CP}^2$  field theory, and the action (5.7) is called an  $SU(3)/[U(1) \times U(1)]$  flag manifold NL $\sigma$ M [149, 150],  $SU(3)/[U(1) \times U(1)]$  describing the manifold of the 3-dimensional matrix  $U$  formed by staking the vectors  $\vec{\phi}_n^T$ ,  $n = 1, 2, 3$  in its rows. The coupling constant  $g$  is the same for all copies of the  $\mathbb{CP}^2$  theories as a consequence of the lattice symmetries of the spin model, and the mapping gives  $g^{-1} = p\sqrt{J_1 J_2 + 2J_1 J_3 + 2J_2 J_3}/(J_1 + J_2)$ . The second line in the action (5.7), where  $\epsilon^{\mu\nu}$  is the Levi-Civita tensor on two space-time indices, is a topological action made of three terms with topological angles  $\theta_n$ ,  $n = 1, 2, 3$ , respectively. The associated topological charges are actually not independent, and one can thus remove one of them from the action. Moreover, thanks to the translational invariance, the two remaining topological angles take the values  $\pm 2\pi p/3$ . Finally the third line of (5.7) is an interaction term with coupling  $\lambda$  which can again be expressed in terms of  $J_1$ ,  $J_2$  and  $J_3$ . It is non-topological as it cannot be rewritten as a total derivative, unlike the second line of the action. A renormalization group analysis shows that the theory in the first line of (5.7) is asymptotically free, and that the  $\lambda$ -term is relevant in the IR [139, 151].

Classical Monte Carlo simulations on the model (5.7) when  $\lambda = 0$  show that [138]: i) when the two remaining independent topological angles vanish, corresponding to  $p$  being an integer multiple of three, the model is gapped for all values of the coupling constant  $g$ ; ii) when the topological angles are chosen as  $\pm 2\pi/3$ , corresponding to

---

<sup>4</sup>Defining the matrix  $U$  such that its  $n$ -th row corresponds to the transposed vector  $\vec{\phi}_n^T$ , then Eq. (5.8) translates into the condition  $UU^\dagger = U^\dagger U = 1$ . The action (5.7) can also be compactly written in terms of  $U(x, \tau)$  and  $U^\dagger(x, \tau)$ , see Eq. (4.6) of Ref. [138].



$p = 1, 2$ , the model is gapped at strong coupling  $g > g_c$  and gapless at weak coupling  $g < g_c$ .

These observations, together with lattice realizations of the  $SU(3)$  chain model, such as the AKLT model extensively discussed in Chapter 4 for  $p = 3$  [118] and the known results on the  $p = 1$  case when  $J_2 = J_3 = 0$  [35], the Lieb-Schulz-Mattis theorem [147, 148] and the apparent analogy with the  $SU(2)$  case naturally leads to the conjecture as stated at the beginning of this section.

## 5.2 The Hamiltonian as a sum of permutations

To make full use of the representation theory of the permutation group presented in Chapter 3 we need to rewrite Hamiltonian (5.2) in terms of permutations. To do so, we first rewrite the operators  $S_i^{\alpha\beta}$  in terms of bosonic operators as follows (we keep  $N$  and  $p$  since the developments are general)

$$S_i^{\alpha\beta} = \sum_{a=1}^p b_{\alpha,a,i}^\dagger b_{\beta,a,i} - \frac{p}{N} \delta_{\alpha\beta} \quad (5.9)$$

where the bosons satisfy the usual commutation relations

$$[b_{\alpha,a,i}, b_{\beta,b,j}^\dagger] = \delta_{\alpha\beta} \delta_{ab} \delta_{ij} \quad (5.10)$$

and where the constraint of  $p$  bosons at each site is imposed

$$\sum_{\alpha=1}^N \sum_{a=1}^p b_{\alpha,a,i}^\dagger b_{\alpha,a,i} = p, \quad \forall i. \quad (5.11)$$

The states of the irrep can be simply expressed in terms of the bosonic operators. For instance, when  $N = 3$  and  $p = 3$  the expressions of the states are (omitting the site index  $i$ )

$ n_A, n_B, n_C\rangle$		
$\boxed{A}\boxed{A}\boxed{A}$	$ 3, 0, 0\rangle$	$b_{A,1}^\dagger b_{A,2}^\dagger b_{A,3}^\dagger  0\rangle$
$\boxed{B}\boxed{B}\boxed{B}$	$ 0, 3, 0\rangle$	$b_{B,1}^\dagger b_{B,2}^\dagger b_{B,3}^\dagger  0\rangle$
$\boxed{C}\boxed{C}\boxed{C}$	$ 0, 0, 3\rangle$	$b_{C,1}^\dagger b_{C,2}^\dagger b_{C,3}^\dagger  0\rangle$
$\boxed{A}\boxed{A}\boxed{B}$	$ 2, 1, 0\rangle$	$\frac{1}{\sqrt{3}} \left( b_{A,1}^\dagger b_{A,2}^\dagger b_{B,3}^\dagger + b_{A,1}^\dagger b_{B,2}^\dagger b_{A,3}^\dagger + b_{B,1}^\dagger b_{A,2}^\dagger b_{A,3}^\dagger \right)  0\rangle$
$\boxed{A}\boxed{B}\boxed{B}$	$ 1, 2, 0\rangle$	$\frac{1}{\sqrt{3}} \left( b_{A,1}^\dagger b_{B,2}^\dagger b_{B,3}^\dagger + b_{B,1}^\dagger b_{A,2}^\dagger b_{B,3}^\dagger + b_{B,1}^\dagger b_{B,2}^\dagger b_{A,3}^\dagger \right)  0\rangle$

## Chapter 5. The 3-box symmetric SU(3) chain

$\boxed{A A C}$	$ 2, 0, 1\rangle$	$\frac{1}{\sqrt{3}} \left( b_{A,1}^\dagger b_{A,2}^\dagger b_{C,3}^\dagger + b_{A,1}^\dagger b_{C,2}^\dagger b_{A,3}^\dagger + b_{C,1}^\dagger b_{A,2}^\dagger b_{A,3}^\dagger \right)  0\rangle$
$\boxed{A C C}$	$ 1, 0, 2\rangle$	$\frac{1}{\sqrt{3}} \left( b_{A,1}^\dagger b_{C,2}^\dagger b_{C,3}^\dagger + b_{C,1}^\dagger b_{A,2}^\dagger b_{C,3}^\dagger + b_{C,1}^\dagger b_{C,2}^\dagger b_{A,3}^\dagger \right)  0\rangle$
$\boxed{B B C}$	$ 0, 2, 1\rangle$	$\frac{1}{\sqrt{3}} \left( b_{B,1}^\dagger b_{B,2}^\dagger b_{C,3}^\dagger + b_{B,1}^\dagger b_{C,2}^\dagger b_{B,3}^\dagger + b_{C,1}^\dagger b_{B,2}^\dagger b_{B,3}^\dagger \right)  0\rangle$
$\boxed{B C C}$	$ 0, 1, 2\rangle$	$\frac{1}{\sqrt{3}} \left( b_{B,1}^\dagger b_{C,2}^\dagger b_{C,3}^\dagger + b_{C,1}^\dagger b_{B,2}^\dagger b_{C,3}^\dagger + b_{C,1}^\dagger b_{C,2}^\dagger b_{B,3}^\dagger \right)  0\rangle$
$\boxed{A B C}$	$ 1, 1, 1\rangle$	$\frac{1}{\sqrt{6}} \left( b_{A,1}^\dagger b_{B,2}^\dagger b_{C,3}^\dagger + \dots \right)  0\rangle$

where the first column contains the Weyl tableaux and in the second column  $|n_A, n_B, n_C\rangle$  is the occupation number of each color  $A, B, C$ . In the last line the ellipse denotes all permutations of the three colors. These states are the ones already introduced in Eq. (3.72).

Inserting Eq. (5.9) into the Hamiltonian one obtains

$$\mathcal{H} = J \sum_i \left( \sum_{\alpha, \beta=1}^N \sum_{a, b=1}^p b_{\alpha, a, i}^\dagger b_{\beta, a, i} b_{\beta, b, i+1}^\dagger b_{\alpha, b, i+1} - \frac{p^2}{N} \right). \quad (5.12)$$

Now observe that the quartic form in bosonic operators can be rewritten as

$$\sum_{a, b=1}^p \sum_{\alpha, \beta=1}^N b_{\alpha, a, i}^\dagger b_{\beta, b, i+1}^\dagger b_{\beta, a, i} b_{\alpha, b, i+1} = \sum_{a, b=1}^p \mathcal{P}_{a, i; b, i+1} \quad (5.13)$$

where  $\mathcal{P}_{a, i; b, i+1}$  is the permutation operator which interchanges the state of the  $a$ -th boson of site  $i$  with the state of the  $b$ -th boson of site  $i+1$ .

For the sake of simplicity, let us number the particles (boxes) from 1 to  $n$  within the chain, with  $n$  the total number of boxes, and introduce the set  $\Gamma_i$  which contains the particle's numbers situated at site  $i$ . For instance, for an SU(3) chain with the 3-box symmetric irrep at each site and  $N_s = 6$  sites in total, the numbering is given in Fig. 5.1. The interaction Hamiltonian between two sites  $i$  and  $j$  then takes the simple form

$$\mathcal{H}_{(i, j)} = 2 \mathbf{T}_i \cdot \mathbf{T}_j = \mathcal{S}_i^{\alpha\beta} \mathcal{S}_j^{\beta\alpha} = \sum_{k \in \Gamma_i} \sum_{l \in \Gamma_j} \mathcal{P}_{k, l} - \frac{p^2}{N} \quad (5.14)$$

where  $\mathcal{P}_{k, l}$  interchanges particle  $k$  with particle  $l$ .

In what follows we shall remove the constant term in this expression and consider the following permutation Hamiltonian,

$$\mathcal{H} = J \sum_i \sum_{k \in \Gamma_i} \sum_{l \in \Gamma_{i+1}} \mathcal{P}_{k, l}. \quad (5.15)$$

$i =$	1	2	3	4	5	6
	<span style="border: 1px solid black; padding: 2px;">1 2 3</span>	<span style="border: 1px solid black; padding: 2px;">4 5 6</span>	<span style="border: 1px solid black; padding: 2px;">7 8 9</span>	<span style="border: 1px solid black; padding: 2px;">10 11 12</span>	<span style="border: 1px solid black; padding: 2px;">13 14 15</span>	<span style="border: 1px solid black; padding: 2px;">16 17 18</span>
$\Gamma_i =$	$\{1, 2, 3\}$	$\{4, 5, 6\}$	$\{7, 8, 9\}$	$\{10, 11, 12\}$	$\{13, 14, 15\}$	$\{16, 17, 18\}$

Figure 5.1: Numbering of particles (boxes) within a chain with  $N_s = 6$  sites.  $\Gamma_i$  is the set of particles living at site  $i$  in a global numbering of particles.

### 5.3 Dealing with the edge states

Since we expect the pure Heisenberg Hamiltonian (5.1) with  $p = 3$  and the AKLT Hamiltonian (see Eq. (4.48) or Eq. (55) of Ref. [118])

$$\mathcal{H} = 5J \sum_i \left( \mathbf{T}_i \cdot \mathbf{T}_{i+1} + \frac{1}{5} (\mathbf{T}_i \cdot \mathbf{T}_{i+1})^2 + \frac{6}{5} \right) \quad (5.16)$$

to lie in the same Haldane phase, for OBC Hamiltonian (5.1) is expected to have low-lying edge states. The nature of the edge states at the AKLT point has been extensively discussed in Section 4.3, and we shall extend the discussion to the case of the Heisenberg model. From a numerical point of view the edge states could be removed by using PBC. However from the perspective of the DMRG, the choice of using PBC has deep consequences: for a given chain length convergence is much more difficult, preventing the study of large systems. For OBC, the presence of edge states is also critical. First, convergence is affected because the edge modes couple to each other between the left and right end of the chain. Secondly the bulk gap is not obtained by accessing the lowest energy state in a given symmetry sector, but the second or the third<sup>5</sup>. Indeed, from Fig. 4.6 we expect the edge states to be adjoint edge modes. This edge modes recombine into all irreps given in Eq. (4.44). When the chain length  $N_s$  is a multiple of three, the ground state is the singlet wave function, and the five other states are low-lying excited states. Thus, to access the singlet-adjoint bulk gap, for instance, one needs to compute the third lowest energy state in the adjoint sector, since the first two lowest energy adjoint states are low-lying and collapse on the ground for increasing system size<sup>6</sup>.

<sup>5</sup>If the different symmetry sectors cannot be targeted, for instance by the use of a standard DMRG code without implementation of the  $SU(3)$  symmetry, one needs to access the 64-th excited state to actually compute the bulk gap from the ground state.

<sup>6</sup>Notice that this is analogous to the  $SU(2)$  spin-1 chain. For OBC, the spin-1/2 edge states couple and form a singlet (ground state) and a low-lying triplet which collapses on the ground state in the thermodynamic limit. To compute the singlet-triplet bulk gap, one thus needs to compute the second lowest energy state in the spin-1 sector, or, if one cannot access the different spin sectors separately, the fourth excited state. The only difference between the  $SU(2)$  and  $SU(3)$  cases, besides the fact that the  $SU(3)$  edge irreps have significantly larger dimension (8 versus 2 for  $SU(2)$ ), is that the edge modes can only form a triplet excitation on top of the singlet ground state, while in the  $SU(3)$   $p = 3$  case, the adjoint

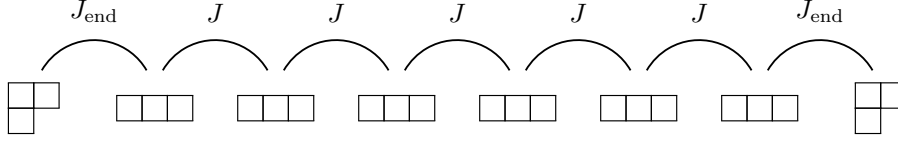


Figure 5.2: Structure of the 3-box symmetric  $SU(3)$  chain, with the adjoint edge spins coupled antiferromagnetically with  $J_{\text{end}} > 0$  to their neighbor [57]. The Heisenberg Hamiltonian corresponding to this chain is given in Eq. (5.17). Figure adapted from Ref. [57] with the permission of the APS, © 2020 American Physical Society.

There is however a way to lift the edge states with OBC, and this is again inspired from the VBS structure of the AKLT state in Fig. 4.6, as well as from what has been done in  $SU(2)$  spin chains [152–156]. We add adjoint edge spins at both ends of the chain, and couple them antiferromagnetically with their 3-box symmetric neighbor in order to form a singlet bond. Figure 5.2 shows the structure of the chain. For any chain length, the ground state lies in the singlet sector, and any excited state is then a bulk excited state. Introducing the end coupling  $J_{\text{end}} > 0$  the Hamiltonian becomes

$$\mathcal{H} = J_{\text{end}} \left( \mathcal{H}_{(1,2)} + \mathcal{H}_{(N_s-1,N_s)} \right) + J \sum_{i=2}^{N_s-1} \mathcal{H}_{(i,i+1)} \quad (5.17)$$

where  $N_s$  is still the total number of sites, including the adjoint edge spins, and where the interaction is given by

$$\mathcal{H}_{(i,i+1)} = \sum_{k \in \Gamma_i} \sum_{l \in \Gamma_{i+1}} \mathcal{P}_{k,l}. \quad (5.18)$$

One can now guess the structure of the lowest energy excited states, which, if the model is gapped, will all be separated from the ground state by a finite gap. Building again on our understanding of the  $SU(2)$  spin-1 chain and on Eq. (4.44) one postulates the existence of five branches of elementary excitations. Indeed, the simplest excitations are obtained by breaking one singlet bond in the VBS. The two unpaired adjoint irreps can recombine and form an adjoint irrep (two times), a 3-box symmetric irrep, its conjugate or a  $[4, 2]$  irrep. Defining the Haldane gap as the bulk gap from the singlet ground state to the elementary excitation, one thus has five Haldane gaps in the model, corresponding to the five elementary excitations.

---

edge modes can form 5 low-lying excitations.

## 5.4 Density matrix renormalization group with $SU(3)$ symmetry

### 5.4.1 Non-abelian symmetries in DMRG

As discussed above, obtaining the bulk gap of Hamiltonian (5.1) without the trick of adding adjoint spins at both ends of the open chain with a standard DMRG code which does not make use of any symmetry would require the calculation of the ground state and of 64 excited states, since the first 63 excited states are low-lying. This is obviously prohibitive. The adjoint edge spins reduce the total number of wave functions to compute to two. However, the dimension of the full Hilbert space, which is  $64 \times 10^{N_s-2}$  for a  $N_s$ -site chain, is a limiting factor. The scaling is the one corresponding to an  $SU(2)$  spin-9/2 chain and only extremely short chains could be studied, or longer chains at the price of a severe truncation of the Hilbert space which forbids any controlled extrapolation.

The implementation of the full  $SU(3)$  symmetry in the DMRG code seems to be the only viable solution to tackle Hamiltonian (5.1) numerically. The route of the implementation of the non-abelian symmetry is usually avoided by DMRG practitioners performing simulations on  $SU(2)$  models. At least three reasons can be found. First, the implementation of the  $U(1)$  (charge conservation, or magnetization conservation) symmetry is standard (it was implemented in the original DMRG papers of White [9, 10]) and already leads to a significant speed-up [11, 157–160]. The other reason is that implementing a non-abelian symmetry is more technical, and, in the most common case of  $SU(2)$  spin systems, the trouble to deal with such technicalities is not *strictly* necessary. Indeed the algorithmic gain (memory and operation complexity) is largely compensated by the use of more powerful clusters. Finally, the full rotational invariance of the spin model is restrictive as it forbids the study of the effects of anisotropies and external fields, of great importance both theoretically and experimentally. Nevertheless, the  $SU(2)$  symmetry has been successfully implemented in DMRG algorithms, with a significant speed-up as long as the total number of DMRG states kept is large enough, as is illustrated for instance in Ref. [161].

The  $SU(2)$  symmetry was first implemented in DMRG using an interaction-round-a-face (IRF) approach for the spin-1/2 chain, where the symmetry is naturally factorized out, and where the fusion rules of  $SU(2)$  are incorporated by the use of Bratteli diagrams [162]. The method was then extended to higher spins, where the benefit of the factorization of the symmetry really comes in [156, 163], and the incorporation of edge spins was carried out in Ref. [156]. In the IRF method, the Wigner-Eckart theorem is used to factorize the matrix elements of the interaction as a product of a “reduced matrix element” and a CGC [164]. The IRF weights, namely the matrix elements of the interaction, are then expressed in closed form in terms of Wigner  $6j$  symbols. Since

exact analytical expressions are known for such coefficients, their calculation can be performed at a very limited cost. However the drawback of this method is that the total number of coefficients which need to be computed increases with the system size and with the local spin at each site.

To overcome this issue, and to provide a more general setup for DMRG with non-abelian symmetries, McCulloch and Gulácsi devised an algorithm again based on the Wigner-Eckart theorem where the blocks themselves transform as irreps of the symmetry group, and where the Clebsch-Gordan series is used to target a specific irrep for the entire chain [165]. By the use of an appropriate density matrix the truncation of the Hilbert space ensures that the total spin is conserved at each step. The method being adaptable to any symmetry group<sup>7</sup>, provided one knows how to compute the associated CGCs, it was used for  $SU(2)$  spin chains but also for systems with  $SO(4)$  and  $U(1) \times SU(2)$  symmetries [158, 165–167]. Interestingly the  $SU(3)$  case was claimed to be under investigation in Ref. [165] but no results were later reported by the authors.

With the advent of the new formulation of the DMRG algorithm in terms of matrix product states [11, 168], the  $SU(2)$  symmetry was introduced in the representation of the tensors [161, 169–171]. The Wigner-Eckart theorem translates into the factorization of each symmetric tensor into the product of a “degeneracy tensor” and a “structural tensor”, the latter containing the CGCs [161, 170]. Implementing the symmetry directly in the tensors makes their use extremely versatile. The different tensor network based methods can then directly incorporate these symmetric tensors and perform the optimizations on the “degeneracy tensors” [170, 171]. In Ref. [171] Weichselbaum described this framework in a generic way, opening the door to the implementation of  $SU(N > 2)$  symmetric tensors to be used in variational algorithms such as the new formulation of the DMRG.

In the first studies of  $SU(N)$ -symmetric spin models [123, 172], the non-abelian symmetry was kept aside because it was considered “inconvenient” [123], and only potentially “useful” [173]. In 2018, two papers made full use of the  $SU(N)$  symmetry for the fundamental irrep at each site, one of them being based on Weichselbaum’s construction [171] and being used to study  $SU(N)$  spin ladders with  $N \leq 6$  [51]. The ladder geometry in this paper brings an additional level of complication and increases at the same time the real need for the non-abelian symmetry to be implemented. The other paper introduced a new DMRG algorithm based on SYTs and SDCs of the symmetric group, and provides numerical results on the  $SU(N)$  Heisenberg chain for  $N$  up to 8 [89].

In this section, we shall extend the latter construction to the case of the 3-box symmetric irrep of  $SU(3)$  at each site. In fact, the generalization applies to the  $p$ -box symmetric

---

<sup>7</sup>In fact, the algorithm simply reduces to the standard formulation of White when the symmetry group is reduced to the  $U(1)$  abelian group [10].

irrep of  $SU(N)$  with  $p$  and  $N$  being general, up to minor changes but at the cost of an increasing algorithmic complexity. We will in particular show how one computes the reduced matrix elements of the interaction using the SDCs of the permutation group, avoiding the need of the more common CGCs. The construction relies on the original formulation of the DMRG by White [9, 10].

### 5.4.2 Description of the algorithm

The DMRG algorithm has been extensively discussed in Ref. [89] for the case of the fundamental irrep of  $SU(N)$  at each site. The structure of the algorithm for the case of the symmetric irrep at each site is exactly the same, up to minor changes. We need in particular to incorporate the adjoint edge states (or any other sort of edge states), and to adapt the genealogy of irreps. This is of course trivial using the Itzykson-Nauenberg rules.

The algorithm is based on the idea of McCulloch [165]: the left and right blocks in DMRG must transform as irreps of the symmetry group. The first truncation of the Hilbert space thus consists in selecting a finite number  $M$  of irreps to describe the left and right blocks. For the case of antiferromagnetic chains, the ground state is expected to live in the irrep with the lowest quadratic Casimir compatible with the total number of boxes and with the local constraints. We thus choose the  $M$  irreps to be the irreps with the lowest quadratic Casimir. For instance, Fig. 5.3 shows the first  $M = 22$  irreps for  $SU(3)$ , together with their eigenvalue of the Casimir, as given in Eq. (3.78). We define the ordered list

$$\mathcal{I}_M = \left\{ \bullet, \square, \begin{array}{|c|c|} \hline \square & \square \\ \hline \end{array}, \begin{array}{|c|c|c|} \hline \square & \square & \square \\ \hline \end{array}, \dots \right\} \quad (5.19)$$

containing these  $M$  irreps. Notice that several of these irreps will never show up in the calculation when considering the 3-box symmetric irrep at each site. This is for instance the case of the irrep  $\begin{array}{|c|c|} \hline \square & \square \\ \hline \end{array} \in \mathcal{I}_{M=22}$  because it has two boxes, which is not a multiple of three. Notice further that in the list  $\mathcal{I}_M$  we have taken the irreps without the columns of  $N = 3$  boxes. When considering a given block of length  $L$  in DMRG, one can simply add columns of  $N$  boxes in order that the total number of boxes is conserved.

Denoting by  $[\beta^i]$  the irrep at the  $i$ -th site and considering now a left block made of  $L$  sites, the relevant irreps are all irreps appearing in the tensor product

$$\bigotimes_{i=1}^L [\beta^i] = \sum_{[\nu]} \mu^{[\nu]} [\nu] \quad (5.20)$$

where the right hand side is a direct sum of irreps  $[\nu]$  with outer multiplicities  $\mu^{[\nu]}$ . The second truncation consists in keeping  $m_L^{[\nu]} < \mu^{[\nu]}$  states to represent the block in the

	0		$\frac{25}{3}$
	$\frac{4}{3}$		$\frac{28}{3}$
	3		$\frac{34}{3}$
	$\frac{10}{3}$		12
	$\frac{16}{3}$		$\frac{40}{3}$
	6		15
	8		

Figure 5.3: List of the first  $M = 22$  irreps of lowest quadratic Casimir for SU(3). The eigenvalue of the quadratic Casimir corresponding to Eq. (3.78) is given beside the irrep(s). Two irreps having the same Casimir are conjugate to each other.

irrep  $[\nu]$ , where  $[\nu]$  appears in the list of  $M$  irreps  $\mathcal{I}_M$ . We denote these states by

$$\left\{ |\xi_1^{[\nu]} \rangle, |\xi_2^{[\nu]} \rangle, \dots, |\xi_{m_L^{[\nu]}}^{[\nu]} \rangle \right\}. \quad (5.21)$$

The total number of states kept at step  $L$  is then simply given by

$$m_L = \sum_{[\nu]} m_L^{[\nu]}. \quad (5.22)$$

We apply a truncation procedure such that  $m_L \leq m$  at each step. Actually we fix  $m$  beforehand and choose the most appropriate distribution of states, namely we choose the  $m_L^{[\nu]}$ 's in order to minimize the total discarded weight while satisfying  $m_L \leq m$ .

### Initialization

To grow the chain up to its final length  $N_s$ , we use the infinite-size DMRG algorithm. Observe that the right block is mirror symmetric to the left block. Denoting by  $\mathcal{H}_L$  the Hamiltonian on the first  $L$  sites, and  $H_L^{[\nu]}$  a matrix representation in the global  $[\nu]$  sector in a basis which respects the SU( $N$ ) symmetry, one starts by constructing  $H_{L=2}^{[\nu]}$  in all relevant sectors  $[\nu]$ , namely all irreps appearing in  $[\beta^1] \otimes [\beta^2]$ . How to construct these



#### 5.4. Density matrix renormalization group with $SU(3)$ symmetry

matrices has been extensively discussed in Refs. [86–88]. In our case where  $[\beta^1] = \begin{smallmatrix} \square & \square \\ \square & \end{smallmatrix}$  and  $[\beta^2] = \begin{smallmatrix} \square & \square & \square & \square \end{smallmatrix}$  one has 4 relevant sectors

$$\begin{smallmatrix} \square & \square \\ \square & \end{smallmatrix} \otimes \begin{smallmatrix} \square & \square & \square & \square \end{smallmatrix} = \begin{smallmatrix} \square & \square & \square \\ \square & \square & \end{smallmatrix} \oplus \begin{smallmatrix} \square & \square & \square & \square \\ \square & \square & \end{smallmatrix} \oplus \begin{smallmatrix} \square & \square & \square & \square \\ \square & \square & \end{smallmatrix} \oplus \begin{smallmatrix} \square & \square & \square & \square & \square \\ \square & \square & \end{smallmatrix}. \quad (5.23)$$

Notice that we have preserved the number of boxes, and that all irreps in the right hand side belong to the list  $\mathcal{I}_{M=22}$  when columns of  $N = 3$  boxes are removed.

We denote by  $\mathcal{I}_M^L$  the list of irreps kept at step  $L$ , and define  $M_L = \text{card}(\mathcal{I}_M^L)$  the number of such irreps. The index  $M$  in  $\mathcal{I}_M^L$  keeps track of the fact that there is a truncation over the  $M$  irreps listed in  $\mathcal{I}_M$ , namely  $\mathcal{I}_M^L$  must be a subset of  $\mathcal{I}_M$ . Here one has

$$\mathcal{I}_{M=22}^{L=2} = \left\{ \begin{smallmatrix} \square & \square \\ \square & \end{smallmatrix}, \begin{smallmatrix} \square & \square & \square & \square \end{smallmatrix}, \begin{smallmatrix} \square & \square & \square & \square \\ \square & \square & \end{smallmatrix}, \begin{smallmatrix} \square & \square & \square & \square & \square \\ \square & \square & \end{smallmatrix} \right\} \subset \mathcal{I}_{M=22}. \quad (5.24)$$

We have removed all columns of  $N$  boxes in the elements of  $\mathcal{I}_M^L$ . Indeed, we know that at step  $L$ , the total number of boxes is  $\sum_{i=1}^L p_i$  where  $p_i = \sum_k \beta_k^i$  since the irrep at site  $i$  is  $[\beta^i] \equiv [\beta_1^i, \beta_2^i, \dots]$ . One can thus easily restore all columns when necessary.

In the example of Eq. (5.23) there is no non-trivial outer multiplicity, namely each irrep in the right hand side appears only once. Thus one has  $m_{L=2}^{[\nu]} = 1, \forall [\nu] \in \mathcal{I}_{M=22}^{L=2}$  and the matrices  $H_{L=2}^{[\nu]}$  are made of a single number.

#### Selecting the new states

Now let us consider the more general case where the left block has  $L \geq 2$  sites, and the Hamiltonian  $\mathcal{H}_L$  on these  $L$  sites is described by the matrices  $H_L^{[\nu]}$ ,  $[\nu] \in \mathcal{I}_M^L$  where  $\mathcal{I}_M^L \subset \mathcal{I}_M$ . To increase the system length by 2 sites one needs to incorporate one site to the left block, and then compute the superblock Hamiltonian. The total Hamiltonian for the chain of length  $2L + 2$  is given by

$$\mathcal{H}_{2L+2} = \mathcal{H}_{L+1}^{\text{left}} + \mathcal{H}_{(L+1, L+2)} + \mathcal{H}_{L+1}^{\text{right}} \quad (5.25)$$

where  $\mathcal{H}_{L+1}^{\text{right}}$  is the Hamiltonian on sites  $L + 2, \dots, 2L + 2$  and is mirror symmetric to  $\mathcal{H}_{L+1}^{\text{left}}$  while  $\mathcal{H}_{(L+1, L+2)}$  joins the left and right blocks. The Hamiltonian  $\mathcal{H}_{L+1}^{\text{left}} \equiv \mathcal{H}_{L+1}$  is itself given by

$$\mathcal{H}_{L+1} = \mathcal{H}_L + \mathcal{H}_{(L, L+1)} \quad (5.26)$$

where  $\mathcal{H}_{(L, L+1)}$  is the interaction Hamiltonian between sites  $L$  and  $L + 1$  and  $\mathcal{H}_L$  is the Hamiltonian on the previous  $L$ -site block, see Fig. 5.4. The Hamiltonian  $\mathcal{H}_L$  is represented by matrices  $\mathcal{H}_L^{[\nu]} \in \mathbb{R}^{m_L^{[\nu]} \times m_L^{[\nu]}}$  in the different sectors  $[\nu] \in \mathcal{I}_M^L$  and their

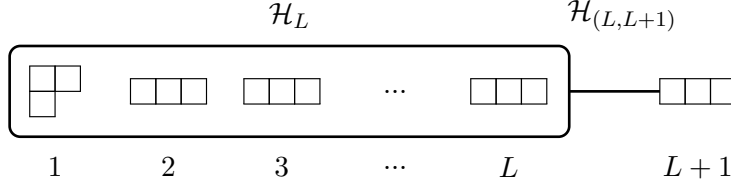


Figure 5.4: The Hamiltonian on the new left block of length  $L + 1$  is made of the Hamiltonian  $\mathcal{H}_L$  on the previous left block of length  $L$  and of the interaction Hamiltonian  $\mathcal{H}_{(L,L+1)}$  between sites  $L$  and  $L + 1$ .

matrix elements are simply given by

$$\left(H_L^{[\nu]}\right)_{i,j} = \langle \xi_i^{[\nu]} | \mathcal{H}_L | \xi_j^{[\nu]} \rangle, \quad 1 \leq i, j \leq m_L^{[\nu]} \quad (5.27)$$

where  $|\xi_j^{[\nu]}\rangle$  is the  $j$ -th eigenstate of the previous reduced density matrix in the sector  $[\nu]$  (see below), and the associated eigenvalues are

$$\left\{ \lambda_1^{[\nu]}, \lambda_2^{[\nu]}, \dots, \lambda_{m_L^{[\nu]}}^{[\nu]} \right\} \equiv \Lambda_L^{[\nu]}. \quad (5.28)$$

Let us introduce some vocabulary. We say that an irrep  $[\chi]$  is a *descendant* of an irrep  $[\nu]$  with respect to an irrep  $[\beta]$  if  $[\chi] \in [\nu] \otimes [\beta]$ . Conversely we say that an irrep  $[\sigma]$  is an *ascendant* of an irrep  $[\nu]$  with respect to an irrep  $[\beta]$  if  $[\nu] \in [\sigma] \otimes [\beta]$ . We can thus form the *genealogy* of an irrep  $[\nu]$  by identifying all its ascendants and all its descendants. We denote by  $n_{\text{asc}}^{[\nu]}$  the total number of ascendants of the irrep  $[\nu]$  and  $n_{\text{desc}}^{[\nu]}$  the total number of its descendants. Figure 5.5 shows the genealogy of the irrep  $[\nu] = [4, 2]$  of SU(3) with respect to the irrep  $[\beta] = [3]$ .

When adding site  $L + 1$  to the left block, the possible irreps for the new block of length  $L + 1$  are then all the descendants of the irreps  $[\nu] \in \mathcal{I}_M^L$  with respect to irrep  $[\beta^{L+1}]$ . We define this ensemble as  $\tilde{\mathcal{I}}_M^{L+1}$ :

$$\begin{aligned} [\chi] \in \tilde{\mathcal{I}}_M^{L+1} &\Leftrightarrow \exists [\nu] \in \mathcal{I}_M^L \text{ such that } [\chi] \in [\nu] \otimes [\beta^{L+1}] \\ &([\chi] \text{ is a descendant of } [\nu] \in \mathcal{I}_M^L). \end{aligned} \quad (5.29)$$

By definition,  $\tilde{\mathcal{I}}_M^{L+1}$  might contain (and actually does contain as soon as  $L$  is larger than a few sites) irreps which do not belong to the list of  $M$  irreps  $\mathcal{I}_M$ . For instance in Fig. 5.5 the descendant  $[7, 2]$  does not belong to  $\mathcal{I}_{M=22}$ . We thus define the list of relevant irreps for the new block of length  $L + 1$  as

$$\mathcal{I}_M^{L+1} = \tilde{\mathcal{I}}_M^{L+1} \cap \mathcal{I}_M. \quad (5.30)$$

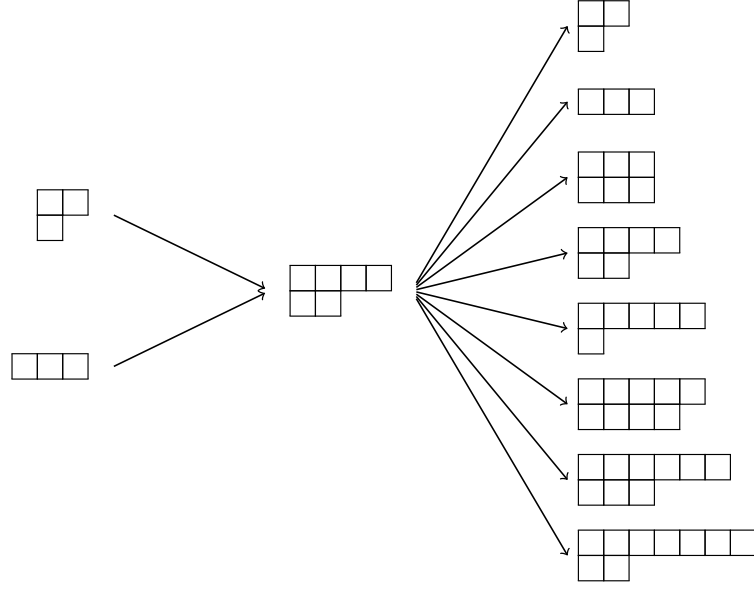


Figure 5.5: The genealogy of the irrep  $[4, 2]$  of  $SU(3)$  with respect to the irrep  $[3]$ . The irrep  $[4, 2]$  has  $n_{\text{asc}}^{[4,2]} = 2$  ascendants and  $n_{\text{desc}}^{[4,2]} = 8$  descendants.

Equation (5.30) is the actual realization of the truncation over the irreps, and we define  $M_{L+1} = \text{card}(\mathcal{I}_M^{L+1})$ .

Now that we have identified the relevant irreps at step  $L + 1$  one needs to distribute the  $m_{L+1} \leq m$  states among the  $M_L$  irreps. One proceeds as follows. We find all ascendants  $[\nu_j^{[\chi]}]$ ,  $1 \leq j \leq n_{\text{asc}}^{[\chi]}$  of each irrep  $[\chi] \in \mathcal{I}_M^{L+1}$  with respect to the irrep  $[\beta^{L+1}]$  and form the lists

$$\mathcal{A}_L^{[\chi]} = \left\{ [\nu_1^{[\chi]}], [\nu_2^{[\chi]}], \dots, [\nu_{n_{\text{asc}}^{[\chi]}}^{[\chi]}] \right\}, \quad [\chi] \in \mathcal{I}_M^{L+1}. \quad (5.31)$$

If the irrep  $[\nu_j^{[\chi]}]$  belongs to  $\mathcal{I}_M^L$  then it points to a set  $\Lambda_L^{[\nu_j^{[\chi]}]}$  of eigenvalues of the reduced density matrix in sector  $[\nu_j^{[\chi]}]$ . One thus build the list of eigenvalues

$$\mathcal{K}_{L+1}^{[\chi]} = \bigcup_{[\nu] \in \mathcal{A}_L^{[\chi]} \cap \mathcal{I}_M^L} \Lambda_L^{[\nu]}. \quad (5.32)$$

Finally the list  $\mathcal{K}_{L+1}$  defined as

$$\mathcal{K}_{L+1} = \bigcup_{[\chi] \in \mathcal{I}_M^{L+1}} \mathcal{K}_{L+1}^{[\chi]} \quad (5.33)$$

contains all relevant eigenvalues coming from step  $L$ , with possible repetitions. Since the cardinal of  $\mathcal{K}_{L+1}$  is larger than  $m_L$  the truncation on the states then consists in

## Chapter 5. The 3-box symmetric SU(3) chain

---

selecting the  $m_{L+1} = \min \{\text{card}(\mathcal{K}_{L+1}), m\}$  states corresponding to the  $m_{L+1}$  largest elements in  $\mathcal{K}_{L+1}$ . Since each element  $\lambda \in \mathcal{K}_{L+1}$  is labeled by an irrep  $[\nu] \in \mathcal{I}_M^L$  and an index  $1 \leq j \leq m_L^{[\nu]}$  and since the irrep  $[\nu]$  is itself an ascendant of an irrep  $[\chi] \in \mathcal{I}_M^{L+1}$ , one can easily distribute  $m_{L+1}^{[\chi]}$  states to the irrep  $[\chi]$ , and one keeps track of the origin of these states. One further defines  $m_{[\chi],L+1}^{[\nu]}$  as the number of states attributed to the irrep  $[\chi]$  coming from the irrep  $[\nu]$  and one has

$$\sum_{[\nu]} m_{[\chi],L+1}^{[\nu]} = m_{L+1}^{[\chi]}. \quad (5.34)$$

Knowing the distribution of the states in the different irreps  $[\chi]$  one introduces two new quantities. First, we define the set of irreps containing at least one state

$$\mathcal{J}_{M,m}^{L+1} = \{[\chi] \in \mathcal{I}_M^{L+1} | m_{L+1}^{[\chi]} > 0\}. \quad (5.35)$$

Second, one defines the total number of effective states

$$m_{\text{eff}} = \sum_{[\chi] \in \mathcal{J}_{M,m}^{L+1}} \dim([\chi]) m_{L+1}^{[\chi]}. \quad (5.36)$$

From  $\mathcal{J}_{M,m}^{L+1}$  one can verify that the truncation of the Hilbert space does not depend on  $M$ , but only on  $m$ . Indeed, if  $M$  is chosen large enough, and since we look at antiferromagnetic chains, only the  $\text{card}(\mathcal{J}_{M,m}^{L+1}) \ll \text{card}(\mathcal{I}_M^{L+1})$  irreps with the smallest quadratic Casimir will be “occupied”. This is illustrated in Fig. 5.6.

The total Hilbert space on the left block is thus described by the decomposition

$$\mathcal{H}^{\text{left}} = \bigoplus_{[\chi] \in \mathcal{J}_{M,m}^{L+1}} m_{L+1}^{[\chi]} [\chi] \quad (5.37)$$

and the Hilbert space on the right block  $\mathcal{H}^{\text{right}}$  is the same during this part where the chain length grows up to its final size.

For each irrep  $[\chi]$  one can separate all the elements of  $\mathcal{K}_{L+1}^{[\chi]}$  into two sets  $\mathcal{K}_{L+1}^{[\chi],\text{kept}}$  and  $\mathcal{K}_{L+1}^{[\chi],\text{disc}}$  such that  $\text{card}(\mathcal{K}_{L+1}^{[\chi],\text{kept}}) = m_{L+1}^{[\chi]}$  and  $\mathcal{K}_{L+1}^{[\chi],\text{kept}} \cup \mathcal{K}_{L+1}^{[\chi],\text{disc}} = \mathcal{K}_{L+1}^{[\chi]}$ .

The discarded weight  $W_{L+1}^{[\chi]}$  at step  $L+1$  in sector  $[\chi]$  is then simply defined as

$$W_{L+1}^{[\chi]} = g_{[\beta^{L+1}]}^{[\chi]} \sum_{\lambda \in \mathcal{K}_{L+1}^{[\chi],\text{disc}}} \lambda \quad (5.38)$$

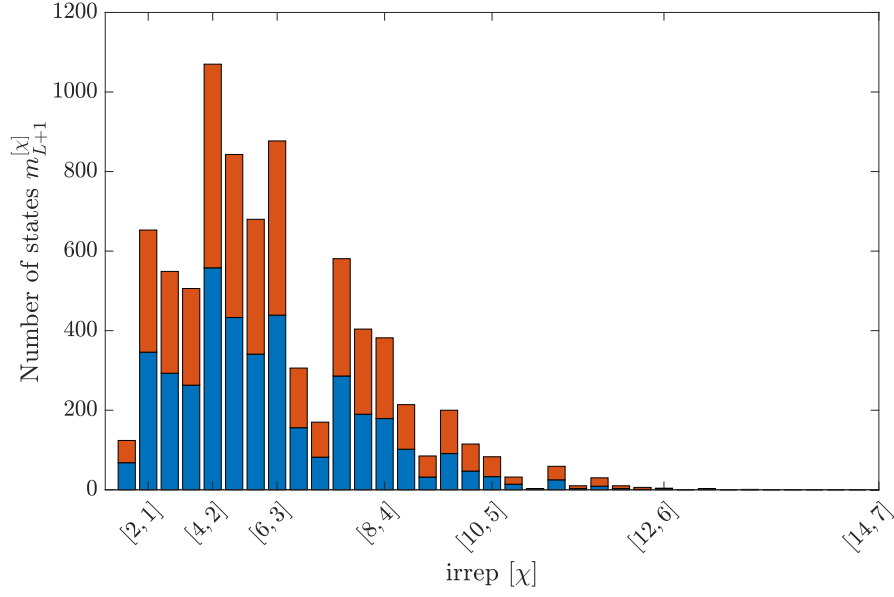


Figure 5.6: Typical distribution of  $m = 4000$  (blue) and  $m = 8000$  (blue and orange) states in the different irreps  $[\chi]$ . The irreps are sorted in ascending order of quadratic Casimir from left to right. For readability, only the self-conjugate irreps are labeled, and we have shown the first 36 irreps only, while  $M$  was chosen much larger ( $M = 300$ ) to ensure that the truncation does not depend on  $M$ . After a few starting steps, the distribution  $m_{L+1}^{[\chi]}$  of states in the different irreps does not change significantly with respect to  $L$ . The effective number of states kept associated to these distributions are  $m_{\text{eff}} = 195268$  and  $m_{\text{eff}} = 412420$ , respectively.

where the symmetry factor  $g_{[\beta^{L+1}]}^{[\chi]}$  is

$$g_{[\beta^{L+1}]}^{[\chi]} = \frac{\dim([\chi])}{\dim([\beta^{L+1}])} \quad (5.39)$$

and the total discarded weight is<sup>8</sup>

$$W_{L+1} = \sum_{[\chi] \in \mathcal{J}_{M,m}^{L+1}} W_{L+1}^{[\chi]}. \quad (5.40)$$

As a side remark, one observes that the selection of states described above does actually not minimize the discarded weight. To actually minimize the discarded weight one would first need to multiply all the elements of  $\mathcal{K}_{L+1}$  by the correct symmetry factor  $g_{[\beta^{L+1}]}^{[\chi]}$  and then select the largest elements. Proceeding this way would in general

<sup>8</sup>Notice that this is equivalent to Eq. (6) of Ref. [89].

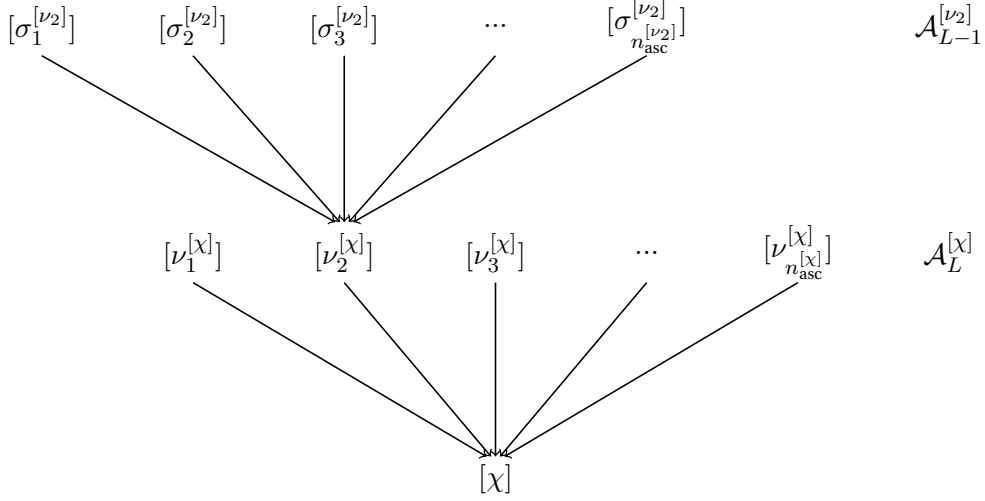


Figure 5.7: Ascendancy tree of the irrep  $[\chi]$ . The first level ascendants are all the irreps  $[\nu_j^{[\chi]}] \in \mathcal{A}_L^{[\chi]}$  and the second level ascendants are all the ascendants of the ascendants of  $[\chi]$ . We have only shown the second level ascendants stemming from the ascendant  $[\nu_2^{[\chi]}] \equiv [\nu_2]$  and forming the set  $\mathcal{A}_{L-1}^{[\nu_2]}$ , for readability.

lead to a different selection of states leading to a lower total discarded weight. However we have observed that this selection scheme is in practice less optimal for the minimization of the energy.

### Hamiltonian on the left block

Now that the relevant states have been selected one can build the new left block of length  $L + 1$ . To build the matrix  $H_L^{[\chi]}$  which represents the Hamiltonian  $\mathcal{H}_L$  in the sector  $[\chi] \in \mathcal{J}_{M,m}^{L+1}$  one simply needs to concatenate the restrictions to the first  $m_{[\chi],L+1}^{[\nu]}$  states of the matrices  $H_L^{[\nu]}$  for  $[\nu] \in \mathcal{A}_L^{[\chi]}$ . The matrix  $H_L^{[\chi]}$  is thus a block-diagonal matrix, each block being of dimension  $m_{[\chi],L+1}^{[\nu]}$ .

The construction of the matrix representation of the new left block follows by constructing the matrix representation  $H_{(L,L+1)}^{[\chi]}$  of the Hamiltonian  $\mathcal{H}_{(L,L+1)}$ . We do this with the help of the genealogy of irreps. Indeed, since  $\mathcal{H}_{(L,L+1)}$  acts only on sites  $L$  and  $L + 1$ , namely on the last  $p_L + p_{L+1}$  particles, the goal is to find all the states corresponding to irreps which are identical at step  $L - 1$ . For any  $[\chi] \in \mathcal{J}_{M,m}^{L+1} \subset \mathcal{I}_M^{L+1}$  one has already introduced the set of ascendants  $\mathcal{A}_L^{[\chi]}$ . One further introduces  $\mathcal{A}_{L-1}^{[\nu_j^{[\chi]}]}$ ,  $[\nu_j^{[\chi]}] \in \mathcal{A}_L^{[\chi]}$  with  $1 \leq j \leq n_{asc}^{[\chi]}$  the set of all ascendants of the irrep  $[\nu_j^{[\chi]}]$  which is itself an ascendant of  $[\chi]$ . This leads to an *ascendancy tree* as pictured in Fig. 5.7.

#### 5.4. Density matrix renormalization group with $SU(3)$ symmetry

From the ascendance tree one can identify branches with a common second level ascendant, as shown in Fig. 5.8(a) in the general case, and Fig. 5.8(b) for a concrete example. The matrix elements of the interaction  $H_{(L,L+1)}^{[\chi]}$  then follow using the technology developed in Refs. [87, 88], considering that the irreps with the colored boxes are representants of equivalence classes of SYTs<sup>9</sup>. For the case illustrated in Fig. 5.8(c), for instance, one has

$$\begin{aligned}
 \langle \begin{array}{|c|c|c|c|c|} \hline \square & \square & \square & \square & \square \\ \hline \square & \square & \square & \square & \square \\ \hline \square & \square & \square & \square & \square \\ \hline \end{array} \mid \mathcal{H}_{(L,L+1)} \mid \begin{array}{|c|c|c|c|c|} \hline \square & \square & \square & \square & \square \\ \hline \square & \square & \square & \square & \square \\ \hline \square & \square & \square & \square & \square \\ \hline \end{array} \rangle &= \frac{73}{20}, \\
 \langle \begin{array}{|c|c|c|c|c|} \hline \square & \square & \square & \square & \square \\ \hline \square & \square & \square & \square & \square \\ \hline \square & \square & \square & \square & \square \\ \hline \end{array} \mid \mathcal{H}_{(L,L+1)} \mid \begin{array}{|c|c|c|c|c|} \hline \square & \square & \square & \square & \square \\ \hline \square & \square & \square & \square & \square \\ \hline \square & \square & \square & \square & \square \\ \hline \end{array} \rangle &= \frac{4\sqrt{6}}{5}, \\
 \langle \begin{array}{|c|c|c|c|c|} \hline \square & \square & \square & \square & \square \\ \hline \square & \square & \square & \square & \square \\ \hline \square & \square & \square & \square & \square \\ \hline \end{array} \mid \mathcal{H}_{(L,L+1)} \mid \begin{array}{|c|c|c|c|c|} \hline \square & \square & \square & \square & \square \\ \hline \square & \square & \square & \square & \square \\ \hline \square & \square & \square & \square & \square \\ \hline \end{array} \rangle &= \frac{4\sqrt{6}}{5}, \\
 \langle \begin{array}{|c|c|c|c|c|} \hline \square & \square & \square & \square & \square \\ \hline \square & \square & \square & \square & \square \\ \hline \square & \square & \square & \square & \square \\ \hline \end{array} \mid \mathcal{H}_{(L,L+1)} \mid \begin{array}{|c|c|c|c|c|} \hline \square & \square & \square & \square & \square \\ \hline \square & \square & \square & \square & \square \\ \hline \square & \square & \square & \square & \square \\ \hline \end{array} \rangle &= \frac{33}{5}.
 \end{aligned}$$

#### Construction of the superblock

To construct the Hamiltonian of the entire chain of length  $N_s = 2L + 2$  we select a target sector (or global sector)  $[\gamma]$  in which we build its matrix. One thus first needs to combine the left and right blocks constructed in the previous step in order to reach the global sector, and then construct the matrix of the interaction between the left and right blocks, as in Eq. (5.25). To identify all contributing sectors one simply defines the following set,

$$\bar{\mathcal{J}}_{M,m}^{L+1} = \left\{ [\chi] \in \mathcal{J}_{M,m}^{L+1} \mid \exists [\chi'] \in \mathcal{J}_{M,m}^{L+1} \text{ such that } [\gamma] \in [\chi] \otimes [\chi'] \right\}. \quad (5.41)$$

One thus has  $\bar{\mathcal{J}}_{M,m}^{L+1} \subseteq \mathcal{J}_{M,m}^{L+1}$  and all irreps belonging to the complement of  $\bar{\mathcal{J}}_{M,m}^{L+1}$  in  $\mathcal{J}_{M,m}^{L+1}$  can be removed since they do not allow to access the global  $[\gamma]$  sector. One thus restricts the Hilbert space of the left block to these irreps (compare to Eq. (5.37))

$$\mathcal{H}^{\text{left}} = \bigoplus_{[\chi] \in \bar{\mathcal{J}}_{M,m}^{L+1}} m_{L+1}^{[\chi]} [\chi] \quad (5.42)$$

<sup>9</sup>An equivalence class of SYTs is an ensemble of SYTs satisfying some local constraints, translating into the fact that particles of a given site occupy the same boxes. All SYTs of the same equivalence class are thus related by permutations of particles within each site [87, 88].

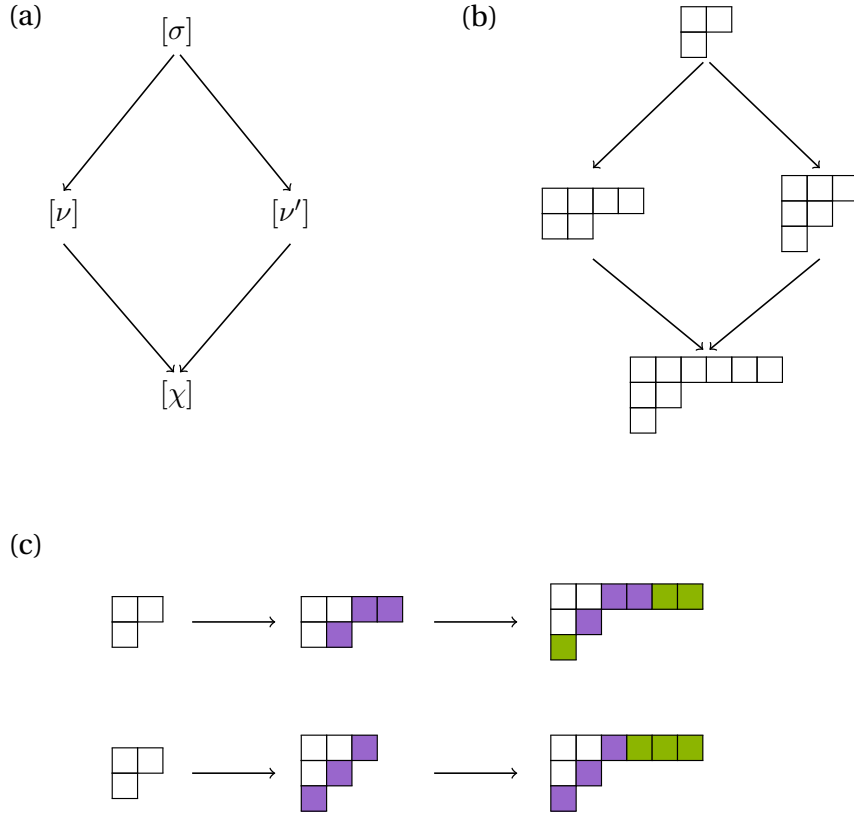


Figure 5.8: (a) Two branches of the ascendance tree of the irrep  $[\chi]$  which have a common second level ascendant  $[\sigma]$ . (b) A concrete example where the ascendance is with respect to the 3-box symmetric irrep  $\square\square\square$ , namely along each arrow there is a tensor product with the irrep  $\square\square\square$ . (c) The two branches corresponding to (b), where we have kept track of the positions of the particles added at each level.

and similarly for the right block. For each couple of irreps in  $\bar{\mathcal{J}}_{M,m}^{L+1}$  one defines a multiplicity matrix

$$M_{[\chi],[\chi']}^{[\gamma]} = ([\chi][\chi'][\gamma]), \quad \forall [\chi], [\chi'] \in \bar{\mathcal{J}}_{M,m}^{L+1} \quad (5.43)$$

containing the outer multiplicity of the irrep  $[\gamma]$  in the tensor product of the irreps  $[\chi]$  and  $[\chi']$ , and the associated boolean matrix

$$B_{[\chi],[\chi']}^{[\gamma]} = \text{Bool}(M_{[\chi],[\chi']}^{[\gamma]}) = \begin{cases} 1 & \text{if } M_{[\chi],[\chi']}^{[\gamma]} > 0 \\ 0 & \text{otherwise} \end{cases} \quad \forall [\chi], [\chi'] \in \bar{\mathcal{J}}_{M,m}^{L+1}. \quad (5.44)$$

In the rest of this chapter, and this is one of the main limitations in the algorithm in its



## 5.4. Density matrix renormalization group with SU(3) symmetry

current state, we restrict ourselves to the irreps  $[\gamma]$  such that

$$M_{[\chi],[\chi']}^{[\gamma]} = B_{[\chi],[\chi']}^{[\gamma]}, \quad \forall [\chi], [\chi'] \in \bar{\mathcal{J}}_{M,m}^{L+1}. \quad (5.45)$$

In other words we only consider global irreps  $[\gamma]$  which can appear *at most* once in the tensor product of two irreps. For SU( $N$ ) with  $N > 2$  this is clearly a limitation since outer multiplicities do occur. In particular, for the study of the chain illustrated in Fig. 5.2 we avoid the global adjoint sector, since its multiplicity in the tensor product of an adjoint from the left block and an adjoint from the right block, for instance, is two. In the outlook of this chapter we argue that this limitation can be overcome in light of Section 3.1.8.

The total Hilbert space on  $N_s = 2L + 2$  sites is then given by

$$\mathcal{H} = \bar{\mathcal{H}}^{\text{left}} \otimes \bar{\mathcal{H}}^{\text{right}} \quad (5.46)$$

and the matrices of the left and right blocks in this space are obtained as (see Eq. (12) of Ref. [89])

$$H_{L+1}^{\text{left},[\gamma]} = \bigoplus_{B_{[\chi],[\chi']}^{[\gamma]}=1} H_{L+1}^{[\chi]} \otimes \mathbb{1}_{L+1}^{[\chi']} \quad (5.47)$$

and

$$H_{L+1}^{\text{right},[\gamma]} = \bigoplus_{B_{[\chi],[\chi']}^{[\gamma]}=1} \mathbb{1}_{L+1}^{[\chi]} \otimes H_{L+1}^{[\chi']}. \quad (5.48)$$

In Eqs. (5.47) and (5.48) the identity matrices  $\mathbb{1}_{L+1}^{[\chi']}$  and  $\mathbb{1}_{L+1}^{[\chi]}$  are of dimension  $m_{L+1}^{[\chi']}$  and  $m_{L+1}^{[\chi]}$ , respectively, and one must of course take care of respecting the structure of  $\mathcal{H}$  when building the matrices of the left and right blocks in this space.

The basis states of the Hilbert space in Eq. (5.46) are labeled by two irreps and two integers,

$$|\xi_i^{[\chi]}\rangle_{\text{left}} \otimes |\xi_j^{[\chi']}\rangle_{\text{right}} \equiv |\xi_i^{[\chi]}; \xi_j^{[\chi']}\rangle, \quad [\chi], [\chi'] \in \bar{\mathcal{J}}_{M,m}^{L+1}, \quad 1 \leq i \leq m_{L+1}^{[\chi]}, \quad 1 \leq j \leq m_{L+1}^{[\chi']}. \quad (5.49)$$

The last thing to be constructed is the matrix of the interaction  $\mathcal{H}_{(L+1,L+2)}$  between the left and right blocks (see Eq. (5.25)) in this basis. We shall argue that the solution is provided by the SDCs. There are three important reasons for this:

- The matrix elements of  $\mathcal{H}_{(L+1,L+2)}$  can *only* be computed easily in the standard basis of SYTs for the global irrep  $[\gamma]$ , by use of the Young rules.
- In the standard basis, namely in a basis made of SYTs corresponding to the global irrep  $[\gamma]$ , the matrix elements of  $\mathcal{H}_{(L+1,L+2)}$  *only* depend on the locations of particles corresponding to sites  $L + 1$  and  $L + 2$ .

- The positions of the particles of site  $L + 1$  and  $L + 2$  in the irreps  $[\chi], [\chi'] \in \bar{\mathcal{J}}_{M,m}^{L+1} \subset \mathcal{I}_M^{L+1}$  can be retrieved since we have kept track of the genealogy of each state. For instance in Fig. 5.8(c) these positions are indicated by green boxes for the irrep  $[\chi] = [6, 2, 1]$ .

The procedure is now natural: we shall rewrite the basis states in the standard basis, because one can then compute easily the reduced matrix elements using the Young rules. Furthermore, the reduced matrix elements will only depend on the positions of the particles of sites  $L + 1$  and  $L + 2$ . Thus the reduced matrix elements can be written

$$\left\langle [\gamma], \begin{matrix} [\chi_3] & [\chi_4] \\ l_3 & l_4 \end{matrix} \left| \mathcal{H}_{(L+1,L+2)} \right| [\gamma], \begin{matrix} [\chi_1] & [\chi_2] \\ l_1 & l_2 \end{matrix} \right\rangle \quad (5.50)$$

where  $l_k$  identifies the locations of the particles of site  $L + 1$  (respectively  $L + 2$ ) in the irreps  $[\chi_1]$  and  $[\chi_3]$  (respectively  $[\chi_2]$  and  $[\chi_4]$ ), and where we have indicated that the reduced matrix elements are computed in the global  $[\gamma]$  sector. We have purposely used a notation similar to the one used for the basis elements of the non-standard (or subduced) basis of  $\mathcal{S}_n$  in Eq. (3.21). There are two differences: first, we have replaced  $m_k$ , the identifier of a SYT for the irrep  $[\nu_k]$  by  $l_k$  which only gives the locations of the particles of site  $L + 1$  or  $L + 2$ . This is because  $\mathcal{H}_{(L+1,L+2)}$  only acts on these particles. Secondly, there is no multiplicity index  $\tau$  in Eq. (5.50). This is because we have restricted ourselves to a global sector  $[\gamma]$  satisfying Eq. (5.45). Thus, the multiplicity index is implicitly  $\tau = 1$ . The ket and the bra in the matrix elements (5.50) are then actually some representative of a basis vector of the non-standard basis. The SDCs allow us to rewrite these representative in the standard basis and to use the Young rules to compute the reduced matrix element of the interaction between the left and right blocks. In the next part, we explain how to do this using the technology of Section 3.1.7.

### Calculation of the reduced matrix elements of the interaction

We denote by  $n$  the total number of particles in the irrep  $[\gamma]$  when all columns of  $N$  boxes are kept, and  $n_k$  the number of boxes in the irrep  $[\chi_k]$  in Eq. (5.50). In the case of the chain illustrated in Fig. 5.2, for instance, one has  $n = 3N_s = 6(L + 1)$  where  $N_s = 2(L + 1)$  is the length of the entire chain, and there are three particles per site. The particles living on site  $L + 1$  and  $L + 2$  are indexed by the elements of  $\Gamma_{L+1}$  and  $\Gamma_{L+2}$  (see Fig. 5.1) which take the values

$$\Gamma_{L+1} = \{n_1 - p_{L+1} + 1, n_1 - p_{L+1} + 2, \dots, n_1\}, \quad \Gamma_{L+2} = \{n_1 + 1, n_1 + 2, \dots, n_1 + p_{L+2}\} \quad (5.51)$$

where  $p_i$  is the total number of particles at site  $i$ .

#### 5.4. Density matrix renormalization group with SU(3) symmetry

To keep track of the positions of the  $p_{L+1}$  and  $p_{L+2}$  last particles in the irreps  $[\chi_k]$  in Eq. (5.50) one can for instance take  $l_k$  to be the rows of the bottom corners occupied by these particles. For instance, if in the irrep  $[\chi_1] = [4, 2]$  the last three particles are situated at the positions of the crosses in

$$\begin{array}{|c|c|c|c|} \hline & & \times & \times \\ \hline & \times & & \\ \hline \end{array} \quad (5.52)$$

then one simply takes  $l_1 = (1, 1, 2)$  which are the rows of each cross in the irrep  $[\chi_1]$ .

Let us now define  $[\chi'_1]$  to be the irrep obtained from  $[\chi_1]$  by removing the boxes at the bottom corners  $l_1$  ( $[\chi'_1]$  is thus an ascendant of  $[\chi_1]$  with respect to the irrep  $[\beta^{L+1}]$ ). We construct a SYT  $Y_{m_1(l_1)}^{[\chi_1]}$  for the irrep  $[\chi_1]$  as follows. We begin by positioning the  $p_{L+1}$  last numbers in descending order in  $[\chi_1]$  from the lowest bottom corner of  $l_1$  to the highest. We then fill the remaining irrep  $[\chi'_1]$  such that  $Y_{m_1(l_1)'}^{[\chi'_1]}$  corresponds to the smallest SYT in the LLOS. For instance,

$$([\chi_1], l_1) = \begin{array}{|c|c|c|c|} \hline & & \times & \times \\ \hline & \times & & \\ \hline \end{array} \longrightarrow \begin{array}{|c|c|c|c|} \hline & & 4 & 5 \\ \hline & 6 & & \\ \hline \end{array} \longrightarrow \begin{array}{|c|c|c|c|} \hline 1 & 2 & 4 & 5 \\ \hline 3 & 6 & & \\ \hline \end{array} =: Y_{m_1(l_1)}^{[\chi_1]}. \quad (5.53)$$

The actual choice of the SYT  $Y_{m_1(l_1)'}^{[\chi'_1]}$  is not important, because the SDCs are independent of  $m_1$  and because the interaction  $\mathcal{H}_{(L+1, L+2)}$  does not involve these particles. In other words, we could equally well have chosen the largest SYT in the LLOS for  $Y_{m_1(l_1)'}^{[\chi'_1]}$ , or any other SYT for the irrep  $[\chi'_1]$ . Conversely, it is crucial to position the last  $p_{L+1}$  particles from top to bottom because this corresponds to our choice of the *representative* SYT of the equivalence class [87].

For the right block, we proceed similarly. For instance,

$$([\chi_2], l_2) = \begin{array}{|c|c|c|c|} \hline & & \times & \times \\ \hline & \times & & \\ \hline \end{array} \longrightarrow \begin{array}{|c|c|c|c|} \hline & & 4 & 5 \\ \hline & 6 & & \\ \hline \end{array} \longrightarrow \begin{array}{|c|c|c|c|} \hline 1 & 2 & 4 & 5 \\ \hline 3 & 6 & & \\ \hline \end{array} =: Y_{m_2(l_2)}^{[\chi_2]}. \quad (5.54)$$

Now we have actually formally defined the ket in the reduced matrix element (compare to Eq. (3.21))

$$\left| \begin{array}{c} [\gamma], \begin{array}{cc} [\chi_1] & [\chi_2] \\ l_1 & l_2 \end{array} \end{array} \right\rangle \equiv \left| \begin{array}{c} [\gamma], \begin{array}{cc} [\chi_1] & [\chi_2] \\ m_1(l_1) & m_2(l_2) \end{array} \end{array} \right\rangle \quad (5.55)$$

where the right hand side is strictly speaking a basis vector of the non-standard basis since  $m_1(l_1)$  and  $m_2(l_2)$  are proper SYTs for the irreps  $[\chi_1]$  and  $[\chi_2]$ , respectively.

One can now expand this basis vector of the non-standard basis onto the standard basis. There is one subtlety, however. When constructing the CSCO of  $\mathcal{S}_n$  in the eigenfunction method, one needs to remember that the  $p_{L+2}$  largest numbers in  $Y_{m_2(l_2)}^{[\chi_2]}$  actually correspond to the numbers in  $\Gamma_{L+2}$  and, as such, are the smallest in the right block. One can thus renumber the boxes in  $Y_{m_2(l_2)}^{[\chi_2]}$  such that number  $j$  is mapped onto  $n-j+1$ .

## Chapter 5. The 3-box symmetric SU(3) chain

For the example above (where  $n_1 = n_2 = 6$ ,  $n = 12$ ) the renumbering is

$$Y_{m_2(l_2)}^{[\nu_2]} = \begin{array}{|c|c|c|c|} \hline 1 & 2 & 4 & 5 \\ \hline 3 & 6 & & \\ \hline \end{array} \longrightarrow \tilde{Y}_{m_2(l_2)}^{[\nu_2]} = \begin{array}{|c|c|c|c|} \hline 12 & 11 & 9 & 8 \\ \hline 10 & 7 & & \\ \hline \end{array}. \quad (5.56)$$

The tableau  $\tilde{Y}_{m_2(l_2)}^{[\nu_2]}$  is not strictly speaking a SYT, but it is convenient to work with this object rather than with  $Y_{m_2(l_2)}^{[\nu_2]}$  when computing the CSCO of  $\mathcal{S}_n$ . We shall put a star on the SDCs to remember this subtlety when computing the CSCO of  $\mathcal{S}_n$ ,

$$\left\langle \begin{array}{c|c} [\gamma] & [\chi_1] \quad [\chi_2] \\ m & m_1(l_1) \quad *m_2(l_2) \end{array} \right\rangle. \quad (5.57)$$

If  $Y_{m_2(l_2)}^{[\chi_2]}$  is not the first SYT in the LLOS for the irrep  $[\chi_2]$  then we need to deal with the Yamanouchi relative phase as explained in Section 3.1.7, starting with the first SYT  $m_2 = 1$  and acting with a sequence of operations which transform  $Y_{m_2=1}^{[\chi_2]}$  into  $Y_{m_2(l_2)}^{[\chi_2]}$ <sup>10</sup>. Once this is done we have an expansion of the basis vector of the non-standard basis onto the standard Yamanouchi basis,

$$\left| \begin{array}{c|c} [\gamma] & [\chi_1] \quad [\chi_2] \\ m & m_1(l_1) \quad *m_2(l_2) \end{array} \right\rangle = \sum_{m_{e.c.}} \left| \begin{array}{c} [\gamma] \\ m_{e.c.} \end{array} \right\rangle \left\langle \begin{array}{c|c} [\gamma] & [\chi_1] \quad [\chi_2] \\ m_{e.c.} & m_1(l_1) \quad *m_2(l_2) \end{array} \right\rangle. \quad (5.58)$$

Now the important point is that  $|Y_{m_{e.c.}}^{[\gamma]}\rangle$  itself should be understood as a linear combination of SYTs in order to implement the local symmetry at sites  $L + 1$  and  $L + 2$ . This is the major difference with the case of one particle per site treated in Ref. [89]. The SYT  $Y_{m_{e.c.}}^{[\gamma]}$  in Eq. (5.58) is actually the SYT of an *equivalence class* in the language of Ref. [87]. Since there is only one state per equivalence class in the symmetric case, it is easy to find out the exact expression of the state by using the appropriate projector which symmetrizes particles of sites  $L + 1$  and  $L + 2$ . Finally,

$$\left| \begin{array}{c|c} [\nu] & [\nu_1] \quad [\nu_2] \\ m & m_1(l_1) \quad *m_2(l_2) \end{array} \right\rangle = \sum_m F_{m_1(l_1), *m_2(l_2)}^{[\gamma], [\chi_1], [\chi_2]} \left| \begin{array}{c} [\nu] \\ m \end{array} \right\rangle \quad (5.59)$$

where  $F_{m_1(l_1), *m_2(l_2)}^{[\gamma], [\chi_1], [\chi_2]}$  is a combination of SDCs and of coefficients which implement the symmetrization with respect to sites  $L + 1$  and  $L + 2$ , and where  $|Y_m^{[\gamma]}\rangle$  are now the SYTs for the irrep  $[\gamma]$ .

Once the same steps have been followed for the bra in Eq. (5.50), the matrix element of the interaction can straightforwardly be computed using the Young rules. From this procedure one deduces a few simple rules:

<sup>10</sup>Notice that in Eq. (5.54) we could have used the last SYT in the LLOS for the irrep  $[\chi'_2]$  obtained from  $[\chi_2]$  by removing the boxes in the bottom corners described by  $l_2$ . When fixing the Yamanouchi relative phase, one should then check if the obtained SYT  $Y_{m_2(l_2)}^{[\chi'_2]}$  corresponds to the last SYT in the LLOS for the irrep  $[\chi_2]$ . This will lead to a different, yet fully equivalent, set of SDCs.

## 5.5. The SU(3) AKLT model with 3-box symmetric irrep

1. (trivial) If the multiplicity  $M_{[\chi_1], [\chi_2]}^{[\gamma]} = 0$  then the reduced matrix element vanishes.
2. If the ascendant irreps of  $[\chi_1]$  and  $[\chi_3]$  are not the same, then the reduced matrix element vanishes.
3. If the ascendant irreps of  $[\chi_2]$  and  $[\chi_4]$  are not the same, then the reduced matrix element vanishes.

Appendix H provides a complete example of calculation of a reduced matrix element of the interaction [57].

### Reduced density matrices

The Hamiltonian of the chain of length  $N_s = 2L + 2$  can be diagonalized and we obtain a ground state wave function

$$|\Psi\rangle = \sum_{[\chi], [\chi']} \sum_{i,j} \Psi_{i,j}^{[\chi], [\chi']} |\xi_i^{[\chi]}\rangle \otimes |\xi_j^{[\chi']}\rangle. \quad (5.60)$$

For each sector  $[\chi]$  one can define a reduced density matrix  $\rho^{[\chi]}$  with matrix elements [89]

$$\rho_{i,j}^{[\chi]} = \frac{1}{\dim([\chi])} \sum_{[\chi'], k} (\Psi_{i,k}^{[\chi], [\chi']})^* \Psi_{j,k}^{[\chi], [\chi']}. \quad (5.61)$$

The full diagonalization of each reduced density matrix leads to a new set of eigenvalues  $\Lambda_{L+1}^{[\chi]}$  and of eigenstates  $|\xi_j^{[\chi]}\rangle$ . These eigenvectors are then used to rewrite the Hamiltonian matrices  $H_{L+1}^{[\chi]}$  in the new basis. Moreover one can extract the entanglement entropy from the eigenvalues of the density matrices [89]

$$S = - \sum_{[\chi] \in \tilde{\mathcal{J}}_{M,m}^{L+1}} \dim([\chi]) \sum_i \lambda_i^{[\chi]} \ln(\lambda_i^{[\chi]}). \quad (5.62)$$

## 5.5 The SU(3) AKLT model with 3-box symmetric irrep

The AKLT model of Greiter and Rachel is a good starting point for a numerical analysis of the Heisenberg model. The Hamiltonian can be written in terms of permutations using the general AKLT construction presented in Chapter 4 and Section 5.2. We obtain

$$\mathcal{H}_{\text{AKLT}} = J_{\text{end}} \left( \mathcal{H}_{(1,2)} + \mathcal{H}_{(N_s-1, N_s)} \right) + J \sum_{i=2}^{N_s-2} \left( \mathcal{H}_{(i, i+1)} + \frac{1}{4} \mathcal{H}_{(i, i+1)}^2 + \frac{3}{4} \right) \quad (5.63)$$

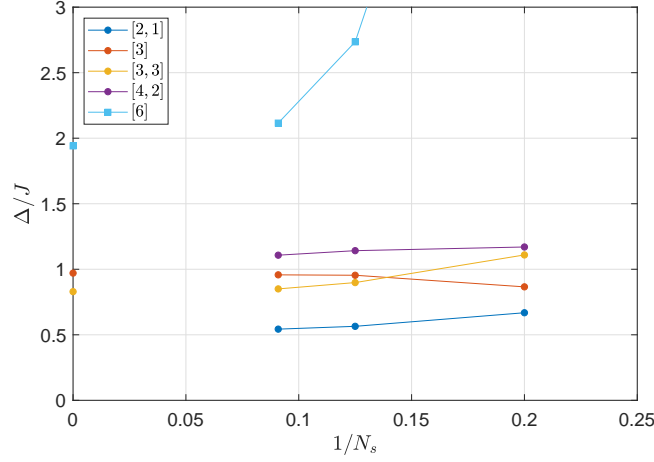


Figure 5.9: Finite-size gaps of the AKLT model in the symmetry sectors corresponding to the elementary excitations and in the 6-box symmetric sector for PBC. DMRG data in the thermodynamic limit in the  $[3]$ ,  $[3,3]$  and  $[6]$  sectors are indicated. Figure adapted from Ref. [57] with the permission of the APS, © 2020 American Physical Society.

where the interaction  $\mathcal{H}_{(i,i+1)}$  is given in Eq. (5.18) and where we have incorporated the Heisenberg exchange to the adjoint edge spins. In what follows, all results are for  $J_{\text{end}}/J = 1$ .

We first investigate the gap using ED. Indeed the correlation length  $\xi = 1/\ln 5$  is short and we expect to be able to see signs of convergence on small chains. Moreover one is not limited to some specific sectors as it is the case for DMRG. Figure 5.9 shows the gap of the AKLT Hamiltonian with PBC versus inverse chain length in the symmetry sectors corresponding to the so-called elementary excitations, and in the 6-box symmetric sector. All sectors show a good convergence towards a finite value, with a smallest gap in the adjoint sector.

The adjoint sector, however, is not reachable using the DMRG algorithm developed in Section 5.4 in its current state. One studies instead the  $[3]$ ,  $[3,3]$  and  $[6]$  sectors in Fig. 5.10. In the two former cases, a good accuracy can be obtained with a very limited number of states. In the latter case, although we have kept only the first  $M = 76$  irreps, one sees a good convergence towards a value  $\Delta_{[6]} = 2\Delta_{[3]}$ . This shows that the first  $[6]$  excitation is not an elementary excitation but a composite excitation made of two  $[3]$  excitations which repel each other.

This nature can be exhibited by computing the bond energy along the chain, which is readily obtained in the DMRG. Figure 5.11 shows the bond energy along the chain in the three same sectors as Fig. 5.10. For the irreps  $[3]$  and  $[3,3]$  the bond energy displays a single peak structure, showing that these excitations are elementary, while in the  $[6]$

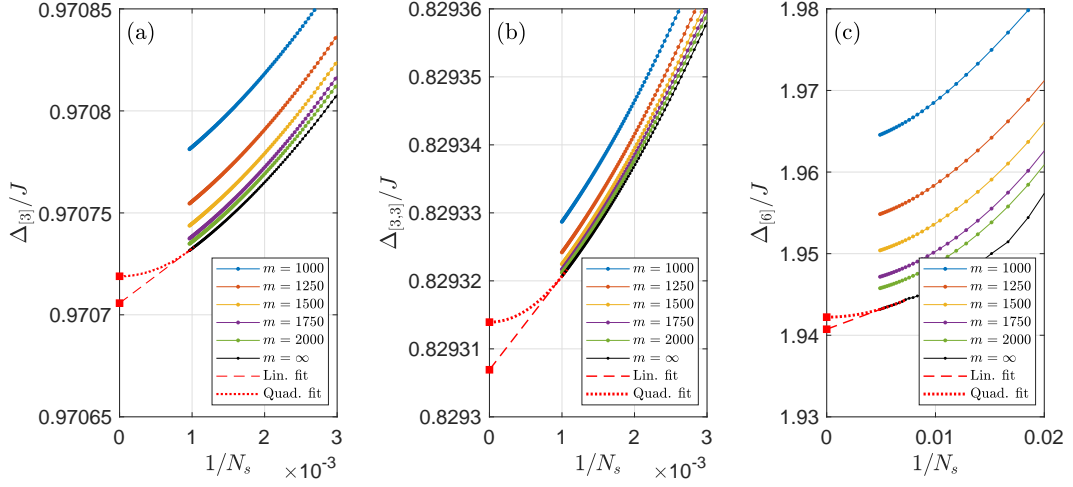


Figure 5.10: Gaps of the AKLT model from the singlet sector to (a) the 3-box symmetric sector  $[3]$ , (b) its conjugate sector  $[3, 3]$  and (c) the 6-box symmetric sector  $[6]$ . Figure adapted from Ref. [57] with the permission of the APS, © 2020 American Physical Society.

sector one observes a double peak structure, corresponding to the two elementary excitations which repel each other [174].

These numerical results are in agreement with the structure of the spectrum that we proposed in Section 5.3. The singlet ground state is separated from the first elementary excited states by finite gaps, and these elementary excitations are all those coming from the tensor product of two adjoint irreps. More complicated excitations are obtained by combining elementary excitations, which can be in the  $[2, 1]$ ,  $[3]$ ,  $[3, 3]$  and  $[4, 2]$  sectors. For instance, the  $[6]$  excitation studied above comes from the combination of two  $[3]$  elementary excitations.

## 5.6 The $SU(3)$ Heisenberg model with 3-box symmetric irrep

### 5.6.1 Haldane gaps

We turn now to the study of the pure Heisenberg model. Figures 5.12(a)-(b) show the singlet- $[3]$  and singlet- $[3, 3]$  gaps versus inverse chain length obtained by DMRG. Although the gap curves do not show a convergence in the system size, as it was obviously the case for the AKLT model, we clearly see that the gaps will extrapolate towards strictly positive values. From the finite- $m$  data, we proceed as follows to extract an estimate of the gaps in the thermodynamic limit. First we extrapolate the lowest energy in each sector (singlet,  $[3]$  and  $[3, 3]$ ) with respect to the discarded weight. This

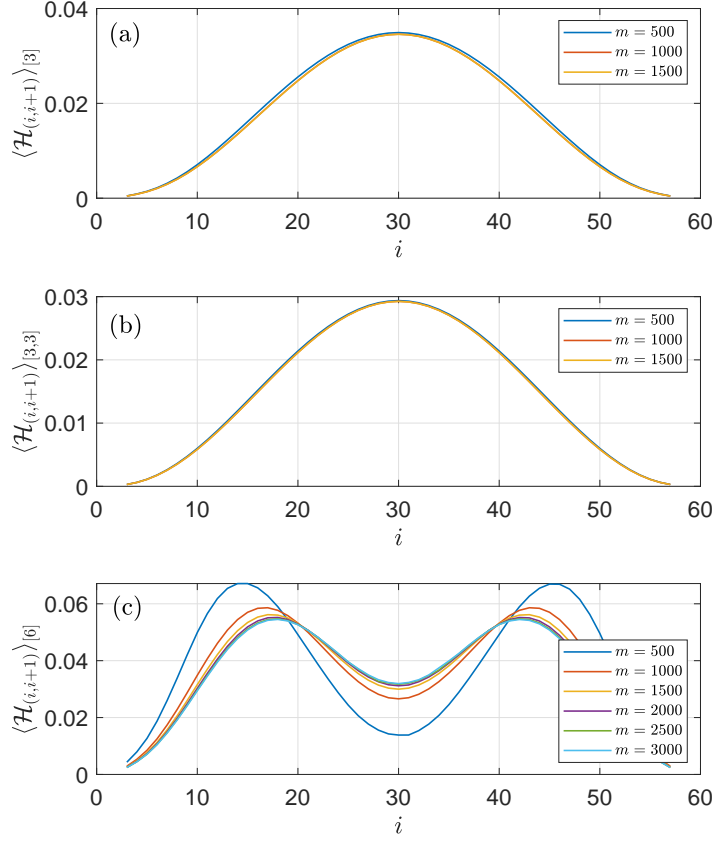


Figure 5.11: Bond energy along the AKLT chain in the (a) [3], (b) [3, 3] and (c) [6] sectors. The double peak structure in (c) together with the gap value show that the first [6] excitation is made of two [3] excitations. In each plot we have subtracted the contribution of the ground state (singlet sector). Figure adapted from Ref. [57] with the permission of the APS, © 2020 American Physical Society.

leads to the black curves labeled  $m = \infty$  in Fig. 5.12(a)-(b). The extrapolation to the thermodynamic limit is obtained by following Schollwöck in Ref. [154]. Extrapolation of the  $m = \infty$  curves in a linear way leads to lower bounds for the gaps. Since these curves clearly extrapolate to strictly positive values, the model has a finite gap in the [3] and [3, 3] sectors. For each sector an upper bound can be obtained from the scaling of the gap at large length scale. Indeed for a gapped system, at length scale  $N_s \gg \xi$  where  $\xi$  is the correlation length and we take the lattice spacing  $a = 1$ , the gap should behave quadratically with respect to the inverse chain length,

$$\Delta(N_s) = \Delta_\infty + \frac{v^2 \pi^2}{\Delta_\infty N_s^2} \quad (5.64)$$



## 5.6. The SU(3) Heisenberg model with 3-box symmetric irrep

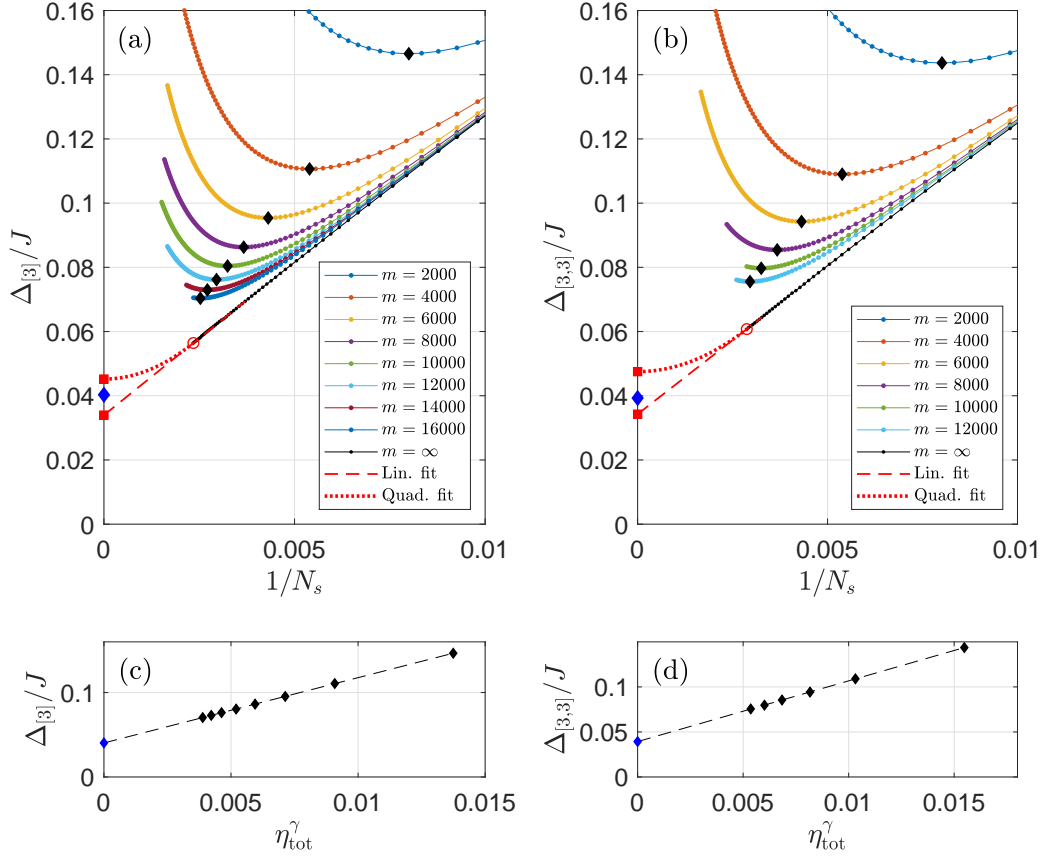


Figure 5.12: (a)-(b) Finite-size gap from the singlet sector to the 3-box symmetric sector and  $[3, 3]$  sector. (c)-(d) Extrapolation of the minimum of each finite  $m$  curve with respect to the total discarded weight. Figure adapted from Ref. [57] with the permission of the APS, © 2020 American Physical Society.

where  $\Delta_\infty$  is the thermodynamic gap and  $v = \xi \Delta_\infty$ . There is thus a crossover between the linear regime and the quadratic regime. Since we do not see the emergence of the quadratic regime in our data, we assume that it develops at length scale just larger than the largest system size that we have investigated. This is indicated by the red circles in Fig. 5.12(a)-(b), and we fit a parabola tangent to these points, leading to an approximate upper bound for the gap in each sector.

One observes that the gap curves at finite  $m$  in Fig. 5.12(a)-(b) go through a minimum and then increase to large values as the system size increases. This is a purely numerical effect [154–156]. At the minimum, the accumulated error on the gap due to the truncation becomes larger than the decrease of the gap due to the increase of the system size. We thus use the value at the minimum as the smallest estimate of the gap at this specific value of  $m$ . One uses these minimal values of the gap at finite

$m$  and perform an extrapolation with respect to the total discarded weight, which is the sum of the discarded weights in the singlet and in the  $[3]$ , or  $[3, 3]$  sectors [156]. Figures 5.12(c)-(d) show these extrapolations, and one sees that the thermodynamic gaps, reported as blue diamonds in Fig. 5.12(a)-(b) lie between the lower and upper bounds derived above.

### 5.6.2 Entanglement entropy

The results presented in Fig. 5.12 are already showing unambiguously the existence of a gap in the  $[3]$  and  $[3, 3]$  sectors, and, as a consequence, in all other sectors of elementary excitations, as we will see below, thus showing that the Heisenberg Hamiltonian is gapped. To bring one more evidence we have studied the curvature of the entanglement entropy in the singlet sector. For a critical model the entanglement entropy follows the Calabrese-Cardy formula [175]

$$S(x) = \frac{c}{6} \ln \left( \frac{2N_s}{\pi} \sin \left( \frac{\pi x}{N_s} \right) \right) + c_1 \quad (5.65)$$

where  $c$  is the central charge of the associated CFT and  $c_1$  is a non-universal constant. For critical SU( $N$ ) spin chains, the CFT describing the low-energy behavior is the SU( $N$ ) <sub>$k$</sub>  WZW model with central charge

$$c = \frac{k(N^2 - 1)}{N + k}. \quad (5.66)$$

The critical SU( $N$ ) Heisenberg models are expected to flow to the stable SU( $N$ )<sub>1</sub> fixed point, except if finely tuned to the integrable points [142, 143]. For the SU(3) chain with 3-box symmetric irrep at each site, the smallest possible central charge compatible with an SU(3) <sub>$k$</sub>  WZW CFT is the level one CFT giving  $c = 2$ . In Figure 5.13(a) one shows the entanglement entropy of a chain with  $N_s = 300$  sites. Despite the large system size, there is no evidence for a clear plateau. A plateau in the entanglement entropy would rule out the possibility of a gapless spectrum. However, the curvature – or “central charge” obtained by fitting the Calabrese-Cardy formula in the middle of the chain – yet non-zero, is smaller than  $c = 2$ , and is compatible with a vanishing curvature in the thermodynamic limit, as shown in Fig. 5.13(b). The analysis of the entanglement entropy in the singlet ground state thus shows that the spectrum of the Heisenberg chain is gapped. This is in agreement with the finite gaps found in the  $[3]$  and  $[3, 3]$  sectors, but goes beyond these results. Indeed, the flat entanglement entropy in the thermodynamic limit tells us that all symmetry sectors are gapped, in particular all symmetry sectors associated to the elementary excitations. This information thus compensates for our inability to study the adjoint and  $[4, 2]$  sectors with DMRG. In the next section, we give another argument for a gapped spectrum in all sectors of elementary excitations.

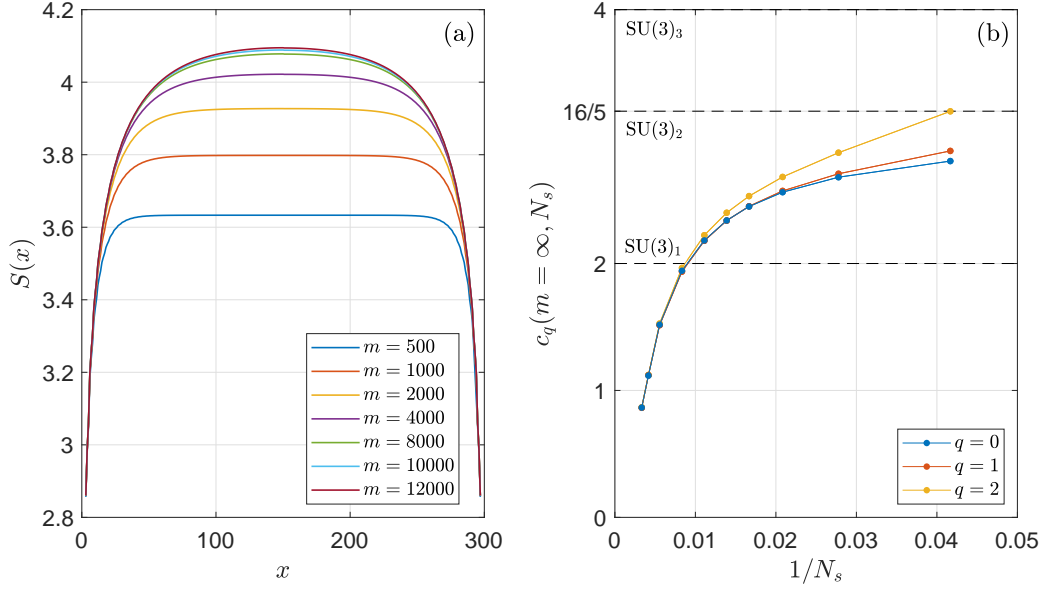


Figure 5.13: (a) Entanglement entropy of the ground state in the singlet sector for a chain of length  $N_s = 300$  sites. (b) Extrapolated central charge versus inverse chain length. The three series  $q = 0, 1, 2$  correspond to the central charge  $c_q$  obtained by fitting the Calabrese-Cardy formula over the points  $x = 3n + q$  with  $n$  an integer. Figure adapted from Ref. [57] with the permission of the APS, © 2020 American Physical Society.

### 5.6.3 Analysis of the spectrum

To summarize we have shown that the antiferromagnetic Heisenberg model has a finite gap from the singlet ground state to the 3-box symmetric irrep,  $\Delta_{[3]}/J \approx 0.04$ , and also a finite gap to the conjugate sector  $[3, 3]$  of the same order. Moreover, an analysis of the entanglement entropy in the singlet ground state has shown that the “central charge” obtained by fitting the Calabrese-Cardy formula is smaller than  $c = 2$  and it thus incompatible with any  $SU(3)_k$  WZW CFT. In addition, for sufficiently large chains the central charge is even smaller than  $c = 1$ , providing one more argument for a gapped spectrum.

If the spectrum is gapped, however, one expects the smallest gap to be in the adjoint sector, based on ED results on small chains and on the AKLT results presented in Fig. 5.10. One can actually find a lower bound for the singlet-adjoint gap, or for the smallest Haldane gap of the model. Indeed, as we have argued above, the spectrum is made of five branches of elementary excitations, which come from the tensor product of two adjoint irreps: two adjoint excitations and one excitation of each of  $[3]$ ,  $[3, 3]$  and  $[4, 2]$  irreps. Since the 3-box symmetric irrep appears in the tensor product of two adjoint irreps, then the adjoint elementary excitations cannot be low lying. If it were,

this would contradict the existence of a finite gap in the 3-box symmetric sector, since one could create a composite excitation in the 3-box symmetric sector made of two adjoint irreps, which would then be a low-lying excitation. The same reasoning applies to the  $[4, 2]$  irrep. Thus the smallest Haldane gap of the Heisenberg model must be at least twice as small as the 3-box symmetric gap,  $\Delta \geq \Delta_{[3]}/2$ . Taking the lower bound for  $\Delta_{[3]}$  one finally concludes that the gap  $\Delta$  of the 3-box symmetric Heisenberg chain given by Hamiltonian (5.17) satisfies

$$\Delta/J \geq 0.017. \quad (5.67)$$

### 5.7 Conclusion and outlook

Despite being almost the simplest possible  $SU(3)$  chain for which a gap was expected<sup>11</sup>, showing rigorously the existence of a finite gap in the 3-box symmetric spin chain took us on a long journey starting from the implementation of the full  $SU(3)$  symmetry into the DMRG algorithm, studying the associated AKLT model and then turning to the Heisenberg model. The results obtained in this chapter are in agreement with the extension of Haldane's conjecture to  $SU(3)$  chains, and is thus a first confirmation of its validity. Although it has never been really debated whether the 3-box symmetric spin chain was gapped or gapless, in contrast to the spin-1 chain, our results shine light on the early DMRG and ED results on the model [87, 123]. First, the value of the gap is tiny,  $\Delta/J \geq 0.017$ , presumably corresponding to a correlation length of several hundred sites. It would thus be very difficult to extract thermodynamic properties using ED, or even DMRG on small chains, unless sophisticated – and potentially uncontrolled – extrapolation methods are used [75]. Secondly reliable results were obtained using an extensive number of states in the DMRG algorithm, and this was only possible thanks to the direct implementation of the non-abelian symmetry and an efficient calculation of the group theory coefficients.

There are several directions in which the results presented here should be extended. First of all, to provide a complete and accurate answer about the smallest Haldane gap, the model should be studied in the adjoint irrep. Indeed we expect the lowest excitation to lie in this sector. We have not considered the adjoint and also the  $[4, 2]$  sectors as they lead to nontrivial outer multiplicities in the calculation of the reduced matrix elements of the interaction. These multiplicities need to be handled carefully to construct the Hamiltonian on the superblock. Since we have explained a method to deal with the outer multiplicities at the level of the SDCs it should be possible to incorporate consistently the outer multiplicities in the DMRG, and thus to compute directly the gaps in the adjoint and  $[4, 2]$  sectors.

---

<sup>11</sup>The  $SU(3)$  adjoint spin chain is also expected to be gapped, and the local Hilbert space dimension is 8. From this point of view, it is simpler than the 3-box symmetric spin chain studied here.

We have shown that the spectrum of the 3-box symmetric  $SU(3)$  Heisenberg chain is gapped. According to Haldane's conjecture, it is reasonable to extrapolate this result to the  $3n$ -box symmetric chain, with  $n$  an integer. Indeed the mapping from the spin chain onto the  $NL\sigma M$  becomes exact in the limit of an infinite number of boxes in the symmetric irrep. Since the conjecture applies for  $n = 1$ , then we can expect it to apply for  $n > 1$ . While the gap has been extracted for  $SU(2)$  spin chains with integer spin  $S$  up to 6 [8, 74, 75], confirming every time the original Haldane conjecture, it seems that it would be difficult with the technique presented above to extract the gap of the 6-box symmetric  $SU(3)$  chain. Indeed the  $SU(3)/[U(1) \times U(1)]$   $NL\sigma M$  is asymptotically free [138, 151, 176], and the crossover length scale thus increases exponentially with the number of boxes in the Young diagram. Extracting the gap becomes thus exponentially more complicated for bigger irreps.

There is a more promising way to further confirm Haldane's conjecture, however. The 2-box symmetric  $SU(3)$  chain is expected to be gapless, with low-energy excitations described by the  $SU(3)_1$  WZW CFT [138, 142, 151, 176, 177]. The analysis of this model should follow the exact same lines as described in this chapter. In particular, we expect the entanglement entropy to satisfy the Calabrese-Cardy formula with a central charge  $c = 2$  provided the chain length is larger than the crossover length scale. If the chain length is smaller than this crossover length scale, there is no physical reason to observe a  $c = 2$  critical theory. The model being asymptotically free, the strong coupling limit is only present in the IR. The results obtained in Ref. [87], in particular the central charge compatible with the  $SU(3)_2$  WZW CFT simply show that the model was not probed at an appropriate length scale, because of the intrinsic limitations of ED. To really observe more exotic critical theories one must add higher order interactions and fine-tune them at the integrable points derived by Johannesson [143]. At these unstable fixed points the critical theory is the  $SU(3)_p$  WZW CFT where  $p$  is the number of boxes in the symmetric irrep.

We have mentioned several times the importance of the crossover length scale in the Heisenberg model, and its scaling with the number of boxes in the Young diagram. However we have not extracted a precise estimate of this crossover length scale in the case of the 3-box symmetric irrep. Indeed, computing two-point functions in the traditional DMRG language is an expensive calculation. In this respect, it would be interesting to investigate how to translate the DMRG algorithm presented in this chapter "to the age of matrix product states" [168], where the calculation of correlation functions is more transparent and economical. An estimate of the correlation length could also be obtained using a different algorithm, such as the variational uniform matrix product state (VUMPS) algorithm, which optimizes a single tensor for a translationally invariant wave function, and extracts the correlation length from the gap in the associated transfer matrix [146, 178]. It seems however that the traditional route consisting in implementing the  $SU(N)$  symmetry by use of CGCs is not the appropriate one, as the number  $M$  of irreps that can be handled is significantly smaller than with

## Chapter 5. The 3-box symmetric $SU(3)$ chain

---

the technique presented in this chapter [146]. It would thus be particularly interesting to investigate how to implement a VUMPS algorithm making use of SDCs, to avoid both the use of CGCs and the trouble of working with finite-sized chains.

## 6 Summary and outlook

Despite nine decades of intense investigations, the one-dimensional spin models are still a major subject in condensed matter physics. A remarkable aspect of this field of research is the intricate effort of the experimental, theoretical and numerical communities to bring a deeper understanding of the various phenomena exhibited by spin systems. With the advent of experiments with ultracold atoms which realize the  $SU(N)$  Hubbard model, and thus the  $SU(N)$  Heisenberg model at low energy, it is now not only a matter of theoretical curiosity to study these models, which generalize, but also complexify, the  $SU(2)$  models. In this thesis we have studied three different aspects of one-dimensional quantum spin chains with full  $SU(N)$  symmetry. The thesis was organized in two independent parts, the first one focusing on the  $SU(2)$  Heisenberg model and the second part discussing  $SU(N)$  models with generic values of  $N$ , and, in particular,  $N = 3$ .

In Chapter 2 we revisited the  $SU(2)$  Heisenberg chain in the limit of large spin  $S$  and showed that perturbation theory, in the form of SWT, can provide meaningful and accurate results, in spite of the Mermin-Wagner-Coleman theorem. When considering observables which respect the symmetry of the model, namely rotationally invariant observables, the IR divergences which plague the usual perturbative expansions precisely cancel each other between the longitudinal (symmetry-breaking direction) and transverse parts. In addition, we argued that the perturbative regime is of significant interest as it is the relevant one at short distance. Indeed, Haldane mapped the spin chain onto the  $O(3)$  NL $\sigma$ M, which is asymptotically free. The short distance, weak coupling regime thus extends up to a length scale of order  $e^{\pi S}/S$ . For the realistic and experimentally relevant case of  $S = 5/2$ , the crossover length scale is  $\xi \sim 160$ . The perturbative regime should be observable experimentally at distance  $|x| \ll \xi$ , as was demonstrated by comparing with QMC simulations. In this regime the spin-spin correlation function shows a logarithmic decay, in contrast to the strong coupling regime where the decay is exponential for integer spin and algebraic for half-odd-integer spin.

## Chapter 6. Summary and outlook

---

Chapter 3 was devoted to the exposition of elements of group theory related to the  $SU(N)$  group. This chapter did not go beyond the material presented in standard textbooks. Nevertheless, a rather detailed presentation was necessary in anticipation of Chapter 4, and, especially, of Chapter 5. The chapter was mainly focused on the representation theory of the permutation group. Indeed, by the Schur-Weyl duality one can apply the machinery of the symmetric group to the  $SU(N)$  group. We have introduced the important notions of Young diagrams, which are convenient graphical representations of the irreps of the group and which are intensely used throughout Chapters 4 and 5, standard Young tableaux, which are Young diagrams filled with integers, and the Itzykson-Nauenberg (or Littlewood-Richardson) rules, which are the rules for decomposing the tensor product of two arbitrary  $SU(N)$  irreps into a direct sum of irreps.

In Chapter 4 we introduced a generic construction for AKLT models with  $SU(N)$  symmetry and arbitrary self-conjugate edge states, building on group theory notions introduced in Chapter 3, and on the MPS form of the AKLT states. This allowed us to build, for instance, a spin-1 AKLT model having spin-1 edge states. Unlike the original AKLT model, this model was shown to lie in a trivial gapped phase, separated from the Haldane phase by a continuous phase transition with central charge  $c = 1$ , in the  $SU(2)_1$  WZW universality class, in agreement with previous predictions for such a topological phase transition. When generalizing the construction to  $SU(N > 2)$  the new feature is the possibility for non-trivial outer multiplicities of irreps in the tensor product of two irreps. With the method presented in this chapter we showed how to build AKLT parent Hamiltonians having a unique ground state. From a practical point of view, however, the construction becomes intractably complicated when the edge irreps have a larger dimension than the physical irreps. Indeed, to ensure the uniqueness of the ground state one must deal with an injective MPS. The only way to enforce this injectivity condition is to enlarge the MPS. As a consequence, the parent Hamiltonians become longer ranged. The construction was applied to revisit the  $SU(3)$  model with physical 3-box symmetric irrep at each site. In particular, we could show that the edge states belong to the adjoint sector. In the original construction, the nature of the edge states remained mysterious, and the AKLT wave function was not optimal in the MPS sense. The new construction for this AKLT state became an extremely valuable guide for our study of the associated Heisenberg model in Chapter 5. The construction of AKLT states described in this chapter also gives a hint on what AKLT models could lie in SPT phases.

Finally in Chapter 5 we investigated numerically the  $SU(3)$  Heisenberg model with completely symmetric irrep made of three boxes at each site, and showed that it has a finite gap. This result comes as a confirmation of the recent Haldane-type argument for a gapped spectrum when the number  $p$  of boxes in the symmetric irrep is a multiple of three and gapless excitations when  $p$  is not a multiple of three. To unambiguously show the opening of a gap in the  $p = 3$  case, the simplest case where a gap was expected,



---

we developed a DMRG algorithm making full use of the  $SU(3)$  symmetry of the model. The core of the algorithm is the calculation of the so-called reduced matrix elements of the interaction between the left and right blocks in DMRG, using the SDCs of  $SU(3)$  which are in one-to-one correspondence with the SDCs of the symmetric group. The  $SU(3)$  AKLT model with 3-box symmetric irrep at each site, which we presented in Chapter 4 as a model made of virtual adjoint irreps, proved to be extremely useful for the analysis of the spectrum at the Heisenberg point. We argued that there are actually four Haldane gaps in the model, corresponding to five elementary excitations, two of them being adjoint excitations. Based on ED results at the AKLT point we argued that the smallest Haldane gap is the adjoint gap. The weakness of our analysis is the fact that we could not, for technical reasons, directly access the singlet-adjoint gap. Nevertheless, based on the nature of the elementary excitations we argued that if one of the elementary excitation is gapped then all the others should also be gapped.

The search for a gap in the 3-box symmetric  $SU(3)$  chain was motivated by the recent mapping of the spin chain onto a  $NL\sigma M$ . As the  $O(3)$   $NL\sigma M$  relevant in the  $SU(2)$  case, the  $SU(3)/[U(1) \times U(1)]$  flag manifold  $NL\sigma M$  is asymptotically free. This means that the opening of a gap is only seen at length scales larger than the crossover length scale  $\xi$  which scales as  $e^{\alpha p}/p$ ,  $\alpha > 0$ <sup>1</sup>. The value of the gap that we found,  $\Delta_{[3]}/J = 0.040 \pm 0.006$  brings us to a very large correlation length, of order several hundreds sites, although we have not attempted to evaluate precisely this length scale. In any case one sees that the weak coupling regime is significantly more extended in the  $SU(3)$  model than in the  $SU(2)$  spin chain. It would be very interesting to extend the perturbative calculations presented in Chapter 2 to the  $SU(3)$  case. Since experimental realizations of  $SU(N)$  models deal with a limited number of atoms loaded in the optical lattice, the analytical predictions of flavour-wave theory, the analogue of SWT for  $N > 2$ , would be particularly relevant [179–183]. Performing such perturbative calculations, however, would be a rather technical challenge given the difficulties encountered in recent progress on the methods for more than one particle per site [140, 184, 185]. These difficulties arise already at linear order with the presence of zero-energy modes in the flavour-wave spectrum. Even when the flat modes are lifted we expect the linear order to be a rather poor approximation of the spin chain, as we have seen in the  $SU(2)$  case, and it would be necessary to take interactions into account to obtain an accurate description of the model.

Showing the existence of a finite gap in the  $p = 3$   $SU(3)$  chain was conceptually equivalent to the quest for a finite gap in the spin-1 chain in the 1980's. To confirm further the  $SU(3)$  Haldane conjecture, it would be crucial to demonstrate that the model with  $p = 2$  is gapless, and lies in the  $SU(3)_1$  WZW universality class. A possible route is the investigation of the entanglement entropy with the Calabrese-Cardy formula. For the

---

<sup>1</sup>The  $\beta$ -function of the coupling  $g$  being known only at order  $g^2$ , the scaling of the crossover length scale is, to this order,  $\xi \sim e^{\alpha p}$ . However it is unlikely that the unknown  $g^3$  term vanishes.

$p = 3$  case we showed that the central charge decreases as the system size increases and becomes ultimately smaller than one, a sign for a gapped spectrum. For the  $p = 2$  model, the analysis should show a saturation of the central charge converging to  $c = 2$  from above. It has already been shown by ED that, on small systems, the central charge was compatible with the  $SU(3)_2$  WZW universality class, but such a behavior is prevented in the thermodynamic limit since this fixed point is unstable.

Finally, let us mention that the recent development of Haldane's conjectures for the different irreps of  $SU(N > 2)$  motivates further numerical investigations. For the  $SU(2)$  Heisenberg model, the existence of a gap has been confirmed up to spin  $S = 6$ , validating every time Haldane's argument. In fact, the study of the long-distance behavior of the large-spin Heisenberg chain is mainly motivated by the challenging numerical difficulty of extracting a tiny but finite gap rather than being motivated by the need of confirming Haldane's conjecture, which is well established. In this respect, the demonstration of the existence of a gap in the spin-1 chain was the strongest argument in favor of the validity of the conjecture. Indeed, the mapping from the spin chain to the NL $\sigma$ M becomes exact in the large spin limit. It is thus both more complicated and less necessary to show the existence of a gap for the large integer spin models. Conversely the numerical confirmation of  $SU(N > 2)$  Haldane's conjectures is at its premises, where, by opposition, we look at the simplest models, namely the most quantum ones, to confirm their low-energy behavior ! The DMRG algorithm is, at the time of writing this thesis, essentially the only viable numerical method adapted to tackle such models. It is very likely that more sophisticated methods based on tensor networks, such as the promising VUMPS, will permit a more systematic and somehow less troublesome study of  $SU(N)$  spin chains in the relevant lowest dimensional irreps, and will thus provide confirmations of the Haldane conjectures. In any case, given the large local Hilbert space dimension associated with non-trivial irreps of  $SU(N > 2)$  and the intrinsic structure of the group, it appears evident that the implementation of the non-abelian  $SU(N)$  symmetry in the numerical techniques is not only useful but absolutely necessary to obtain reliable results with classical computers.

# A Crossover scale of the NL $\sigma$ M

In this appendix we derive the higher-order corrections to the crossover length scale  $\xi$  in Eq. (2.17) and Eq. (2.18) based on the 4-loop  $\beta$ -function of the NL $\sigma$ M derived in Ref. [73]. We then deduce the corrections to the crossover energy scale  $\Delta$  in Eq. (2.19).

The 4-loop  $\beta$ -function reads [73]

$$\beta(g) = \frac{g^2}{2\pi} + \frac{g^3}{(2\pi)^2} + \frac{5g^4}{4(2\pi)^3} + \frac{23g^5}{12(2\pi)^4} + \mathcal{O}(g^6) \quad \left( \frac{dg}{d \ln L} = \beta(g) \right). \quad (\text{A.1})$$

To simplify a bit the notation we define the coefficients  $\{a_i\}_{i=2}^5$  of the expansion of the  $\beta$ -function in powers of  $g$ ,

$$\beta(g) = \sum_{i=2}^5 a_i g^i + \mathcal{O}(g^6). \quad (\text{A.2})$$

Integrating the renormalization group equation we obtain,

$$\ln \xi = \int_{g_0}^{g_1} \frac{dg}{\beta(g)} \quad (\text{A.3})$$

where  $g_0$  is the bare coupling and  $g_1$  is an arbitrary coupling at length scale  $\xi$ , which is  $g_1 = \mathcal{O}(1)$ .

Now we perform the integral in the right-hand side. We define

$$f(g) = \frac{\beta(g)}{a_2 g^2} - 1 = \frac{a_3}{a_2} g + \frac{a_4}{a_2} g^2 + \frac{a_5}{a_2} g^3 + \mathcal{O}(g^4) \quad (\text{A.4})$$

and obtain

$$\int_{g_0}^{g_1} \frac{dg}{\beta(g)} = \frac{1}{a_2} \int_{g_0}^{g_1} dg \frac{1}{g^2} \frac{1 + f(g) - f(g)}{1 + f(g)} = \frac{1}{a_2} \left( \frac{1}{g_0} - \frac{1}{g_1} \right) - \frac{1}{a_2} J_1 \quad (\text{A.5})$$

## Appendix A. Crossover scale of the $\text{NL}\sigma\text{M}$

---

where

$$J_1 = \int_{g_0}^{g_1} dg \frac{1}{g^2} \frac{f(g)}{1+f(g)}. \quad (\text{A.6})$$

We rewrite  $J_1$  as

$$J_1 = \int_{g_0}^{g_1} dg \frac{1}{g} \frac{f(g)/g}{1+f(g)} = \frac{a_3}{a_2} \int_{g_0}^{g_1} dg \frac{1}{g} \frac{1+f(g) - f(g) + \frac{a_4}{a_3}g + \frac{a_5}{a_3}g^2 + \mathcal{O}(g^3)}{1+f(g)} \quad (\text{A.7})$$

leading to

$$J_1 = \frac{a_3}{a_2} \ln\left(\frac{g_1}{g_0}\right) + \frac{a_3}{a_2} \int_{g_0}^{g_1} dg \frac{1}{g} \frac{\frac{a_4}{a_3}g + \frac{a_5}{a_3}g^2 - f(g) + \mathcal{O}(g^3)}{1+f(g)}. \quad (\text{A.8})$$

One has now

$$J_1 = \frac{a_3}{a_2} \ln\left(\frac{g_1}{g_0}\right) + \frac{a_4}{a_2} J_2 \quad (\text{A.9})$$

where

$$J_2 = \int_{g_0}^{g_1} dg \frac{1 + \frac{a_5}{a_4}g - \frac{a_3}{a_4} \frac{1}{g} f(g) + \mathcal{O}(g^2)}{1+f(g)}. \quad (\text{A.10})$$

This can be rewritten as

$$J_2 = \int_{g_0}^{g_1} dg \frac{d_0 + d_1 g + \mathcal{O}(g^2)}{1+f(g)} \quad (\text{A.11})$$

where

$$d_0 = 1 - \frac{a_3^2}{a_2 a_4}, \quad d_1 = \frac{a_5}{a_4} - \frac{a_3}{a_2}. \quad (\text{A.12})$$

Since  $f(g) = \mathcal{O}(g)$  we can develop

$$\frac{1}{1+f(g)} = 1 - f(g) + \mathcal{O}(g^2) = 1 - \frac{a_3}{a_2}g + \mathcal{O}(g^2). \quad (\text{A.13})$$

Defining  $c_1 = -a_3/a_2$  the coefficient of the linear term in  $g$  in the expansion of  $(1+f(g))^{-1}$  the integral  $J_2$  is given by

$$J_2 = \int_{g_0}^{g_1} dg \left( d_0 + (c_1 d_0 + d_1)g + \mathcal{O}(g^2) \right) \quad (\text{A.14})$$

leading to

$$J_2 = K_2 - d_0 g_0 - \frac{1}{2}(c_1 d_0 + d_1)g_0^2 + \mathcal{O}(g_0^3) \quad (\text{A.15})$$

where  $K_2 = d_0 g_1 + (c_1 d_0 + d_1)g_1^2/2$  is not relevant as it depends on the unknown coupling  $g_1$  at scale  $\xi$ .

---

We thus end up with

$$\ln \xi = \text{const} + \frac{1}{a_2 g_0} - \frac{a_3}{a_2^2} \ln \left( \frac{g_1}{g_0} \right) + \frac{a_4 d_0}{a_2^2} g_0 + \frac{a_4 (c_1 d_0 + d_1)}{2a_2^2} g_0^2 + \mathcal{O}(g_0^3) \quad (\text{A.16})$$

where the first constant term contains all terms depending only on  $g_1$ .

We now define

$$\lambda_1 = \frac{a_4 d_0}{a_2^2} \quad \text{and} \quad \lambda_2 = \frac{a_4 (c_1 d_0 + d_1)}{2a_2^2} \quad (\text{A.17})$$

and exponentiate Eq. (A.16),

$$\xi \propto g_0^{a_3/a_2^2} e^{(a_2 g_0)^{-1}} \exp \left( \lambda_1 g_0 + \lambda_2 g_0^2 + \mathcal{O}(g_0^3) \right). \quad (\text{A.18})$$

Expanding the last exponential and replacing the coefficients by their exact values one finally has

$$\xi \propto g_0 e^{2\pi/g_0} \left( 1 + \frac{g_0}{8\pi} + \frac{23g_0^2}{384\pi^2} + \mathcal{O}(g_0^3) \right). \quad (\text{A.19})$$

Taking  $g_0 = 2/S$  as the bare coupling constant this formula translates into

$$\xi \propto \frac{1}{S} e^{\pi S} \left( 1 + \frac{1}{4\pi S} + \frac{23}{96\pi^2 S^2} + \mathcal{O}(S^{-3}) \right). \quad (\text{A.20})$$

The crossover energy scale is given by  $\Delta = v/\xi$  where  $v = 2JS$  is the spin-wave velocity. One thus has

$$\Delta \propto JS^2 e^{-\pi S} \left( 1 - \frac{1}{4\pi S} - \frac{17}{96\pi^2 S^2} + \mathcal{O}(S^{-3}) \right). \quad (\text{A.21})$$

Figure 2.1 in the main text shows the numerical values of the gap  $\Delta$  and correlation length  $\xi$  obtained by numerical diagonalization together with fits to expressions (A.20) and (A.21) as well as the interpolated values for half-odd-integer spin.



# B Equal-time correlation function from the Hellmann-Feynman theorem

## B.1 Introduction

The aim of this appendix is to derive the equal-time spin-spin correlation function using a modified Hamiltonian and the Hellmann-Feynman theorem [79, 80].

We consider the following Hamiltonian,

$$\tilde{\mathcal{H}}(\lambda) = \mathcal{H} + \mathcal{W}(\lambda) \quad (\text{B.1})$$

where  $\mathcal{H}$  is the Heisenberg Hamiltonian given in Eq. (2.1) and which we recall here for completeness

$$\mathcal{H} = J \sum_i \mathbf{S}_i \cdot \mathbf{S}_{i+1}$$

and

$$\mathcal{W}(\lambda) = \lambda J (-1)^{n+1} \sum_i \mathbf{S}_i \cdot \mathbf{S}_{i+n} \quad (\text{B.2})$$

where the distance  $n$  is fixed and  $\lambda$  is a (small) positive dimensionless parameter. The factor  $(-1)^{n+1}$  ensures that  $\mathcal{W}(\lambda)$  does not frustrate the model.

By the Hellmann-Feynman theorem we obtain

$$\left. \frac{(-1)^{n+1}}{JN_s} \frac{\partial \tilde{E}_0(\lambda)}{\partial \lambda} \right|_{\lambda=0} = \langle \mathbf{S}_i \cdot \mathbf{S}_{i+n} \rangle_{\mathcal{H}} \quad (\text{B.3})$$

where  $\tilde{E}_0(\lambda) = \langle \tilde{\mathcal{H}}(\lambda) \rangle_{\tilde{\mathcal{H}}(\lambda)}$  is the ground state energy of  $\tilde{\mathcal{H}}(\lambda)$  and where  $\langle \cdot \rangle_{\mathcal{H}}$  denotes an expectation value in the ground state of the original Heisenberg Hamiltonian  $\mathcal{H}$ . The equal-time spin-spin correlation function can thus be obtained by computing the ground state energy of the modified Hamiltonian  $\tilde{\mathcal{H}}(\lambda)$  to second order in perturbation theory. To proceed further one needs to treat separately the case of even and odd distance  $n$ .

## B.2 Odd distance

We take  $n$  odd. Thus  $(-1)^{n+1} = 1$  and  $\mathcal{W}(\lambda)$  comes with an overall positive sign.

### B.2.1 Hamiltonian $\mathcal{W}(\lambda)$

We write an expansion of  $\mathcal{W}(\lambda)$  in powers of  $1/S$  in the following way

$$\mathcal{W}(\lambda) = \mathcal{W}^{(0)}(\lambda) + \mathcal{W}^{(2)}(\lambda) + \mathcal{W}^{(4)}(\lambda) + \mathcal{O}(S^{-1}) \quad (\text{B.4})$$

where the first terms take the values (compare to Eq. (2.27), (2.28) and (2.30), respectively)

$$\mathcal{W}^{(0)} = -JN_s S^2 \lambda, \quad (\text{B.5})$$

$$\mathcal{W}^{(2)}(\lambda) = JS\lambda \sum_k \left[ 2a_k^\dagger a_k + \gamma_k(n) (a_k^\dagger a_{-k}^\dagger + a_{-k} a_k) \right] \quad (\text{B.6})$$

with

$$\gamma_k(n) = \cos(kn) \quad (\text{B.7})$$

and

$$\mathcal{W}^{(4)}(\lambda) = -\frac{J\lambda}{2} \sum_{\langle\langle ij \rangle\rangle} (a_i^\dagger a_i a_j a_j + \text{h.c.}) - J\lambda \sum_{\langle\langle ij \rangle\rangle} a_i^\dagger a_j^\dagger a_i a_j. \quad (\text{B.8})$$

In Eq. (B.8) we have used the notation  $\langle\langle ij \rangle\rangle$  to denote all the couples  $(i, j)$  which are separated by a distance  $n$ . In other words we have

$$\sum_{\langle ij \rangle} O_{(i,j)} = \sum_i O_{(i,i+1)} = \frac{1}{2} \sum_i \sum_{\delta=\pm 1} O_{(i,i+\delta)} \quad (\text{B.9})$$

and

$$\sum_{\langle\langle ij \rangle\rangle} O_{(i,j)} = \sum_i O_{(i,i+n)} = \frac{1}{2} \sum_i \sum_{\delta=\pm n} O_{(i,i+\delta)}. \quad (\text{B.10})$$



Equation (B.6) is easily obtained from Eq. (2.52),

$$\begin{aligned}
 \mathcal{W}^{(2)}(\lambda) &= JS\lambda \sum_i \mathcal{O}_{i,i+n}^{(1)} \\
 &= JS\lambda \frac{1}{2} \sum_i \sum_{\delta=\pm n} \mathcal{O}_{i,i+\delta}^{(1)} \\
 &= JS\lambda \frac{1}{2} \sum_i \sum_{\delta=\pm n} \left[ a_i^\dagger a_{i+\delta}^\dagger + a_i a_{i+\delta} + a_i^\dagger a_i + a_{i+\delta}^\dagger a_{i+\delta} \right] \\
 &= JS\lambda \frac{1}{2} \sum_{\delta=\pm n} \sum_k \left[ 2a_k^\dagger a_k + e^{ik\delta} \left( a_k^\dagger a_{-k}^\dagger + a_{-k} a_k \right) \right] \\
 &= JS\lambda \sum_k \left[ 2a_k^\dagger a_k + \cos(kn) \left( a_k^\dagger a_{-k}^\dagger + a_{-k} a_k \right) \right].
 \end{aligned} \tag{B.11}$$

### B.2.2 Hamiltonian $\tilde{\mathcal{H}}(\lambda)$

The total Hamiltonian  $\tilde{\mathcal{H}}(\lambda)$  has the following expansion

$$\tilde{\mathcal{H}}(\lambda) = \tilde{\mathcal{H}}^{(0)}(\lambda) + \tilde{\mathcal{H}}^{(2)}(\lambda) + \tilde{\mathcal{H}}^{(4)}(\lambda) + \mathcal{O}(S^{-1}) \tag{B.12}$$

where  $\tilde{\mathcal{H}}^{(k)}(\lambda) = \mathcal{H}^{(k)} + \mathcal{W}^{(k)}(\lambda)$ . The classical ground state energy is given by

$$\tilde{\mathcal{H}}^{(0)}(\lambda) = -JN_s S^2 (1 + \lambda), \tag{B.13}$$

and the quadratic Hamiltonian by

$$\tilde{\mathcal{H}}^{(2)}(\lambda) = \sum_k \left[ \tilde{A}_k a_k^\dagger a_k - \frac{1}{2} \tilde{B}_k \left( a_k^\dagger a_{-k}^\dagger + a_{-k} a_k \right) \right] \tag{B.14}$$

where we defined

$$\tilde{A}_k = 2JS(1 + \lambda), \quad \tilde{B}_k = -2JS\tilde{\gamma}_k(n), \quad \tilde{\gamma}_k(n) = \gamma_k + \lambda\gamma_k(n). \tag{B.15}$$

In Eq. (B.15) and throughout this appendix we should keep in mind that quantities with a tilde depend explicitly on the parameter  $\lambda$ , although this dependence is removed in the notations to lighten the expressions.

The first order interaction  $\tilde{\mathcal{H}}^{(4)}(\lambda)$  of  $\tilde{\mathcal{H}}(\lambda)$  is given by

$$\begin{aligned}
 \tilde{\mathcal{H}}^{(4)}(\lambda) &= -\frac{J}{2} \sum_{\langle ij \rangle} \left( a_i^\dagger a_i a_j a_j + \text{h.c.} \right) - J \sum_{\langle ij \rangle} a_i^\dagger a_j^\dagger a_i a_j \\
 &\quad - \frac{J\lambda}{2} \sum_{\langle\langle ij \rangle\rangle} \left( a_i^\dagger a_i a_j a_j + \text{h.c.} \right) - J\lambda \sum_{\langle\langle ij \rangle\rangle} a_i^\dagger a_j^\dagger a_i a_j.
 \end{aligned} \tag{B.16}$$

## Appendix B. Equal-time correlation function from the Hellmann-Feynman theorem

### B.2.3 Bogoliubov transformation

Performing a Bogoliubov transformation on the Hamiltonian  $\tilde{\mathcal{H}}^{(2)}(\lambda)$  given in Eq. (B.14) as explained in the main text we obtain the coefficients

$$\tilde{u}_k = \sqrt{\frac{\tilde{A}_k + \tilde{\epsilon}_k}{2\tilde{\epsilon}_k}} \quad \text{and} \quad \tilde{v}_k = -\text{sign}(\tilde{B}_k) \sqrt{\frac{\tilde{A}_k - \tilde{\epsilon}_k}{2\tilde{\epsilon}_k}} \quad (\text{B.17})$$

with the dispersion relation

$$\begin{aligned} \tilde{\epsilon}_k &= \sqrt{\tilde{A}_k^2 - \tilde{B}_k^2} \\ &= 2JS \sqrt{1 + \lambda^2 + 2\lambda - \tilde{\gamma}_k^2(n)} \\ &= 2JS \sqrt{1 - \gamma_k^2 + 2\lambda + \lambda^2 - 2\lambda\gamma_k\gamma_k(n) - \lambda^2\gamma_k^2(n)}. \end{aligned} \quad (\text{B.18})$$

The quadratic Hamiltonian then reads

$$\tilde{\mathcal{H}}^{(2)}(\lambda) = \delta\tilde{\mathcal{E}}^{(2)} + \sum_k \tilde{\epsilon}_k \alpha_k^\dagger \alpha_k \quad (\text{B.19})$$

where

$$\delta\tilde{\mathcal{E}}^{(2)} = -JN_s S(1 + \lambda) + \frac{1}{2} \sum_k \tilde{\epsilon}_k \quad (\text{B.20})$$

is a first order correction to the ground state energy.

### B.2.4 First order interaction

We can now proceed to the treatment of the first order interaction  $\tilde{\mathcal{H}}^{(4)}(\lambda)$ . The solution consists in applying Wick's theorem. It is important to recall that expectation values are taken in the Bogoliubov vacuum of  $\tilde{\mathcal{H}}(\lambda)$ , not the Bogoliubov vacuum of  $\mathcal{H}$ ! Thus, even though  $\mathcal{H}^{(4)}$  does not explicitly involve  $\lambda$ , the coefficients of its expansion in the Bogoliubov basis do.

We obtain

$$\mathcal{H}^{(4)} = \delta\mathcal{E}^{(4)} + \sum_k \left[ \delta\mathcal{E}_k^{(4)} \alpha_k^\dagger \alpha_k + \frac{1}{2} B_k^{(4)} \left( \alpha_k^\dagger \alpha_{-k}^\dagger + \alpha_{-k} \alpha_k \right) \right] + : (4\text{-bosons}) : \quad (\text{B.21})$$

where  $: (4\text{-bosons}) :$  denotes normal ordered terms with four Bogoliubov bosonic operators and where all vertices  $\delta\mathcal{E}^{(4)}$ ,  $\delta\mathcal{E}_k^{(4)}$ ,  $B_k^{(4)}$ , ... depend on  $\lambda$ . Notice in particular that the vertex  $B_k^{(4)}$  was vanishing in the case of  $\lambda = 0$  treated in the main text. The

vertices have the following expressions

$$\begin{aligned}\delta\mathcal{E}^{(4)} &= -JN_s \left\{ (\tilde{n} + \tilde{\Delta})^2 + \tilde{m}(\tilde{m} + \tilde{\delta}) \right\}, \\ \delta\mathcal{E}_k^{(4)} &= (\tilde{u}_k^2 + \tilde{v}_k^2) \delta A_k - 2\tilde{u}_k \tilde{v}_k \delta B_k, \\ B_k^{(4)} &= (\tilde{u}_k^2 + \tilde{v}_k^2) \delta B_k - 2\tilde{u}_k \tilde{v}_k \delta A_k,\end{aligned}\tag{B.22}$$

and

$$\delta A_k = -J \left[ 2(\tilde{\Delta} + \tilde{n}) + \gamma_k(\tilde{\delta} + 2\tilde{m}) \right], \tag{B.23}$$

$$\delta B_k = -J \left[ \tilde{m} + 2(\tilde{\Delta} + \tilde{n})\gamma_k \right], \tag{B.24}$$

where the coefficients  $\tilde{\Delta}$ ,  $\tilde{\delta}$ ,  $\tilde{m}$  and  $\tilde{n}$  are defined as ( $j$  being nearest neighbor of  $i$  and the expectation values are taken in the Bogoliubov vacuum of  $\tilde{\mathcal{H}}(\lambda)$ )

$$\tilde{\Delta} = \langle a_i a_j \rangle = -\frac{1}{N_s} \sum_k \gamma_k \tilde{u}_k \tilde{v}_k, \tag{B.25}$$

$$\tilde{\delta} = \langle a_i^2 \rangle = -\frac{1}{N_s} \sum_k \tilde{u}_k \tilde{v}_k, \tag{B.26}$$

$$\tilde{m} = \langle a_i^\dagger a_j \rangle = \frac{1}{N_s} \sum_k \gamma_k \tilde{v}_k^2, \tag{B.27}$$

$$\tilde{n} = \langle a_i^\dagger a_i \rangle = \frac{1}{N_s} \sum_k \tilde{v}_k^2. \tag{B.28}$$

Now we turn to the treatment of the first order interaction of  $\mathcal{W}(\lambda)$ , namely  $\mathcal{W}^{(4)}(\lambda)$ . The only difference with  $\mathcal{H}^{(4)}(\lambda)$  is the fact that  $i$  and  $j$  are not nearest neighbor anymore, but are separated by a distance  $n$ . So we should simply replace  $\gamma_k$  by  $\gamma_k(n)$ . We define, for those  $(i, j)$  (notice the similarity with  $\tilde{\Delta}$  in Eq. (B.25) and  $\tilde{m}$  in Eq. (B.27))

$$\tilde{\Omega} = \langle a_i a_j \rangle = -\frac{1}{N_s} \sum_k \gamma_k(n) \tilde{u}_k \tilde{v}_k \tag{B.29}$$

and

$$\tilde{p} = \langle a_i^\dagger a_j \rangle = \frac{1}{N_s} \sum_k \gamma_k(n) \tilde{v}_k^2. \tag{B.30}$$

We can now rewrite our  $\mathcal{W}^{(4)}(\lambda)$  as

$$\mathcal{W}^{(4)}(\lambda) = \delta F^{(4)} + \sum_k \left[ \omega_k^{(4)} \alpha_k^\dagger \alpha_k + \frac{1}{2} D_k^{(4)} \left( \alpha_k^\dagger \alpha_{-k}^\dagger + \alpha_{-k} \alpha_k \right) \right] + : (4\text{-bosons}) : \tag{B.31}$$

## Appendix B. Equal-time correlation function from the Hellmann-Feynman theorem

---

where

$$\begin{aligned}\delta F^{(4)} &= -J\lambda N_s \left[ (\tilde{n} + \tilde{\Omega})^2 + \tilde{p}(\tilde{p} + \tilde{\delta}) \right], \\ \omega_k^{(4)} &= (\tilde{u}_k^2 + \tilde{v}_k^2) \delta C_k - 2\tilde{u}_k \tilde{v}_k \delta D_k, \\ D_k^{(4)} &= (\tilde{u}_k^2 + \tilde{v}_k^2) \delta D_k - 2\tilde{u}_k \tilde{v}_k \delta C_k,\end{aligned}\tag{B.32}$$

and

$$\delta C_k = -J\lambda \left[ 2(\tilde{\Omega} + \tilde{n}) + \gamma_k(n)(\tilde{\delta} + 2\tilde{p}) \right],\tag{B.33}$$

$$\delta D_k = -J\lambda \left[ \tilde{p} + 2(\tilde{\Omega} + \tilde{n})\gamma_k(n) \right].\tag{B.34}$$

Regrouping  $\mathcal{H}^{(4)}$  and  $\mathcal{W}^{(4)}(\lambda)$  we end up with

$$\tilde{\mathcal{H}}^{(4)}(\lambda) = \delta \tilde{\mathcal{E}}^{(4)} + \sum_k \left[ \tilde{\mathcal{E}}_k^{(4)} \alpha_k^\dagger \alpha_k + \frac{1}{2} \tilde{\mathcal{B}}_k^{(4)} (\alpha_k^\dagger \alpha_{-k}^\dagger + \alpha_{-k} \alpha_k) \right] + : (4\text{-bosons}) : \tag{B.35}$$

with

$$\delta \tilde{\mathcal{E}}^{(4)} = -JN_s \left[ \left\{ (\tilde{n} + \tilde{\Delta})^2 + \tilde{m}(\tilde{m} + \tilde{\delta}) \right\} + \lambda \left\{ (\tilde{n} + \tilde{\Omega})^2 + \tilde{p}(\tilde{p} + \tilde{\delta}) \right\} \right],\tag{B.36}$$

$$\tilde{\mathcal{E}}_k^{(4)} = (\tilde{u}_k^2 + \tilde{v}_k^2) \delta \mathcal{A}_k - 2\tilde{u}_k \tilde{v}_k \delta \mathcal{B}_k,\tag{B.37}$$

$$\tilde{\mathcal{B}}_k^{(4)} = (\tilde{u}_k^2 + \tilde{v}_k^2) \delta \mathcal{B}_k - 2\tilde{u}_k \tilde{v}_k \delta \mathcal{A}_k\tag{B.38}$$

and

$$\begin{aligned}\delta \mathcal{A}_k &= \delta A_k + \delta C'_k \\ &= -J \left[ 2(\tilde{\Delta} + \tilde{n}) + \gamma_k(\tilde{\delta} + 2\tilde{m}) + \lambda \left\{ 2(\tilde{\Omega} + \tilde{n}) + \gamma_k(n)(\tilde{\delta} + 2\tilde{p}) \right\} \right],\end{aligned}\tag{B.39}$$

$$\begin{aligned}\delta \mathcal{B}_k &= \delta B_k + \delta D_k \\ &= -J \left[ \tilde{m} + 2(\tilde{\Delta} + \tilde{n})\gamma_k + \lambda \left\{ \tilde{p} + 2(\tilde{\Omega} + \tilde{n})\gamma_k(n) \right\} \right].\end{aligned}\tag{B.40}$$

At this order the Hamiltonian reads

$$\begin{aligned}\tilde{\mathcal{H}}(\lambda) &= \tilde{\mathcal{H}}^{(0)} + \delta \tilde{\mathcal{E}}^{(2)} + \delta \tilde{\mathcal{E}}^{(4)} \\ &+ \sum_k \left( \tilde{\epsilon}_k + \tilde{\mathcal{E}}_k^{(4)} \right) \alpha_k^\dagger \alpha_k + \sum_k \frac{1}{2} \tilde{\mathcal{B}}_k^{(4)} (\alpha_k^\dagger \alpha_{-k}^\dagger + \alpha_{-k} \alpha_k) \\ &+ : (4\text{-bosons}) : .\end{aligned}\tag{B.41}$$

The ground state energy of  $\tilde{\mathcal{H}}(\lambda)$  is thus given, to second order in perturbation theory, by

$$\tilde{E}_0(\lambda) = \tilde{\mathcal{H}}^{(0)} + \delta\tilde{\mathcal{E}}^{(2)} + \delta\tilde{\mathcal{E}}^{(4)} + \mathcal{O}(S^{-1}). \quad (\text{B.42})$$

Using Eq. (B.3) one can obtain the correlation function from this expression. We perform the derivation separately at first and second order.

### B.2.5 Analysis at first order

We focus on the two first terms in Eq. (B.42). First observe that

$$\left. \frac{\partial \tilde{\epsilon}_k}{\partial \lambda} \right|_{\lambda=0} = 2JS \frac{1 - \gamma_k \gamma_k(n)}{\sqrt{1 - \gamma_k^2}}. \quad (\text{B.43})$$

One has

$$\left. \frac{\partial \tilde{\mathcal{H}}^{(0)}}{\partial \lambda} \right|_{\lambda=0} = -JN_s S^2 \quad (\text{B.44})$$

and

$$\left. \frac{\partial \delta\tilde{\mathcal{E}}^{(2)}}{\partial \lambda} \right|_{\lambda=0} = -JN_s S + \frac{1}{2} \sum_k \left. \frac{\partial \tilde{\epsilon}_k}{\partial \lambda} \right|_{\lambda=0}. \quad (\text{B.45})$$

We thus obtain

$$\begin{aligned} \frac{1}{JN_s} \left. \frac{\partial \tilde{E}_0(\lambda)}{\partial \lambda} \right|_{\lambda=0} &= -S^2 - S + \frac{S}{N_s} \sum_k \frac{1 - \gamma_k \gamma_k(n)}{\sqrt{1 - \gamma_k^2}} + \mathcal{O}(S^0) \\ &= -S^2 - S + \frac{S}{2\pi} \int_{-\pi}^{\pi} dk \frac{1 - \gamma_k \gamma_k(n)}{\sqrt{1 - \gamma_k^2}} + \mathcal{O}(S^0) \\ &= -S^2 - S + \frac{S}{2\pi} \int_{-\pi}^{\pi} dk \frac{1 - \cos(k) \cos(kn)}{|\sin(k)|} + \mathcal{O}(S^0) \\ &= -S^2 - S + \frac{S}{\pi} \int_0^{\pi} dk \frac{1 - \cos(k) \cos(kn)}{\sin(k)} + \mathcal{O}(S^0) \\ &= -S^2 - S + \frac{2S}{\pi} \int_0^{\pi/2} dk \left[ \frac{1}{\sin(k)} - \frac{\cos(kn)}{\tan(k)} \right] + \mathcal{O}(S^0) \\ &= -S^2 - S + \frac{2S}{\pi} J_1(n) + \mathcal{O}(S^0) \\ &= -S^2 \left[ 1 + \frac{1}{S} \left( 1 - \frac{2}{\pi} J_1(n) \right) + \mathcal{O}(S^{-2}) \right] \\ &= \langle \mathbf{S}_i \cdot \mathbf{S}_{i+n} \rangle \text{ up to first order, } n \text{ odd} \end{aligned} \quad (\text{B.46})$$

where  $J_1(n)$  is given in Eq. (2.63).

## Appendix B. Equal-time correlation function from the Hellmann-Feynman theorem

### B.2.6 Analysis at second order

The second order contribution is obtained with the calculation of

$$\frac{1}{JN_s} \left. \frac{\partial}{\partial \lambda} \right|_{\lambda=0} \delta \tilde{\mathcal{E}}^{(4)} \quad (\text{B.47})$$

and  $\delta \tilde{\mathcal{E}}^{(4)}$  is given in Eq. (B.36). We need to pay attention to the fact that everything depends on  $\lambda$  since  $\tilde{u}_k$  and  $\tilde{v}_k$  depend on  $\lambda$ . We have

$$\begin{aligned} \frac{\partial}{\partial \lambda} \delta \tilde{\mathcal{E}}^{(4)} = & -JN_s \left[ \left\{ 2(\tilde{n} + \tilde{\Delta})(\partial_\lambda \tilde{n} + \partial_\lambda \tilde{\Delta}) + \partial_\lambda \tilde{m}(\tilde{m} + \tilde{\delta}) + \tilde{m}(\partial_\lambda \tilde{m} + \partial_\lambda \tilde{\delta}) \right\} \right. \\ & \left. + (\tilde{n} + \tilde{\Omega})^2 + \tilde{p}(\tilde{p} + \tilde{\delta}) + \lambda \{ \dots \} \right]. \end{aligned} \quad (\text{B.48})$$

Observe that the two last terms in the second line vanish when we set  $\lambda = 0$  because  $\tilde{\delta}(\lambda = 0) = \tilde{m}(\lambda = 0) = \tilde{p}(\lambda = 0) = 0$ . The derivative at  $\lambda = 0$  is finally expressed as

$$\left. \frac{\partial}{\partial \lambda} \right|_{\lambda=0} \delta \tilde{\mathcal{E}}^{(4)} = -JN_s \left[ 2(n + \Delta)(\partial_\lambda \tilde{n}|_{\lambda=0} + \partial_\lambda \tilde{\Delta}|_{\lambda=0}) + (n + \Omega)^2 \right] \quad (\text{B.49})$$

where all quantities in the right-hand side are evaluated at  $\lambda = 0$  (thus we have removed the tildes on the factors which do not have a  $\lambda$ -derivative).

Let us compute all these quantities. From Eq. (B.15)

$$\frac{\partial}{\partial \lambda} \tilde{A}_k = 2JS \quad \text{and} \quad \frac{\partial}{\partial \lambda} \tilde{B}_k = -2JS\gamma_k(n). \quad (\text{B.50})$$

Using now the definitions in Eq. (B.17) and (B.18) we obtain

$$\partial_\lambda \tilde{u}_k = \frac{1}{4} \sqrt{\frac{2\tilde{\epsilon}_k}{\tilde{A}_k + \tilde{\epsilon}_k}} \frac{(\partial_\lambda \tilde{A}_k + \partial_\lambda \tilde{\epsilon}_k)\tilde{\epsilon}_k - \partial_\lambda \tilde{\epsilon}_k(\tilde{A}_k + \tilde{\epsilon}_k)}{\tilde{\epsilon}_k^2} \quad (\text{B.51})$$

and

$$\partial_\lambda \tilde{v}_k = -2\delta(\tilde{B}_k)\partial_\lambda \tilde{B}_k \sqrt{\frac{\tilde{A}_k - \tilde{\epsilon}_k}{2\tilde{\epsilon}_k}} - \frac{1}{4} \text{sign}(\tilde{B}_k) \sqrt{\frac{2\tilde{\epsilon}_k}{\tilde{A}_k - \tilde{\epsilon}_k}} \frac{(\partial_\lambda \tilde{A}_k - \partial_\lambda \tilde{\epsilon}_k)\tilde{\epsilon}_k - \partial_\lambda \tilde{\epsilon}_k(\tilde{A}_k - \tilde{\epsilon}_k)}{\tilde{\epsilon}_k^2}. \quad (\text{B.52})$$

The first term in this expression vanishes at  $\lambda = 0$  because  $\sqrt{(A_k - \epsilon_k)/(2\epsilon_k)}$  vanishes when  $B_k = 0$ . We then obtain

$$\begin{aligned} \partial_\lambda \tilde{n}|_{\lambda=0} + \partial_\lambda \tilde{\Delta}|_{\lambda=0} &= \frac{1}{N_s} \sum_k [2v_k \partial_\lambda \tilde{v}_k|_{\lambda=0} - \gamma_k(\partial_\lambda \tilde{u}_k|_{\lambda=0} v_k + u_k \partial_\lambda \tilde{v}_k|_{\lambda=0})] \\ &= 0. \end{aligned} \quad (\text{B.53})$$

As a consequence only the last term in Eq. (B.49) survives. It is given by

$$n + \Omega = \frac{1}{N_s} \sum_k v_k (v_k - \gamma_k(n) u_k) \quad (\text{B.54})$$

and is IR finite. Applying Eq. (B.3) we get

$$\begin{aligned} C_{i,i+n}^{(2)} &= \frac{1}{JN_s} \left. \frac{\partial}{\partial \lambda} \right|_{\lambda=0} \delta \tilde{\mathcal{E}}^{(4)} \\ &= - (n + \Omega)^2 \\ &= - \left( \frac{1}{N_s} \sum_k v_k (v_k - \gamma_k(n) u_k) \right)^2 \\ &= - \frac{1}{4} \left( C_{i,i+n}^{(1)} \right)^2 \\ &= - \frac{1}{4} \left( 1 - \frac{2}{\pi} J_1(n) \right)^2 \end{aligned} \quad (\text{B.55})$$

where  $J_1(n)$  is given in Eq. (2.63).

The final expression for the correlation function to second order in perturbation theory is thus given by

$$\langle \mathbf{S}_i \cdot \mathbf{S}_{i+n} \rangle = -S^2 \left[ 1 + \frac{1}{S} \left( 1 - \frac{2}{\pi} J_1(n) \right) + \frac{1}{4S^2} \left( 1 - \frac{2}{\pi} J_1(n) \right)^2 + \mathcal{O}(S^{-3}) \right], \quad n \text{ odd.} \quad (\text{B.56})$$

This corresponds to Eq. (2.61) obtained in standard Rayleigh-Schödinger perturbation theory with  $n$  odd.

## B.3 Even distance

We take now  $n$  even and strictly positive (the case  $n = 0$  is trivial), leading to  $\mathcal{W}(\lambda)$  with an overall minus sign,

$$\mathcal{W}(\lambda) = -\lambda J \sum_i \mathbf{S}_i \cdot \mathbf{S}_{i+n}, \quad \lambda > 0. \quad (\text{B.57})$$

### B.3.1 Hamiltonian $\mathcal{W}(\lambda)$

We write the same expansion

$$\mathcal{W}(\lambda) = \mathcal{W}^{(0)}(\lambda) + \mathcal{W}^{(2)}(\lambda) + \mathcal{W}^{(4)}(\lambda) + \mathcal{O}(S^{-1}) \quad (\text{B.58})$$

and we have

$$\mathcal{W}^{(0)}(\lambda) = -JN_s S^2 \lambda \quad (\text{B.59})$$

## Appendix B. Equal-time correlation function from the Hellmann-Feynman theorem

---

and

$$\mathcal{W}^{(2)}(\lambda) = 2JS\lambda \sum_k (1 - \gamma_k(n)) a_k^\dagger a_k. \quad (\text{B.60})$$

The first order interaction  $\mathcal{W}^{(4)}(\lambda)$  is expressed by

$$\mathcal{W}^{(4)}(\lambda) = -J\lambda \sum_{\langle\langle ij \rangle\rangle} \mathcal{O}_{ij}^{(2)} \quad (\text{B.61})$$

where  $\mathcal{O}_{ij}^{(2)}$  is given in Eq. (2.53) (first line), leading to

$$\mathcal{W}^{(4)}(\lambda) = \frac{J\lambda}{2} \sum_{\langle\langle ij \rangle\rangle} \left( a_i^\dagger a_i^\dagger a_i a_j + \text{h.c.} \right) - J\lambda \sum_{\langle\langle ij \rangle\rangle} a_i^\dagger a_j^\dagger a_i a_j \quad (\text{B.62})$$

where the notation  $\langle\langle ij \rangle\rangle$  denotes again all couples  $(i, j)$  separated by a distance  $n$ .

### B.3.2 Hamiltonian $\tilde{\mathcal{H}}(\lambda)$

The procedure is exactly the same as above. We obtain

$$\tilde{\mathcal{H}}^{(0)}(\lambda) = -JN_s S^2 (1 + \lambda), \quad (\text{B.63})$$

$$\tilde{\mathcal{H}}^{(2)}(\lambda) = \sum_k \left[ \tilde{A}_k a_k^\dagger a_k - \frac{1}{2} \tilde{B}_k \left( a_k^\dagger a_{-k}^\dagger + a_{-k} a_k \right) \right] \quad (\text{B.64})$$

with

$$\tilde{A}_k = 2JS (1 + \lambda(1 - \gamma_k(n))) \quad \text{and} \quad \tilde{B}_k = -2JS\gamma_k \quad (\text{B.65})$$

and

$$\begin{aligned} \tilde{\mathcal{H}}^{(4)}(\lambda) = & -\frac{J}{2} \sum_{\langle ij \rangle} \left( a_i^\dagger a_i a_j + \text{h.c.} \right) - J \sum_{\langle ij \rangle} a_i^\dagger a_j^\dagger a_i a_j \\ & + \frac{J\lambda}{2} \sum_{\langle\langle ij \rangle\rangle} \left( a_i^\dagger a_i^\dagger a_i a_j + \text{h.c.} \right) - J\lambda \sum_{\langle\langle ij \rangle\rangle} a_i^\dagger a_j^\dagger a_i a_j. \end{aligned} \quad (\text{B.66})$$

### B.3.3 Bogoliubov transformation

The Bogoliubov transformation is performed as above. In particular Eq. (B.17) holds with the definitions of  $\tilde{A}_k$  and  $\tilde{B}_k$  given in Eq. (B.65). One obtains the dispersion relation

$$\tilde{\epsilon}_k = \sqrt{\tilde{A}_k^2 - \tilde{B}_k^2} = 2JS \sqrt{1 - \gamma_k^2 + 2\lambda(1 - \gamma_k(n)) + \lambda^2(1 - \gamma_k(n))^2}. \quad (\text{B.67})$$



The quadratic Hamiltonian then reads

$$\tilde{\mathcal{H}}^{(2)}(\lambda) = \delta\tilde{\mathcal{E}}^{(2)} + \sum_k \tilde{\epsilon}_k \alpha_k^\dagger \alpha_k \quad (\text{B.68})$$

where

$$\delta\tilde{\mathcal{E}}^{(2)} = -JN_s S(1 + \lambda) + \frac{1}{2} \sum_k \tilde{\epsilon}_k. \quad (\text{B.69})$$

### B.3.4 First order interaction

We only need to look at the first order interaction coming from  $\mathcal{W}(\lambda)$  since we have already treated  $\mathcal{H}^{(4)}(\lambda)$  above.

Proceeding in a similar fashion as for  $n$  odd we obtain the constant term

$$\delta F^{(4)} = -J\lambda N_s \left[ (\tilde{n} - \tilde{p})^2 + \tilde{\Omega}(\tilde{\Omega} - \tilde{\delta}) \right] \quad (\text{B.70})$$

where  $\tilde{\Omega}$  and  $\tilde{p}$  are defined according to Eq. (B.29) and (B.30), respectively, but with  $i - j$  even.

Bringing the contribution of  $\mathcal{H}^{(4)}$  and the one of  $\mathcal{W}^{(4)}(\lambda)$  leads to

$$\tilde{\mathcal{H}}^{(4)}(\lambda) = \delta\tilde{\mathcal{E}}^{(4)} + (\text{2-bosons}) + (\text{4-bosons}) \quad (\text{B.71})$$

with

$$\delta\tilde{\mathcal{E}}^{(4)} = -JN_s \left[ \left\{ (\tilde{n} + \tilde{\Delta})^2 + \tilde{m}(\tilde{m} + \tilde{\Delta}) \right\} + \lambda \left\{ (\tilde{n} - \tilde{p})^2 + \tilde{\Omega}(\tilde{\Omega} - \tilde{\delta}) \right\} \right]. \quad (\text{B.72})$$

The ground state energy of  $\tilde{\mathcal{H}}(\lambda)$  is thus given by

$$\tilde{E}_0(\lambda) = \tilde{\mathcal{H}}^{(0)} + \delta\tilde{\mathcal{E}}^{(2)} + \delta\tilde{\mathcal{E}}^{(4)} + \mathcal{O}(S^{-1}) \quad (\text{B.73})$$

and one is ready to use Eq. (B.3) to derive the correlation function  $\langle \mathbf{S}_i \cdot \mathbf{S}_{i+n} \rangle$  at even distance  $n$ .

### B.3.5 Analysis at first order

Observe that

$$\frac{\partial \tilde{\epsilon}_k}{\partial \lambda} = 2JS \frac{1 - \gamma_k(n) + \lambda(1 - \gamma_k(n))^2}{\tilde{\epsilon}_k(\lambda)/(2JS)}. \quad (\text{B.74})$$

## Appendix B. Equal-time correlation function from the Hellmann-Feynman theorem

The equal-time correlation function up to first order is thus given by

$$\begin{aligned}
-\frac{1}{JN_s} \left. \frac{\partial \tilde{E}_0(\lambda)}{\partial \lambda} \right|_{\lambda=0} &= S^2 + S - \frac{S}{N_s} \sum_k \frac{1 - \gamma_k(n)}{\sqrt{1 - \gamma_k^2}} + \mathcal{O}(S^0) \\
&= S^2 + S - \frac{S}{2\pi} \int_{-\pi}^{\pi} dk \frac{1 - \gamma_k(n)}{\sqrt{1 - \gamma_k^2}} + \mathcal{O}(S^0) \\
&= S^2 + S - \frac{S}{2\pi} \int_{-\pi}^{\pi} dk \frac{1 - \cos(kn)}{|\sin(k)|} + \mathcal{O}(S^0) \\
&= S^2 + S - \frac{S}{\pi} \int_0^{\pi} dk \frac{1 - \cos(kn)}{\sin(k)} + \mathcal{O}(S^0) \\
&= S^2 + S - \frac{2S}{\pi} \int_0^{\pi/2} dk \frac{1 - \cos(kn)}{\sin(k)} + \mathcal{O}(S^0) \\
&= S^2 + S - \frac{2S}{\pi} J_0(n) + \mathcal{O}(S^0) \\
&= S^2 \left[ 1 + \frac{1}{S} \left( 1 - \frac{2}{\pi} J_0(n) \right) + \mathcal{O}(S^{-2}) \right] \\
&= \langle \mathbf{S}_i \cdot \mathbf{S}_{i+n} \rangle \text{ at first order, } n \text{ even}
\end{aligned} \tag{B.75}$$

where the integral  $J_0(n)$  is defined in Eq. (2.62).

### B.3.6 Analysis at second order

The derivative of  $\delta \tilde{\mathcal{E}}^{(4)}$  is given by

$$\begin{aligned}
\frac{\partial}{\partial \lambda} \delta \tilde{\mathcal{E}}^{(4)} &= -JN_s \left[ \left\{ 2(\tilde{n} + \tilde{\Delta})(\partial_\lambda \tilde{n} + \partial_\lambda \tilde{\Delta}) + \partial_\lambda \tilde{m}(\tilde{m} + \tilde{\delta}) + \tilde{m}(\partial_\lambda \tilde{m} + \partial_\lambda \tilde{\delta}) \right\} \right. \\
&\quad \left. + (\tilde{n} - \tilde{p})^2 + \tilde{\Omega}(\tilde{\Omega} - \tilde{\delta}) + \lambda \{ \dots \} \right].
\end{aligned} \tag{B.76}$$

The first part which is in the curly bracket  $\{ \}$  is exactly the same as in the case of odd distance, Eq. (B.48). It vanishes when we set  $\lambda$  to zero. The next to last term,  $\tilde{\Omega}(\tilde{\Omega} - \tilde{\delta}) = 0$  because  $\tilde{\Omega}(\lambda = 0) = \tilde{\delta}(\lambda = 0) = 0$ . Thus after setting  $\lambda$  to 0 we are left with

$$\left. \frac{\partial}{\partial \lambda} \right|_{\lambda=0} \delta \tilde{\mathcal{E}}^{(4)} = -JN_s (n - p)^2 \tag{B.77}$$

where we have remove the tildes. We have

$$n - p = \frac{1}{N_s} \sum_k v_k^2 (1 - \gamma_k(n)) \tag{B.78}$$

which is IR finite. Applying Equ. (B.3) gives

$$\begin{aligned}
 -\frac{1}{JN_s} \frac{\partial}{\partial \lambda} \Big|_{\lambda=0} \delta \tilde{\mathcal{E}}^{(4)} &= (n-p)^2 \\
 &= \left( \frac{1}{N_s} \sum_k v_k^2 (1 - \gamma_k(n)) \right)^2 \\
 &= \frac{1}{4} \left( C_{i,i+n}^{(1)} \right)^2 \\
 &= \frac{1}{4} \left( 1 - \frac{2}{\pi} J_0(n) \right)^2.
 \end{aligned} \tag{B.79}$$

Dealing with the peculiar case of  $n = 0$  we obtain the final expression of the equal-time spin-spin correlation function at even distance

$$\langle \mathbf{S}_i \cdot \mathbf{S}_{i+n} \rangle = S^2 \left[ 1 + \frac{1}{S} \left( 1 - \frac{2}{\pi} J_0(n) \right) + \frac{1}{4S^2} \left( 1 - \frac{2}{\pi} J_0(n) - \delta_{n,0} \right)^2 + \mathcal{O}(S^{-3}) \right]. \tag{B.80}$$

This equation corresponds again to Eq. (2.61) obtained in standard Rayleigh-Schrödinger perturbation theory for  $n$  even.

## B.4 Summary

Bringing together Eq. (B.56) and (B.80) we obtain a generic expression for the equal-time spin-spin correlation function of the Heisenberg chain to second order in perturbation theory

$$\langle \mathbf{S}_i \cdot \mathbf{S}_{i+n} \rangle = (-1)^n S^2 \left[ 1 + \frac{1}{S} \left( 1 - \frac{2}{\pi} J_\alpha(n) \right) + \frac{1}{4S^2} \left( 1 - \frac{2}{\pi} J_\alpha(n) - \delta_{n,0} \right)^2 + \mathcal{O}(S^{-3}) \right] \tag{B.81}$$

where  $\alpha = n \pmod{2}$  and the integrals  $J_0(n)$  and  $J_1(n)$  are defined in Eq. (2.62) and (2.63), respectively. This shows the equivalence of both approaches to extract the equal-time two-point function of spin operators, the direct perturbative expansion of  $\langle \mathbf{S}_i \cdot \mathbf{S}_j \rangle$  in powers of  $1/S$  using standard Rayleigh-Schrödinger perturbation theory and the derivation of the correlation function from the ground state energy of a modified Hamiltonian using the Hellmann-Feynman theorem.



# C Asymptotic form of the integrals $J_0(n)$ and $J_1(n)$

In this appendix we show that the long distance behavior of the integrals  $J_0(n)$  and  $J_1(n)$  defined in Eq. (2.62) and (2.63), respectively, and which we rewrite here

$$\begin{aligned} J_0(n) &= \int_0^{\pi/2} dk \frac{1 - \cos(kn)}{\sin k} & n \text{ even,} \\ J_1(n) &= \int_0^{\pi/2} dk \left[ \frac{1}{\sin k} - \frac{\cos(kn)}{\tan k} \right] & n \text{ odd} \end{aligned}$$

is given by

$$J_0(n) = \ln 2 + \gamma + \ln |n| + \mathcal{O}(n^{-4}) \quad n \text{ even,} \quad (\text{C.1})$$

$$J_1(n) = \ln 2 + \gamma + \ln |n| - \frac{1}{2n^2} + \mathcal{O}(n^{-4}) \quad n \text{ odd} \quad (\text{C.2})$$

where  $\gamma \simeq 0.577$  is the Euler-Mascheroni constant. Equation (C.1) has been shown in great details in Ref. [55]. Here we focus on Eq. (C.2), but the procedure is exactly similar. Before proceeding to the proof of Eq. (C.2) we derive a useful result.

**Proposition:** Taking  $n$  even the integral

$$\mathcal{I}_n = \int_0^{\pi/2} dk \cos(nk) \left( \frac{1}{\sin k} - \frac{1}{k} \right) \quad (\text{C.3})$$

satisfies

$$\mathcal{I}_n = \frac{4(-1)^{n/2}}{\pi^2 n^2} + \mathcal{O}(n^{-4}). \quad (\text{C.4})$$

**Proof:** The proof of this result is given in Ref. [55]. We follow the same steps. First we write

$$f(k) = \frac{1}{\sin k} - \frac{1}{k} = \frac{1}{k} \left( \frac{1}{\text{sinc } k} - 1 \right) \quad (\text{C.5})$$

### Appendix C. Asymptotic form of the integrals $J_0(n)$ and $J_1(n)$

---

and write its Taylor expansion as

$$\frac{1}{\text{sinc } k} = \sum_{p=0}^{\infty} k^{2p} \left[ \sum_{m=0}^{\infty} \frac{(-1)^m}{(2m+3)!} k^{2m} \right]^p \quad (\text{C.6})$$

which is valid since  $k \in [0, \pi/2]$ . One has then

$$f(k) = \sum_{m=0}^{\infty} a_m k^{2m+1} \quad \text{for } k \in [0, \pi/2] \quad (\text{C.7})$$

where the coefficients are expressed in terms of the first Bernoulli numbers  $B_{2l}$  as

$$a_m = \frac{2(-1)^m (2^{2m+1} - 1) B_{2(m+1)}}{(2m+2)!}. \quad (\text{C.8})$$

The integral  $\mathcal{I}_n$  is thus given by

$$\mathcal{I}_n = \sum_{m=0}^{\infty} a_m \mathcal{J}_m(n) \quad (\text{C.9})$$

where

$$\mathcal{J}_m(n) = \int_0^{\pi/2} dk k^{2m+1} \cos(nk). \quad (\text{C.10})$$

These integrals can be expressed in terms of the generalized hypergeometric function  ${}_pF_q(\mathbf{a}; \mathbf{b}; z)$  as

$$\mathcal{J}_m(n) = \frac{1}{2} \left( \frac{\pi}{2} \right)^{2m+2} \frac{1}{m+1} {}_1F_2 \left( \mathbf{a}; \mathbf{b}; -\frac{n^2 \pi^2}{16} \right) \quad (\text{C.11})$$

with

$$\mathbf{a} = m+1 \quad \text{and} \quad \mathbf{b} = \left( \frac{1}{2}, m+2 \right). \quad (\text{C.12})$$

The integral  $\mathcal{J}_0$  for  $n$  integer is given by

$$\mathcal{J}_0(n) = \begin{cases} \frac{(-1)^{n/2} - 1}{n^2} & \text{for } n \text{ even,} \\ -\frac{1}{n^2} + \frac{(-1)^{(n-1)/2} \pi}{2n} & \text{for } n \text{ odd.} \end{cases} \quad (\text{C.13})$$

Using Eq. (C.13) and integration by parts it can be easily proved by recurrence that [55]

$$|\mathcal{J}_m(n)| = \mathcal{O} \left( \frac{1}{n^2} \right) \quad \text{for } n \text{ even.} \quad (\text{C.14})$$

The proof actually follows from the important relation

$$\mathcal{J}_m(n) = (-1)^{n/2} \frac{2m+1}{n^2} \left( \frac{\pi}{2} \right)^{2m} - \frac{2m(2m+1)}{n^2} \mathcal{J}_{m-1}(n), \quad m > 0. \quad (\text{C.15})$$

To compute the  $\mathcal{O}(n^{-2})$  term in  $\mathcal{I}_n$  we make use of Eq. (C.15) and of the form of the

---

derivative of  $f$

$$\frac{df(k)}{dk} = \frac{1}{k^2} - \cot k \csc k = \sum_{m=0}^{\infty} a_m (2m+1) k^{2m} \quad (\text{C.16})$$

leading to

$$\begin{aligned} \frac{(-1)^{n/2}}{n^2} \frac{df(\pi/2)}{dk} &= \frac{4(-1)^{n/2}}{\pi^2 n^2} = \sum_{m=0}^{\infty} a_m (-1)^{n/2} \frac{2m+1}{n^2} \left(\frac{\pi}{2}\right)^{2m} \\ &= \sum_{m=0}^{\infty} a_m \mathcal{J}_m(n) + \mathcal{O}(n^{-4}). \end{aligned} \quad (\text{C.17})$$

This proves Eq. (C.4).

□

Now we proceed to the proof of Eq. (C.2). Without loss of generality we take  $n$  positive. We begin by rewriting the integrand in  $J_1(n)$  as

$$\begin{aligned} g(k) &= \frac{1}{\sin k} - \frac{\cos(nk)}{\tan k} \\ &= \frac{1}{\sin k} - \frac{1}{k} \\ &\quad - \cos k \cos(nk) \left( \frac{1}{\sin k} - \frac{1}{k} \right) \\ &\quad - \frac{\cos k \cos(nk) - 1}{k}. \end{aligned} \quad (\text{C.18})$$

The integral  $J_1(n)$  thus decomposes into three parts

$$J_1(n) = \int_0^{\pi/2} dk g(k) = I_1 - I_2 + I_3. \quad (\text{C.19})$$

The integrals  $I_1$  and  $I_3$  are easily computed

$$I_1 = \int_0^{\pi/2} dk \left( \frac{1}{\sin k} - \frac{1}{k} \right) = \ln \left( \frac{4}{\pi} \right) \quad (\text{C.20})$$

and

$$\begin{aligned}
 I_3 &= - \int_0^{\pi/2} dk \frac{\cos k \cos(nk) - 1}{k} \\
 &= - \frac{1}{2} \left( \int_0^{\pi/2} dk \frac{\cos(k(n-1)) - 1}{k} + \int_0^{\pi/2} dk \frac{\cos(k(n+1)) - 1}{k} \right) \\
 &= - \frac{1}{2} \left( \int_0^{(n-1)\pi/2} dt \frac{\cos t - 1}{t} + \int_0^{(n+1)\pi/2} dt \frac{\cos t - 1}{t} \right) \\
 &= - \frac{1}{2} (-2\gamma - \ln((n-1)\pi/2) - \ln((n+1)\pi/2) + \text{Ci}((n-1)\pi/2) + \text{Ci}((n+1)\pi/2)) \\
 &= \gamma + \ln(\pi/2) + \frac{1}{2} (\ln(n-1) + \ln(n+1) - \text{Ci}((n-1)\pi/2) - \text{Ci}((n+1)\pi/2)) \\
 &= \gamma + \ln(\pi/2) + \ln(\sqrt{n^2-1}) - \frac{1}{2} (\text{Ci}((n-1)\pi/2) + \text{Ci}((n+1)\pi/2)) \\
 &= \gamma + \ln(\pi/2) + \ln(\sqrt{n^2-1}) + \frac{2(-1)^{(n-1)/2}}{\pi^2} \left( \frac{1}{(n-1)^2} - \frac{1}{(n+1)^2} \right) + \mathcal{O}(n^{-4})
 \end{aligned} \tag{C.21}$$

where Ci is the Cosine integral which satisfies

$$\int_0^x dt \frac{\cos t - 1}{t} = \text{Ci}(x) - \gamma - \ln(x). \tag{C.22}$$

In the last line of Eq. (C.21) we used the asymptotic behavior of this function given by

$$\text{Ci}(m\pi) \sim \frac{\sin(m\pi)}{m\pi} - \frac{\cos(m\pi)}{m^2\pi^2} + \mathcal{O}(m^{-4}) = \frac{(-1)^{m+1}}{m^2\pi^2} + \mathcal{O}(m^{-4}), \quad m \in \mathbb{Z} \tag{C.23}$$

and the fact that since  $n$  is odd,  $n \pm 1$  is even.

The second integral  $I_2$  is expressed as

$$\begin{aligned}
 I_2 &= \int_0^{\pi/2} dk \cos k \cos(nk) \left( \frac{1}{\sin k} - \frac{1}{k} \right) \\
 &= \frac{1}{2} \left( \int_0^{\pi/2} dk \cos((n-1)k) \left( \frac{1}{\sin(k)} - \frac{1}{k} \right) + \int_0^{\pi/2} dk \cos((n+1)k) \left( \frac{1}{\sin(k)} - \frac{1}{k} \right) \right) \\
 &= \frac{1}{2} (\mathcal{I}_{n-1} + \mathcal{I}_{n+1}).
 \end{aligned} \tag{C.24}$$

where  $\mathcal{I}_{n-1}$  and  $\mathcal{I}_{n+1}$  are defined in Eq. (C.3) ( $n \pm 1$  are even). Using Eq. (C.4) we obtain

$$I_2 = \frac{2(-1)^{(n-1)/2}}{\pi^2} \left( \frac{1}{(n-1)^2} - \frac{1}{(n+1)^2} \right) + \mathcal{O}(n^{-4}). \tag{C.25}$$

Expanding the logarithm in Eq. (C.21) as

$$\ln(\sqrt{n^2-1}) = \ln n + \ln(\sqrt{1-n^{-2}}) = \ln n - \frac{1}{2n^2} + \mathcal{O}(n^{-4}) \tag{C.26}$$



---

we finally obtain

$$J_1(n) = \ln 2 + \gamma + \ln n - \frac{1}{2n^2} + \mathcal{O}(n^{-4}). \quad (\text{C.27})$$

□

To show Eq. (C.1) we proceed similarly. We rewrite the integrand of  $J_0(n)$  as

$$\begin{aligned} g(k) &= \frac{1 - \cos(nk)}{\sin k} \\ &= \frac{1}{\sin k} - \frac{1}{k} \\ &\quad - \cos(nk) \left( \frac{1}{\sin k} - \frac{1}{k} \right) \\ &\quad - \frac{\cos(nk) - 1}{k} \end{aligned} \quad (\text{C.28})$$

and define the three following integrals

$$I_1 = \int_0^{\pi/2} dk \left( \frac{1}{\sin k} - \frac{1}{k} \right) = \ln \left( \frac{4}{\pi} \right), \quad (\text{C.29})$$

$$I_3 = \int_0^{\pi/2} dk \frac{\cos(nk) - 1}{k} = \text{Ci}(n\pi/2) - \gamma - \ln(n\pi/2) \quad (\text{C.30})$$

and

$$I_2 = \int_0^{\pi/2} dk \cos(nk) \left( \frac{1}{\sin k} - \frac{1}{k} \right) \quad (\text{C.31})$$

such that

$$J_0(n) = I_1 - I_2 - I_3. \quad (\text{C.32})$$

We note that  $I_2 \equiv \mathcal{I}_n$  given in Eq. (C.3). Using Eq. (C.4) and the asymptotic behavior of the Cosine integral in Eq. (C.23) one obtains the desired result.

□



# D Calculations at finite temperature

In this appendix we provide details on the calculation of the dynamical structure factor, of the equal-time structure factor and of the equal-time correlation function of the Heisenberg chain to second order in perturbation theory at inverse temperature  $\beta$ . The calculation relies on the imaginary-time (or imaginary frequency) Green's functions of HP bosons. We shall first derive these Green's functions and then turn to the dynamical structure factor. The material contained in this appendix has been reported in Ref. [55], although with significantly less details.

## D.1 Free Bogoliubov Green's function

We begin by computing the free Green's function of Bogoliubov bosons defined as

$$\mathcal{G}^0(k, \tau) = -\langle T_\tau \alpha_k(\tau) \alpha_k^\dagger(0) \rangle_0 = -\text{Tr} \left( \rho_0 T_\tau \alpha_k(\tau) \alpha_k^\dagger(0) \right) \quad (\text{D.1})$$

where  $\rho_0$  is the free density matrix defined as

$$\rho_0 = \frac{1}{Z_0} e^{-\beta \mathcal{H}^{(2)}} \quad (\text{D.2})$$

with  $Z_0 = \text{Tr} \left( e^{-\beta \mathcal{H}^{(2)}} \right)$ . The Green's function in Eq. (D.1) is easily computed

$$\mathcal{G}^0(k, \tau) = -\frac{e^{-\epsilon_k \tau}}{e^{\beta \epsilon_k} - 1} \left( e^{\beta \epsilon_k} \theta(\tau) + \theta(-\tau) \right). \quad (\text{D.3})$$

Introducing the bosonic Matsubara frequencies  $\omega_n = 2n\pi/\beta$  the Matsubara Green's function is given by

$$\mathcal{G}^0(k, i\omega_n) = \frac{1}{i\omega_n - \epsilon_k} \quad (\text{D.4})$$

which is indeed the generic form of a free bosonic propagator at finite temperature.

## D.2 Free HP Green's functions

With Eq. (D.3) one can now extract the free Green's functions of HP operators

$$\mathbb{G}^0(k, \tau) = -\text{Tr} \left( \rho_0 T_\tau \begin{pmatrix} a_k(\tau) \\ a_{-k}^\dagger(\tau) \end{pmatrix} \begin{pmatrix} a_k^\dagger(0) & a_{-k}(0) \end{pmatrix} \right) \quad (\text{D.5})$$

using the inverse Bogoliubov transformation

$$a_k = u_k \alpha_k - v_k \alpha_{-k}^\dagger, \quad a_{-k}^\dagger = u_k \alpha_{-k}^\dagger - v_k \alpha_k. \quad (\text{D.6})$$

For instance the first diagonal Green's function reads

$$\begin{aligned} \mathbb{G}_{11}^0(k, \tau) &= -\langle T_\tau a_k(\tau) a_k^\dagger(0) \rangle_0 \\ &= -\langle T_\tau (u_k \alpha_k(\tau) - v_k \alpha_{-k}^\dagger(\tau)) (u_k \alpha_k^\dagger(0) - v_k \alpha_{-k}(0)) \rangle_0 \\ &= -u_k^2 \langle T_\tau \alpha_k(\tau) \alpha_k^\dagger(0) \rangle_0 - v_k^2 \langle T_\tau \alpha_{-k}^\dagger(\tau) \alpha_{-k}(0) \rangle_0 \\ &= u_k^2 \mathcal{G}^0(k, \tau) + v_k^2 \mathcal{G}^0(-k, -\tau). \end{aligned} \quad (\text{D.7})$$

Moreover,  $\mathbb{G}_{22}^0(k, \tau) = \mathbb{G}_{11}^0(k, -\tau)$  and  $\mathbb{G}_{12}^0(k, \tau) = \mathbb{G}_{21}^0(k, \tau)$  are obtained in a similar fashion

$$\mathbb{G}_{12}^0(k, \tau) = -\langle T_\tau a_k(\tau) a_{-k}(0) \rangle_0 = -u_k v_k \left( \mathcal{G}^0(k, \tau) + \mathcal{G}^0(k, -\tau) \right). \quad (\text{D.8})$$

The frequency Green's functions are then

$$\mathbb{G}^0(k, i\omega_n) = \frac{1}{(i\omega_n)^2 - \epsilon_k^2} \begin{pmatrix} A_k + i\omega_n & B_k \\ B_k & A_k - i\omega_n \end{pmatrix}. \quad (\text{D.9})$$

## D.3 Perturbative expansion for the HP Green's functions

We illustrate the calculation of the Green's functions of HP bosons in SWT with the case of the diagonal  $\mathbb{G}_{11}$ . We have

$$\begin{aligned} \mathbb{G}_{11}(k, \tau) &= -\langle T_\tau a_k(\tau) a_k^\dagger(0) \rangle \\ &= -\text{Tr} \left( \rho T_\tau a_k(\tau) a_k^\dagger(0) \right) \\ &= -\text{Tr} \left( \rho_0 T_\tau a_k(\tau) a_k^\dagger(0) \exp \left( -\int_0^\beta d\tau_1 \mathcal{V}(\tau_1) \right) \right) \\ &= \mathbb{G}_{11}^0(k, \tau) + \int_0^\beta d\tau_1 \langle T_\tau a_k(\tau) a_k^\dagger(0) \mathcal{V}(\tau_1) \rangle_0 + \dots \end{aligned} \quad (\text{D.10})$$

Approximating  $\mathcal{V} \simeq \mathcal{H}^{(4)}$  given in Eq. (2.35) and using Wick's theorem one ends up with an expansion of the Green's function with a first order correction. The truly important

point is that we then use Dyson's equation to define the interacting Green's function in a compact way

$$[\mathbb{G}(k, i\omega_n)]^{-1} = [\mathbb{G}^0(k, i\omega_n)]^{-1} - \Sigma(k, i\omega_n) \quad (\text{D.11})$$

where  $\Sigma(k, i\omega_n)$  is the self-energy and is extracted from the expansion of the Green's function using  $\mathcal{H}^{(4)}$  as the interaction. In particular, to this order the self-energy is independent of the frequency and is given by

$$\Sigma(k) = -\frac{2J\kappa_\beta}{S} \begin{pmatrix} 1 & \gamma_k \\ \gamma_k & 1 \end{pmatrix}. \quad (\text{D.12})$$

This leads to the Green's function given in Eq. (2.76).

## D.4 Longitudinal structure factor

The longitudinal part of the dynamical structure factor will exhibit a two-magnon continuum, as can be seen from the HP transformation. Keeping only these two-magnon terms one has

$$\tilde{S}_k^z(\tau) \tilde{S}_{-k}^z(0) \rightarrow \frac{1}{N_s} \sum_{p,q} a_{q-k}^\dagger(\tau) a_q(\tau) a_{k+p}^\dagger(0) a_p(0). \quad (\text{D.13})$$

It is indeed convenient to perform all calculations with the rotated spin operators and to shift momentum by  $\pi$  at the very end.

Taking the expectation value of this term and using Wick's theorem we have

$$\begin{aligned} \langle T_\tau a_{q-k}^\dagger(\tau) a_q(\tau) a_{k+p}^\dagger(0) a_p(0) \rangle &= \langle T_\tau a_{q-k}^\dagger(\tau) a_{k+p}^\dagger(0) \rangle \langle T_\tau a_q(\tau) a_p(0) \rangle \\ &+ \langle T_\tau a_{q-k}^\dagger(\tau) a_p(0) \rangle \langle T_\tau a_q(\tau) a_{k+p}^\dagger(0) \rangle \\ &+ \dots \end{aligned} \quad (\text{D.14})$$

where ... denotes terms where operators are contracted at equal time and thus simply give constant contributions. We can rewrite this using our definitions of the thermal Green's functions,

$$\begin{aligned} \langle T_\tau a_{q-k}^\dagger(\tau) a_q(\tau) a_{k+p}^\dagger(0) a_p(0) \rangle &= \delta_{q-k, -(k+p)} \delta_{q, -p} \mathbb{G}_{21}(q-k, \tau) \mathbb{G}_{12}(q, \tau) \\ &+ \delta_{q-k, p} \delta_{-q, k+p} \mathbb{G}_{22}(q-k, \tau) \mathbb{G}_{11}(q, \tau) \\ &+ \dots \end{aligned} \quad (\text{D.15})$$

Observe that formally we should have used  $\mathbb{G}_{jl}^0$  in this expression since we only need to compute this expectation value in the free theory. However in doing so we would ignore the correction to the dispersion relation. Using the interacting Green's functions  $\mathbb{G}_{jl}$  is thus necessary to incorporate consistently the first order corrections to the energy. We

## Appendix D. Calculations at finite temperature

---

thus obtain

$$F_{2\text{-magnon}}^{zz}(k, i\omega_n) = - \int_0^\beta d\tau e^{i\omega_n \tau} \frac{1}{N_s} \sum_q [\mathbb{G}_{12}(q-k, \tau) \mathbb{G}_{12}(q, \tau) + \mathbb{G}_{22}(q-k, \tau) \mathbb{G}_{11}(q, \tau)]. \quad (\text{D.16})$$

Performing the  $\tau$ -integral this becomes

$$F_{2\text{-magnon}}^{zz}(k, i\omega_n) = - \frac{1}{N_s} \sum_q \frac{1}{\beta} \sum_m [\mathbb{G}_{12}(q-k, i\omega_n - i\omega_m) \mathbb{G}_{12}(q, i\omega_m) + \mathbb{G}_{22}(q-k, i\omega_n - i\omega_m) \mathbb{G}_{11}(q, i\omega_m)]. \quad (\text{D.17})$$

Now we begin with the computationally intensive parts. We rewrite  $F_{2\text{-magnon}}^{zz}(k, i\omega_n)$  as

$$-F_{2\text{-magnon}}^{zz}(k, i\omega_n) = X_1(k, i\omega_n) + X_2(k, i\omega_n) \quad (\text{D.18})$$

where

$$X_1(k, i\omega_n) = \frac{1}{N_s} \sum_q \frac{1}{\beta} \sum_m \mathbb{G}_{12}(q-k, i\omega_n - i\omega_m) \mathbb{G}_{12}(q, i\omega_m) \quad (\text{D.19})$$

and

$$X_2(k, i\omega_n) = \frac{1}{N_s} \sum_q \frac{1}{\beta} \sum_m \mathbb{G}_{22}(q-k, i\omega_n - i\omega_m) \mathbb{G}_{11}(q, i\omega_m). \quad (\text{D.20})$$

Inserting the expressions of the Green's functions given in Eq. (2.76) one obtains

$$X_1(k, i\omega_n) = \frac{1}{N_s} \sum_q p_\beta^2 B_{q-k} B_q S_1(k, q, i\omega_n) \quad (\text{D.21})$$

and

$$\begin{aligned} X_2(k, i\omega_n) &= \frac{1}{N_s} \sum_q p_\beta A_q (p_\beta A_{q-k} - i\omega_n) S_1(k, q, i\omega_n) \\ &+ \frac{1}{N_s} \sum_q (p_\beta (A_q + A_{q-k}) - i\omega_n) S_2(k, q, i\omega_n) \\ &+ \frac{1}{N_s} \sum_q S_3(k, q, i\omega_n) \end{aligned} \quad (\text{D.22})$$

where we defined

$$p_\beta = 1 + \frac{|\kappa_\beta|}{S} \quad (\text{D.23})$$

and where the Matsubara sums  $S_l(k, q, i\omega_n)$ ,  $l = 1, 2, 3$  are given by

$$S_1(k, q, i\omega_n) = \frac{1}{\beta} \sum_m \frac{1}{(i\omega_m)^2 - \xi_q^2} \frac{1}{(i\omega_m - i\omega_n)^2 - \xi_{k-q}^2}, \quad (\text{D.24})$$

$$S_2(k, q, i\omega_n) = \frac{1}{\beta} \sum_m \frac{i\omega_m}{(i\omega_m)^2 - \xi_q^2} \frac{1}{(i\omega_m - i\omega_n)^2 - \xi_{k-q}^2}, \quad (\text{D.25})$$

$$S_3(k, q, i\omega_n) = \frac{1}{\beta} \sum_m \frac{(i\omega_m)^2}{(i\omega_m)^2 - \xi_q^2} \frac{1}{(i\omega_m - i\omega_n)^2 - \xi_{k-q}^2}. \quad (\text{D.26})$$

Let us now explicitly compute the Matsubara sum  $S_1(k, q, i\omega_n)$  to illustrate the procedure. First we rewrite it as

$$S_1(k, q, i\omega_n) = \frac{1}{\beta} \sum_m \frac{1}{(i\omega_m - \xi_q)(i\omega_m + \xi_q)} \frac{1}{(i(\omega_m - \omega_n) - \xi_{k-q})(i(\omega_m - \omega_n) + \xi_{k-q})}. \quad (\text{D.27})$$

Defining

$$f_1(z) = \frac{1}{(z - \xi_q)(z + \xi_q)(z - i\omega_n - \xi_{k-q})(z - i\omega_n + \xi_{k-q})} \quad (\text{D.28})$$

we have

$$S_1(k, q, i\omega_n) = \frac{1}{\beta} \sum_m f_1(i\omega_m). \quad (\text{D.29})$$

The function  $f_1(z)$  has simple poles at

$$z_A = \xi_q, \quad z_B = -\xi_q, \quad z_C = i\omega_n + \xi_{k-q}, \quad z_D = i\omega_n - \xi_{k-q}. \quad (\text{D.30})$$

We also define the Bose-Einstein distribution

$$n_B(z) = \frac{1}{e^{\beta z} - 1} \quad (\text{D.31})$$

which has poles along the imaginary axis at  $z = i\omega_m = i2\pi m/\beta, m \in \mathbb{Z}$ .

In order to compute the Matsubara sum  $S_1$  we use Cauchy's theorem. Choosing the contour  $\mathcal{C}$  depicted in Fig. D.1 we obtain

$$\oint_{\mathcal{C}} \frac{dz}{2\pi i} f_1(z) n_B(z) = 0 \quad (\text{D.32})$$

leading to

$$\sum_m \text{Res}(f_1 \cdot n_B, i\omega_m) = - \sum_{j=A,B,C,D} \text{Res}(f_1 \cdot n_B, z_j). \quad (\text{D.33})$$

The residue at  $i\omega_m$  can be computed easily and are simply given by

$$\text{Res}(f_1 \cdot n_B, i\omega_m) = \frac{1}{\beta} f_1(i\omega_m). \quad (\text{D.34})$$

Thus

$$S_1(k, q, i\omega_n) = - \sum_{j=A,B,C,D} \text{Res}(f_1 \cdot n_B, z_j). \quad (\text{D.35})$$

## Appendix D. Calculations at finite temperature

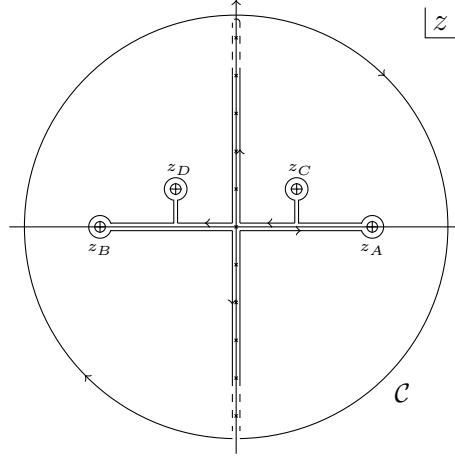


Figure D.1: Integration contour for the calculation of the Matsubara sum  $S_1(k, q, i\omega_n)$ . The poles along the imaginary axis are located at  $z = i\omega_m$  where  $\omega_m$  are the bosonic Matsubara frequencies.

The residues at the poles of  $f_1$  are also easily obtained:

$$\text{Res}(f_1 \cdot n_B, \xi_q) = \frac{n_B(\xi_q)}{2\xi_q(i\omega_n - \xi_q - \xi_{k-q})(i\omega_n - \xi_q + \xi_{k-q})}, \quad (\text{D.36})$$

$$\text{Res}(f_1 \cdot n_B, -\xi_q) = \frac{-n_B(-\xi_q)}{2\xi_q(i\omega_n + \xi_q - \xi_{k-q})(i\omega_n + \xi_q + \xi_{k-q})}, \quad (\text{D.37})$$

$$\text{Res}(f_1 \cdot n_B, i\omega_n + \xi_{k-q}) = \frac{n_B(\xi_{k-q})}{2\xi_{k-q}(i\omega_n - \xi_q + \xi_{k-q})(i\omega_n + \xi_q + \xi_{k-q})}, \quad (\text{D.38})$$

$$\text{Res}(f_1 \cdot n_B, i\omega_n - \xi_{k-q}) = \frac{-n_B(-\xi_{k-q})}{2\xi_{k-q}(i\omega_n - \xi_q - \xi_{k-q})(i\omega_n + \xi_q - \xi_{k-q})}. \quad (\text{D.39})$$

One can now use the following identity satisfied by the Bose-Einstein distribution

$$n_B(-z) = -e^{\beta z} n_B(z) \quad (\text{D.40})$$

which leads to

$$n_B(z) + n_B(-z) = -1, \quad n_B(z) - n_B(-z) = \coth\left(\frac{\beta z}{2}\right) \quad (\text{D.41})$$

to rewrite the residues as

$$\text{Res}(f_1 \cdot n_B, \xi_q) + \text{Res}(f_1 \cdot n_B, -\xi_q) = \frac{\coth\left(\frac{\beta \xi_q}{2}\right) \left((i\omega_n)^2 + \xi_q^2 - \xi_{k-q}^2\right) - 2i\omega_n \xi_q}{2\xi_q \left[(i\omega_n)^2 - (E_{k,q}^+)^2\right] \left[(i\omega_n)^2 - (E_{k,q}^-)^2\right]} \quad (\text{D.42})$$



and

$$\begin{aligned} \text{Res}(f_1 \cdot n_B, i\omega_n + \xi_{k-q}) + \text{Res}(f_1 \cdot n_B, i\omega_n - \xi_{k-q}) = \\ \frac{\coth\left(\frac{\beta\xi_{k-q}}{2}\right) \left((i\omega_n)^2 - \xi_q^2 + \xi_{k-q}^2\right) + 2i\omega_n \xi_{k-q}}{2\xi_{k-q} \left[(i\omega_n)^2 - (E_{k,q}^+)^2\right] \left[(i\omega_n)^2 - (E_{k,q}^-)^2\right]} \end{aligned} \quad (\text{D.43})$$

where

$$E_{k,q}^+ = \xi_q + \xi_{k-q}, \quad E_{k,q}^- = \xi_q - \xi_{k-q}. \quad (\text{D.44})$$

Finally,

$$S_1(k, q, i\omega_n) = \frac{s_1(k, q, i\omega_n)}{\left[(i\omega_n)^2 - (E_{k,q}^+)^2\right] \left[(i\omega_n)^2 - (E_{k,q}^-)^2\right]} \quad (\text{D.45})$$

with

$$s_1(k, q, i\omega_n) = -\frac{\left((i\omega_n)^2 + \xi_q^2 - \xi_{k-q}^2\right) \coth\left(\frac{\beta\xi_q}{2}\right)}{2\xi_q} - \frac{\left((i\omega_n)^2 - \xi_q^2 + \xi_{k-q}^2\right) \coth\left(\frac{\beta\xi_{k-q}}{2}\right)}{2\xi_{k-q}}. \quad (\text{D.46})$$

The Matsubara sums  $S_2(k, q, i\omega_n)$  and  $S_3(k, q, i\omega_n)$  are obtained in the exact same way, using  $f_2(z) = z f_1(z)$  and  $f_3(z) = z^2 f_1(z)$ , respectively. One gets

$$S_l(k, q, i\omega_n) = \frac{s_l(k, q, i\omega_n)}{\left[(i\omega_n)^2 - (E_{k,q}^+)^2\right] \left[(i\omega_n)^2 - (E_{k,q}^-)^2\right]}, \quad l = 2, 3 \quad (\text{D.47})$$

with

$$s_2(k, q, i\omega_n) = -\frac{i\omega_n}{2\xi_{k-q}} \left[ 2\xi_q \xi_{k-q} \coth\left(\frac{\beta\xi_q}{2}\right) + \left\{ (i\omega_n)^2 - \xi_q^2 - \xi_{k-q}^2 \right\} \coth\left(\frac{\beta\xi_{k-q}}{2}\right) \right] \quad (\text{D.48})$$

and

$$\begin{aligned} s_3(k, q, i\omega_n) = & -\frac{1}{2\xi_{k-q}} \left[ \xi_q \xi_{k-q} \left\{ (i\omega_n)^2 + \xi_q^2 - \xi_{k-q}^2 \right\} \coth\left(\frac{\beta\xi_q}{2}\right) \right. \\ & \left. + \left\{ -(2i\omega_n \xi_{k-q})^2 + [(i\omega_n)^2 + \xi_{k-q}^2][(i\omega_n)^2 - \xi_q^2 + \xi_{k-q}^2] \right\} \coth\left(\frac{\beta\xi_{k-q}}{2}\right) \right]. \end{aligned} \quad (\text{D.49})$$

Coming back to the 2-magnon part of the longitudinal structure factor one has

$$\begin{aligned} -F_{2\text{-magnon}}^{zz}(k, i\omega_n) = & \frac{1}{N_s} \sum_q (P_{k,q} - i\omega_n Q_{k,q}) S_1(k, q, i\omega_n) \\ & + \frac{1}{N_s} \sum_q (R_{k,q} - i\omega_n) S_2(k, q, i\omega_n) \\ & + \frac{1}{N_s} \sum_q S_3(k, q, i\omega_n) \end{aligned} \quad (\text{D.50})$$

## Appendix D. Calculations at finite temperature

---

where we defined the functions  $P_{k,q}$ ,  $Q_{k,q}$  and  $R_{k,q}$  as

$$P_{k,q} = p_\beta^2 (A_q A_{k-q} + B_q B_{k-q}), \quad (\text{D.51})$$

$$Q_{k,q} = p_\beta A_q, \quad (\text{D.52})$$

$$R_{k,q} = p_\beta (A_q + A_{q-k}). \quad (\text{D.53})$$

The next step is the analytical continuation to real frequency, followed by taking the imaginary part of the expression. The analytical continuation is defined by

$$i\omega_n \rightarrow \omega + i\eta \quad \text{and} \quad (i\omega_n)^2 \rightarrow \omega^2 + i \text{sign}(\omega)\eta \quad (\text{D.54})$$

while Sokhotsky's formula is useful for extracting the imaginary part

$$\frac{1}{x \pm i\eta} = \text{PV} \frac{1}{x} \mp i\pi \delta(x) \quad (\text{D.55})$$

where PV denotes the principal value.

Let us illustrate the calculation with the third line of Eq. (D.50). The analytical continuation reads

$$S_3(k, q, i\omega_n) \rightarrow \frac{s_3(k, q, \omega)}{\left[ \omega^2 - (E_{k,q}^+)^2 + i \text{sign}(\omega)\eta \right] \left[ \omega^2 - (E_{k,q}^-)^2 + i \text{sign}(\omega)\eta \right]}. \quad (\text{D.56})$$

Taking now the imaginary part of this expression one obtains (we omit here the factor  $s_3$  in the numerator as it is purely real after the analytical continuation)

$$\text{Im} \left[ \frac{1}{\left[ \omega^2 - (E_{k,q}^+)^2 + i \text{sign}(\omega)\eta \right] \left[ \omega^2 - (E_{k,q}^-)^2 + i \text{sign}(\omega)\eta \right]} \right] = -\pi \text{sign}(\omega) \mathcal{P}(k, q, \omega) \quad (\text{D.57})$$

where

$$\mathcal{P}(k, q, \omega) = \text{PV} \frac{1}{\omega^2 - (E_{k,q}^-)^2} \delta(\omega^2 - (E_{k,q}^+)^2) + \text{PV} \frac{1}{\omega^2 - (E_{k,q}^+)^2} \delta(\omega^2 - (E_{k,q}^-)^2). \quad (\text{D.58})$$

The delta functions can be rewritten as

$$\delta(\omega^2 - (E_{k,q}^+)^2) = \frac{1}{2E_{k,q}^+} \left( \delta(\omega - E_{k,q}^+) + \delta(\omega + E_{k,q}^+) \right) \quad (\text{D.59})$$

and

$$\delta(\omega^2 - (E_{k,q}^-)^2) = \frac{1}{2|E_{k,q}^-|} \left( \delta(\omega - E_{k,q}^-) + \delta(\omega + E_{k,q}^-) \right). \quad (\text{D.60})$$

We have used the fact that  $E_{k,q}^+$  is positive, unlike  $E_{k,q}^-$ , to remove the absolute value in

the prefactor of Eq. (D.59).

Thus the third line of Eq. (D.50) becomes

$$\text{Im} \left[ \lim_{i\omega_n \rightarrow \omega + i\eta} \frac{1}{N_s} \sum_q S_3(k, q, i\omega_n) \right] = -\frac{\pi \text{sign}(\omega)}{N_s} \sum_q s_3(k, q, \omega) \mathcal{P}(k, q, \omega). \quad (\text{D.61})$$

We can now compute the four terms appearing in the right-hand side of this expression. The first one is given by

$$-\frac{\pi \text{sign}(\omega)}{N_s} \sum_q s_3(k, q, \omega) \times \text{PV} \frac{1}{\omega^2 - (E_{k,q}^-)^2} \times \frac{1}{2E_{k,q}^+} \times \delta(\omega - E_{k,q}^+). \quad (\text{D.62})$$

Since the delta function vanishes unless  $\omega = E_{k,q}^+$  this can be rewritten as

$$-\frac{\pi}{N_s} \sum_q s_3(k, q, E_{k,q}^+) \times \text{PV} \frac{1}{(E_{k,q}^+)^2 - (E_{k,q}^-)^2} \times \frac{1}{2E_{k,q}^+} \times \delta(\omega - E_{k,q}^+) \quad (\text{D.63})$$

where we used the fact that  $\text{sign}(E_{k,q}^+) = 1$ . Now the principal value is well defined and one obtains

$$-\frac{\pi}{N_s} \sum_q s_3(k, q, E_{k,q}^+) \times \frac{1}{4\xi_q \xi_{k-q}} \times \frac{1}{2E_{k,q}^+} \times \delta(\omega - E_{k,q}^+). \quad (\text{D.64})$$

Doing the algebra we finally obtain for this contribution

$$\frac{\pi}{N_s} \sum_q \frac{\xi_q \left[ \coth\left(\frac{\beta\xi_q}{2}\right) + \coth\left(\frac{\beta\xi_{k-q}}{2}\right) \right]}{8\xi_{k-q}} \times \delta(\omega - E_{k,q}^+). \quad (\text{D.65})$$

The three other contributions are evaluated in a similar way and we obtain

$$-\frac{\pi}{N_s} \sum_q \frac{\xi_q \left[ \coth\left(\frac{\beta\xi_q}{2}\right) + \coth\left(\frac{\beta\xi_{k-q}}{2}\right) \right]}{8\xi_{k-q}} \times \delta(\omega + E_{k,q}^+), \quad (\text{D.66})$$

$$-\frac{\pi}{N_s} \sum_q \frac{\xi_q \left[ \coth\left(\frac{\beta\xi_q}{2}\right) - \coth\left(\frac{\beta\xi_{k-q}}{2}\right) \right]}{8\xi_{k-q}} \times \delta(\omega - E_{k,q}^-), \quad (\text{D.67})$$

and

$$\frac{\pi}{N_s} \sum_q \frac{\xi_q \left[ \coth\left(\frac{\beta\xi_q}{2}\right) - \coth\left(\frac{\beta\xi_{k-q}}{2}\right) \right]}{8\xi_{k-q}} \times \delta(\omega + E_{k,q}^-). \quad (\text{D.68})$$

## Appendix D. Calculations at finite temperature

Finally the third line of Eq. (D.50) is given by

$$\begin{aligned} \text{Im} \left[ \lim_{i\omega_n \rightarrow \omega + i\eta} \frac{1}{N_s} \sum_q S_3(k, q, i\omega_n) \right] \\ = \frac{\pi}{N_s} \sum_q \frac{\xi_q \left[ \coth\left(\frac{\beta\xi_q}{2}\right) + \coth\left(\frac{\beta\xi_{k-q}}{2}\right) \right]}{8\xi_{k-q}} \left[ \delta(\omega - E_{k,q}^+) - \delta(\omega + E_{k,q}^+) \right] \\ - \frac{\pi}{N_s} \sum_q \frac{\xi_q \left[ \coth\left(\frac{\beta\xi_q}{2}\right) - \coth\left(\frac{\beta\xi_{k-q}}{2}\right) \right]}{8\xi_{k-q}} \left[ \delta(\omega - E_{k,q}^-) - \delta(\omega + E_{k,q}^-) \right]. \end{aligned} \quad (\text{D.69})$$

This expression has a form suitable for numerical integration. We should then multiply this quantity by  $2(1 + n_B(\omega))$  to obtain the contribution of the  $S_3$  term to  $S^{zz}(k, \omega; \beta)^{1,2}$ .

For completeness we write the contributions of the second line of Eq. (D.50)

$$\begin{aligned} \text{Im} \left[ \lim_{i\omega_n \rightarrow \omega + i\eta} \frac{1}{N_s} \sum_q (R_{k,q} - i\omega_n) S_2(k, q, i\omega_n) \right] \\ = -\frac{\pi}{N_s} \sum_q \frac{1}{8\xi_{k-q}} \left[ \left\{ \coth\left(\frac{\beta\xi_q}{2}\right) + \coth\left(\frac{\beta\xi_{k-q}}{2}\right) \right\} \left\{ (R_{k,q} - E_{k,q}^+) \delta(\omega - E_{k,q}^+) \right. \right. \\ \left. \left. + (R_{k,q} + E_{k,q}^+) \delta(\omega + E_{k,q}^+) \right\} - \left\{ \coth\left(\frac{\beta\xi_q}{2}\right) - \coth\left(\frac{\beta\xi_{k-q}}{2}\right) \right\} \times \right. \\ \left. \left\{ (R_{k,q} - E_{k,q}^-) \delta(\omega - E_{k,q}^-) + (R_{k,q} + E_{k,q}^-) \delta(\omega + E_{k,q}^-) \right\} \right] \end{aligned} \quad (\text{D.70})$$

and of the first line

$$\begin{aligned} \text{Im} \left[ \lim_{i\omega_n \rightarrow \omega + i\eta} \frac{1}{N_s} \sum_q (P_{k,q} - i\omega_n Q_{k,q}) S_1(k, q, i\omega_n) \right] \\ = \frac{\pi}{N_s} \sum_q \frac{1}{8\xi_q \xi_{k-q}} \left[ \left\{ \coth\left(\frac{\beta\xi_q}{2}\right) + \coth\left(\frac{\beta\xi_{k-q}}{2}\right) \right\} \left\{ (P_{k,q} - E_{k,q}^+ Q_{k,q}) \delta(\omega - E_{k,q}^+) \right. \right. \\ \left. \left. - (P_{k,q} + E_{k,q}^+ Q_{k,q}) \delta(\omega + E_{k,q}^+) \right\} - \left\{ \coth\left(\frac{\beta\xi_q}{2}\right) - \coth\left(\frac{\beta\xi_{k-q}}{2}\right) \right\} \times \right. \\ \left. \left\{ (P_{k,q} - E_{k,q}^- Q_{k,q}) \delta(\omega - E_{k,q}^-) - (P_{k,q} + E_{k,q}^- Q_{k,q}) \delta(\omega + E_{k,q}^-) \right\} \right]. \end{aligned} \quad (\text{D.71})$$

The final expression in Eq. (2.79) is obtained from these equations by trivial algebra.

<sup>1</sup>Notice that Eq. (D.69) should not be multiplied by  $-2(1 + n_B(\omega))$  because the minus signs from Eq. (2.70) and (2.71) cancel each other.

<sup>2</sup>Momentum should still be shifted by  $\pi$  to take into account the rotation of spin operators along the  $x$  axis that we performed in the very beginning.

## D.5 Transverse structure factor

The calculation of the transverse part of the dynamical structure factor is significantly easier. We first use the HP transformation and write

$$\begin{aligned}
 \tilde{S}_k^x(\tau)\tilde{S}_{-k}^x(0) &= \frac{S}{2} \left( a_k(\tau)a_{-k}(0) + a_k(\tau)a_k^\dagger(0) + a_{-k}^\dagger(\tau)a_{-k}(0) + a_{-k}^\dagger(\tau)a_k^\dagger(0) \right) \\
 &\quad - \frac{1}{8N_s} \sum_{p,q} \left( a_k(\tau)a_{p+q+k}^\dagger(0)a_p(0)a_q(0) + a_{p+q-k}^\dagger(\tau)a_p(\tau)a_q(\tau)a_{-k}(0) \right. \\
 &\quad \quad \quad + a_k(\tau)a_p^\dagger(0)a_q^\dagger(0)a_{p+q-k}(0) + a_{p+q-k}^\dagger(\tau)a_p(\tau)a_q(\tau)a_k^\dagger(0) \\
 &\quad \quad \quad + a_{-k}^\dagger(\tau)a_{p+q+k}^\dagger(0)a_p(0)a_q(0) + a_p^\dagger(\tau)a_q^\dagger(\tau)a_{p+q+k}(\tau)a_{-k}(0) \\
 &\quad \quad \quad \left. + a_{-k}^\dagger(\tau)a_p^\dagger(0)a_q^\dagger(0)a_{p+q-k}(0) + a_p^\dagger(\tau)a_q^\dagger(\tau)a_{p+q+k}(\tau)a_k^\dagger(0) \right) \\
 &\quad + \mathcal{O}(S^{-1}).
 \end{aligned} \tag{D.72}$$

Looking at the leading order contribution given by the first line of this expression one obtains

$$F^{xx}(k, i\omega_n) = \frac{S}{2} \sum_{j,l} \mathbb{G}_{jl}(k, i\omega_n). \tag{D.73}$$

The analytic continuation is now trivial and we obtain

$$S^{xx}(k, \omega; \beta) = -\frac{2Sp_\beta(A_k + B_k)}{1 - e^{-\beta\omega}} \text{Im} \left[ \frac{1}{\omega^2 - \xi_k^2 + i\eta \text{sign}(\omega)} \right]. \tag{D.74}$$

Using Sokhotsky's formula in Eq. (D.55) one can develop the imaginary part as

$$\begin{aligned}
 S^{xx}(k, \omega; \beta) &= \frac{2S\pi p_\beta(A_k + B_k)\text{sign}(\omega)}{1 - e^{-\beta\omega}} \delta(\omega^2 - \xi_k^2) \\
 &= \frac{2S\pi p_\beta(A_k + B_k)\text{sign}(\omega)}{1 - e^{-\beta\omega}} \frac{1}{2\xi_k} (\delta(\omega - \xi_k) + \delta(\omega + \xi_k)) \\
 &= \frac{S\pi\text{sign}(\omega)}{1 - e^{-\beta\omega}} \left| \tan\left(\frac{k}{2}\right) \right| (\delta(\omega - \xi_k) + \delta(\omega + \xi_k)).
 \end{aligned} \tag{D.75}$$

We observe that the transverse structure factor is positive for negative and positive frequencies, and gives contributions only along the single-magnon branch  $\omega = \pm\xi_k$ .

Now let us look at the first order correction to this result, given by the 4-boson terms in Eq. (D.72). As an example, the expectation value of the first term,

$$\langle T_\tau a_k(\tau) a_{p+q+k}^\dagger(0^+) a_p(0) a_q(0) \rangle \tag{D.76}$$

## Appendix D. Calculations at finite temperature

is treated as follows with Wick's theorem

$$\begin{aligned} \langle T_\tau a_k(\tau) a_{p+q+k}^\dagger(0^+) a_p(0) a_q(0) \rangle &= \delta_{p,-q} \mathbb{G}_{11}^0(k, \tau) \mathbb{G}_{12}^0(p, 0) + \delta_{k,-p} \mathbb{G}_{12}^0(k, \tau) \mathbb{G}_{22}^0(q, 0^+) \\ &\quad + \delta_{k,-q} \mathbb{G}_{12}^0(k, \tau) \mathbb{G}_{22}^0(p, 0^+). \end{aligned} \quad (\text{D.77})$$

We have used the free Green's function  $\mathbb{G}_{jl}^0(k, \tau)$  since the contribution is  $\mathcal{O}(S^0)$ . However we will soon replace them by the interacting Green's functions to consistently take into account the correction to the dispersion relation due to the first order interaction in the Hamiltonian. After summing over  $p$  and  $q$  we get

$$\begin{aligned} \frac{1}{N_s} \sum_{p,q} \langle T_\tau a_k(\tau) a_{p+q+k}^\dagger(0^+) a_p(0) a_q(0) \rangle \\ = \mathbb{G}_{11}^0(k, \tau) \underbrace{\left( \frac{1}{N_s} \sum_q \mathbb{G}_{12}^0(q, 0) \right)}_{=0} + 2 \mathbb{G}_{12}^0(k, \tau) \underbrace{\left( \frac{1}{N_s} \sum_q \mathbb{G}_{22}^0(q, 0^+) \right)}_{=n_\beta} = 2n_\beta \mathbb{G}_{12}^0(k, \tau). \end{aligned} \quad (\text{D.78})$$

Performing the same steps for all 4-boson terms in Eq. (D.72) and performing then the Fourier transform we obtain the following contribution

$$\frac{S}{2} \left( -\frac{1}{4S} \right) 4n_\beta \sum_{j,l} \mathbb{G}_{jl}^0(k, i\omega_n). \quad (\text{D.79})$$

Now we see that if we were to perform the analytic continuation on this equation, followed by the use of Sokhotsky's formula, we would end up with a single-magnon branch at  $\omega = \epsilon_k$ . This is of course forbidden since the magnon dispersion relation is given by  $\xi_k$ , which incorporates the first order temperature-dependant correction generated by  $\mathcal{H}^{(4)}$ . To avoid this issue, we simply replace  $\mathbb{G}^0(k, i\omega_n)$  by  $\mathbb{G}(k, i\omega_n)$ . This replacement only affects order  $S^{-1}$  or smaller. The contribution is then precisely of the same form as the one coming from the 2-boson terms. We thus end up with

$$S^{xx}(k, \omega; \beta) = \frac{S\pi \text{sign}(\omega)}{1 - e^{-\beta\omega}} \left( 1 - \frac{n_\beta}{S} \right) \left| \tan \left( \frac{k}{2} \right) \right| (\delta(\omega - \xi_k) + \delta(\omega + \xi_k)). \quad (\text{D.80})$$

## D.6 Real-space correlation function

Let us turn now to the calculation of the real-space equal-time correlation function at finite temperature. To perform this calculation, we rewrite each term of the operator  $\mathbf{S}_i \cdot \mathbf{S}_j$  in Eq. (2.51) in Fourier space. For even distance  $|i - j|$  one has

$$\mathcal{O}_{ij}^{(1)} = \frac{1}{N_s} \sum_{k_1, k_2} \left[ e^{-ik_1 r_i + ik_2 r_j} + e^{-ik_1 r_j + ik_2 r_i} - e^{-i(k_1 - k_2) r_i} - e^{-i(k_1 - k_2) r_j} \right] a_{k_1}^\dagger a_{k_2} \quad (\text{D.81})$$

and

$$\mathcal{O}_{ij}^{(2)} = \frac{1}{N_s^2} \sum_{k_1, k_2, k_3, k_4} f^{(2)}(k_1, k_2, k_3, k_4; r_i, r_j) a_{k_1}^\dagger a_{k_2}^\dagger a_{k_3} a_{k_4} \quad (\text{D.82})$$

with

$$\begin{aligned} f^{(2)}(k_1, k_2, k_3, k_4; r_i, r_j) = & e^{-ik_1 r_i - ik_2 r_j + ik_3 r_i + ik_4 r_j} \\ & - \frac{1}{4} \left( e^{-ik_1 r_j - ik_2 r_j + ik_3 r_i + ik_4 r_j} + e^{-ik_1 r_i - ik_2 r_j + ik_3 r_i + ik_4 r_i} \right. \\ & \left. + e^{-ik_1 r_i - ik_2 r_j + ik_3 r_j + ik_4 r_j} + e^{-ik_1 r_i - ik_2 r_i + ik_3 r_i + ik_4 r_j} \right). \end{aligned} \quad (\text{D.83})$$

Now we give a positive imaginary time  $0^+$  to all creation operators in order to respect the ordering, and evaluate all expectation values using Wick's theorem. The first expectation value is given by

$$\langle a_{k_1}^\dagger a_{k_2} \rangle = \langle a_{k_1}^\dagger(0^+) a_{k_2}(0) \rangle = -\delta_{k_1, k_2} \mathbb{G}_{22}(-k_1, 0^+) = -\delta_{k_1, k_2} \mathbb{G}_{11}(k_1, 0^-). \quad (\text{D.84})$$

The first order term thus reads

$$\langle \mathcal{O}_{ij}^{(1)} \rangle = -\frac{2}{N_s} \sum_k (\gamma_k(r) - 1) \mathbb{G}_{11}(k, 0^-). \quad (\text{D.85})$$

Similarly the expectation value of the string of operators in Eq. (D.82) is given by

$$\begin{aligned} \langle a_{k_1}^\dagger(0^+) a_{k_2}^\dagger(0^+) a_{k_3}(0) a_{k_4}(0) \rangle = & \delta_{k_1, -k_2} \delta_{k_3, -k_4} \mathbb{G}_{12}(k_1, 0) \mathbb{G}_{12}(k_3, 0) \\ & + (\delta_{k_1, k_3} \delta_{k_2, k_4} + \delta_{k_1, k_4} \delta_{k_2, k_3}) \mathbb{G}_{11}(k_1, 0^-) \mathbb{G}_{11}(k_2, 0^-). \end{aligned} \quad (\text{D.86})$$

This leads to

$$\begin{aligned} \langle \mathcal{O}_{ij}^{(2)} \rangle = & \left( \frac{1}{N_s} \sum_k (\gamma_k(r) - 1) \mathbb{G}_{11}(k, 0^-) \right)^2 \\ & + \left( \frac{1}{N_s} \sum_k \gamma_k(r) \mathbb{G}_{12}(k, 0) \right) \left( \frac{1}{N_s} \sum_k (\gamma_k(r) - 1) \mathbb{G}_{12}(k, 0) \right). \end{aligned} \quad (\text{D.87})$$

To evaluate these expressions, we use the Green's functions obtained after using Dyson's equation. This has the advantage of taking self-consistently into account the first order correction to the dispersion relation coming from  $\mathcal{H}^{(4)}$ . The Green's functions then

## Appendix D. Calculations at finite temperature

---

simply read

$$\mathbb{G}_{11}(k, 0^+) = -\frac{u_k^2 e^{\beta \xi_k} + v_k^2}{e^{\beta \xi_k} - 1}, \quad (\text{D.88})$$

$$\mathbb{G}_{11}(k, 0^-) = -\frac{v_k^2 e^{\beta \xi_k} + u_k^2}{e^{\beta \xi_k} - 1}, \quad (\text{D.89})$$

$$\mathbb{G}_{12}(k, 0^\pm) = u_k v_k \coth\left(\frac{\beta \xi_k}{2}\right) \quad (\text{D.90})$$

and  $\mathbb{G}_{22}(k, 0^\pm) = \mathbb{G}_{22}(k, 0^\mp)$ . With this, one observes that the second line in Eq. (D.87) vanishes.

Let us now give the expressions for odd distance  $|i - j|$  between the spins. In Fourier space, the first order term of the correlator reads

$$\begin{aligned} \mathcal{O}_{ij}^{(1)} &= \frac{1}{N_s} \sum_{k_1, k_2} \left( e^{-i(k_1 - k_2)r_i} + e^{-i(k_1 - k_2)r_j} \right) a_{k_1}^\dagger a_{k_2} \\ &+ \frac{1}{N_s} \sum_{k_1, k_2} e^{-i(k_1 r_i + k_2 r_j)} \left( a_{k_1}^\dagger a_{k_2}^\dagger + a_{k_1} a_{k_2} \right) \end{aligned} \quad (\text{D.91})$$

leading to

$$\langle \mathcal{O}_{ij}^{(1)} \rangle = -\frac{2}{N_s} \sum_k \mathbb{G}_{11}(k, 0^-) - \frac{2}{N_s} \sum_k \gamma_k(r) \mathbb{G}_{12}(k, 0). \quad (\text{D.92})$$

The second order term  $\mathcal{O}_{ij}^{(2)}$  in the correlator is given by

$$\begin{aligned} \mathcal{O}_{ij}^{(2)} &= -\frac{1}{N_s^2} \sum_{k_1, k_2, k_3, k_4} e^{-ik_1 r_i - ik_2 r_j + ik_3 r_i + ik_4 r_j} a_{k_1}^\dagger a_{k_2}^\dagger a_{k_3} a_{k_4} \\ &- \frac{1}{4N_s^2} \sum_{k_1, k_2, k_3, k_4} \left( e^{-ik_1 r_i + ik_2 r_i + ik_3 r_i + ik_4 r_j} + e^{-ik_1 r_j + ik_2 r_i + ik_3 r_j + ik_4 r_j} \right) a_{k_1}^\dagger a_{k_2} a_{k_3} a_{k_4} \\ &- \frac{1}{4N_s^2} \sum_{k_1, k_2, k_3, k_4} \left( e^{-ik_1 r_i - ik_2 r_i - ik_3 r_j + ik_4 r_i} + e^{-ik_1 r_i - ik_2 r_j - ik_3 r_j + ik_4 r_j} \right) a_{k_1}^\dagger a_{k_2}^\dagger a_{k_3}^\dagger a_{k_4}. \end{aligned} \quad (\text{D.93})$$

After some algebra one gets

$$\langle \mathcal{O}_{ij}^{(2)} \rangle = -\left( \frac{1}{N_s} \sum_k (\mathbb{G}_{11}(k, 0^-) + \gamma_k(r) \mathbb{G}_{12}(k, 0)) \right)^2. \quad (\text{D.94})$$



# E Cancellation of divergences in the equal-time structure factor

In this appendix we demonstrate that the divergences occuring in the transverse and longitudinal parts of the equal-time structure factor cancel each other when considering the  $O(3)$  invariant structure factor defined as

$$S(k) = 2S^{xx}(k) + S^{zz}(k). \quad (\text{E.1})$$

The structure factor is given in Eq. (2.90). We shall here focus on the last term which contains the integral. Our aim is to show that this integral is IR finite.

We define

$$f(k, q) = \frac{1}{|\sin(q)|} \left( \frac{1 - \cos(q) \cos(k+q)}{|\sin(k+q)|} - 2 \tan(k/2) \right). \quad (\text{E.2})$$

This is the integrand in Eq. (2.90) up to two minor changes. First we have put an absolute value on the prefactor  $1/|\sin q|$ . This has no effect on  $S(k)$  since integration is on  $q \in [0, \pi]$ , but will prove to be useful later. Second we have removed the absolute value on the last term. This is allowed since we take  $k \in [0, \pi]$ . Our aim is to show that

$$I(k) = \int_0^\pi dq f(k, q) \quad (\text{E.3})$$

is IR finite. Observe that  $f(k, q)$  is  $\pi$ -periodic in  $q$  thanks to the additionnal absolute value on the  $\sin q$  factor. Defining

$$g(k, q) = f(k, q + k), \quad h(k, q) = f(k, -q - 2k) \quad (\text{E.4})$$

it is then trivial to show that

$$I(k) = \int_0^\pi dq g(k, q) = \int_0^\pi dq h(k, q) \quad (\text{E.5})$$

if the integral is convergent. The important point is that both  $g(k, q)$  and  $h(k, q)$  are divergent for  $q = \pi - 2k, \pi - k$  if  $2k < \pi$  or for  $q = 2(\pi - k), \pi - k$  if  $2k > \pi$ . Now let us

## Appendix E. Cancellation of divergences in the equal-time structure factor

---

rewrite  $I(k)$  as

$$\begin{aligned} I(k) &= \frac{1}{2} \left( \int_0^\pi dq g(k, q) + \int_0^\pi dq h(k, q) \right) \\ &= \frac{1}{2} \int_0^\pi dq (g(k, q) + h(k, q)) \\ &= \int_0^\pi dq G(k, q) \end{aligned} \quad (\text{E.6})$$

where

$$G(k, q) = \frac{1 - \cos(k + q) \cos(2k + q) - \tan(k/2) (|\sin(2k + q)| + |\sin(k + q)|)}{|\sin(2k + q)| |\sin(k + q)|}. \quad (\text{E.7})$$

There are two  $q$  points which require some attention, because the denominator in  $G(k, q)$  vanishes for  $q = \pi - 2k, \pi - k$  if  $2k < \pi$  or for  $q = \pi - k, 2(\pi - k)$  if  $2k > \pi$ . We study the behavior of  $G(k, q)$  close to these points (we consider the case  $\pi - 2k > 0$ ).

We begin by taking  $q = \pi - 2k - \delta$  with  $\delta > 0$ . We obtain

$$G(k, \pi - 2k - \delta) = \frac{1 - \cos(\delta) \cos(k + \delta) - \tan(k/2) (|\sin(k + \delta)| + |\sin(\delta)|)}{|\sin(k + \delta)| |\sin(\delta)|}. \quad (\text{E.8})$$

Taking  $\delta > 0$  sufficiently small we can remove all absolute values in this expression, and expand the trigonometric functions in  $\delta$  in order to keep all singular terms in  $\delta$  as well as terms of order  $\mathcal{O}(\delta^{-1})$  and  $\mathcal{O}(\delta^0)$ . We then obtain

$$\begin{aligned} G(k, \pi - 2k - \delta) &= \frac{1}{\delta \sin(k)} (1 - \cos(k) - \tan(k/2) \sin(k)) \\ &\quad - \frac{1}{\sin(k)} (\sin(k) - \cos(k) \tan(k/2) - \tan(k/2)) \\ &\quad + \mathcal{O}(\delta) \\ &\longrightarrow 0 \text{ when } \delta \rightarrow 0. \end{aligned} \quad (\text{E.9})$$

The  $1/\delta$  term and the constant term cancel because we have the two following trigonometric identities

$$1 - \cos(k) - \tan(k/2) \sin(k) = 0, \quad (\text{E.10})$$

$$\sin(k) - (1 + \cos(k)) \tan(k/2) = 0. \quad (\text{E.11})$$

In other words

$$\lim_{\delta \rightarrow 0^+} G(k, \pi - 2k - \delta) = 0 \quad (\text{E.12})$$

such that  $G(k, q)$  is everywhere well-defined for  $q \in [0, \pi - 2k[$  and is not divergent when  $q \rightarrow \pi - 2k$  from below.

Now we take  $q = \pi - 2k + \delta$  with  $\delta > 0$ , namely we study the right neighborhood of  $\pi - 2k$ . Again we can take  $\delta$  sufficiently small and remove the absolute values. We

---

obtain

$$G(k, \pi - 2k + \delta) = \frac{1 - \cos(k - \delta) \cos(\delta) - (\sin(k - \delta) + \sin(\delta)) \tan(k/2)}{\sin(\delta) \sin(k - \delta)}. \quad (\text{E.13})$$

After the same sort of algebra we get

$$\begin{aligned} G(k, \pi - 2k + \delta) &= \frac{1}{\delta \sin(k)} \underbrace{(1 - \cos(k) - \sin(k) \tan(k/2))}_{=0} \\ &\quad - \frac{1}{\sin(k)} \underbrace{(\sin(k) - \cos(k) \tan(k/2) + \tan(k/2))}_{=2 \tan(k/2)} + \mathcal{O}(\delta) \\ &\longrightarrow -\frac{2 \tan(k/2)}{\sin(k)} \text{ when } \delta \rightarrow 0. \end{aligned} \quad (\text{E.14})$$

Thus  $G(k, q)$  has a well-defined limit on the right of  $q = \pi - 2k$ ,

$$\lim_{\delta \rightarrow 0^+} G(k, \pi - 2k + \delta) = -\frac{2 \tan(k/2)}{\sin(k)}. \quad (\text{E.15})$$

From Eqs. (E.12) and (E.15) we see that  $G(k, q)$  has a discontinuity at  $q = \pi - 2k$ , but the derivative of  $G(k, q)$  with respect to  $q$  is well defined in the neighborhood of  $\pi - 2k$ .

We look now at the neighborhood of the second singularity of  $G$ , namely  $q = \pi - k$ . Taking  $q = \pi - k - \delta$ ,  $\delta > 0$  we see that  $G(k, \pi - k - \delta)$  has the exact same form as in Eq. (E.13). This is easily justified as follows. Observe that if we restore the absolute value on the  $\tan(k/2)$  factor in  $G(k, q)$  then we can change variables and define

$$u = 2k + q, \quad v = k + q \quad (\text{E.16})$$

and

$$\bar{G}(u, v) = G(k(u, v), q(u, v)). \quad (\text{E.17})$$

Then  $\bar{G}$  is even under permutation of  $u$  and  $v$ ,  $\bar{G}(u, v) = \bar{G}(v, u)$ . Thus  $G(k, q)$  has a well-defined limit on the left of  $\pi - k$ ,

$$\lim_{\delta \rightarrow 0^+} G(k, \pi - k - \delta) = -\frac{2 \tan(k/2)}{\sin(k)}. \quad (\text{E.18})$$

Finally we take  $q = \pi - k + \delta$ ,  $\delta > 0$  and, for the same reason as above,  $G(k, \pi - k + \delta)$  has the exact same form as Eq. (E.8). Thus  $G(k, q)$  has a well-defined limit on the right of  $\pi - k$ ,

$$\lim_{\delta \rightarrow 0^+} G(k, \pi - k + \delta) = 0. \quad (\text{E.19})$$

We have thus found a function  $G(k, q)$  everywhere well defined except at  $\pi - k$  and

## Appendix E. Cancellation of divergences in the equal-time structure factor

---

$\pi - 2k$  or  $\pi - k$  and  $2(\pi - k)$  where it is discontinuous, but where the derivative on the left and on the right are well defined, such that

$$I(k) = \int_0^\pi dq G(k, q) \tag{E.20}$$

thus showing that the integral itself is well defined in the sense that the divergences of  $f(k, q)$  for  $q \in [0, \pi]$  cancel each other and lead to a finite result. We can thus compute  $I(k)$  by integrating exactly  $G(k, q)$  numerically.

# F $\mathfrak{su}(3)$ generators in the symmetric irreps

## F.1 2-box symmetric irrep

The generators of  $\mathfrak{su}(3)$  in the 6-dimensional symmetric irrep  $\square\square$  are given by the following expressions, where  $T_3$  and  $T_8$  are diagonal:

$$T_1 = \begin{pmatrix} 0 & 1/\sqrt{2} & 0 & 0 & 0 & 0 \\ 1/\sqrt{2} & 0 & 0 & 1/\sqrt{2} & 0 & 0 \\ 0 & 0 & 0 & 0 & 1/2 & 0 \\ 0 & 1/\sqrt{2} & 0 & 0 & 0 & 0 \\ 0 & 0 & 1/2 & 0 & 0 & 0 \\ 0 & 0 & 0 & 0 & 0 & 0 \end{pmatrix}$$

$$T_2 = i \begin{pmatrix} 0 & -1/\sqrt{2} & 0 & 0 & 0 & 0 \\ 1/\sqrt{2} & 0 & 0 & -1/\sqrt{2} & 0 & 0 \\ 0 & 0 & 0 & 0 & -1/2 & 0 \\ 0 & 1/\sqrt{2} & 0 & 0 & 0 & 0 \\ 0 & 0 & 1/2 & 0 & 0 & 0 \\ 0 & 0 & 0 & 0 & 0 & 0 \end{pmatrix}$$

$$T_3 = \text{diag}\left(1, 0, \frac{1}{2}, -1, -\frac{1}{2}, 0\right)$$

$$T_4 = \begin{pmatrix} 0 & 0 & 1/\sqrt{2} & 0 & 0 & 0 \\ 0 & 0 & 0 & 0 & 1/2 & 0 \\ 1/\sqrt{2} & 0 & 0 & 0 & 0 & 1/\sqrt{2} \\ 0 & 0 & 0 & 0 & 0 & 0 \\ 0 & 1/2 & 0 & 0 & 0 & 0 \\ 0 & 0 & 1/\sqrt{2} & 0 & 0 & 0 \end{pmatrix}$$

$$T_5 = i \begin{pmatrix} 0 & 0 & -1/\sqrt{2} & 0 & 0 & 0 \\ 0 & 0 & 0 & 0 & -1/2 & 0 \\ 1/\sqrt{2} & 0 & 0 & 0 & 0 & -1/\sqrt{2} \\ 0 & 0 & 0 & 0 & 0 & 0 \\ 0 & 1/2 & 0 & 0 & 0 & 0 \\ 0 & 0 & 1/\sqrt{2} & 0 & 0 & 0 \end{pmatrix}$$

$$T_6 = \begin{pmatrix} 0 & 0 & 0 & 0 & 0 & 0 \\ 0 & 0 & 1/2 & 0 & 0 & 0 \\ 0 & 1/2 & 0 & 0 & 0 & 0 \\ 0 & 0 & 0 & 0 & 1/\sqrt{2} & 0 \\ 0 & 0 & 0 & 1/\sqrt{2} & 0 & 1/\sqrt{2} \\ 0 & 0 & 0 & 0 & 1/\sqrt{2} & 0 \end{pmatrix}$$

$$T_7 = i \begin{pmatrix} 0 & 0 & 0 & 0 & 0 & 0 \\ 0 & 0 & -1/2 & 0 & 0 & 0 \\ 0 & 1/2 & 0 & 0 & 0 & 0 \\ 0 & 0 & 0 & 0 & -1/\sqrt{2} & 0 \\ 0 & 0 & 0 & 1/\sqrt{2} & 0 & -1/\sqrt{2} \\ 0 & 0 & 0 & 0 & 1/\sqrt{2} & 0 \end{pmatrix}$$

$$T_8 = \text{diag} \left( \frac{1}{\sqrt{3}}, \frac{1}{\sqrt{3}}, -\frac{1}{2\sqrt{3}}, \frac{1}{\sqrt{3}}, -\frac{1}{2\sqrt{3}}, -\frac{2}{\sqrt{3}} \right).$$

They satisfy the normalization condition (see Eq. (3.77))

$$\text{Tr} (T_i T_j) = \frac{5}{2} \delta_{ij}.$$

## F.2 3-box symmetric irrep

The generators of  $\mathfrak{su}(3)$  in the 10-dimensional symmetric irrep  $\square\square\square$  are given by the following expressions, where  $T_3$  and  $T_8$  are diagonal:

$$T_1 = \begin{pmatrix} 0 & \sqrt{3}/2 & 0 & 0 & 0 & 0 & 0 & 0 & 0 & 0 \\ \sqrt{3}/2 & 0 & 0 & 1 & 0 & 0 & 0 & 0 & 0 & 0 \\ 0 & 0 & 0 & 0 & 1/\sqrt{2} & 0 & 0 & 0 & 0 & 0 \\ 0 & 1 & 0 & 0 & 0 & 0 & \sqrt{3}/2 & 0 & 0 & 0 \\ 0 & 0 & 1/\sqrt{2} & 0 & 0 & 0 & 0 & 1/\sqrt{2} & 0 & 0 \\ 0 & 0 & 0 & 0 & 0 & 0 & 0 & 0 & 1/2 & 0 \\ 0 & 0 & 0 & \sqrt{3}/2 & 0 & 0 & 0 & 0 & 0 & 0 \\ 0 & 0 & 0 & 0 & 1/\sqrt{2} & 0 & 0 & 0 & 0 & 0 \\ 0 & 0 & 0 & 0 & 0 & 1/2 & 0 & 0 & 0 & 0 \\ 0 & 0 & 0 & 0 & 0 & 0 & 0 & 0 & 0 & 0 \end{pmatrix}$$

$$T_2 = i \begin{pmatrix} 0 & -\sqrt{3}/2 & 0 & 0 & 0 & 0 & 0 & 0 & 0 & 0 \\ \sqrt{3}/2 & 0 & 0 & -1 & 0 & 0 & 0 & 0 & 0 & 0 \\ 0 & 0 & 0 & 0 & -1/\sqrt{2} & 0 & 0 & 0 & 0 & 0 \\ 0 & 1 & 0 & 0 & 0 & 0 & -\sqrt{3}/2 & 0 & 0 & 0 \\ 0 & 0 & 1/\sqrt{2} & 0 & 0 & 0 & 0 & -1/\sqrt{2} & 0 & 0 \\ 0 & 0 & 0 & 0 & 0 & 0 & 0 & 0 & -1/2 & 0 \\ 0 & 0 & 0 & \sqrt{3}/2 & 0 & 0 & 0 & 0 & 0 & 0 \\ 0 & 0 & 0 & 0 & 1/\sqrt{2} & 0 & 0 & 0 & 0 & 0 \\ 0 & 0 & 0 & 0 & 0 & 1/2 & 0 & 0 & 0 & 0 \\ 0 & 0 & 0 & 0 & 0 & 0 & 0 & 0 & 0 & 0 \end{pmatrix}$$

$$T_3 = \text{diag}\left(\frac{3}{2}, \frac{1}{2}, 1, -\frac{1}{2}, 0, \frac{1}{2}, -\frac{3}{2}, -1, -\frac{1}{2}, 0\right)$$

$$T_4 = \begin{pmatrix} 0 & 0 & \sqrt{3}/2 & 0 & 0 & 0 & 0 & 0 & 0 & 0 \\ 0 & 0 & 0 & 0 & 1/\sqrt{2} & 0 & 0 & 0 & 0 & 0 \\ \sqrt{3}/2 & 0 & 0 & 0 & 0 & 1 & 0 & 0 & 0 & 0 \\ 0 & 0 & 0 & 0 & 0 & 0 & 0 & 1/2 & 0 & 0 \\ 0 & 1/\sqrt{2} & 0 & 0 & 0 & 0 & 0 & 0 & 1/\sqrt{2} & 0 \\ 0 & 0 & 1 & 0 & 0 & 0 & 0 & 0 & 0 & \sqrt{3}/2 \\ 0 & 0 & 0 & 0 & 0 & 0 & 0 & 0 & 0 & 0 \\ 0 & 0 & 0 & 1/2 & 0 & 0 & 0 & 0 & 0 & 0 \\ 0 & 0 & 0 & 0 & 1/\sqrt{2} & 0 & 0 & 0 & 0 & 0 \\ 0 & 0 & 0 & 0 & 0 & \sqrt{3}/2 & 0 & 0 & 0 & 0 \end{pmatrix}$$

$$T_5 = i \begin{pmatrix} 0 & 0 & -\sqrt{3}/2 & 0 & 0 & 0 & 0 & 0 & 0 & 0 \\ 0 & 0 & 0 & 0 & -1/\sqrt{2} & 0 & 0 & 0 & 0 & 0 \\ \sqrt{3}/2 & 0 & 0 & 0 & 0 & -1 & 0 & 0 & 0 & 0 \\ 0 & 0 & 0 & 0 & 0 & 0 & 0 & -1/2 & 0 & 0 \\ 0 & 1/\sqrt{2} & 0 & 0 & 0 & 0 & 0 & 0 & -1/\sqrt{2} & 0 \\ 0 & 0 & 1 & 0 & 0 & 0 & 0 & 0 & 0 & -\sqrt{3}/2 \\ 0 & 0 & 0 & 0 & 0 & 0 & 0 & 0 & 0 & 0 \\ 0 & 0 & 0 & 1/2 & 0 & 0 & 0 & 0 & 0 & 0 \\ 0 & 0 & 0 & 0 & 1/\sqrt{2} & 0 & 0 & 0 & 0 & 0 \\ 0 & 0 & 0 & 0 & 0 & \sqrt{3}/2 & 0 & 0 & 0 & 0 \end{pmatrix}$$

$$T_6 = \begin{pmatrix} 0 & 0 & 0 & 0 & 0 & 0 & 0 & 0 & 0 & 0 \\ 0 & 0 & 1/2 & 0 & 0 & 0 & 0 & 0 & 0 & 0 \\ 0 & 1/2 & 0 & 0 & 0 & 0 & 0 & 0 & 0 & 0 \\ 0 & 0 & 0 & 0 & 1/\sqrt{2} & 0 & 0 & 0 & 0 & 0 \\ 0 & 0 & 0 & 1/\sqrt{2} & 0 & 1/\sqrt{2} & 0 & 0 & 0 & 0 \\ 0 & 0 & 0 & 0 & 1/\sqrt{2} & 0 & 0 & 0 & 0 & 0 \\ 0 & 0 & 0 & 0 & 0 & 0 & 0 & \sqrt{3}/2 & 0 & 0 \\ 0 & 0 & 0 & 0 & 0 & 0 & \sqrt{3}/2 & 0 & 1 & 0 \\ 0 & 0 & 0 & 0 & 0 & 0 & 0 & 1 & 0 & \sqrt{3}/2 \\ 0 & 0 & 0 & 0 & 0 & 0 & 0 & 0 & \sqrt{3}/2 & 0 \end{pmatrix}$$



$$T_7 = i \begin{pmatrix} 0 & 0 & 0 & 0 & 0 & 0 & 0 & 0 & 0 & 0 \\ 0 & 0 & -1/2 & 0 & 0 & 0 & 0 & 0 & 0 & 0 \\ 0 & 1/2 & 0 & 0 & 0 & 0 & 0 & 0 & 0 & 0 \\ 0 & 0 & 0 & 0 & -1/\sqrt{2} & 0 & 0 & 0 & 0 & 0 \\ 0 & 0 & 0 & 1/\sqrt{2} & 0 & -1/\sqrt{2} & 0 & 0 & 0 & 0 \\ 0 & 0 & 0 & 0 & 1/\sqrt{2} & 0 & 0 & 0 & 0 & 0 \\ 0 & 0 & 0 & 0 & 0 & 0 & 0 & -\sqrt{3}/2 & 0 & 0 \\ 0 & 0 & 0 & 0 & 0 & 0 & \sqrt{3}/2 & 0 & -1 & 0 \\ 0 & 0 & 0 & 0 & 0 & 0 & 0 & 1 & 0 & -\sqrt{3}/2 \\ 0 & 0 & 0 & 0 & 0 & 0 & 0 & 0 & \sqrt{3}/2 & 0 \end{pmatrix}$$

$$T_8 = \text{diag} \left( \frac{\sqrt{3}}{2}, \frac{\sqrt{3}}{2}, 0, \frac{\sqrt{3}}{2}, 0, -\frac{\sqrt{3}}{2}, \frac{\sqrt{3}}{2}, 0, -\frac{\sqrt{3}}{2}, -\sqrt{3} \right).$$

They satisfy the normalization condition (see Eq. (3.77))

$$\text{Tr} (T_i T_j) = \frac{15}{2} \delta_{ij}.$$



## G Example of calculation of subduction coefficients

In this Appendix, the calculation of SDCs is illustrated with a simple example. We take  $[\nu] = [4, 4, 3]$ ,  $[\nu_1] = [3, 3, 1]$  and  $[\nu_2] = [2, 1, 1]$  (thus  $n_1 = 7$ ,  $n_2 = 4$  and  $n = n_1 + n_2 = 11$ ).

First, we build all SYTs for the irrep  $[\nu]$  which are compatible with the irrep  $[\nu_1]$ . To perform the calculation of the SDCs, we take the largest SYT  $Y_{m_1=h[\nu_1]}^{[\nu_1]}$  but this choice is arbitrary since the SDCs do not depend on  $m_1$ . The 6 relevant SYTs  $Y_m^{[\nu]}$  ordered in ascending order of the LLOS are given by

$$\begin{array}{|c|c|c|c|} \hline 1 & 4 & 6 & 8 \\ \hline 2 & 5 & 7 & 9 \\ \hline 3 & 10 & 11 & \\ \hline \end{array}, \quad \begin{array}{|c|c|c|c|} \hline 1 & 4 & 6 & 8 \\ \hline 2 & 5 & 7 & 10 \\ \hline 3 & 9 & 11 & \\ \hline \end{array}, \quad \begin{array}{|c|c|c|c|} \hline 1 & 4 & 6 & 9 \\ \hline 2 & 5 & 7 & 10 \\ \hline 3 & 8 & 11 & \\ \hline \end{array}, \quad \begin{array}{|c|c|c|c|} \hline 1 & 4 & 6 & 8 \\ \hline 2 & 5 & 7 & 11 \\ \hline 3 & 9 & 10 & \\ \hline \end{array}, \quad \begin{array}{|c|c|c|c|} \hline 1 & 4 & 6 & 9 \\ \hline 2 & 5 & 7 & 11 \\ \hline 3 & 8 & 10 & \\ \hline \end{array}, \quad \begin{array}{|c|c|c|c|} \hline 1 & 4 & 6 & 10 \\ \hline 2 & 5 & 7 & 11 \\ \hline 3 & 8 & 9 & \\ \hline \end{array}. \quad (\text{G.1})$$

These SYTs define the Yamanouchi basis  $|Y_m^{[\nu]}\rangle$ ,  $m = 1, \dots, 6$  in which the CSCO of  $\mathcal{S}_{n_2}$  will be solved.

There are 3 SYTs  $Y_{m_2}^{[\nu_2]}$  associated with the irrep  $[\nu_2]$  (again in ascending order of the LLOS from left to right)

$$\begin{array}{|c|c|} \hline 1 & 2 \\ \hline 3 & \\ \hline 4 & \\ \hline \end{array}, \quad \begin{array}{|c|c|} \hline 1 & 3 \\ \hline 2 & \\ \hline 4 & \\ \hline \end{array}, \quad \begin{array}{|c|c|} \hline 1 & 4 \\ \hline 2 & \\ \hline 3 & \\ \hline \end{array}. \quad (\text{G.2})$$

We shall begin with the calculation of the SDCs for the smallest SYT  $m_2 = 1$  and then derive the other SDCs using Eq. (3.33).

To solve the CSCO of  $\mathcal{S}_{n_2}$  in the Yamanouchi basis  $|Y_m^{[\nu]}\rangle$  we compute the quadratic

## Appendix G. Example of calculation of subduction coefficients

Casimir of the canonical group chain of  $\mathcal{S}_{n_2}$  associated to  $Y_{m_2=1}^{[\nu_2]}$ . One has:

$$\begin{aligned} \begin{array}{|c|c|} \hline 1 & 2 \\ \hline 3 & \\ \hline 4 & \\ \hline \end{array} : C'_2(n_2 = 4) &= \mathcal{P}_{8,9} + \mathcal{P}_{8,10} + \mathcal{P}_{9,10} + \mathcal{P}_{8,11} + \mathcal{P}_{9,11} + \mathcal{P}_{10,11} = \lambda_2^{[\nu_2]} = -2 \\ \begin{array}{|c|c|} \hline 1 & 2 \\ \hline 3 & \\ \hline & \\ \hline \end{array} : C'_2(n_2 - 1 = 3) &= \mathcal{P}_{8,9} + \mathcal{P}_{8,10} + \mathcal{P}_{9,10} = \lambda_2^{[\nu'_2]} = 0 \\ \begin{array}{|c|c|} \hline 1 & 2 \\ \hline & \\ \hline & \\ \hline \end{array} : C'_2(n_2 - 2 = 2) &= \mathcal{P}_{8,9} = \lambda_2^{[\nu''_2]} = 1 \end{aligned} \quad (\text{G.3})$$

where  $\mathcal{P}_{i,j} \equiv (i, j)$  is the permutation operator which interchanges  $i$  with  $j$  and where  $\lambda_2^{[\nu]}$  is the eigenvalue of the quadratic Casimir operator given in Eq. (3.5).

The goal is now to find the state

$$\left| [\nu], 1 \begin{array}{cc} [\nu_1] & [\nu_2] \\ m_1 & 1 \end{array} \right\rangle$$

written in the basis of Eq. (G.1), which satisfies the three equations in (G.3) simultaneously (we have kept  $m_1$  arbitrary, but the calculation is performed with  $m_1 = h^{[\nu_1]}$ , as discussed above). This state will thus be expressed as

$$\left| [\nu], 1 \begin{array}{cc} [\nu_1] & [\nu_2] \\ m_1 & 1 \end{array} \right\rangle = \sum_m \left| \begin{array}{c} [\nu] \\ m \end{array} \right\rangle \left\langle \begin{array}{c} [\nu] \\ m \end{array} \right| \left| [\nu], 1 \begin{array}{cc} [\nu_1] & [\nu_2] \\ m_1 & 1 \end{array} \right\rangle \quad (\text{G.4})$$

where the multiplicity index is  $\tau = 1$ .

To lighten a bit the notation, we use

$$|\Phi_1\rangle \equiv \left| [\nu], 1 \begin{array}{cc} [\nu_1] & [\nu_2] \\ m_1 & 1 \end{array} \right\rangle. \quad (\text{G.5})$$

From a numerical point of view it is useful to reduce as much as possible the number of operators in the equations. One thus rewrite Eq. (G.3) as

$$\begin{aligned} (\mathcal{P}_{8,9} - 1) |\Phi_1\rangle &= 0 \\ (\mathcal{P}_{8,10} + \mathcal{P}_{9,10} + 1) |\Phi_1\rangle &= 0 \\ (\mathcal{P}_{8,11} + \mathcal{P}_{9,11} + \mathcal{P}_{10,11} + 2) |\Phi_1\rangle &= 0. \end{aligned} \quad (\text{G.6})$$

One then builds the operator  $\mathcal{O}$  defined as

$$\mathcal{O} = (\mathcal{P}_{8,9} - 1)^2 + (\mathcal{P}_{8,10} + \mathcal{P}_{9,10} + 1)^2 + (\mathcal{P}_{8,11} + \mathcal{P}_{9,11} + \mathcal{P}_{10,11} + 2)^2 \quad (\text{G.7})$$

and finds its kernel in the basis of SYTs for the irrep  $[\nu]$  given in Eq. (G.1). We find

$$|\Phi_1\rangle \equiv \left| [\nu], 1 \begin{smallmatrix} [\nu_1] \\ m_1 \end{smallmatrix} \begin{smallmatrix} [\nu_2] \\ 1 \end{smallmatrix} \right\rangle = \frac{\sqrt{15}}{8} \left| \begin{array}{|c|c|c|c|} \hline 1 & 4 & 6 & 8 \\ \hline 2 & 5 & 7 & 10 \\ \hline 3 & 9 & 11 & \\ \hline \end{array} \right\rangle + \frac{5}{8} \left| \begin{array}{|c|c|c|c|} \hline 1 & 4 & 6 & 9 \\ \hline 2 & 5 & 7 & 10 \\ \hline 3 & 8 & 11 & \\ \hline \end{array} \right\rangle - \frac{\sqrt{5}}{8} \left| \begin{array}{|c|c|c|c|} \hline 1 & 4 & 6 & 8 \\ \hline 2 & 5 & 7 & 11 \\ \hline 3 & 9 & 10 & \\ \hline \end{array} \right\rangle \\ - \frac{5}{8\sqrt{3}} \left| \begin{array}{|c|c|c|c|} \hline 1 & 4 & 6 & 9 \\ \hline 2 & 5 & 7 & 11 \\ \hline 3 & 8 & 10 & \\ \hline \end{array} \right\rangle + \frac{1}{\sqrt{6}} \left| \begin{array}{|c|c|c|c|} \hline 1 & 4 & 6 & 10 \\ \hline 2 & 5 & 7 & 11 \\ \hline 3 & 8 & 9 & \\ \hline \end{array} \right\rangle. \quad (\text{G.8})$$

The coefficients in this expression are the SDCs. Notice in particular that the coefficient of the first SYT in the expansion is chosen positive to satisfy the overall phase convention.

We can now compute the SDCs associated to the other SYTs for the irrep  $[\nu_2]$ .

Let us consider the second SYT (in ascending order of the LLOS)  $m_2 = 2$ . We first find the sequence of permutations which brings  $Y_1^{[\nu_2]}$  onto  $Y_{m_2=2}^{[\nu_2]}$ :

$$Y_1^{[\nu_2]} = \begin{array}{|c|c|} \hline 1 & 2 \\ \hline 3 & \\ \hline 4 & \\ \hline \end{array} \xrightarrow{(2,3)} \begin{array}{|c|c|} \hline 1 & 3 \\ \hline 2 & \\ \hline 4 & \\ \hline \end{array} = Y_{m_2=2}^{[\nu_2]}. \quad (\text{G.9})$$

The axial distance from 2 to 3 in the SYT  $Y_1^{[\nu_2]}$  being +2 we obtain, using the Young rules in Eq. (3.17),

$$\mathcal{P}_{2,3} \left| \begin{array}{|c|c|} \hline 1 & 2 \\ \hline 3 & \\ \hline 4 & \\ \hline \end{array} \right\rangle = -\frac{1}{2} \left| \begin{array}{|c|c|} \hline 1 & 2 \\ \hline 3 & \\ \hline 4 & \\ \hline \end{array} \right\rangle + \frac{\sqrt{3}}{2} \left| \begin{array}{|c|c|} \hline 1 & 3 \\ \hline 2 & \\ \hline 4 & \\ \hline \end{array} \right\rangle. \quad (\text{G.10})$$

One then defines the operator  $T_2 \in \mathcal{S}_{n_2}(1, \dots, n_2)$  as

$$T_2 = \frac{\mathcal{P}_{2,3} + \frac{1}{2}}{\sqrt{3}/2} \quad (\text{G.11})$$

which is such that

$$|Y_{m_2=2}^{[\nu_2]}\rangle = \left| \begin{array}{|c|c|} \hline 1 & 3 \\ \hline 2 & \\ \hline 4 & \\ \hline \end{array} \right\rangle = T_2 \left| \begin{array}{|c|c|} \hline 1 & 2 \\ \hline 3 & \\ \hline 4 & \\ \hline \end{array} \right\rangle = T_2 |Y_1^{[\nu_2]}\rangle. \quad (\text{G.12})$$

Now we apply on the state  $|\Phi_1\rangle$  the operator  $T'_2 \in \mathcal{S}_{n_2}(n_1 + 1, \dots, n)$  obtained from  $T_2$  by transforming the permutation  $\mathcal{P}_{i,j}$  acting in  $\mathcal{S}_{n_2}(1, \dots, n_2)$  onto the permutation  $\mathcal{P}_{i+n_1, j+n_1}$  acting on the irrep  $[\nu]$ . This defines the state  $|\Phi_2\rangle$  which will contain the SDCs associated to  $Y_{m_2=2}^{[\nu_2]}$ ,

$$|\Phi_2\rangle = T'_2 |\Phi_1\rangle = \frac{\mathcal{P}_{9,10} + \frac{1}{2}}{\sqrt{3}/2} |\Phi_1\rangle. \quad (\text{G.13})$$

## Appendix G. Example of calculation of subduction coefficients

Using again the Young rules to extract the action of  $\mathcal{P}_{9,10}$  in the Yamanouchi basis  $|Y_m^{[\nu]}\rangle$  we finally obtain

$$|\Phi_2\rangle \equiv \left| [\nu], 1 \begin{array}{cc} [\nu_1] & [\nu_2] \\ m_1 & 2 \end{array} \right\rangle = \frac{1}{3}\sqrt{\frac{5}{2}} \left| \begin{array}{|c|c|c|c|} \hline 1 & 4 & 6 & 8 \\ \hline 2 & 5 & 7 & 9 \\ \hline 3 & 10 & 11 & \\ \hline \end{array} \right\rangle + \frac{5\sqrt{5}}{24} \left| \begin{array}{|c|c|c|c|} \hline 1 & 4 & 6 & 8 \\ \hline 2 & 5 & 7 & 10 \\ \hline 3 & 9 & 11 & \\ \hline \end{array} \right\rangle - \frac{5}{8\sqrt{3}} \left| \begin{array}{|c|c|c|c|} \hline 1 & 4 & 6 & 9 \\ \hline 2 & 5 & 7 & 10 \\ \hline 3 & 8 & 11 & \\ \hline \end{array} \right\rangle \\ - \frac{\sqrt{15}}{8} \left| \begin{array}{|c|c|c|c|} \hline 1 & 4 & 6 & 8 \\ \hline 2 & 5 & 7 & 11 \\ \hline 3 & 9 & 10 & \\ \hline \end{array} \right\rangle + \frac{3}{8} \left| \begin{array}{|c|c|c|c|} \hline 1 & 4 & 6 & 9 \\ \hline 2 & 5 & 7 & 11 \\ \hline 3 & 8 & 10 & \\ \hline \end{array} \right\rangle. \quad (\text{G.14})$$

Finally let us consider the last SYT  $Y_{m_2=3}^{[\nu_2]}$ . The sequence of operations which transforms  $Y_1^{[\nu_2]}$  onto this SYT is

$$Y_1^{[\nu_2]} = \begin{array}{|c|c|} \hline 1 & 2 \\ \hline 3 & 4 \\ \hline \end{array} \xrightarrow{(2,3)} \begin{array}{|c|c|} \hline 1 & 3 \\ \hline 2 & 4 \\ \hline \end{array} \xrightarrow{(3,4)} \begin{array}{|c|c|} \hline 1 & 4 \\ \hline 2 & 3 \\ \hline \end{array} = Y_{m_2=3}^{[\nu_2]}. \quad (\text{G.15})$$

We then define the operator

$$T_2 = \frac{\mathcal{P}_{3,4} + \frac{1}{3}}{\sqrt{8/3}} \frac{\mathcal{P}_{2,3} + \frac{1}{2}}{\sqrt{3/2}} \quad (\text{G.16})$$

which is such that

$$|Y_{m_2=3}^{[\nu_2]}\rangle = \left| \begin{array}{|c|c|} \hline 1 & 4 \\ \hline 2 & 3 \\ \hline \end{array} \right\rangle = T_2 \left| \begin{array}{|c|c|} \hline 1 & 2 \\ \hline 3 & 4 \\ \hline \end{array} \right\rangle = T_2 |Y_1^{[\nu_2]}\rangle. \quad (\text{G.17})$$

Defining  $T'_2$  as

$$T'_2 = \frac{\mathcal{P}_{10,11} + \frac{1}{3}}{\sqrt{8/3}} \frac{\mathcal{P}_{9,10} + \frac{1}{2}}{\sqrt{3/2}} \quad (\text{G.18})$$

one gets

$$|\Phi_3\rangle \equiv \left| [\nu], 1 \begin{array}{cc} [\nu_1] & [\nu_2] \\ m_1 & 3 \end{array} \right\rangle = T'_2 |\Phi_1\rangle \\ = \frac{\sqrt{5}}{3} \left| \begin{array}{|c|c|c|c|} \hline 1 & 4 & 6 & 8 \\ \hline 2 & 5 & 7 & 9 \\ \hline 3 & 10 & 11 & \\ \hline \end{array} \right\rangle - \frac{1}{3}\sqrt{\frac{5}{2}} \left| \begin{array}{|c|c|c|c|} \hline 1 & 4 & 6 & 8 \\ \hline 2 & 5 & 7 & 10 \\ \hline 3 & 9 & 11 & \\ \hline \end{array} \right\rangle + \frac{1}{\sqrt{6}} \left| \begin{array}{|c|c|c|c|} \hline 1 & 4 & 6 & 9 \\ \hline 2 & 5 & 7 & 10 \\ \hline 3 & 8 & 11 & \\ \hline \end{array} \right\rangle. \quad (\text{G.19})$$

The method presented above for the calculation of the SDCs, although being convenient because extremely simple, is not ideal in actual calculations when the total number  $n$  of boxes increases. Indeed, the number of SYTs for the irrep  $[\nu]$  compatible with the irrep  $[\nu_1]$  increases dangerously with  $n$  and  $n_2$ . Thus it becomes more and more difficult to build the operator  $\mathcal{O}$  in Eq. (G.7), and to extract its kernel. To overcome this issue, a “shortcut” has been devised in Ref. [89]. Instead of seeing  $[\nu_2]$  as a tensor product of fundamental irreps one interprets the irrep  $[\nu_2]$  as being obtained from the tensor product of fully antisymmetric irreps. Actually, one can also interpret

---

it as being obtained from a tensor product of fully symmetric irreps. This trick allows us to drastically reduce the algorithmic complexity and it is absolutely necessary to implement it when SDCs for bigger irreps need to be computed. We shall not repeat here the details of the procedure as it can straightforwardly be obtained from the development above and following Ref. [89].





# H Example of calculation of a reduced matrix element

In this appendix we illustrate the procedure to compute the  $SU(3)$  reduced matrix element of the interaction

$$\left\langle [\gamma], \begin{smallmatrix} [\chi_3] \\ \mathbf{l}_3 \end{smallmatrix} \begin{smallmatrix} [\chi_4] \\ \mathbf{l}_4 \end{smallmatrix} \left| \mathcal{H}_{(L+1, L+2)} \right| [\gamma], \begin{smallmatrix} [\chi_1] \\ \mathbf{l}_1 \end{smallmatrix} \begin{smallmatrix} [\chi_2] \\ \mathbf{l}_2 \end{smallmatrix} \right\rangle \quad (\text{H.1})$$

when

$$([\chi_1], \mathbf{l}_1) = \begin{array}{|c|c|c|c|} \hline & & \times & \times \\ \hline & \times & & \\ \hline \end{array}, \quad ([\chi_2], \mathbf{l}_2) = \begin{array}{|c|c|c|c|} \hline & & \times & \times \\ \hline & \times & & \\ \hline \end{array}, \quad (\text{H.2})$$

$$([\chi_3], \mathbf{l}_3) = \begin{array}{|c|c|c|} \hline & & \times \\ \hline & \times & \\ \hline \times & & \\ \hline \end{array}, \quad ([\chi_4], \mathbf{l}_4) = \begin{array}{|c|c|c|} \hline & & \times \\ \hline & \times & \\ \hline \times & & \\ \hline \end{array} \quad (\text{H.3})$$

and the global singlet irrep

$$[\gamma] = \begin{array}{|c|c|c|c|} \hline & & & \\ \hline & & & \\ \hline & & & \\ \hline & & & \\ \hline \end{array}. \quad (\text{H.4})$$

This example was provided in Ref. [57]. We give here a number of additional details on this calculation.

We will show that

$$\left\langle [\gamma], \begin{smallmatrix} [\chi_3] \\ \mathbf{l}_3 \end{smallmatrix} \begin{smallmatrix} [\chi_4] \\ \mathbf{l}_4 \end{smallmatrix} \left| \mathcal{H}_{(L+1, L+2)} \right| [\gamma], \begin{smallmatrix} [\chi_1] \\ \mathbf{l}_1 \end{smallmatrix} \begin{smallmatrix} [\chi_2] \\ \mathbf{l}_2 \end{smallmatrix} \right\rangle = \frac{2\sqrt{6}}{5}. \quad (\text{H.5})$$

The multiplicity index  $\tau$  takes a single value  $\tau = 1$  because the target irrep  $[\gamma]$  appears only once in the tensor products  $[\chi_1] \otimes [\chi_2]$  and  $[\chi_3] \otimes [\chi_4]$ , and is thus ignored in the basis elements of the non-standard basis.

## Appendix H. Example of calculation of a reduced matrix element

First, we proceed to the following replacements

$$([\chi_1], l_1) = \begin{array}{|c|c|c|c|} \hline & & \times & \times \\ \hline & & & \\ \hline \end{array} \rightarrow \begin{array}{|c|c|c|c|} \hline & & 4 & 5 \\ \hline & 6 & & \\ \hline \end{array} \rightarrow \begin{array}{|c|c|c|c|} \hline 1 & 2 & 4 & 5 \\ \hline 3 & 6 & & \\ \hline \end{array} =: Y_{m_1(l_1)}^{[\chi_1]}, \quad (\text{H.6})$$

and

$$([\chi_2], l_2) = \begin{array}{|c|c|c|c|} \hline & & \times & \times \\ \hline & & & \\ \hline \end{array} \rightarrow \begin{array}{|c|c|c|c|} \hline & & 4 & 5 \\ \hline & 6 & & \\ \hline \end{array} \rightarrow \begin{array}{|c|c|c|c|} \hline 1 & 2 & 4 & 5 \\ \hline 3 & 6 & & \\ \hline \end{array} =: Y_{m_2(l_2)}^{[\chi_2]}. \quad (\text{H.7})$$

Solving the CSCO we obtain that the ket is expressed with a single term,

$$\left| [\gamma], \begin{array}{c} [\chi_1] \\ l_1 \end{array} \begin{array}{c} [\chi_2] \\ l_2 \end{array} \right\rangle = \left| \begin{array}{|c|c|c|c|} \hline 1 & 2 & 4 & 5 \\ \hline 3 & 6 & 7 & 10 \\ \hline 8 & 9 & 11 & 12 \\ \hline \end{array} \right\rangle \equiv \left| \begin{array}{|c|c|c|c|} \hline & & & \\ \hline & & & \\ \hline & & & \\ \hline \end{array} \right\rangle. \quad (\text{H.8})$$

We have of course dealt with the Yamanouchi relative phase since  $Y_{m_2(l_2)}^{[\chi_2]}$  is not the first SYT in the LLOS for the shape  $[\chi_2]$ .

The Young tableau in the middle of Eq. (H.8) is the *representative* of the equivalence class given in the right. In other words, it is a representative of a state satisfying the local symmetry at sites  $L + 1$  and  $L + 2$ . In order not to confuse it with a Yamanouchi basis vector, we should use the Young diagram (not the Young tableau) with the color scheme to denote this state. The colors allow us to keep track of the positions of the particles at sites  $L + 1$  and  $L + 2$ . Notice that in general, in Eq. (H.8) we would obtain a linear combination of representatives of equivalence classes. One must now rewrite Eq. (H.8) in the Yamanouchi basis. This is easily done using Ref. [87]. We obtain

$$\begin{aligned} \left| [\gamma], \begin{array}{c} [\chi_1] \\ l_1 \end{array} \begin{array}{c} [\chi_2] \\ l_2 \end{array} \right\rangle &= \left| \begin{array}{|c|c|c|c|} \hline & & & \\ \hline & & & \\ \hline & & & \\ \hline \end{array} \right\rangle \\ &= \frac{1}{9} \left| \begin{array}{|c|c|c|c|} \hline 1 & 2 & 4 & 5 \\ \hline 3 & 6 & 7 & 10 \\ \hline 8 & 9 & 11 & 12 \\ \hline \end{array} \right\rangle + \frac{\sqrt{2}}{9} \left| \begin{array}{|c|c|c|c|} \hline 1 & 2 & 4 & 6 \\ \hline 3 & 5 & 7 & 10 \\ \hline 8 & 9 & 11 & 12 \\ \hline \end{array} \right\rangle + \frac{1}{3} \sqrt{\frac{2}{3}} \left| \begin{array}{|c|c|c|c|} \hline 1 & 2 & 5 & 6 \\ \hline 3 & 4 & 7 & 10 \\ \hline 8 & 9 & 11 & 12 \\ \hline \end{array} \right\rangle \\ &+ \frac{\sqrt{2}}{9} \left| \begin{array}{|c|c|c|c|} \hline 1 & 2 & 4 & 5 \\ \hline 3 & 6 & 8 & 10 \\ \hline 7 & 9 & 11 & 12 \\ \hline \end{array} \right\rangle + \frac{2}{9} \left| \begin{array}{|c|c|c|c|} \hline 1 & 2 & 4 & 6 \\ \hline 3 & 5 & 8 & 10 \\ \hline 7 & 9 & 11 & 12 \\ \hline \end{array} \right\rangle + \frac{2}{3\sqrt{3}} \left| \begin{array}{|c|c|c|c|} \hline 1 & 2 & 5 & 6 \\ \hline 3 & 4 & 8 & 10 \\ \hline 7 & 9 & 11 & 12 \\ \hline \end{array} \right\rangle \\ &+ \frac{1}{3} \sqrt{\frac{2}{3}} \left| \begin{array}{|c|c|c|c|} \hline 1 & 2 & 4 & 5 \\ \hline 3 & 6 & 9 & 10 \\ \hline 7 & 8 & 11 & 12 \\ \hline \end{array} \right\rangle + \frac{2}{3\sqrt{3}} \left| \begin{array}{|c|c|c|c|} \hline 1 & 2 & 4 & 6 \\ \hline 3 & 5 & 9 & 10 \\ \hline 7 & 8 & 11 & 12 \\ \hline \end{array} \right\rangle + \frac{2}{3} \left| \begin{array}{|c|c|c|c|} \hline 1 & 2 & 5 & 6 \\ \hline 3 & 4 & 9 & 10 \\ \hline 7 & 8 & 11 & 12 \\ \hline \end{array} \right\rangle. \end{aligned} \quad (\text{H.9})$$

We can now apply the interaction  $\mathcal{H}_{(L+1, L+2)}$  on this expansion using the Young rules (in the right-hand side of the following equation, each SYT should be written in a ket;

we omit the ket to lighten the notation)

$$\begin{aligned}
& \mathcal{H}_{(L+1,L+2)} \left| [\gamma], \begin{smallmatrix} [\chi_1] \\ l_1 \end{smallmatrix} \begin{smallmatrix} [\chi_2] \\ l_2 \end{smallmatrix} \right\rangle = \\
& -\frac{1}{45} \begin{smallmatrix} 1 & 2 & 4 & 5 \\ 3 & 6 & 7 & 10 \\ 8 & 9 & 11 & 12 \end{smallmatrix} - \frac{\sqrt{2}}{45} \begin{smallmatrix} 1 & 2 & 4 & 5 \\ 3 & 6 & 8 & 10 \\ 7 & 9 & 11 & 12 \end{smallmatrix} - \frac{1}{15} \sqrt{\frac{2}{3}} \begin{smallmatrix} 1 & 2 & 4 & 5 \\ 3 & 6 & 9 & 10 \\ 7 & 8 & 11 & 12 \end{smallmatrix} - \frac{\sqrt{2}}{45} \begin{smallmatrix} 1 & 2 & 4 & 6 \\ 3 & 5 & 7 & 10 \\ 8 & 9 & 11 & 12 \end{smallmatrix} - \frac{2}{45} \begin{smallmatrix} 1 & 2 & 4 & 6 \\ 3 & 5 & 8 & 10 \\ 7 & 9 & 11 & 12 \end{smallmatrix} \\
& - \frac{2}{15\sqrt{3}} \begin{smallmatrix} 1 & 2 & 4 & 6 \\ 3 & 5 & 9 & 10 \\ 7 & 8 & 11 & 12 \end{smallmatrix} - \frac{1}{15} \sqrt{\frac{2}{3}} \begin{smallmatrix} 1 & 2 & 5 & 6 \\ 3 & 4 & 7 & 10 \\ 8 & 9 & 11 & 12 \end{smallmatrix} - \frac{2}{15\sqrt{3}} \begin{smallmatrix} 1 & 2 & 5 & 6 \\ 3 & 4 & 8 & 10 \\ 7 & 9 & 11 & 12 \end{smallmatrix} - \frac{2}{15} \begin{smallmatrix} 1 & 2 & 5 & 6 \\ 3 & 4 & 9 & 10 \\ 7 & 8 & 11 & 12 \end{smallmatrix} \\
& + \frac{1}{40} \sqrt{\frac{3}{2}} \begin{smallmatrix} 1 & 2 & 4 & 7 \\ 3 & 5 & 8 & 10 \\ 6 & 9 & 11 & 12 \end{smallmatrix} + \frac{3}{40\sqrt{2}} \begin{smallmatrix} 1 & 2 & 4 & 7 \\ 3 & 5 & 9 & 10 \\ 6 & 8 & 11 & 12 \end{smallmatrix} + \frac{3}{40\sqrt{2}} \begin{smallmatrix} 1 & 2 & 4 & 8 \\ 3 & 5 & 7 & 10 \\ 6 & 9 & 11 & 12 \end{smallmatrix} + \frac{1}{8} \sqrt{\frac{3}{10}} \begin{smallmatrix} 1 & 2 & 4 & 9 \\ 3 & 5 & 7 & 10 \\ 6 & 8 & 11 & 12 \end{smallmatrix} \\
& + \frac{1}{8} \sqrt{\frac{3}{10}} \begin{smallmatrix} 1 & 2 & 4 & 8 \\ 3 & 5 & 9 & 10 \\ 6 & 7 & 11 & 12 \end{smallmatrix} + \frac{3}{8\sqrt{10}} \begin{smallmatrix} 1 & 2 & 4 & 9 \\ 3 & 5 & 8 & 10 \\ 6 & 7 & 11 & 12 \end{smallmatrix} + \frac{3}{40\sqrt{2}} \begin{smallmatrix} 1 & 2 & 4 & 7 \\ 3 & 6 & 8 & 10 \\ 5 & 9 & 11 & 12 \end{smallmatrix} + \frac{3}{40} \sqrt{\frac{3}{2}} \begin{smallmatrix} 1 & 2 & 4 & 7 \\ 3 & 6 & 9 & 10 \\ 5 & 8 & 11 & 12 \end{smallmatrix} \\
& + \frac{3}{40} \sqrt{\frac{3}{2}} \begin{smallmatrix} 1 & 2 & 4 & 8 \\ 3 & 6 & 7 & 10 \\ 5 & 9 & 11 & 12 \end{smallmatrix} + \frac{3}{8\sqrt{10}} \begin{smallmatrix} 1 & 2 & 4 & 9 \\ 3 & 6 & 7 & 10 \\ 5 & 8 & 11 & 12 \end{smallmatrix} + \frac{3}{8\sqrt{10}} \begin{smallmatrix} 1 & 2 & 4 & 9 \\ 3 & 6 & 9 & 10 \\ 5 & 7 & 11 & 12 \end{smallmatrix} + \frac{3}{8} \sqrt{\frac{3}{10}} \begin{smallmatrix} 1 & 2 & 4 & 9 \\ 3 & 6 & 8 & 10 \\ 5 & 7 & 11 & 12 \end{smallmatrix} \\
& + \frac{3}{40\sqrt{2}} \begin{smallmatrix} 1 & 2 & 5 & 7 \\ 3 & 4 & 8 & 10 \\ 6 & 9 & 11 & 12 \end{smallmatrix} + \frac{3}{40} \sqrt{\frac{3}{2}} \begin{smallmatrix} 1 & 2 & 5 & 7 \\ 3 & 4 & 9 & 10 \\ 6 & 8 & 11 & 12 \end{smallmatrix} + \frac{3}{40} \sqrt{\frac{3}{2}} \begin{smallmatrix} 1 & 2 & 5 & 8 \\ 3 & 4 & 7 & 10 \\ 6 & 9 & 11 & 12 \end{smallmatrix} + \frac{3}{8\sqrt{10}} \begin{smallmatrix} 1 & 2 & 5 & 9 \\ 3 & 4 & 7 & 10 \\ 6 & 8 & 11 & 12 \end{smallmatrix} \\
& + \frac{3}{8\sqrt{10}} \begin{smallmatrix} 1 & 2 & 5 & 8 \\ 3 & 4 & 9 & 10 \\ 6 & 7 & 11 & 12 \end{smallmatrix} + \frac{3}{8} \sqrt{\frac{3}{10}} \begin{smallmatrix} 1 & 2 & 5 & 9 \\ 3 & 4 & 8 & 10 \\ 6 & 7 & 11 & 12 \end{smallmatrix} + \frac{1}{8} \sqrt{\frac{3}{10}} \begin{smallmatrix} 1 & 2 & 6 & 7 \\ 3 & 4 & 8 & 10 \\ 5 & 9 & 11 & 12 \end{smallmatrix} + \frac{3}{8\sqrt{10}} \begin{smallmatrix} 1 & 2 & 6 & 7 \\ 3 & 4 & 9 & 10 \\ 5 & 8 & 11 & 12 \end{smallmatrix} \\
& + \frac{3}{8\sqrt{10}} \begin{smallmatrix} 1 & 2 & 6 & 8 \\ 3 & 4 & 7 & 10 \\ 5 & 9 & 11 & 12 \end{smallmatrix} + \frac{1}{8} \sqrt{\frac{3}{2}} \begin{smallmatrix} 1 & 2 & 6 & 9 \\ 3 & 4 & 7 & 10 \\ 5 & 8 & 11 & 12 \end{smallmatrix} + \frac{1}{8} \sqrt{\frac{3}{2}} \begin{smallmatrix} 1 & 2 & 6 & 8 \\ 3 & 4 & 9 & 10 \\ 5 & 7 & 11 & 12 \end{smallmatrix} + \frac{3}{8\sqrt{2}} \begin{smallmatrix} 1 & 2 & 6 & 9 \\ 3 & 4 & 8 & 10 \\ 5 & 7 & 11 & 12 \end{smallmatrix} \\
& + \frac{1}{8} \sqrt{\frac{3}{10}} \begin{smallmatrix} 1 & 2 & 5 & 7 \\ 3 & 6 & 8 & 10 \\ 4 & 9 & 11 & 12 \end{smallmatrix} + \frac{3}{8\sqrt{10}} \begin{smallmatrix} 1 & 2 & 5 & 7 \\ 3 & 6 & 9 & 10 \\ 4 & 8 & 11 & 12 \end{smallmatrix} + \frac{3}{8\sqrt{10}} \begin{smallmatrix} 1 & 2 & 5 & 8 \\ 3 & 6 & 7 & 10 \\ 4 & 9 & 11 & 12 \end{smallmatrix} + \frac{1}{8} \sqrt{\frac{3}{2}} \begin{smallmatrix} 1 & 2 & 5 & 9 \\ 3 & 6 & 7 & 10 \\ 4 & 8 & 11 & 12 \end{smallmatrix} \\
& + \frac{1}{8} \sqrt{\frac{3}{2}} \begin{smallmatrix} 1 & 2 & 5 & 8 \\ 3 & 6 & 9 & 10 \\ 4 & 7 & 11 & 12 \end{smallmatrix} + \frac{3}{8\sqrt{2}} \begin{smallmatrix} 1 & 2 & 5 & 9 \\ 3 & 6 & 8 & 10 \\ 4 & 7 & 11 & 12 \end{smallmatrix} + \frac{3}{8\sqrt{10}} \begin{smallmatrix} 1 & 2 & 6 & 7 \\ 3 & 5 & 8 & 10 \\ 4 & 9 & 11 & 12 \end{smallmatrix} + \frac{3}{8} \sqrt{\frac{3}{10}} \begin{smallmatrix} 1 & 2 & 6 & 7 \\ 3 & 5 & 9 & 10 \\ 4 & 8 & 11 & 12 \end{smallmatrix} \\
& + \frac{3}{8} \sqrt{\frac{3}{10}} \begin{smallmatrix} 1 & 2 & 6 & 8 \\ 3 & 5 & 7 & 10 \\ 4 & 9 & 11 & 12 \end{smallmatrix} + \frac{3}{8\sqrt{2}} \begin{smallmatrix} 1 & 2 & 6 & 9 \\ 3 & 5 & 7 & 10 \\ 4 & 8 & 11 & 12 \end{smallmatrix} + \frac{3}{8\sqrt{2}} \begin{smallmatrix} 1 & 2 & 6 & 8 \\ 3 & 5 & 9 & 10 \\ 4 & 7 & 11 & 12 \end{smallmatrix} + \frac{3}{8} \sqrt{\frac{3}{2}} \begin{smallmatrix} 1 & 2 & 6 & 9 \\ 3 & 5 & 8 & 10 \\ 4 & 7 & 11 & 12 \end{smallmatrix}.
\end{aligned}$$

(H.10)

We have clustered the SYTs into two groups. The first 9 SYTs obviously belong to the equivalence class that we have already encountered,

$$\begin{smallmatrix} & & & \\ & & & \\ & & & \\ & & & \end{smallmatrix}$$

(H.11)

## Appendix H. Example of calculation of a reduced matrix element

while the 36 last SYTs belong to another equivalence class,

$$\begin{array}{|c|c|c|c|} \hline & & \text{orange} & \text{blue} \\ \hline & \text{orange} & \text{blue} & \\ \hline \text{orange} & & & \\ \hline \end{array}. \quad (\text{H.12})$$

Looking at Eq. (H.9) (or performing the change of basis explicitly) one rewrites Eq. (H.10) as

$$\mathcal{H}_{(L+1,L+2)} \left| [\gamma], \begin{smallmatrix} [\chi_1] \\ \mathbf{l}_1 \end{smallmatrix} \begin{smallmatrix} [\chi_2] \\ \mathbf{l}_2 \end{smallmatrix} \right\rangle = -\frac{1}{5} \left| \begin{array}{|c|c|c|c|} \hline & & \text{orange} & \text{orange} \\ \hline & \text{orange} & \text{blue} & \\ \hline \text{blue} & & & \\ \hline \end{array} \right\rangle + \frac{2\sqrt{6}}{5} \left| \begin{array}{|c|c|c|c|} \hline & & \text{orange} & \text{blue} \\ \hline & \text{orange} & \text{blue} & \\ \hline \text{orange} & & & \\ \hline \end{array} \right\rangle. \quad (\text{H.13})$$

Now we look at the bra in Eq. (H.1). We proceed to the following replacement

$$([\chi_3], \mathbf{l}_3) = \begin{array}{|c|c|c|} \hline & & \times \\ \hline & \times & \\ \hline \times & & \\ \hline \end{array} \longrightarrow \begin{array}{|c|c|c|} \hline & & 4 \\ \hline & 5 & \\ \hline 6 & & \\ \hline \end{array} \longrightarrow \begin{array}{|c|c|c|} \hline 1 & 2 & 4 \\ \hline 3 & 5 & \\ \hline 6 & & \\ \hline \end{array} =: Y_{m_3(\mathbf{l}_3)}^{[\chi_3]}, \quad (\text{H.14})$$

and

$$([\chi_4], \mathbf{l}_4) = \begin{array}{|c|c|c|} \hline & & \times \\ \hline & \times & \\ \hline \times & & \\ \hline \end{array} \longrightarrow \begin{array}{|c|c|c|} \hline & & 4 \\ \hline & 5 & \\ \hline 6 & & \\ \hline \end{array} \longrightarrow \begin{array}{|c|c|c|} \hline 1 & 2 & 4 \\ \hline 3 & 5 & \\ \hline 6 & & \\ \hline \end{array} =: Y_{m_4(\mathbf{l}_4)}^{[\chi_4]}. \quad (\text{H.15})$$

Solving the CSCO we get that the bra is expanded in terms of a single state

$$\left\langle [\gamma], \begin{smallmatrix} [\chi_3] \\ \mathbf{l}_3 \end{smallmatrix} \begin{smallmatrix} [\chi_4] \\ \mathbf{l}_4 \end{smallmatrix} \right| = \left\langle \begin{array}{|c|c|c|c|} \hline & & \text{orange} & \text{blue} \\ \hline & \text{orange} & \text{blue} & \\ \hline \text{orange} & & & \\ \hline \end{array} \right|. \quad (\text{H.16})$$

One can now compute the overlap between Eq. (H.13) and (H.16)

$$\left\langle [\gamma], \begin{smallmatrix} [\chi_3] \\ \mathbf{l}_3 \end{smallmatrix} \begin{smallmatrix} [\chi_4] \\ \mathbf{l}_4 \end{smallmatrix} \right| \mathcal{H}_{(L+1,L+2)} \left| [\gamma], \begin{smallmatrix} [\chi_1] \\ \mathbf{l}_1 \end{smallmatrix} \begin{smallmatrix} [\chi_2] \\ \mathbf{l}_2 \end{smallmatrix} \right\rangle = \frac{2\sqrt{6}}{5}. \quad (\text{H.17})$$

We shall note now that this matrix element will occur when the chain length  $N_s = 2(L+1)$  satisfies  $L = 3q+1$  where  $q$  is any positive integer. Thus, once the number of irreps  $M$  has been fixed, there is a finite number of reduced matrix elements to compute.

# Bibliography

- [1] W. Heisenberg, [Z. Phys. \*\*49\*\*, 580 \(1928\)](#).
- [2] F. Bloch, [Z. Phys. \*\*61\*\*, 206 \(1930\)](#).
- [3] H. Bethe, [Z. Phys. \*\*71\*\*, 205 \(1931\)](#).
- [4] J. C. Bonner and M. E. Fisher, [Phys. Rev. \*\*135\*\*, A640 \(1964\)](#).
- [5] H. Q. Lin, [Phys. Rev. B \*\*42\*\*, 6561 \(1990\)](#).
- [6] H. G. Evertz, G. Lana, and M. Marcu, [Phys. Rev. Lett. \*\*70\*\*, 875 \(1993\)](#).
- [7] H. G. Evertz and M. Marcu, [Nucl. Phys. B \(Proc. Suppl.\) \*\*30\*\*, 277 \(1993\)](#).
- [8] S. Todo and K. Kato, [Phys. Rev. Lett. \*\*87\*\*, 047203 \(2001\)](#).
- [9] S. R. White, [Phys. Rev. Lett. \*\*69\*\*, 2863 \(1992\)](#).
- [10] S. R. White, [Phys. Rev. B \*\*48\*\*, 10345 \(1993\)](#).
- [11] S. Östlund and S. Rommer, [Phys. Rev. Lett. \*\*75\*\*, 3537 \(1995\)](#).
- [12] G. Vidal, [Phys. Rev. Lett. \*\*91\*\*, 147902 \(2003\)](#).
- [13] J. Jordan, R. Orús, G. Vidal, F. Verstraete, and J. I. Cirac, [Phys. Rev. Lett. \*\*101\*\*, 250602 \(2008\)](#).
- [14] G. Vidal, [Phys. Rev. Lett. \*\*101\*\*, 110501 \(2008\)](#).
- [15] M. Mourigal, M. Enderle, A. Klöpperpieper, J.-S. Caux, A. Stunault, and H. M. Rønnow, [Nat. Phys. \*\*9\*\*, 435 \(2013\)](#).
- [16] J. P. Renard, M. Verdaguer, L. P. Regnault, W. A. C. Erkelens, J. Rossat-Mignod, J. Ribas, W. G. Stirling, and C. Vettier, [J. Appl. Phys. \*\*63\*\*, 3538 \(1988\)](#).
- [17] S. Ma, C. Broholm, D. H. Reich, B. J. Sternlieb, and R. W. Erwin, [Phys. Rev. Lett. \*\*69\*\*, 3571 \(1992\)](#).

## Bibliography

---

- [18] L. P. Regnault, J. Rossat-Mignod, and J. P. Renard, *J. Magn. Magn. Mat.* **104-107**, 869 (1992).
- [19] W. J. L. Buyers, R. M. Morra, R. L. Armstrong, M. J. Hogan, P. Gerlach, and K. Hirakawa, *Phys. Rev. Lett.* **56**, 371 (1986).
- [20] M. Steiner, K. Kakurai, J. K. Kjems, D. Petitgrand, and R. Pynn, *J. Appl. Phys.* **61**, 3953 (1987).
- [21] R. M. Morra, W. J. L. Buyers, R. L. Armstrong, and K. Hirakawa, *Phys. Rev. B* **38**, 543 (1988).
- [22] I. A. Zaliznyak, *J. Appl. Phys.* **91**, 8390 (2002).
- [23] M. Niel, C. Cros, G. Le Flem, M. Pouchard, and P. Hagenmuller, *Physica B+C* **86-88**, 702 (1977).
- [24] K. Hirakawa, H. Ikeda, H. Kadowaki, and K. Ubukoshi, *J. Phys. Soc. Jpn.* **52**, 2882 (1983).
- [25] C. Payen, P. Molinie, P. Colombet, and G. Fillion, *J. Mag. Mag. Mat.* **84**, 95 (1990).
- [26] C. Payen, H. Mutka, J. Soubeyroux, P. Molinié, and P. Colombet, *J. Magn. Magn. Mat.* **104-107**, 797 (1992), proceedings of the International Conference on Magnetism, Part II.
- [27] P. Day, A. Gregson, D. Leech, M. Hutchings, and B. Rainford, *J. Magn. Magn. Mat.* **14**, 166 (1979).
- [28] Y. Tazuke, H. Tanaka, K. Iio, and K. Nagata, *J. Phys. Soc. Jpn.* **53**, 3191 (1984).
- [29] M. Hagiwara, Y. Idutsu, Z. Honda, and S. Yamamoto, *J. Phys.: Conf. Ser.* **400**, 032014 (2012).
- [30] S. K. Niesen, O. Heyer, T. Lorenz, and M. Valldor, *J. Magn. Magn. Mat.* **323**, 2575 (2011).
- [31] F. D. M. Haldane, *Phys. Rev. Lett.* **50**, 1153 (1983).
- [32] F. D. M. Haldane, *Phys. Lett. A* **93**, 464 (1983).
- [33] Uimin, .
- [34] C. K. Lai, *J. Math. Phys.* **15**, 1675 (1974).
- [35] B. Sutherland, *Phys. Rev. B* **12**, 3795 (1975).
- [36] C. Itoi and M.-H. Kato, *Phys. Rev. B* **55**, 8295 (1997).
- [37] K. I. Kugel and D. I. Khomski, *Sov. Phys. Usp.* **25**, 231 (1982).

- 
- [38] P. Corboz, M. Lajkó, A. M. Läuchli, K. Penc, and F. Mila, [Phys. Rev. X \*\*2\*\*, 041013 \(2012\)](#).
  - [39] M. G. Yamada, M. Oshikawa, and G. Jackeli, [Phys. Rev. Lett. \*\*121\*\*, 097201 \(2018\)](#).
  - [40] C. Wu, J.-p. Hu, and S.-c. Zhang, [Phys. Rev. Lett. \*\*91\*\*, 186402 \(2003\)](#).
  - [41] C. Honerkamp and W. Hofstetter, [Phys. Rev. Lett. \*\*92\*\*, 170403 \(2004\)](#).
  - [42] M. A. Cazalilla, A. Ho, and M. Ueda, [New J. Phys. \*\*11\*\*, 103033 \(2009\)](#).
  - [43] A. V. Gorshkov, M. Hermele, V. Gurarie, C. Xu, P. S. Julienne, J. Ye, P. Zoller, E. Demler, M. D. Lukin, and A. Rey, [Nat. Phys. \*\*6\*\*, 289 \(2010\)](#).
  - [44] S. Taie, R. Yamazaki, S. Sugawa, and Y. Takahashi, [Nat. Phys. \*\*8\*\*, 825 \(2012\)](#).
  - [45] H. Nonne, M. Moliner, S. Capponi, P. Lecheminant, and K. Totsuka, [Europhys. Lett. \*\*102\*\*, 37008 \(2013\)](#).
  - [46] G. Pagano, M. Mancini, G. Cappellini, P. Lombardi, F. Schäfer, H. Hu, X.-J. Liu, J. Catani, C. Sias, M. Inguscio, *et al.*, [Nat. Phys. \*\*10\*\*, 198 \(2014\)](#).
  - [47] F. Scazza, C. Hofrichter, M. Höfer, P. De Groot, I. Bloch, and S. Fölling, [Nat. Phys. \*\*10\*\*, 779 \(2014\)](#).
  - [48] X. Zhang, M. Bishof, S. L. Bromley, C. V. Kraus, M. S. Safronova, P. Zoller, A. M. Rey, and J. Ye, [Science \*\*345\*\*, 1467 \(2014\)](#).
  - [49] C. Hofrichter, L. Riegger, F. Scazza, M. Höfer, D. R. Fernandes, I. Bloch, and S. Fölling, [Phys. Rev. X \*\*6\*\*, 021030 \(2016\)](#).
  - [50] S. Capponi, P. Lecheminant, and K. Totsuka, [Ann. Phys. \*\*367\*\*, 50 \(2016\)](#).
  - [51] A. Weichselbaum, S. Capponi, P. Lecheminant, A. M. Tsvelik, and A. M. Läuchli, [Phys. Rev. B \*\*98\*\*, 085104 \(2018\)](#).
  - [52] M. E. Beverland, G. Alagic, M. J. Martin, A. P. Koller, A. M. Rey, and A. V. Gorshkov, [Phys. Rev. A \*\*93\*\*, 051601 \(2016\)](#).
  - [53] N. D. Mermin and H. Wagner, [Phys. Rev. Lett. \*\*17\*\*, 1133 \(1966\)](#).
  - [54] S. Coleman, [Commun. Math. Phys. \*\*31\*\*, 259 \(1973\)](#).
  - [55] S. Gozel, F. Mila, and I. Affleck, [Phys. Rev. Lett. \*\*123\*\*, 037202 \(2019\)](#).
  - [56] S. Gozel, D. Poilblanc, I. Affleck, and F. Mila, [Nucl. Phys. B \*\*945\*\*, 114663 \(2019\)](#).
  - [57] S. Gozel, P. Nataf, and F. Mila, [Phys. Rev. Lett. \*\*125\*\*, 057202 \(2020\)](#).
  - [58] J. des Cloizeaux and J. J. Pearson, [Phys. Rev. \*\*128\*\*, 2131 \(1962\)](#).

## Bibliography

---

- [59] A. B. Zamolodchikov and A. B. Zamolodchikov, *Ann. Phys.* **120**, 253 (1979).
- [60] A. B. Zamolodchikov and A. B. Zamolodchikov, *Nucl. Phys. B* **379**, 602 (1992).
- [61] A. M. Polyakov, *Phys. Lett. B* **59**, 79 (1975).
- [62] D. J. Gross and F. Wilczek, *Phys. Rev. Lett.* **30**, 1343 (1973).
- [63] H. D. Politzer, *Phys. Rev. Lett.* **30**, 1346 (1973).
- [64] M. Takahashi, *Phys. Rev. B* **40**, 2494 (1989).
- [65] M. Takahashi, *Prog. Theor. Phys.* **101**, 487 (1990).
- [66] T. Holstein and H. Primakoff, *Phys. Rev.* **58**, 1098 (1940).
- [67] E. Fradkin, *Field theories of condensed matter physics* (Cambridge University Press, 2013).
- [68] I. Affleck, *J. Phys.: Condens. Matter* **1**, 3047 (1989).
- [69] I. Affleck, Private communication.
- [70] A. Auerbach, *Interacting Electrons and Quantum Magnetism* (Springer-Verlag New York, 1994).
- [71] K. G. Wilson and J. Kogut, *Phys. Rep.* **12**, 75 (1974).
- [72] E. Brézin and J. Zinn-Justin, *Phys. Rev. B* **14**, 3110 (1976).
- [73] W. Bernreuther and F. J. Wegner, *Phys. Rev. Lett.* **57**, 1383 (1986).
- [74] S. Todo, H. Matsuo, and H. Shitara, *Comput. Phys. Comm.* **239**, 84 (2019).
- [75] H. Nakano, N. Todoroki, and T. Sakai, *J. Phys. Soc. Jpn.* **88**, 114702 (2019).
- [76] S. Todo, H. Matsuo, and H. Shitara, “Loop Cluster Monte Carlo Simulation of Quantum Magnets Based on Global Union-Find Algorithm,” (2013), The International Conference for High Performance Computing, Networking, Storage and Analysis.
- [77] S. Elitzur, *Nucl. Phys. B* **212**, 501 (1983).
- [78] F. David, *Commun. Math. Phys.* **81**, 149 (1981).
- [79] H. Hellmann, *Z. Phys.* **85**, 180 (1933).
- [80] R. P. Feynman, *Phys. Rev.* **56**, 340 (1939).
- [81] S. Doniach and E. H. Sondheimer, *Green’s functions for solid state physicists* (World Scientific Publishing, 1974).



- 
- [82] R. Dingle, M. E. Lines, and S. L. Holt, [Phys. Rev. \*\*187\*\*, 643 \(1969\)](#).
  - [83] R. J. Birgeneau, R. Dingle, M. T. Hutchings, G. Shirane, and S. L. Holt, [Phys. Rev. Lett. \*\*26\*\*, 718 \(1971\)](#).
  - [84] M. T. Hutchings, G. Shirane, R. J. Birgeneau, and S. L. Holt, [Phys. Rev. B \*\*5\*\*, 1999 \(1972\)](#).
  - [85] A. Alex, M. Kalus, A. Huckleberry, and J. von Delft, [J. Math. Phys. \*\*52\*\*, 023507 \(2011\)](#).
  - [86] P. Nataf and F. Mila, [Phys. Rev. Lett. \*\*113\*\*, 127204 \(2014\)](#).
  - [87] P. Nataf and F. Mila, [Phys. Rev. B \*\*93\*\*, 155134 \(2016\)](#).
  - [88] K. Wan, P. Nataf, and F. Mila, [Phys. Rev. B \*\*96\*\*, 115159 \(2017\)](#).
  - [89] P. Nataf and F. Mila, [Phys. Rev. B \*\*97\*\*, 134420 \(2018\)](#).
  - [90] A. Young, [Proc. London Math. Soc. \*\*s1-33\*\*, 97 \(1900\)](#).
  - [91] J.-Q. Chen, D. F. Collinson, and M.-J. Gao, [J. Math. Phys. \*\*24\*\*, 2695 \(1983\)](#).
  - [92] J.-Q. Chen, J. Ping, and F. Wang, [Group representation theory for physicists](#) (World Scientific Publishing Company, 2002).
  - [93] W. Pfeifer, [The Lie algebras  \$su\(N\)\$](#)  (Springer, 2003).
  - [94] M. Hamermesh, [Group theory and its application to physical problems](#) (Dover Publications, 2012).
  - [95] D. E. Littlewood, [J. Lond. Math. Soc. \*\*s1-31\*\*, 89 \(1956\)](#).
  - [96] W. Fulton, [Young Tableaux: With Applications to Representation Theory and Geometry](#), London Mathematical Society Student Texts (Cambridge University Press, 1996).
  - [97] A. Nijenhuis and H. S. Wilf, [Combinatorial Algorithms: For Computers and Calculators](#), 2nd ed. (Academic Press, 1978).
  - [98] A. Young, [Proc. London Math. Soc. \*\*s2-34\*\*, 196 \(1932\)](#).
  - [99] T. Yamanouchi, [Proc. Phys.-Math. Soc. Jpn. 3rd Series \*\*19\*\*, 436 \(1937\)](#).
  - [100] D. E. Rutherford, [Substitutional analysis](#) (Edinburgh University Press, 1948).
  - [101] W. Fulton and J. Harris, [Representation Theory: A First Course](#) (Springer, 2013).
  - [102] T. Toyoda, [J. Phys. Soc. Jpn. \*\*19\*\*, 1757 \(1964\)](#).
  - [103] J. F. Cornwell, [Group Theory in Physics, Volume II](#) (Academic Press, 1984).

## Bibliography

---

- [104] K. Pilch and A. N. Schellekens, *J. Math. Phys.* **25**, 3455 (1984).
- [105] C. Itzykson and M. Nauenberg, *Rev. Mod. Phys.* **38**, 95 (1966).
- [106] L. C. Biedenharn, *J. Math. Phys.* **4**, 436 (1963).
- [107] G. E. Baird and L. C. Biedenharn, *J. Math. Phys.* **4**, 1449 (1963).
- [108] G. E. Baird and L. C. Biedenharn, *J. Math. Phys.* **5**, 1723 (1964).
- [109] G. E. Baird and L. C. Biedenharn, *J. Math. Phys.* **5**, 1730 (1964).
- [110] G. E. Baird and L. C. Biedenharn, *J. Math. Phys.* **6**, 1847 (1965).
- [111] N. J. Vilenkin and A. U. Klimyk, *Representation of Lie groups and special functions: Volume 1: Simplest Lie Groups, Special Functions and Integral Transforms* (Kluwer Academic Publishers, 1991).
- [112] N. J. Vilenkin and A. U. Klimyk, *Representation of Lie groups and special functions: Volume 2: Class I Representations, Special Functions, and Integral Transforms* (Kluwer Academic Publishers, 1993).
- [113] N. J. Vilenkin and A. U. Klimyk, *Representation of Lie groups and special functions: Volume 3: Classical and quantum groups and special functions* (Kluwer Academic Publishers, 1992).
- [114] J.-S. Huang, *Lectures on representation theory* (World Scientific, 1999).
- [115] I. Affleck, T. Kennedy, E. H. Lieb, and H. Tasaki, *Phys. Rev. Lett.* **59**, 799 (1987).
- [116] I. Affleck, T. Kennedy, E. H. Lieb, and H. Tasaki, *Commun. Math. Phys.* **115**, 477 (1988).
- [117] M. Greiter, S. Rachel, and D. Schuricht, *Phys. Rev. B* **75**, 060401(R) (2007).
- [118] M. Greiter and S. Rachel, *Phys. Rev. B* **75**, 184441 (2007).
- [119] H. Katsura, T. Hirano, and V. E. Korepin, *J. Phys. A: Math. Theor.* **41**, 135304 (2008).
- [120] T. Morimoto, H. Ueda, T. Momoi, and A. Furusaki, *Phys. Rev. B* **90**, 235111 (2014).
- [121] A. Roy and T. Quella, *Phys. Rev. B* **97**, 155148 (2018).
- [122] K. Duivenvoorden and T. Quella, *Phys. Rev. B* **87**, 125145 (2013).
- [123] S. Rachel, R. Thomale, M. Führinger, P. Schmitteckert, and M. Greiter, *Phys. Rev. B* **80**, 180420(R) (2009).
- [124] D. P. Arovas, A. Auerbach, and F. D. M. Haldane, *Phys. Rev. Lett.* **60**, 531 (1988).

- 
- [125] H.-H. Tu, G.-M. Zhang, T. Xiang, Z.-X. Liu, and T.-K. Ng, [Phys. Rev. B \*\*80\*\*, 014401 \(2009\)](#).
  - [126] M. Fannes, B. Nachtergaele, and R. F. Werner, [Commun. Math. Phys. \*\*144\*\*, 443 \(1992\)](#).
  - [127] B. Nachtergaele, [Commun. Math. Phys. \*\*175\*\*, 565 \(1996\)](#).
  - [128] D. Perez-Garcia, F. Verstraete, M. M. Wolf, and J. I. Cirac, [arXiv:quant-ph/0608197 \(2006\)](#).
  - [129] M. Sanz, D. Pérez-García, M. M. Wolf, and J. I. Cirac, [IEEE Trans. Inf. Theory \*\*56\*\*, 4668 \(2010\)](#).
  - [130] N. Schuch, D. Pérez-García, and I. Cirac, [Phys. Rev. B \*\*84\*\*, 165139 \(2011\)](#).
  - [131] M. den Nijs and K. Rommelse, [Phys. Rev. B \*\*40\*\*, 4709 \(1989\)](#).
  - [132] M. Hagiwara, K. Katsumata, I. Affleck, B. I. Halperin, and J. P. Renard, [Phys. Rev. Lett. \*\*65\*\*, 3181 \(1990\)](#).
  - [133] F. Pollmann, A. M. Turner, E. Berg, and M. Oshikawa, [Phys. Rev. B \*\*81\*\*, 064439 \(2010\)](#).
  - [134] F. Pollmann, E. Berg, A. M. Turner, and M. Oshikawa, [Phys. Rev. B \*\*85\*\*, 075125 \(2012\)](#).
  - [135] L. Tsui, Y.-T. Huang, H.-C. Jiang, and D.-H. Lee, [Nucl. Phys. B \*\*919\*\*, 470 \(2017\)](#).
  - [136] A. Moreo, [Phys. Rev. B \*\*36\*\*, 8582 \(1987\)](#).
  - [137] T. Ziman and H. J. Schulz, [Phys. Rev. Lett. \*\*59\*\*, 140 \(1987\)](#).
  - [138] M. Lajkó, K. Wamer, F. Mila, and I. Affleck, [Nucl. Phys. B \*\*924\*\*, 508 \(2017\)](#).
  - [139] M. Lajkó, K. Wamer, F. Mila, and I. Affleck, [Nucl. Phys. B \*\*949\*\*, 114781 \(2019\)](#).
  - [140] K. Wamer, F. H. Kim, M. Lajkó, F. Mila, and I. Affleck, [Phys. Rev. B \*\*100\*\*, 115114 \(2019\)](#).
  - [141] K. Wamer, M. Lajkó, F. Mila, and I. Affleck, [Nucl. Phys. B \*\*952\*\*, 114932 \(2020\)](#).
  - [142] P. Lecheminant, [Nucl. Phys. B \*\*901\*\*, 510 \(2015\)](#).
  - [143] H. Johannesson, [Nucl. Phys. B \*\*270\*\*, 235 \(1986\)](#).
  - [144] L. A. Takhtajan, [Phys. Lett. A \*\*87\*\*, 479 \(1982\)](#).
  - [145] H. M. Babujian, [Phys. Lett. A \*\*90\*\*, 479 \(1982\)](#).
  - [146] L. Vanderstraeten and F. Verstraete, Private communication.

## Bibliography

---

- [147] E. Lieb, T. Schultz, and D. Mattis, [Ann. Phys. \*\*16\*\*, 407 \(1961\)](#).
- [148] I. Affleck and E. H. Lieb, [Lett. Math. Phys. \*\*12\*\*, 57 \(1986\)](#).
- [149] D. Bykov, [Commun. Math. Phys. \*\*322\*\*, 807 \(2013\)](#).
- [150] H. T. Ueda, Y. Akagi, and N. Shannon, [Phys. Rev. A \*\*93\*\*, 021606 \(2016\)](#).
- [151] K. Ohmori, N. Seiberg, and S.-H. Shao, [SciPost Phys. \*\*6\*\*, 17 \(2019\)](#).
- [152] S. R. White and D. A. Huse, [Phys. Rev. B \*\*48\*\*, 3844 \(1993\)](#).
- [153] U. Schollwöck and T. Jolicoeur, [Europhys. Lett. \*\*30\*\*, 493 \(1995\)](#).
- [154] U. Schollwöck, O. Golinelli, and T. Jolicoeur, [Phys. Rev. B \*\*54\*\*, 4038 \(1996\)](#).
- [155] X. Wang, S. Qin, and L. Yu, [Phys. Rev. B \*\*60\*\*, 14529 \(1999\)](#).
- [156] T. Wada, [Phys. Rev. E \*\*61\*\*, 3199 \(2000\)](#).
- [157] S. Ramasesha, S. K. Pati, H. R. Krishnamurthy, Z. Shuai, and J. L. Brédas, [Phys. Rev. B \*\*54\*\*, 7598 \(1996\)](#).
- [158] I. P. McCulloch, [J. Stat. Mech.: Theory Exp. \*\*2007\*\*, P10014 \(2007\)](#).
- [159] S. Singh, R. N. C. Pfeifer, and G. Vidal, [Phys. Rev. B \*\*83\*\*, 115125 \(2011\)](#).
- [160] ITensor Library <http://itensor.org>.
- [161] S. Singh and G. Vidal, [Phys. Rev. B \*\*86\*\*, 195114 \(2012\)](#).
- [162] G. Sierra and T. Nishino, [Nucl. Phys. B \*\*495\*\*, 505 \(1997\)](#).
- [163] T. Wada and T. Nishino, [Comput. Phys. Comm. \*\*142\*\*, 164 \(2001\)](#), conference on Computational Physics 2000: “New Challenges for the New Millenium”.
- [164] J. M. Román, G. Sierra, J. Dukelsky, and M. A. Martín-Delgado, [J. Phys. A: Math. Gen. \*\*31\*\*, 9729 \(1998\)](#).
- [165] I. P. McCulloch and M. Gulácsi, [Europhys. Lett. \*\*57\*\*, 852 \(2002\)](#).
- [166] I. P. McCulloch and M. Gulácsi, [Phil. mag. lett. \*\*81\*\*, 447 \(2001\)](#).
- [167] G. Alvarez, [Comput. Phys. Commun. \*\*183\*\*, 2226 \(2012\)](#).
- [168] U. Schollwöck, [Ann. Phys. \*\*326\*\*, 96 \(2011\)](#).
- [169] S. Singh, R. N. C. Pfeifer, and G. Vidal, [Phys. Rev. A \*\*82\*\*, 050301 \(2010\)](#).
- [170] S. Singh, H.-Q. Zhou, and G. Vidal, [New J. Phys. \*\*12\*\*, 033029 \(2010\)](#).
- [171] A. Weichselbaum, [Ann. Phys. \*\*327\*\*, 2972 \(2012\)](#).

- [172] M. Fühlinger, S. Rachel, R. Thomale, M. Greiter, and P. Schmitteckert, [Ann. Phys. \*\*17\*\*, 922 \(2008\)](#).
- [173] S. R. Manmana, K. R. A. Hazzard, G. Chen, A. E. Feiguin, and A. M. Rey, [Phys. Rev. A \*\*84\*\*, 043601 \(2011\)](#).
- [174] E. S. Sørensen and I. Affleck, [Phys. Rev. Lett. \*\*71\*\*, 1633 \(1993\)](#).
- [175] P. Calabrese and J. Cardy, [J. Stat. Mech. \*\*2004\*\*, P06002 \(2004\)](#).
- [176] Y. Tanizaki and T. Sulejmanpasic, [Phys. Rev. B \*\*98\*\*, 115126 \(2018\)](#).
- [177] Y. Yao, C.-T. Hsieh, and M. Oshikawa, [Phys. Rev. Lett. \*\*123\*\*, 180201 \(2019\)](#).
- [178] V. Zauner-Stauber, L. Vanderstraeten, M. T. Fishman, F. Verstraete, and J. Haegeman, [Phys. Rev. B \*\*97\*\*, 045145 \(2018\)](#).
- [179] N. Papanicolaou, [Nucl. Phys. B \*\*240\*\*, 281 \(1984\)](#).
- [180] N. Papanicolaou, [Nucl. Phys. B \*\*305\*\*, 367 \(1988\)](#).
- [181] A. Joshi, M. Ma, F. Mila, D. N. Shi, and F. C. Zhang, [Phys. Rev. B \*\*60\*\*, 6584 \(1999\)](#).
- [182] A. V. Chubukov, [J. Phys.: Condens. Mat. \*\*2\*\*, 1593 \(1990\)](#).
- [183] M. Mathur and D. Sen, [J. of Math. Phys. \*\*42\*\*, 4181 \(2001\)](#).
- [184] F. H. Kim, K. Penc, P. Nataf, and F. Mila, [Phys. Rev. B \*\*96\*\*, 205142 \(2017\)](#).
- [185] F. H. Kim, F. F. Assaad, K. Penc, and F. Mila, [Phys. Rev. B \*\*100\*\*, 085103 \(2019\)](#).



## List of publications

- [3] *Haldane gap of the three-box symmetric  $SU(3)$  chain*,  
[Samuel Gozel](#), Pierre Nataf, and Frédéric Mila,  
[Phys. Rev. Lett. \*\*125\*\*, 057202 \(2020\)](#).
- [2] *Asymptotic freedom and large spin antiferromagnetic chains*,  
[Samuel Gozel](#), Frédéric Mila, and Ian Affleck,  
[Phys. Rev. Lett. \*\*123\*\*, 037202 \(2019\)](#).
- [1] *Novel families of  $SU(N)$  AKLT states with arbitrary self-conjugate edge states*,  
[Samuel Gozel](#), Didier Poilblanc, Ian Affleck, and Frédéric Mila,  
[Nucl. Phys. B \*\*945\*\*, 114663 \(2019\)](#).





# Samuel GOZEL

EPFL SB IPHYS CTMC  
BSP 718 (Cubotron Unil)  
Route de la Sorge  
1015 Lausanne  
Switzerland

20/11/1992  
Swiss  
+41 21 693 05 14  
[samuel.gozel@epfl.ch](mailto:samuel.gozel@epfl.ch)

## Education

---

09/2016-12/2020	<b>EPFL, Swiss Federal Institute of Technology, Lausanne</b> Doctoral studies in the Chair of Condensed Matter Theory, co-supervised by Prof. Frédéric Mila & Prof. Ian Affleck (based in UBC, Vancouver, Canada)
09/2016-08/2017	<b>UBC, University of British Columbia, Vancouver</b> Visiting International Research Student in the Stewart Blusson Quantum Matter Institute, Group of Prof. Ian Affleck
09/2014-07/2016	<b>EPFL, Swiss Federal Institute of Technology, Lausanne</b> Master in Physics with Minor in Computational Science and Engineering
09/2011-07/2014	Bachelor in Physics
08/2008-07/2011	<b>Gymnase cantonal de Nyon (High school), Nyon</b> Federal bilingual maturity (French-German), scientific options

## Technical skills

---

<b>Programming</b>	<ul style="list-style-type: none"><li>• Proficient in Matlab, C++ (with object orientation), C</li><li>• Good knowledge of Mathematica, basic notions of Python</li><li>• Use of version control system (Git)</li><li>• Use of HPCs</li><li>• Basics of OpenMP</li></ul>
<b>Numerical methods</b>	Computational linear algebra, finite element methods

## Languages

---

<b>English</b>	C1. Over 14 months in Vancouver (Canada) as part of my PhD (one 12-months stay and several shorter term visits)
<b>German</b>	B1/B2. Bilingual maturity: exchange for 3 months in Germany in 2009
<b>French</b>	Mother tongue

## Awards

---

<b>2016</b>	<b>Prof. Ian Affleck and Stewart Blusson Quantum Matter Institute (UBC)</b> PhD Award
<b>2011</b>	<b>Gymnase cantonal de Nyon (High school)</b> <ul style="list-style-type: none"><li>• Award of Excellence in Physics</li><li>• Award of Excellence in Mathematics &amp; Physics</li></ul>

## Talks

---

10/2019	Workshop "Trends in Theory of Correlated Materials", Kyoto (Japan) <i>SU(3) 3-box symmetric spin chains</i>
08/2019	Swiss Physical Society Meeting, Zürich (Switzerland) <i>Novel families of SU(N) AKLT states with arbitrary self-conjugate edge states</i>
08/2019	Summer School "Quantum Magnetism", Lausanne (Switzerland) <i>Novel families of SU(N) AKLT states with arbitrary self-conjugate edge states</i>

## Doctoral schools, Workshops and Conferences

---

07-09/10/2019	(invited) Swiss-Japan Workshop "Trends in Theory of Correlated Materials", Kyoto (Japan)
27-30/08/2019	Swiss Physical Society Meeting, Zürich (Switzerland)
19-23/08/2019	Summer School "Quantum Magnetism", Lausanne (Switzerland)
01-03/05/2019	Workshop "Interacting Majorana Fermions", Vancouver (Canada)
01-13/10/2018	Workshop "Topological phases in condensed matter and cold atoms", Cargese (Corsica, France)
29-31/08/2018	Swiss Workshop on Materials, MaNEP, Les Diablerets (Switzerland)
20-24/08/2018	Summer school "New Trends in Chiral Magnetism", Lausanne (Switzerland)
04-08/06/2018	Conference "Trends in Quantum Magnetism", Bad Honnef (Germany)
26-28/04/2018	Symposium "30 years of AKLT: Interacting Systems in Low Dimensions", Vancouver (Canada)
18/02-03/03/2018	Workshop "Entanglement in Strongly Correlated Systems", Benasque (Spain)
5-10/11/2017	European Tensor Network School, Ghent (Belgium)

## Short research stays

---

24/04-09/05/2019	UBC, Vancouver (Canada)
08/09-29/09/2018	
19/04-07/05/2018	

## Teaching assistantship

---

09/2019-12/2019	PHYS-419 Solid State Physics III (EPFL)
02/2019-06/2019	PHYS-210 Computational Physics II (EPFL)
02/2018-06/2018	
09/2017-12/2017	PHYS-315 Statistical Physics I (EPFL)
09/2016-12/2016	PHYS-101 Energy and Waves (UBC)